

**METAMORPHOSIS IN TELEOSTS: A
COMPARATIVE STUDY BETWEEN THE
FLATFISH *HIPPOGLOSSUS*
HIPPOGLOSSUS AND THE ROUND FISH
*SPARUS AURATUS***

MARCO ANTÓNIO CAMPINHO

This dissertation is submitted
for the degree of Doctor of Philosophy

School of Biosciences
Cardiff University

UMI Number: U584916

All rights reserved

INFORMATION TO ALL USERS

The quality of this reproduction is dependent upon the quality of the copy submitted.

In the unlikely event that the author did not send a complete manuscript and there are missing pages, these will be noted. Also, if material had to be removed, a note will indicate the deletion.



UMI U584916

Published by ProQuest LLC 2013. Copyright in the Dissertation held by the Author.
Microform Edition © ProQuest LLC.

All rights reserved. This work is protected against
unauthorized copying under Title 17, United States Code.



ProQuest LLC
789 East Eisenhower Parkway
P.O. Box 1346
Ann Arbor, MI 48106-1346

Declaration

I hereby declare that my dissertation contains material that has not been submitted for a degree or diploma or any other qualification at any other university. The contents of this thesis are of exclusive responsibility of the author.

Acknowledgments

I want to acknowledge the Fundação Para a Ciência e Tecnologia (FCT) for funding this research (SFRH/BD/6133/2001).

I would like to thank to my supervisor Dr. Glen E. Sweeney for giving me the opportunity to carry out this PhD at Cardiff University and for all his friendship, support and knowledge throughout this years. I feel that I have walked some big steps in my knowledge, vision and understanding of biology thanks to you.

I would like to thank Professor Deborah Power for so enthusiastically supporting me, trusted me and above all believed in my potential as a biologist and for being my mentor since I started working in science. This PhD would not have been possible without Professor Debbie. Above all I would like to thank your friendship and all your determination to keep me going forward and better all the time. I hope one day I can repay everything you have taught me by giving all this knowledge to someone else.

I also want to thanks Professor Adelino Canário for having me in his lab and give me all the support needed to do this PhD. Specially in statistical analysis and problems where he always helped me a lot.

I want to thank all my friends in Cardiff, Dave, Tim, Gareth, Marion and Pete for making the lab a great place to work. I would specially like to thank all the friendship and support of my lab colleges in Cardiff, Paul, Lynda and Malyka, for the excellent times we had, their friendship and help. Specially Malyka for being like a big sister to me during my time in Cardiff.

I also want to thank all my colleges in Faro for their friendship and support. With a special thanks for my good friends Rute and Juan with whom I discussed results and from which the discussion of thesis has gain a lot. Would like to thanks the significant help by Rita Costa in halibut deiodinase *in situ* hybridization experiments and Rita Jacinto in the radioimmunoassay experiments. Also would like to give special thanks my good friend Bruno with whom I have found and explored so many bioinformatics tools used in this thesis, my great friend Nádia that made an outstanding impact in this work in every histological analysis.

A special thanks to my parents and my brother for their support without which this PhD would have not been possible.

A very special thanks for my girlfriend and companion Amélia for her support and endless patience with me during all this time.

Abstract

Metamorphosis is the developmental process by which larvae become adult-like juveniles. In both amphibia and flatfish thyroid hormones (THs) have been shown to drive metamorphosis and probably also influence the larval to juvenile transition in roundfish. Remarkably little is known about the regulation and expression of deiodinase genes that are responsible for TH metabolism or the TH-responsive genes at this developmental stage in teleosts. The objective of this thesis was to characterise the potential role of deiodinases in the metamorphosis of the Atlantic halibut (*Hippoglossus hippoglossus*), a flatfish and the analogous larval to juvenile transition in a roundfish the gilthead sea bream (*Sparus auratus*).

Fast and slow muscle Troponin-T genes were cloned from both species and found to be differentially regulated by THs. Species specific differences were found in TnT genes and their expression profiles during development which probably reflect the significant differences in muscle ontogeny between these teleosts. A halibut epidermal-keratin gene was also isolated and shown to be differentially expressed in skin during metamorphosis and related to molecular, cellular and histological changes that occur at this time. Genes encoding all three deiodinase enzymes (which regulate intracellular TH levels in target tissues) were isolated from both halibut and sea bream and their expression profile was correlated to molecular and cellular changes in muscle during the larval to juvenile transition in both teleosts.

The results presented here strongly suggest that despite the significant morphological differences that exist between halibut metamorphosis and sea bream larval to juvenile transition the overall relationships between deiodinases expression is conserved suggesting that THs have a similar role in both these processes.

Communications in meetings

M.A. Campinho, D.M. Power, G.E. Sweeney. Effect of T3 and methimazole treatment in Troponin T gene expression in sea bream juveniles. Fifth International Symposium on Fish Endocrinology, Castellon, Spain, September, 2004.

Campinho, M.A., Power, D.M. and Sweeney, G.: Isolation and identification of two slow troponin T genes in the *Sparus aurata*: In silico comparative genomic analysis with *Fugu rubripes*. COST action 925 - The importance of prenatal events for postnatal muscle growth in relation to the quality of muscle based foods, 2004. Porto, Portugal.

Campinho, MA, Power, DM, Sweeney, GE. Deiodinase expression during halibut metamorphosis: Quantitative PCR analysis. International Marine Biotechnology Conference, New Foundland, Canada, 2005

M.A. Campinho, N. Silva, G. E. Sweeney and D.M. Power. Molecular, histological and morphological changes in skin of halibut during metamorphosis. 5º Congresso de la Asociación Ibérica de Endocrinología Comparada, 2005. Faro, Portugal.

Publications

Campinho, M.A., Power, D.M. and Sweeney, G.E. Identification and analysis of teleost slow muscle troponin T (sTnT) and intronless TnT genes. *Gene* 361 (2005) 67-79.

Campinho, M.A., Power, D.M. and Sweeney, G. Isolation and identification of two slow troponin T genes in the *Sparus aurata*: In silico comparative genomic analysis with *Fugu rubripes*. *Archives of Animal Breeding* 48 (2005) 77-78.

Campinho, M.A., Silva, N., Sweeney, G.E., Power, D.M. Molecular, cellular and histological changes in skin from a larval to an adult phenotype during bony fish metamorphosis. *Cell and Tissue Research* (2007) Feb;327(2):267-84.

Campinho, M.A., Sweeney, G.E., Power, D.M. Regulation of Troponin T expression during muscle development in Sea Bream (*Sparus auratus*, Linnaeus): the potential role of thyroid hormones. *Journal of Experimental Biology* (2006) Dec 1;209(Pt 23):4751-67.

Campinho, M. A., Silva, N., Nowell, M. A., Llewellyn, L., Sweeney, G. E., Sweeney and Power, D. M. *Troponin T* isoform expression is modulated during Atlantic Halibut metamorphosis (Submitted).

Submissions to GenBank database

The halibut and sea bream cDNAs isolated and fully described in the thesis were submitted to Genbank database with the following accession numbers:

Halibut: hhKer1 (DQ364242); efTnThh (DQ680173); fTnThh-1 (DQ680174); fTnThh-2 (DQ680175), AfTnThh-1 (DQ680176); AfTnThh-2 (DQ680177); AfTnThh-3 (DQ680178); AfTnThh-4 (DQ680179); sTnT2hh (DQ680172); hhD1 (DQ856302); hhD2 (DQ856304); hhD3 (DQ856303).

Sea bream: efTnTsb (DQ473445); LfTnTsb (DQ473444); afTnTsb (DQ473443); sTnT1sb-1 (AY684301); sTnT2sb (AY684302); iTnTsb (AY953294); saD1 (DQ888894); saD2 (DQ888895); saD3 (DQ888896).

Table of contents

Declaration	i
Acknowledgments	ii
Abstract	iii
Communications in meetings	iv
Publications	iv
Submissions to GenBank	iv
Table of contents	v
List of figures	ix
List of tables	xix
Abbreviations	xx
Chapter 1: General introduction	1
1.1.1 The Atlantic Halibut (<i>Hippoglossus hippoglossus</i>)	4
1.1.2 The Gilthead Sea Bream (<i>Sparus auratus</i>)	5
1.2 Metamorphosis	7
1.2.1 Thyroid Hormones	11
1.2.1.1 Thyroid Hormones Production	12
1.2.1.2 Regulation of Thyroid Hormones Production	14
1.2.1.3 Transport and Cellular Intake of TH	15
1.3 Deiodination	16
1.2.1 Type I Deiodinase	17
1.2.2 Type II Deiodinase	20
1.2. 3 Type III Deiodinase	24
1.2.4 Deiodinases in development of vertebrates	28
1.4 Thyroid hormone receptors	31
1.4.1 Role of TRs in mediating TH action in vertebrate development	35
1.5 Molecular markers of fish metamorphosis	37
1.5.1 Troponin T	39
1.5.2 Epidermal keratin genes	40
Chapter 2: Molecular, cellular and histological changes in skin from a larval to an adult phenotype during halibut metamorphosis.	41
2.1 Introduction	42
2.2 Materials and methods	44
2.2.1 cDNA isolation of an epidermal type I keratin – hhKer1	44
2.2.2 Phylogenetic analysis	45
2.2.3 Putative genomic organization	47
2.2.4 Animal and tissue sampling	47
2.2.5 Total RNA extraction	48
2.2.6 Northern Blot	48
2.2.7 Semi-Quantitative RT-PCR analysis of halibut keratin expression during Halibut metamorphosis	49
2.2.7 Radioimmunoassay for thyroid hormones	50
2.2.8 Histology	51
2.2.9 In situ hybridisation	51
2.3 Results	53
2.3.1 Halibut keratin 1 (hhKer1)	53
2.3.2 hhKer1 expression and T4 levels during halibut metamorphosis	58

2.3.3 Skin development and hhKer1 spatial temporal pattern of expression during halibut metamorphosis	61
2.4 Discussion	66
2.4.1 Halibut larval epidermal keratin type I gene – hhKer1	66
2.4.2 Halibut metamorphosis and molecular and histological changes in skin	69
Chapter 3: Troponin T isoform expression is modulated during Atlantic Halibut metamorphosis	74
3.1 Introduction	75
3.2 Materials and methods	76
3.2.1 TnT cDNA library screening	76
3.2.2 Phylogenetic analysis	77
3.2.3 Putative genomic organisation of halibut TnT genes	79
3.2.4 Animal sampling	79
3.2.4 Total RNA extraction	80
3.2.5 Northern Blot	80
3.2.6 Semi-Quantitative RT-PCR analysis of TnT expression during halibut metamorphosis	81
3.2.7 In situ hybridisation	82
3.2.8 Radioimmunoassay for thyroid hormones	84
3.3 Results	85
3.3.1 Halibut TnT genes	85
3.3.2 Putative genomic organization of halibut skeletal TnT genes	87
3.3.3 Tissue specificity of halibut TnT genes	90
3.3.4 Phylogenetic analysis of Halibut TnT genes	91
3.3.5 TnT expression during halibut metamorphosis	94
3.3.6 Muscle Growth and Ontogeny	98
3.3.7 Spatial-temporal expression pattern of halibut TnT genes during metamorphosis	100
3.3.8 TH levels in metamorphosing halibut	101
3.4 Discussion	103
3.4.1 Halibut TnT genes	103
3.4.2 Halibut TnT genes expression during metamorphosis	106
Chapter 4: Deiodinases present a coordinated pattern of expression throughout Hippoglossus hippoglossus (Atlantic halibut) metamorphosis	111
4.1 Introduction	112
4.2 Material and Methods	114
4.2.1 cDNA isolation of halibut D1 and D3	114
4.2.2 RT-PCR cloning of halibut D2	115
4.2.3 Phylogenetic analysis	116
4.2.4 Animal and tissue sampling	116
4.2.5 Total RNA extraction	117
4.2.6 Quantitative Taqman RT-PCR analysis	117
4.2.7 Radioimmunoassay for T4 and T3	119
4.2.8 In situ hybridisation	119
4.3 Results	121
4.3.1 Halibut deiodinase genes	121
4.3.2 Halibut deiodinases expression during metamorphosis – Taqman Quantitative RT-PCR	127

4.3.3 T4 and T3 profile during halibut metamorphosis	129
4.3.4 Deiodinase expression in skin during halibut metamorphosis	131
4.3.5 Halibut deiodinase expression in muscle during halibut metamorphosis	134
4.4 Discussion	136
4.4.1 Halibut deiodinase genes	136
4.4.2 Deiodinase in coordination of halibut metamorphosis	137
4.4.3 Deiodinase expression in skin and muscle during halibut metamorphosis	140
Chapter 5: Regulation of Troponin T expression during muscle development in Sea Bream: The potential role of thyroid hormones	145
5.1 Introduction	146
5.2 Materials and Methods	148
5.2.1 Sea bream fTnT cDNA Library Screen	148
5.2.2 Strategy for cDNA library screening for sea bream sTnT genes	148
5.2.3 RT-PCR cloning of the sea bream intronless TnT gene (iTnTsb)	150
5.2.4 Animal and Tissue Sampling	150
5.2.5 Total RNA extraction	151
5.2.6 Northern blot	151
5.2.7 Identification in silico of fTnT variants in other teleosts	152
5.2.8 Phylogenetic analysis of sea bream TnT genes	153
5.2.9 Putative genomic organisation of sea bream TnT gene	155
5.2.10 First strand cDNA synthesis	155
5.2.11 Developmental expression of sea bream TnT genes - Semi-Quantitative RT-PCR analysis	156
5.2.12 Experiments - T3 and Methimazol treatment	157
5.2.13 Sea bream TnT genes in T3 and Methimazol-treated animals – Semi -Quantitative RT-PCR analysis	159
5.2.14 TH extraction and Radioimmunoassay	159
5.2.15 Thyroid follicular activity analysis	160
5.2.16 Statistical analysis	160
5.3 Results	161
5.3.1 Characterization of sea bream fast TnT isoforms	161
5.3.2 Characterization of cloned sea bream sTnT and iTnT genes	166
5.3.3 Northern blot analysis	169
5.3.4 In silico identification of fTnT variants in other teleosts	171
5.3.5 Phylogenetic analysis of sea bream TnT genes	174
5.3.6 Putative genomic organisation of the sea bream fTnT gene	177
5.3.7 Putative genomic organization of fish sTnT genes and iTnT	179
5.3.8 Developmental analysis of sea bream fTnT – semi-quantitative RT-PCR	180
5.3.9 Tissue specific and developmental expression of sTnT1sb, sTnT2sb and iTnTsb – semi-quantitative RT-PCR	182
5.3.10 T3 and Methimazol treatments – sea bream TnT expression	184
5.3.11 T3 and Methimazol treatments: TH levels and thyrocyte activity	190
5.4 Discussion	193
5.4.1 Molecular characterization of sea bream fTnT gene – fTnTsb	193
5.4.2 Molecular characterisation of the sTnT and iTnT genes found in Sea bream	196
5.4.3 Developmental expression from embryonic stages to adult of fTnTsb	200
5.4.4 Developmental expression of the sea bream sTnT	201
5.4.5 Sea bream TnT genes TH responsiveness	204

Chapter 6: Coordination of deiodinase and thyroid hormone receptor expression during the larval to the juvenile transition in sea bream	207
6.1 Introduction	208
6.2 Material and Methods	211
6.2.1 Isolation of sea bream D1 and D3 cDNAs	211
6.2.2 RT-PCR cloning of sea bream D2	211
6.2.3 Phylogenetic analysis	212
6.2.4 Animal Sampling	213
6.2.5 Animal treatments	213
6.2.6 Total RNA extraction	214
6.2.7 First strand cDNA synthesis	214
6.2.8 Developmental expression of sea bream D1, D2 and D3 – semi-quantitative RT-PCR analysis	214
6.2.9 Developmental expression of sea bream TR α and TR β - Taqman Quantitative RT-PCR analysis	216
6.3 Results	218
6.3.1 Isolation of sea bream deiodinases cDNA	218
6.3.2 Phylogenetic relationships of sea bream deiodinases	221
6.3.3 Developmental expression of sea bream deiodinases	223
6.3.4 Developmental expression of sea bream TR α and TR β	226
6.3.5 T3 and methimazol treatments - sea bream deiodinases expression	228
6.3.6 T3 and methimazol treatments - sea bream TR α and TR β expression	231
6.4 Discussion	234
6.4.1 Molecular characterisation of sea bream deiodinases	234
6.4.2 Sea bream deiodinases, TR α and TR β present coordinated expression during development	235
6.4.3 Effect of T3 and methimazol treatment in sea bream deiodinase and TR expression	237
Chapter 7: General conclusions	241
7.1 Future research in TH action in teleost development	246
Appendix I	248
References	254

List of Figures

- Figure 1.1.** Proposed phylogenetic relationship of fishes and their relative abundance in the fossil record. Note that the teleostei are the latest bony fish group to arise although there are the largest group of modern fishes (adapted from (Langeland and A., 1997)). 2
- Figure 1.2.** Representation of the Atlantic Halibut, *Hippoglossus hippoglossus* (adapted from www.fishbase.org, 2000). 4
- Figure 1.3.** Representation of the Sea Bream, *Sparus aurata* (adapted from ww.fishbase.org,2000). 6
- Figure 1.4.** Structural formula of thyroxine (T4) and 3, 5, 3'-triiodothyronine (T3). 11
- Figure 1.5.** Structural formula of rT3 and T2. 12
- Figure 1.6.** (A) Conformational changes of Tg necessary to permit the correct positioning of MIT and DIT residues for TH formation (www.thyroidmanager.org, 2003). (B) Proposed coupling reaction of iodotyrosines in Tg. The free radicals could combine to generate the iodothyronine residue (at the tyrosine acceptor site) and a dehydroalanine residue (at the tyrosine donor site), which in the presence of H₂O converts into a serine (Adapted from (Gavaret et al., 1980; Gavaret et al., 1981)). 14
- Figure 1.7.** Metabolism of thyroid hormones by the three known vertebrate deiodinases. 17
- Figure 1.8.** Scheme representing the proposed enzymatic action of D1. D1 converts iodothyronines by taking a iodine in position 5' and forming an intermediary that is recovered by the action of thiol groups like DTT (taken from www.thyroidmanager.org, 2003). 19
- Figure 1.9.** Scheme representing the proposed action of D2. The Se group in D2 interacts and constitutes a intermediate with T4 that after thiol action results in the production of T3 and the regeneration of the enzyme (adapted from (Kuiper et al., 2002)). 22
- Figure 1.10.** Proposed action of thyroid hormone receptors. The TR is bound to DNA in the TRE located upstream of the initiation site as a heterodimer with the RXR receptors. The plasma circulating T4 enters the cell, it is converted to T3 in the cytoplasm and enters the nucleus where it binds with TR. The binding of the hormone to its receptor causes a conformational changes in the TR-RXR heterodimer and, depending of the target gene promoter context and other factors, will enhance or repress gene expression (adapted from www.thyroidmanager.org, 2003). 32
- Figure 1.11.** Domain structure of Thyroid Hormone Receptors. The N-terminal A/B domain contains the AF-1 site where other transcription factors interact. C domain contains the two- zinc finger structure that binds to DNA, and the E domain contains the ligand binding pocket as well as the AF-2 region that directly contacts coactivator peptides (adapted from (Nilsson et al., 2001). 33

Figure 1.12. Thyroid Response Element (TRE) consensus sequence. The sequence depicted represents the most common direct repeat TRE. Other TRE's have the same sequence although they can be present as a palindrome or an inverted sequence. 34

Figure 2.1. (A) Predicted protein sequence of hhKer1 showing the characteristic protein domains typical of type I keratins. X represent STRING deduced type I keratin signatures. (B) Maximum-parsimony phylogenetic tree for vertebrate type I keratins. The bar represents 10% sequence divergence. 55

Figure 2.2. Diagram representing the putative teleost Ker1 gene organization predicted using the Tetraodon genome. Lines represent introns and non-coding genomic sequence whereas boxes represent exons. The grey area in exon I and VIII represent, respectively, the 5' and 3'UTR. The white area represents the N-terminal head region and left facing bars areas represent Coil 1A domain while right facing bars represent Coil1B domain. Vertical bar area represent the linker region between Coil 1 and Coil 2 domains, with the black colored areas represent the latter domain. White area with black dots represent the tail domain. 57

Figure 2.3. Northern blot analysis of hhKer1 expression during halibut metamorphosis from larvae (Stage 5, Stg5; Stage 6, Stg6), beginning of metamorphosis (Stage 7, Stg7), early climax (Stage 8, Stg8), climax (Stage 9, Stg9) to fully metamorphosed juveniles (Stage 10, Stg10) and adult skin (AdSkin). (A) Northern blot probed with 32P-dCTP labelled 3'UTR of hhKer1 cDNA. (B) Ethidium bromide stained gel loaded with 3µg of total RNA per metamorphic stage. 58

Figure 2.4. (A) RT-PCR analysis of expression of hhKer1 during halibut metamorphosis, and in adult halibut skin. The expression of 18s rRNA is also shown and used as an internal reference. (B) hhKer1:18s rRNA expression ratio during halibut metamorphosis, and in adult skin. C- control (no template). (C) Whole body T4 levels (ng T4/mg animal) during halibut metamorphosis. In Figure 2.4C "a" denotes no significant statistical differences observed (HSM, $p>0.05$) in T4 levels between stages with the same letter; "b" denotes significant statistical differences between stage 9 (HSM, $p<0.001$) T4 levels and all the other stages; and "c" denotes statistical significant differences between T4 levels of juveniles after metamorphosis (Stg10) and all other previous stages (Stage 5 to 8, HSM, $p<0.001$; stage 9, HSM, $p=0.003$). 60

Figure 2.5. Masson trichrome staining (A-F) and detection of keratin filaments by fluorescence microscopy (A'-F') in halibut skin during development. EC, epithelial cells; LB, larval basal cells; DE, dermal endothelial cells; LSB, larval supra-basal cells; ASB, adult supra-basal cells; AB, adult basal cells; *, mucus cells; arrowheads in E,F indicate fibroblast-like cells in the collagen lamella; arrow in F denotes melanocyte; arrowheads in A'-E', indicate fluorescent keratin in basal cells and supra-basal cells; cl, collagen lamella. Note the fluorescent background on muscle fibers underlining the dermis. Scale bar = 10µm. 63

Figure 2.6. In situ hybridisation expression of hhKer1 (A-F) and saColl1a1 (A'-F') in halibut skin during development. hhKer1 transcript is present in the larval basal cells and larval supra-basal cells before metamorphosis (A-D) disappearing at the metamorphic climax (E-F). Col 1a1 is expressed in larval basal cells until the metamorphic climax (A'-E') and in dermal endothelial cells in all the stages observed 65

(arrowheads A'-F'), some expression is also detected in the fibroblasts present in the dermis (arrow in E'- F'). LSB, larval supra-basal cell; LB, larval basal cell; Scale bar = 10µm.

Figure 2.7. Schematic representation of the ontogeny of halibut basal epidermal cells. Pre-metamorphic larval basal epidermal cells are oval and contain keratin bundles and express hhKer1 and Colla1. Adult basal epidermal cells are cuboid and lack all the preceding markers. 70

Figure 3.1. Clustal X multiple alignment of predicted protein sequences from halibut fTnThh cDNA isoforms, AfTnThh and sTnT2hh cDNAs. Shaded areas represent sequence similarity. The N-terminal hypervariable region and Tropomyosin- and Troponin I-binding regions are indicated. 87

Figure 3.2. Genomic organization of *Tetraodon* fTnTtn (A), AfTnTtn (B) and sTnT2tn (C). Open rectangles represent untranslated regions, while shading represents coding exons. The striped rectangles represent alternatively spliced exons. The arrowheads pointing upwards depict the ATG translational start codon. The three *Tetraodon* TnT genes have a very similar genomic organizations with exon I containing the start of the 5'UTR, the ATG start site is located in exon II and the last exon codes for the last C-terminal amino acids as well as the entire 3'UTR. In the fTnT gene exons IV and V are alternatively spliced both in *Tetraodon* and halibut. In the AfTnT gene exon VI is alternatively spliced in *Tetraodon* but seems to be constitutive in halibut (see Discussion). 90

Figure 3.3. (A) Northern blot analysis of the expression of halibut fTnThh, AfTnThh and sTnT2hh genes in adult white muscle (W), red muscle (R), heart (H) and liver (L). All images represent 48 hour exposures. Ethidium bromide gel image is shown to give an indication of the quantity of total RNA loaded per sample. (B) RT-PCR analysis of expression of fTnThh, AfTnThh and sTnT2hh in halibut adult white (WM) and red (RM) muscle and heart (H). The 18s rRNA is shown and was used for normalisation. The graphs on the right of the fTnThh and AfTnThh gels represent, respectively, expression of the different fTnThh or AfTnThh isoforms relative to 18s rRNA. 92

Figure 3.4. Maximum parsimony phylogenetic tree using the predicted protein sequence of the different halibut TnT cDNA isolated and that of other vertebrates (table 3.1) retrieved from Genebank and the Medaka EST database (see Materials and Methods). The bar in the bottom left-hand corner represents 10% sequence divergence. The abbreviations are described in Table 3.1. 93

Figure 3.5. Expression of fTnThh gene during halibut metamorphosis. Ethidium bromide gel image of RT-PCR amplified fTnThh and 18s rRNA (A). White arrowheads indicate different fTnThh isoforms. Graphs represent fTnThh expression relative to 18s rRNA (B) and the ratio between the different fTnThh isoforms (C). C- indicates the no-template control. 95

Figure 3.6. Expression of AfTnThh gene during halibut metamorphosis. Ethidium bromide gel image of AfTnThh and 18s rRNA (A). C- represents none-template control. White arrowheads indicate the different AfTnThh isoforms found. Graphs present the expression of the different AfTnThh isoforms found relative to 18s rRNA (B) and the 96

ratio between the different AfTnThh isoforms (C). The predicted protein sequence of the amplified halibut AfTnThh isoforms is given (D). The largest product, AfTnThh-1 (439 bp) is identical to the AfTnThh cDNA isolated by library screening and includes all alternatively spliced exons; AfTnThh-2 (412 bp; DQ680177) lacks exons IV and VII but exon V is maintained; AfTnThh-3 (301 bp; DQ680178) is composed of exon IV and VII but exon V is spliced out; and in AfTnThh-4 (283 bp; DQ680179) only exon IV is spliced in and all other alternatively spliced exons (exons V and VII) are spliced out. All the halibut AfTnThh isoforms detected contain exon VI and neither the isoform expression pattern nor the ratio between these AfTnThh isoforms is altered during metamorphosis.

Figure 3.7. Ethidium bromide gel image of sTnT2hh and 18s rRNA expression during halibut metamorphosis (A). Graphs present the relative expression of sTnThh2 after normalisation with 18s rRNA during halibut metamorphosis (B). C- represents non-template control. 97

Figure 3.8. Schematic representation of the muscle ontogeny in halibut from larvae (stage 5) to juvenile (stage 10) and the overall expression pattern of TnT. There is a general increase in myotome number and volume during development with new myotomes originating from the most dorsal and ventral regions. Note that throughout muscle ontogeny, prior to and after metamorphosis, bilateral symmetry is maintained in a sagittal plane. In pre-metamorphic stage 5 halibut efTnThh (dots) is most highly expressed in the most apical and lateral sides of the myotomes, regions which are associated with the larval white muscle hyperplastic growth regions. As white muscle fibers increase in size the expression of efTnThh isoforms disappears with the exception of scattered satellite cells. When the animals reach the beginning of metamorphic climax (Stage 8) all mature white muscle fibers express the fTnThh-1 and -2 isoforms (light shading). At climax (stage 9) and in juvenile (stage 10) white muscle fTnThh-1 and -2 isoforms are expressed with varying intensity (dots in juvenile myotome - regions with higher expression). In pre-metamorphic halibut red muscle all cells express sTnT2hh and AfTnThh (red area). The expression of the red muscle specific Troponin T genes is constant and restricted to the outer red muscle throughout halibut metamorphosis and in juvenile animals. 99

Figure 3.9. *In situ hybridization* showing the expression of halibut embryonic/larval fTnT (A-D), 3'UTR-fTnT probe (E-H), AfTnT (I-L) and sTnT2 (M-P) in transverse sections of halibut larvae. Pre-metamorphic stage 5 larvae: A, E, I, M; pre-metamorphic stage 6 larvae: B, F, J and N; larvae at the beginning of climax (stage 8): C, G, K and O; larvae at metamorphic climax: D; post-metamorphic juveniles: H, L and P. In C arrowheads depict efTnT expression in putative myogenic satellite cells. Hybridized probe is evident as a purple/brown colouration in the sections. Scale bars, 50 µm. 101

Figure 3.10. Thyroid hormones profile during halibut metamorphosis. a – denotes no significant differences in T3 levels between stages. b – denotes no significant difference in T4 and T3 levels between stages. c – denotes significant differences in T4 levels with stage 9 and 10. d – denotes significant statistical differences in T4 levels with stages 7, 9 and 10. e – denotes significant statistical differences in T4 levels with stages 5, 9 and 10. 102

Figure 4.1. Halibut D1 (A) and D3 (B) cDNA sequences and predicted protein sequences. The double underline in (A) represents the TGA Sec insertion codon. In (A) and (B) the single underline represent the putative polyadenylation signal, the sequences in bold the SECISearch predicted SECIS element and the (*) denotes the termination codon. SECISearch predicted hhD1 (A') and hhD3 (B') SECIS element. The boxed region in (A') and (B') represent the SECIS core while the bold letters represent conserved SECIS nucleotides. Halibut D2 RT-PCR isolated nucleotide and predicted peptide sequences (C). The double underline in (C) represents the TGA Sec insertion codon and the boxed amino acids conserved vertebrate D2 amino acids. Red lines in (A) and (B) above sequences indicate hhD1 and hhD3 digoxigenin-labelled cRNA probes template sequence used for in situ hybridizations. In the case of hhD2 the entire DNA sequence isolated was used. 124

Figure 4.2. Maximum parsimony phylogenetic tree for halibut deiodinase protein sequence in relation to other vertebrate deiodinase protein sequences. The *H. roretzi* iodothyronine deiodinase was used as the outgroup. The bar represents 10% dissimilarity. 126

Figure 4.3. (A) Whole-body quantitative RT-PCR expression analysis of halibut D1, D2 and D3 during halibut metamorphosis normalised against 18s rRNA expression. * - denotes significant statistical differences between expression of hhD3 ($p < 0.05$). ¥ - denotes significant statistical difference between expression of D1 and D2 ($p < 0.05$). (B) Ratio of the expression of the different halibut deiodinases during halibut metamorphosis. (C) Thyroid hormones profile during halibut metamorphosis. a - denotes no significant differences in T3 levels between stages. b - denotes no significant difference in T4 and T3 levels between stages. c - denotes significant differences in T4 levels with stage 9 and 10. d - denotes significant statistical differences in T4 levels with stages 7, 9 and 10. e - denotes significant statistical differences with stages 5, 9 and 10. 130

Figure 4.4. *In situ* expression of hhD2 (A-E) and hhD3 (A'-E') in halibut skin during metamorphosis. Stage 5, A and A'; Stage 6 B and B'; Stage 8 C and C'; Stage 9 D and D' and; Stage 10 E and E'. Arrowheads in B, B', C, C', D and D' denote dermal endothelial cells while in E denote collagen bound fibroblast-like cells. Small arrows in C and C' denote the outermost epithelial cells of the epidermis. The bar represents 10µm. 133

Figure 4.5. *In situ* expression of hhD2 (A-H) and hhD3 (A'-H') in halibut white (A, A', C, C', E, E', G and G') and red (B, B', D, D', F, F', H and H') muscle during halibut metamorphosis. Stage 5, A, A', B and B'; Stage 8 C, C', D and D'; Stage 9 E, E', F and F' and; Stage 10 G, G', H and H'. Arrowheads in B and B' denote cells that are closely associated with mature white muscle fibres. Arrowheads in F denote cells associated with mature red muscle fibres. SRM- superficial red muscle cells; WF- white muscle fibre; RF - red muscle fibre. The bar represents 10µm. 135

Figure 4.6. Schematic representation of the ontogeny of halibut basal epidermal cells. Pre-metamorphic larval basal epidermal cells are oval and contain keratin bundles show expression of hhKer1 and Coll1α1 as well as low expression of hhD2 and hhD3. As metamorphic climax is reached T3 levels elevate and in larval basal epidermal cells hhD2 expression increases while hhD3 is no longer expressed. When halibut reaches the 142

post-metamorphic juvenile stage the adult basal epidermal cells have become cuboidal and no expressions of hhKer1, Col1_1 or keratin bundles are detected; hhD2 expression has ceased completely while hhD3 is now highly expressed. The coordinated pattern of expression between hhD2 and hhD3 seems to be involved in the change from a larval to an adult differentiation of epidermal basal cells during metamorphosis thus further implying the role of TH as one of the most important factors for differentiation and maintenance of larval and adult characters of halibut skin.

Figure 4.7. Schematic representation of the muscle ontogeny in the halibut during metamorphosis. Only one epaxial quadrant is shown for easy representation. In pre-metamorphic stage 5 halibut expression of efTnThh (dark blue) is co-localised with the expression of both hhD2 and hhD3 (green) specifically in the most apical and lateral sides of the myotomes which is associated with the larval white muscle hyperplasic growth regions. Moreover, the expression of efTnThh, hhD2 and hhD3 is localised in the small diameter fibers on those myotome regions as white muscle fibers increase in size expression of the three genes disappears. When the animals reach the beginning of metamorphic climax (Stage 8) all mature white muscle fibers express the fTnThh-1 and -2 isoforms (light blue area) while the apical and lateral hyperplasic muscle growth region are almost depleted and putative satellite cells start to intersperse the white muscle fibers. These satellite cells also co-express efTnThh, hhD2 and hhD3. With climax and in juvenile white muscle efTnThh is totally downregulated and only the other fTnThh isoforms are expressed (light blue area; the slightly darker blue dots in juvenile myotome represents regions where expression of fTnThh-1 and -2 isoforms is stronger) in white muscle but hhD2 and hhD3 continue to be expressed in the presumed muscle satellite cells. In pre-metamorphic halibut red muscle all cells express sTnT2hh and AfTnThh (red area) and no expression of hhD2 and hhD3 is detected. As development progresses and halibut larvae reach the beginning of climax hhD2 and hhD3 expression are observed in small cells across the red muscle. The expression of the red muscle specific Troponin T genes is constant throughout halibut metamorphosis and in juvenile animals. However, in the case of deiodinases at climax only hhD2 expression (yellow dots) is observed in red muscle and only in scattered oval cells. By juvenile stage no halibut deiodinase is expressed in halibut red muscle. These observations strongly suggest that different TH levels are important for different differentiation status of halibut white and red muscle from larvae to adult and further highlight the coordination between hhD2 and hhD3 in that process. Drawings are not in scale.

144

Figure 5.1. Nucleotide sequence and deduced protein sequence of the sea bream fTnT isoforms isolated. Putative isoform efTnTsb (A), isoform afTnTsb (B) and LfTnTsb (C) are shown. The ATG translation initiation codon is shown in bold as well as the TAG STOP codon, which is also represented by an asterisk (*). The Kozak consensus sequence is underlined and the double underline indicates the polyadenylation signal. (D) Clustal X (Thompson et al., 1997) multiple nucleotide sequence alignment of sea bream fTnT cDNAs. The position of Forward and Reverse primers used for RT-PCR expression analysis are indicated by arrows.

163

Figure 5.2. Multiple sequence alignment of the deduced amino acid sequence of sea bream sTnT1, sTnT2 and iTnT. Identical amino acids are denoted by a dot, gaps introduced to maximise similarity are indicated by hyphens.

167

Figure 5.3. Northern blot analysis of the distribution of sea bream *fTnT*, *sTnT1sb* and *sTnT2sb*. Total RNA from sea bream adult white muscle (1), adult red muscle (2), adult heart (3) and adult liver (4) was used for northern blotting and probed with ³²P-dCTP labelled 3'UTR of clone *sTnT1sb* and *sTnT2sb*. A single low abundance transcript of ~1260 nucleotides corresponding to *sTnT1* was restricted to adult sea bream red muscle. A highly abundant transcript of ~1000 nucleotides corresponding to *sTnT2sb* was detected in adult sea bream red muscle. A very abundant transcript of ~1000 nucleotides, corresponding to *fTnT*, is detected in the white muscle lane and, much less abundantly, in red muscle also. The ethidium bromide-stained northern gel is also shown (rRNA) to illustrate that similar amounts of RNA were loaded in each lane. 170

Figure 5.4. ClustalX (Thompson et al., 1997) multiple sequence alignment of the cDNA (A) and putative protein sequences (B) of *efTnTsb*, *afTnTsb* and *LfTnTsb* isoforms. Shaded areas correspond to identical residues. Accession numbers: *efTnTsb*, DQ473445; *afTnTsb*, DQ473443; *LfTnTsb*, DQ473444; *efTnTtn*, CR660426; *LfTnTtn*, CR658326; *aTnTtn*, CR658422; *fTnTmd-2*, BJ728074; *fTnTmd-1*, BJ729852; *fTnTss*, AAC24595; *fTnTgm*, AAM21701; *fTnTazf*, NP571640; *fTnTbzf-2*, BC065452; *fTnTbzf-1*, AF425741. 173

Figure 5.5. Phylogenetic analysis of vertebrate TnT genes derived from maximum parsimony using the sequence of *Caenorhabditis elegans* (TnT Ce, GenBank accession no. NP_509076.1) as the outgroup. The phylogenetic tree was constructed using 1000 bootstrap replicates (Fitch, 1971), bootstrap values are indicated as percentages. Species identification and accession numbers for sequences used in the analysis were as follows in Table 5.1. 176

Figure 5.6. Genomic organisation of the putative sea bream, *Fugu* and *Tetraodon* *fTnT* gene predicted after Spidey analysis using the sea bream *fTnT* isoform cDNA sequence isolated and the *Fugu* scaffold 1617. The same analysis was carried out using the sea bream *fTnT* isoforms isolated and *Tetraodon* scaffold SCAF7217, but including also the *Tetraodon* full-length cDNA clones CR660426, CR658422 and CR657382. The black boxed areas represent constitutive protein coding regions while the empty boxes represent untranslated regions. White blocks bearing black diagonal lines represent alternatively spliced untranslated exons, while black blocks bearing white diagonal lines represent protein coding alternatively spliced exons. Exon II contains the ATG initiation codon (arrowhead) and is composed of part of the 5'UTR and the start of the coding region. The sea bream, *Fugu* and *Tetraodon* *fTnT* locus has 14 exons from which exon I, and XIV represent untranslated exons. The exon numbers represented with an asterisk denote alternatively spliced exons. Exon V represents the larval specific exon. Flush junction boundaries in exons indicate that they start or end in intact codons; saw tooth boundaries indicate that the upstream exon donates one nt to the codon while the other two are contributed by the downstream exon; concave/convex exon boundaries indicate that codon splitage takes place by the upstream exon donating two nt while the downstream exon contributes with one. The *efTnTsb* isoform results from the incorporation of all exons except exon I. The *afTnTsb* isoform results from splicing of exons I-IV and VI-XIV while in the *LfTnTsb* isoform exons I-III and VI-XIV are spliced. Both, *afTnTsb* and *LfTnTsb*, have an extra 5'UTR exon, exon I, which is absent from the *efTnTsb*. Sequence conservation between this region (exon I) of the presumed adult sea bream *fTnT* cDNAs and the genomic sequence of *Tetraodon* was higher than 88%. 178

Figure 5.7. (A) Putative genomic organisation of the *Fugu sTnT2* gene predicted by Spidey analysis using *sTnT2sb* cDNA sequence isolated and *Fugu* scaffold 1711. Exons are represented by shaded rectangles, nontranslated exonic sequence is indicated by open rectangles. The putative exons are indicated in roman numerals. Exon I contains the ATG initiation codon (arrow head) as well as part of the 5'UTR (white box area of exon 1). The predicted gene is composed of 12 exons. Exon 12 contains the 3'UTR of the *sTnT2sb* gene. (B) Representation of the sea bream sTnT2 protein sequence showing protein regions encoded by the putative exons. 180

Figure 5.8. Developmental expression of sea bream *fTnT* isoforms and *18s* ribosomal RNA (*18s* rRNA) assessed by RT-PCR, reaction products fractionated on a 2.5% agarose gel (A). Embryos from 12, 18 and 36hpf, larvae from 1 to 75 dph and juveniles of 89 dph were analysed. Adult white (WM) and red (RM) muscle, heart (H) and liver (L) were also analysed. A no template, negative control was used (C-). Three bands are detected which are products of the sea bream *fTnTsb* gene. B1, B2 and B3 represent respectively, *efTnTsb*, *afTnTsb* and *LfTnTsb*. Graphic (B) represents the average of expression of each *fTnT* isoform in relation to *18s* rRNA of three samples. Error bars represent standard error. Graphic (C) depicts the ratio between the different sea bream *fTnT* isoforms. 182

Figure 5.9. (A) RT-PCR analysis of the expression of *sTnT1sb*, *sTnT2sb* and *iTnTsb* during sea bream embryonic (12 hpf until 36 hpf), larval (1 dph until 46 dph) and juvenile development (64 dph until 89 dph), and in adult white muscle (WM), red muscle (RM), heart (H) and liver (L). (B-D) Graphical representation, indicated as relative units, of the expression of *sTnT1sb* band 1 and band 2 (B), *sTnT2sb* (C) and *iTnTsb* (D), normalised with respect to expression *18S* rRNA. Results are the mean + standard error of 3 independent samples per developmental time analysed. (E) The two *sTnT1sb* RT-PCR products of 332 bp (band 1) and 353 bp (band 2) respectively, were sequenced to establish their identity. A ClustalX alignment of the two *sTnT1sb* putative protein sequences is shown. Identical amino acids are denoted by a dot, gaps introduced to maximise similarity are indicated by hyphens. 184

Figure 5.10. Expression of sea bream *fTnT* gene isoforms *afTnTsb* (higher molecular weight), *LfTnTsb* (lower molecular weight) and *18s* rRNA assessed by RT-PCR after 7 (64 dph), 18 (75dph) and 31 days (89 dph) treatment with T3, methimazol and control animals. Reaction products fractionated on a 2.5% agarose gel (A) and respective graphical representation of relative expression of isoform *afTnTsb* (B) and *LfTnTsb* (C) against *18s*. In (D) the ratio *afTnTsb*:*LfTnTsb* is presented. The *efTnTsb* isoform is not represented graphically since no expression is detected in any treatment at any sampling point. In the graphs "a" represents significant statistical differences between all treatments; "b" represents significant statistical differences between control and T3-treated group, but no differences when the methimazol-treated group is compared either with the control or T3-treated animals; "c" represents no significant statistical differences are found between control and T3-treated animals but methimazol is significantly different. 186

Figure 5.11. Expression of sea bream *sTnT2*, *iTnT* genes and *18s* rRNA determined by RT-PCR after 7 (64 dph), 18 (75 dph) and 31 (89 dph) days of treatment with T3, methimazol or in control animals. Reaction products fractionated on a 2.5% agarose gel 187

(A) and respective graphical representation of the relative *sTnT2sb* expression in relation to *18s* rRNA (B). The *iTnTsb* gene is not represented graphically since no expression is detected in any treatment group at any sampling time. No significant statistical differences are found in *sTnT2sb* expression between any of the treatments at any sampling time.

Figure 5.12. Expression of sea bream *sTnT1sb* gene isoforms *sTnT1sb-1* (lower molecular weight), *sTnT1sb-2* (higher molecular weight) and *18s* rRNA determined by RT-PCR after 7 (64 dph), 18 (75 dph) and 31 (89 dph) days of treatment with T3 and methimazol or in control animals. Reaction products fractionated on a 2.5% agarose gel (A) and respective graphical representation of relative expression of isoform *sTnT1sb-1* (B) and *sTnT1sb-2* (C) against *18s* rRNA. In (D) the ratio *sTnT1sb-1*:*sTnT1sb-2* is represented. In graphs “a” represents significant statistical differences between control and the other treatments but no differences between T3 and methimazol; “b” represents significant statistical differences between control and methimazol-treated group, but no differences between the T3-treated group and the control or methimazol-treated animals. 189

Figure 5.13. Sea bream whole body thyroid hormone levels, (A) T4 and (B) T3 levels in sea bream treated with T3, methimazol or in control animals (n=5 per sampling time and treatment). Levels are measured after 7 (64 dph), 18 (75 dph) and 31 (89 dph) days of treatment. “a” – denotes a statistical significant difference (HSD, p<0.001) between T3 and the other two experimental groups. 191

Figure 5.14. (A) Follicle number per slide at the level of the vomer bone (n=3 animals per treatment) in T3, methimazol and control sea bream after 7 (64 dph), 18 (75 dph) and 31 (89 dph) days of treatment. (B) Thyrocyte cell height measured in order to determine thyroid activity. “a” – denotes statistical significant differences between the T3 treated and the other two experimental groups; “b” – denotes significant statistical differences between the three experimental groups and; “c” - denotes significant statistical differences between methimazol and the other two treatment groups. (C) Thyroid follicles in control and treated animals at each sampling point. The scale bar represents 100 µm. Black asterisk denotes a thyroid follicle. 193

Figure 6.1. Nucleotide sequence and deduced protein sequence of sea bream deiodinases cDNAs saD1 (A) and saD3 (B). The double underline elicits the Sec (U) insertion codon TGA while (*) denotes the termination codon. In (B) the underlined denotes the putative poly(A) signal. The SECIS element of saD1 (A) and saD3 (B) is in depicted in bold. The SECISearch predicted SECIS element hairpin is shown for saD1 (A') and saD3 (B'). In both (A) and (B) the SECIS core is boxed and the conserved adenosines as well as the conserved SECIS core nucleotides are in bold. In (C) is represented the RT-PCR isolated saD2 nucleotide sequence and the predicted peptide sequence. The TGA Sec (U) insertion codon is double undelined. The boxed aa's represent highly conserved residues. 220

Figure 6.2. Maximum parsimony phylogenetic tree for halibut deiodinase protein sequence in relation to other vertebrate deiodinase protein sequences. The *H. roretzi* iodothyronine deiodinase was used as the outgroup. The bar represents 10% dissimilarity. 222

Figure 6.3. Semi quantitative RT-PCR expression of saD1 (A), saD2 (B) and saD3 (C) in sea bream embryonic, larval and juvenile stages. Ethidium bromide agarose gel and graphic representation of sea bream deiodinase genes normalised with 18s rRNA expression. 225

Figure 6.4. Taqman quantitative real-time RT-PCR expression of saTR α and saTR β in sea bream embryonic, larval and juvenile stages (A). The (*) denotes significant statistical differences between expression of saTR α and saTR β . Representation of the expression ratio saTR α :saTR β in sea bream embryos, larvae and juveniles (B). 228

Figure 6.5. Expression of sea bream deiodinase genes and 18s rRNA assessed by semi-quantitative RT-PCR after 7 (64dph), 18 (75dph) and 31 days (89dph) treatment with T3, methimazol and control animals. Reaction products fractionated on a agarose gel and respective graphical representation of relative expression saD1 (A), saD2 (B) and saD3 (C) against 18s. In the graphs “a” represents significant statistical differences between the control and the other experimental groups (HSD, $p < 0.05$); “b” represents significant statistical differences between methimazol and the other two experimental groups (HSD, $p < 0.05$); “c” represents significant statistical differences between all experimental groups (HSD, $p < 0.05$); “d” denotes statistical significant differences between the control and methimazol groups (HSD, $p < 0.05$). 231

Figure 6.6. Graphic representation of expression of sea bream saTR α (A) and saTR β (B) genes normalised with 18s rRNA assessed by Taqman quantitative real-time RT-PCR after 7 (64dph), 18 (75dph) and 31 days (89dph) treatment with T3, methimazol and control animals. In graphs (A) and (B) “a” represents significant statistical differences between methimazol and the other two experimental groups and; “d” denotes statistical significant differences between the T3 group and the other two experimental groups. Graphic representation of the expression ratio saTR α :saTR β (C). 233

List of tables

Table 2.1. Exon size of epidermal type I keratin from the putative teleost <i>Ker1</i> , <i>X. laevis XK81</i> (Miyatani et al. 1986), <i>H. sapiens Ker12</i> (Nishida et al. 1997) and <i>Ker17</i> (Trojanovsky et al. 1992) genes.	68
Table 3.1. Vertebrate TnT sequences used in phylogenetic analysis	78
Table 3.2. Restriction enzymes used to produce 3'UTR probes for northern blot hybridization.	80
Table 3.3. Primer sequence and concentration used for RT-PCR analysis of fTnThh, AfTnThh and sTnT2hh during halibut metamorphosis.	82
Table 4.1. Quantitative RT-PCR primers and Taqman probes sequences and respective concentration used to analyse halibut D1, D2 and D3 expression normalised with 18s rRNA expression. The PCR efficiencies are also given.	118
Table 5.1. Vertebrate TnT sequences used in phylogenetic analysis.	154
Table 5.2. Protein sequence identity matrix after ClustalX (Thompson et al., 1997) multiple alignment. Sea bream sequences are shown in light grey.	166
Table 5.3. Amino acid identity matrix derived after ClustalX (Thompson et al., 1997) multiple alignment. Sea bream results are shown in light grey.	169
Table 6.1. Sea bream deiodinase primers sequences used for developmental analysis of expression	215
Table 6.2. Quantitative RT-PCR primers and Taqman probes sequences and respective concentration used to analyse sea bream TR α and TR β expression and respective PCR efficiencies.	217

Abbreviations

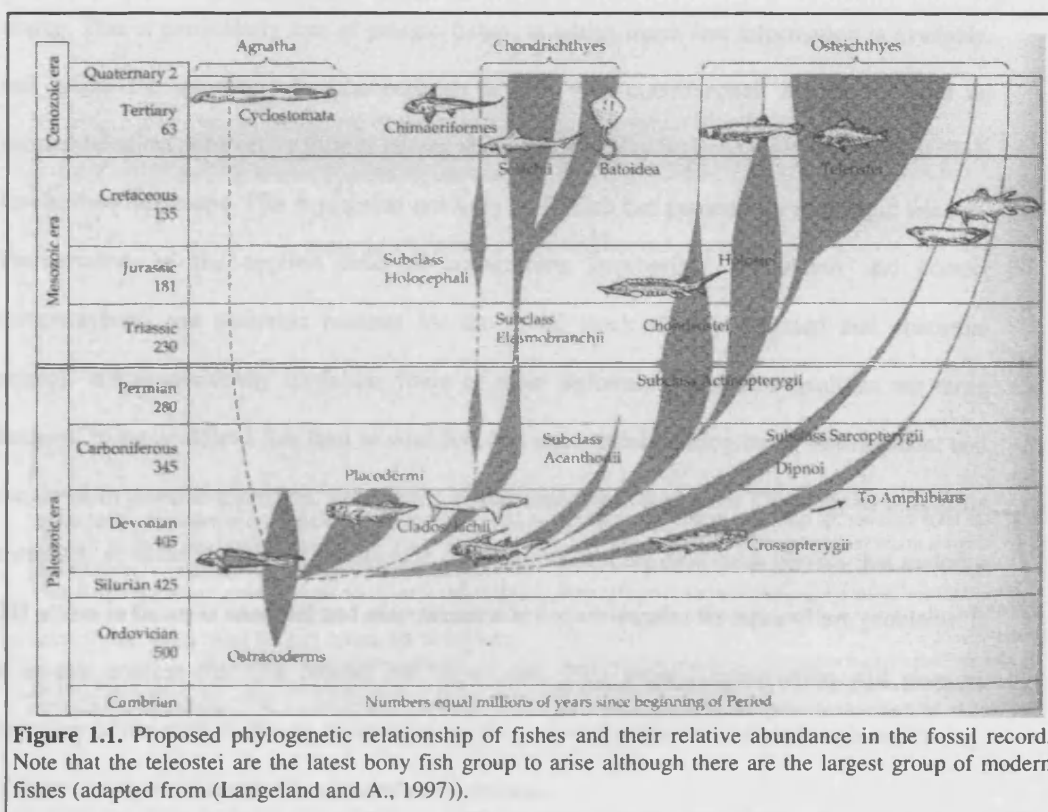
μg	micrograms
μl	microliter
μM	micromolar
aa	amino acid
AfTnT	Atypical fast TnT
APES	aminopropyltriethoxysilane
BCIP	5-bromo-4-chloro-indolylphosphate
bFGF	Basic Fibroblast Growth Factor
bp	base pairs
cAMP	cyclic adenosine monophosphate
cDNA	complementary DNA
cTnT	cardiac TnT
D1	iodothyronine deiodinase 1
D2	iodothyronine deiodinase 2
D3	iodothyronine deiodinase 3
DEPC	Diethyl pyrocarbonate
DIT	Diiido tyrosine
DNA	Deoxyribonucleic acid
dNTP	deoxynucleotide triphosphates
Dpf	days post-fertilization
Dph	days post-hatch
DTT	DL-Dithiothreitol
EDTA	Ethylenediamine tetra acetic acid
fTnT	fast muscle TnT
Hpf	hours post-fertilization
IPTG	Isopropyl-beta-D-thiogalactoside
IRD	Inner Ring Deiodination
ISH	In situ hybridization
iTnT	intronless TnT
kb	kilobase
kDa	kilodaltons
Ker1	epidermal keratin 1
mg	milligrams
MIT	Monoiodo tyrosine
MHC	Myosin heavy chain
ml	millilitres
MLC	Myosin light chain
mRNA	messenger RNA
NBT	Nitroblu tetrazolium chloride
NCoA	Nuclear receptor co-activator
NCoR	Nuclear receptor co-repressor
NIS	Sodium Iodine Symporter
nt	nucleotide
ORD	Outer Ring Deiodination
PCR	polymerase chain reaction
PEG	Polyethylene Glycol
Pfu	plaque forming units
qPCR	quantitative PCR
RER	Rough Endoplasmatic Reticulum
RIA	Radioimmunoassay
RNA	Ribonucleic acid
rRNA	ribosomal RNA

RT	reverse transcriptase
SECIS	Selenocysteine-insertion sequence
SDS	Sodium dodecyl sulphate
SSC	saline sodium citrate buffer
sTnT	slow muscle TnT
TBE	Tris-Borate-EDTA buffer
Tg	Thyroglobulin
TH	Thyroid hormones
Tm	Tropomyosin
TnC	Troponin C
TnI	Troponin I
TnT	Troponin T
TPA	12- <i>O</i> -tetradecanoyl phorbol 13-acetate
TPO	Thyropoxidase
TR	Thyroid hormone receptor
TSH	Thyroid Releasing Hormone, Thyrotrophin
UTR	Untranslated region
X-gal	5-Bromo-4-Chloro-3-indoxyl-beta-D-galactopyranoside

CHAPTER 1

GENERAL INTRODUCTION

The present thesis will focus on the thyroid hormone (TH) axis in fishes and in particular the most successful group of vertebrates, the teleosts, of which there are over 25,000 living species. The living fishes do not constitute a natural phyletic group, rather they are composed of three different classes (Fig. 1.1) jawless fish (Agnatha), the cartilaginous fish (Chondrichthyes), and the bony fish (Osteichthyes). The bony fish is in turn composed by the Sarcopterygii subclass, that gave rise to land vertebrates, and by the Actinopterygii subclass, constituted in its majority by the teleostei that comprised about 24,000 species. The divergence of Actinopterygii fish from the Sarcopterygii fish, ancestor of all land vertebrates, is thought to occur at about 405 million years ago in the Devonian period.



Teleostei is the most diversified vertebrate group and is currently composed of 23,500 species (corresponding about 96% of all fish species) organised in 38 orders, 426 families and 4064 genera (Nelson, 1994). They first evolved around 200 million years ago and present a wide range variation from morphology to behaviour, ecology and physiology (Miya et al.,

2003). The model species studied in this thesis are the Atlantic halibut (*Hippoglossus hippoglossus*) and the gilthead sea bream (*Sparus auratus*) which belong to the pleuronectiforms and perciformes respectively.

Current evidence suggests that in common with flatfish, pelagic fishes undergo a transition from larvae to juvenile that is homologous to anuran metamorphosis and is dependent on the thyroid axis. In fish information concerning the developmental relationships of the different elements of the thyroid axis, namely deiodinases and thyroid hormone receptors (TRs), that act cooperatively to bring about the thyroid hormones-mediated action, is very scarce. This is particularly true of pelagic fishes, in which much less information is available, and where the question of metamorphosis is still very controversial. Moreover, from an endocrinological perspective little is known about the interplay between thyroid hormones (TH) levels, deiodinase and TRs expression not only in flatfish but particularly in pelagic teleosts. Furthermore, in the applied field of aquaculture, appropriate TH action and correct metamorphosis are desirable features for the brood stock since malformed and abnormal animals are economically unviable. Some of these deformities and abnormalities are more frequent in aquacultured fish than in wild fish and arise mainly during larval development and the larval to juvenile transition. This period is associated with a surge in TH levels as well as its receptors, so understanding the molecular mechanisms and the molecular players that underlie TH action in fishes is essential and may permit a better assessment for aquaculture problems. It is in this context that this project was developed. This general introduction will give an overview of the state-of-the-art about metamorphosis and the role of the thyroid axis and its key players during development in mammals and anurans.

The lack of biological and molecular tools with which to study metamorphosis in teleosts represents a significant barrier to progress. In particular how, why and if metamorphosis also occurs in pelagic teleosts has been largely unexplored. In the present thesis the possible inter-relationships of deiodinases, TRs and TH levels was investigated during metamorphosis of the

flatfish halibut but also in the symmetrical teleost sea bream with special emphasis being given to muscle and skin changes, namely possible changes in expression profiles of muscle and skin specific genes during this developmental time period in response to TH action. By determining the interplay of these factors in TH-driven halibut metamorphosis comparison was made to changes in homologous factors in the round teleost sea bream in order to determine by molecular criteria if the sea bream larvae to juvenile transition could be considered equivalent to the metamorphic TH-driven process of flatfish and, in an ultimate analysis, anurans.

1.1.1 The Atlantic Halibut (*Hippoglossus hippoglossus*)

The Atlantic Halibut belongs to the *Pleuronectidae* family (Fig. 1.2). It is present in the North Atlantic Ocean from the Bay of Biscay to the coast of Virginia in USA. As with all flatfishes, it has a benthic life style when adult. It predated mainly other fishes but also cephalopods and crustaceans. It reaches very significant sizes that can go to a maximum of 2.7 meters total length (www.fishbase.org, 2000) and its development to a mature adult can take as long as 4 years. In common with other flatfishes, halibut hatch as a pelagic larvae and develops through metamorphosis to a benthic fish.

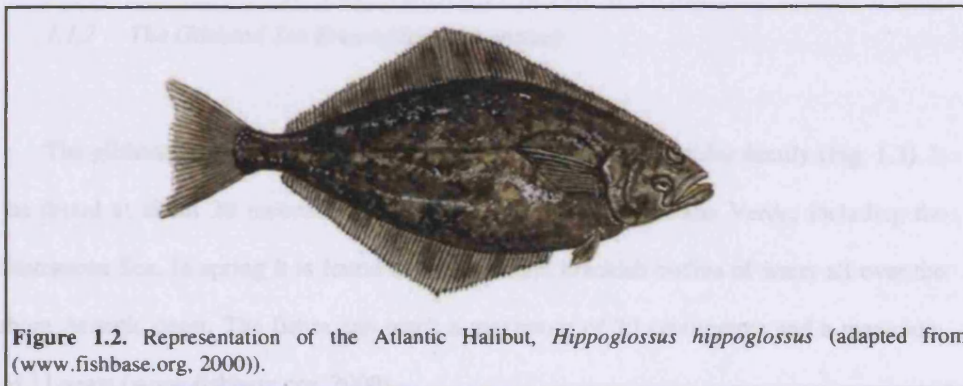


Figure 1.2. Representation of the Atlantic Halibut, *Hippoglossus hippoglossus* (adapted from (www.fishbase.org, 2000)).

The metamorphosis of halibut involves the migration of the left eye to the right side of the head and the conversion of the right side of the pelagic larvae into the dorsal side of the adult

fish. Inclusive the right side of the larvae becomes pigmented and several other biochemical modifications occur led through differential gene expression and endocrine pathways.

The species is now included in the IUCN (International Union for Conservation of Nature and Natural Resources) red list of endangered species and in Icelandic waters the capture has fallen from 1583 tons in 1994 to 497 tons in 2000. Since the species is considered to be of economic importance in northern European countries where halibut is starting to be extensively farmed (to try to overcome the fall in captures) it has become a very important species to study and several reports about its biology have been published (Helvik et al., 1991; Helvik and Walther, 1992; Naess et al., 1995; Helvik and Karlsen, 1996; Ronnestad et al., 1997; Shields et al., 1997; Harboe et al., 1998; Naess and Lie, 1998; Pittman et al., 1998; Ronnestad et al., 1998; Llewellyn et al., 1999; Shields et al., 1999; Hamre et al., 2001a; Hamre et al., 2001b; Hamre et al., 2002; Solbakken et al., 2002; Hamre et al., 2003a; Hamre et al., 2003b; Saele et al., 2003). Moreover, 30-90% of juveniles from hatcheries present deformities arising at metamorphosis which leads to a substantial decrease in their market value, thereby undermining the industry and stressing the need for a better understanding of the phenomenon of metamorphosis in halibut.

1.1.2 *The Gilthead Sea Bream (Sparus auratus)*

The gilthead Sea Bream (*Sparus auratus*) belongs to the *Sparidae* family (Fig. 1.3). It can be found at about 30 metres depth from the British Isles to Cabo Verde, including the Mediterranean Sea. In spring it is found in estuaries and brackish bodies of water all over the Southern Atlantic coast. The fishes can reach a maximum of 70 centimetres and a maximum age of 11 years (www.fishbase.org, 2000).

The sea bream has 48 chromosomes (Bejar et al., 1997) and like many other marine fishes develops from floating embryos that are part of the zooplankton. The embryos and larvae float in the Atlantic currents and soon after hatching they start feeding exogenously through predation. The larvae continue growing until 60 to 70 days, at which time it undergoes a transition from larvae to juvenile and at around 90 days fully developed juveniles arise. The juvenile presents new morphological features in relation to the larvae such as the extension of the snout to eye distance and fully developed pelvic and pectoral fins. However, although the larvae to juvenile transition in sea bream occurs in a life period homologous to metamorphosis of flatfishes and also anurans, the morphological changes are less dramatic.

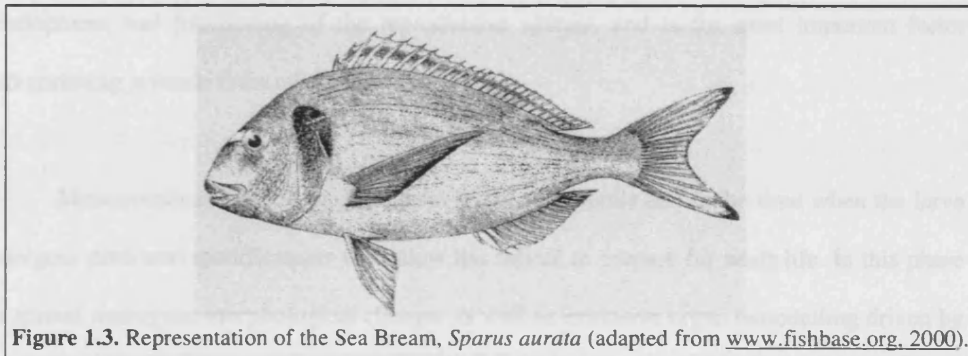


Figure 1.3. Representation of the Sea Bream, *Sparus aurata* (adapted from www.fishbase.org, 2000).

The easy rearing in artificial conditions of this teleost and its high market value, especially in Southern European countries, led to a huge increase in aquaculture with more than 40,000 tons being produced per year. Also due to the easy rearing and availability of sea bream in southern Europe, several marine research centres in Europe have drawn their attention to this euteleost where it is used as a physiological model of marine teleosts, with several genomic libraries available as well a microarray (Dr. Deborah Power, personal communication). Inclusive, it was the first fish species in which the hormone PTHrP (Flanagan et al., 2000) and transthyretin a thyroid transporting protein (Santos and Power, 1999) were cloned. Moreover, sea bream skeletal development is fully described (Faustino and Power, 1998; Faustino and Power, 1999; Faustino and Power, 2001) and an EU project to map the genome is underway.

1.2 Metamorphosis

Lower vertebrates undergo development through distinct phases normally described as embryo, larvae, juvenile and adult. The embryologic development of these animals normally occurs in a protected environment normally encapsulated by an impermeable membrane. The larvae stage starts immediately after hatching and is a transitory stage in which the animal harbours nutrients and gains weight and size to prepare the larvae for the transition to a juvenile. Fish in the juvenile stage although smaller and sexually immature, are already similar in form, behaviour and physiology to adults. The transition to adult is coincident with the full development and functioning of the reproductive system, and is the most important factor distinguishing juvenile from adult animals.

Metamorphosis is the transition from larvae to juvenile and is the time when the larva undergoes profound modifications that allow the animal to prepare for adult life. In this phase the animal undergoes morphological changes as well as extensive organ remodelling driven by specific hormones and extensive expression and repression of genes, as well as the occurrence of varied other molecular mechanisms that give rise to complex gene expression and functioning. This developmental event is very dramatic in urodeles (salamanders) and anurans (frogs and toads) and also in flatfish species. It is ultimately controlled by the thyroid hormones (THs): thyroxine (T4) and; triiodothyronine (T3). Metamorphosis in amphibians is absolutely dependent on THs and is blocked by thyroidectomy (Shi et al., 1986). Importantly, most vertebrates are unable to grow and reach their normal adult form without THs (Turner and Bagnara, 1976; Porterfield and Hendrich, 1993; Huang et al., 1999a; Hernandez et al., 2006). Some of the established actions of thyroid hormones are direct although they are often also required in a permissive role, assisting the action of other hormones (Hadley, 1992).

During metamorphosis in salamanders the external gills regress and lungs develop, at the same time the newt skin dies and gives rise to adult skin enabling the animal to pass from

an aquatic to a terrestrial lifestyle. In the Mexican axolotl, *Ambystoma mexicanum*, T4 treatment induced precocious early development of adult gills, and hind limbs develop digits and increase in size, muscle mass and bone diameter much faster than non-treated animals (Brown, 1997). In anurans metamorphosis is even more dramatic, with all the major tissues of the animal undergoing extensive remodelling. Regression of the tail (due to extensive cell death) is coordinated with limb morphogenesis in such way that the paddle like tail only fully regresses when the limbs are almost completely formed and functional. In *Xenopus laevis*, THs control cell autonomous apoptosis of the white muscle fibres of the tail (Chanoine and Hardy, 2003) and proteolytic enzymes, released by THs induce death of larval skin fibroblasts and digest the red muscle fibres (Schreiber and Brown, 2003). Further evidence of the coordinating action of THs, is the finding in the bullfrog that an epidermal collagenase is up-regulated at metamorphosis (Eisen and Gross, 1965). The same degree of synchronisation also occurs in other organ systems, with regression of the gills only being achieved when the lung and its accessory muscles have completely developed. The skin of the tadpole is replaced by a much more stratified adult skin appropriate to a terrestrial life. In skin, THs are responsible for the onset and control of all molecular and cellular events that mediate apoptosis of the larval skin and the replacement for the adult type (Miyatani et al., 1986; Mathisen and Miller, 1987; Mathisen and Miller, 1989; Nishikawa et al., 1990; Shimizu-Nishikawa and Miller, 1991; Nishikawa et al., 1992; Shimizu-Nishikawa and Miller, 1992; Kawai et al., 1994; Suzuki et al., 2001; Watanabe et al., 2001; Suzuki et al., 2002; Watanabe et al., 2002; Ishida et al., 2003; Schreiber and Brown, 2003). Metamorphosis also leads to physiological adaptation and in the aquatic medium tadpoles are ammonotelic but the adult toads and frogs are ureotelic, and in this way lose much less water in terrestrial environments (Dorit et al., 1991). Additionally, the intestine is shortened and the tadpole teeth are retracted during metamorphosis in preparation for its transition from herbivorous tadpole into carnivorous adult (Schreiber et al., 2005). Extensive remodelling occurs in the central nervous system with its most striking feature the migration of the eyes from a lateral to a central position and the development of binocular vision (Marsh-Armstrong et al., 1999). During this period new neurons arise and connect to

newly formed muscles and bones start to fully ossify from cartilaginous structures (Dorit et al., 1991). Even in anurans that show direct development (i.e. appear to bypass metamorphosis) TH action is needed before a fully developed froglet hatches. In the direct-developing *Eleutherodactylus coqui*, tri-iodothyronine (T3 – the most potent form of TH) is essential for the extensive remodelling of the abdominal musculature, tail regression and complete skin formation that occurs in the latter phases of embryogenesis (Callery and Elinson, 2000). *E. coqui* embryos treated with methimazole (a TH production inhibitor) were shown to recover almost complete development after treatment with exogenous T3 and although initial development of limb is not impaired by methimazole treatment, the final events of elongation of the limbs are dependent on TH (Callery and Elinson, 2000).

In fish, flatfish species present the most dramatic manifestation of metamorphosis. Morphologically this change is marked by the migration of one eye so that both eyes are on the upper side of the head, the alteration of the pigmentation on the upper side of the fish and the transition from pelagic larvae into a benthic adult. Also noteworthy, is the relationship between TH levels and metamorphosis in fish, and a correlation exists between TH levels and the larvae to juvenile transition in a well studied flatfish model, the Japanese flounder *Paralichthys olivaceus*, with TH levels highest at metamorphic climax (Miwa et al., 1988). Similarly it was reported that this surge in TH levels is correlated with stomach development in *P. olivaceus* and *Paralichthys dentatus* (Miwa et al., 1992). In these flatfish, the gastric gland starts developing in premetamorphosis although pepsinogen-like immunoreactivity is detected only after metamorphosis (Miwa et al., 1992), in common with observations in the frog *Rana catesbeiana*. Furthermore, TH treatment results in accelerated gut development and the presence of pepsinogen-like immunoreactivity, whereas thiourea delays stomach development and prevents any pepsinogen-like immunoreactivity in the organ (Miwa et al., 1992). Metamorphosis in flatfish is also accompanied with changes in isoform expression of several muscle genes and haemoglobins. Yamano et al. (1991, 1994) has shown that in *P. olivaceus*, metamorphosis was accompanied by isoform changes in muscle contractile proteins, namely in

Troponin T (TnT) and DTNB (5,5'-dithio-bis-nitrobenzoic acid) myosin light chain isoform expression. Troponin T and DTNB myosin light chains isoform expression was severely affected by thiourea, since fish treated with the chemical were unable to metamorphose and expression of adult characteristic isoforms was impaired (Yamano et al., 1994b). Moreover, TH treatment led to precocious metamorphosis and precocious expression of adult specific isoforms of TnT and DTNB light chains, thus emphasising the control of TH over isoform expression of muscle genes (Yamano et al., 1994b). In the haematopoietic system, pre-metamorphic larvae of *P. olivaceus* have large round erythrocytes, with small round nuclei; as the larvae enter metamorphosis this cell population is substituted by elliptical erythrocytes in such a way that at the end of metamorphosis the juveniles only possess adult type erythrocytes (Miwa and Inui, 1991). TH-treatment was able to induce this change as well as the usual morphologic changes that come with metamorphosis, thus suggesting that THs are able to suppress larval erythropoiesis and stimulate adult, definitive, erythropoiesis (Miwa and Inui, 1991). Although TH is recognised to be responsible for metamorphosis and the pelagic to benthic behaviour shift in flatfish, the nature of metamorphosis in pelagic fish, and the role THs, is much less understood. Notably, maternally derived THs are found in all fish eggs, and TRs are expressed from the early stages of embryonic development (Power et al., 2001). In zebrafish, Brown (1997) showed that THs are necessary for the larva to juvenile transition, whereas methimazole inhibited the transition from larva to juvenile. Interestingly, the effect of THs in zebrafish seem to be confined to the transition from larvae to juvenile, since treatment with methimazole (which would not, however, affect the action of maternal TH) did not affect embryonic and early larval development (Brown, 1997). However, it was shown that methimazole treated animals were unable to fully develop the paired fins, even though the unpaired fins develop normally, suggesting THs stimulated development of the paired fins, analogous to limb development in anurans (Brown, 1997). Again, in common with anurans, THs are responsible for lower jaw posterior migration, paired fin elongation and overall shape modification of the zebrafish larvae into the adult-shaped juvenile (Brown, 1997; Liu and Chan, 2002). THs are also responsible for morphological changes of the swim bladder, gastric gland,

trunk musculature, yolk sac and skin of metamorphosing zebrafish larvae (Liu and Chan, 2002). It was also reported in grouper (*Epinephelus coiodes*) that TH-treated larvae undergo metamorphosis faster than non-treated animals and methimazole-treated larvae were arrested in their larval development (de Jesus et al., 1998). However it was recently found that TH are also important in the transition from embryo to larvae in *D. rerio* and in common with *S. auratus* TR β receptor (Nowell et al., 2001) is already detected since mid-blastula transition further suggesting that TH might be important in early embryonic stages of teleosts (Liu et al., 2000). Nevertheless, the effect of TH in teleosts is still a open matter. It was found that high TH-content in *Morone saxatilis* enhanced embryonic developmental rates but the same effect was not found in salmonids (Leatherland, 1994).

1.2.1 Thyroid Hormones

Thyroid hormones are small hydrophobic molecules that are produced by thyroid follicles and circulate in the plasma bound to thyroid hormone-binding proteins that include albumin, transthyretin (TTR) and thyroxine-binding globulin (Schreiber and Richardson, 1997; Santos and Power, 1999). Thyroxine (T4) is the most abundant form of TH while triiodothyronine (T3) is the active form of the hormone (Fig. 1.4). Iodine comprises 65% and 58% of the molecular weight of T4 and T3 respectively, and is an indispensable component of both hormones.

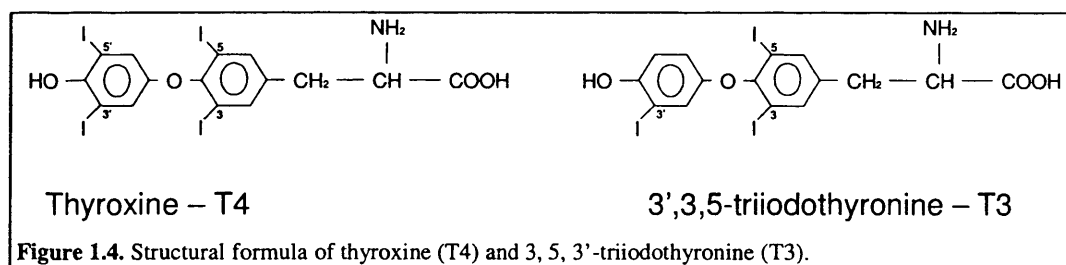
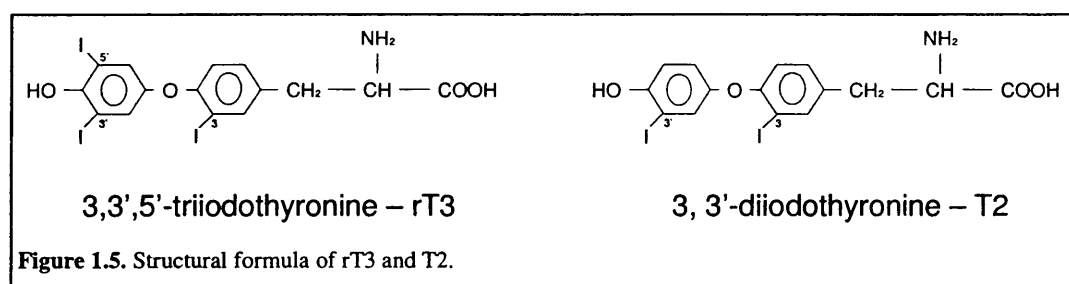


Figure 1.4. Structural formula of thyroxine (T4) and 3, 5, 3'-triiodothyronine (T3).

Thyroid hormones have been identified in the blood of representative species of either lower or higher vertebrates, from cyclostomes to man and are the only iodine-containing

compounds of physiological significance in vertebrates. The metabolites 3,3',5'-triiodothyronine (reverse-T3) and 3,5-diiodotyronin (T2) are other forms of thyroid hormones known (Fig. 1.5) but they have little activity and their physiological significance is still controversial (Kohrle, 2000). It has been reported that rT3 may have a direct action on plasma membrane proteins and T2 has a direct effect on the activation of the respiratory chain in mitochondria since a T2 binding site was identified in a subunit of cytochrome-c-oxidase (Wrutniak-Cabello et al., 2001).



1.2.1.1 Thyroid Hormones Production

The production of THs in vertebrates occurs in the thyrocytes, which are organised in follicles. In higher vertebrates these follicles are organised into the thyroid gland and in fish and other lower vertebrates the thyroid follicles are scattered throughout the pharynx (Dorit et al., 1991; Eales and Brown, 1993; Leatherland, 1994; Fagman et al., 2006). In the thyroid, iodine is taken up through a specialised sodium/iodine symporter (NIS) that is present in the thyrocyte basal membrane (Dai et al., 1996). Thyroglobulin is the most abundant protein in the thyroid gland and it is the major deposit of iodine in the thyroid. In humans, Tg is encoded by a 200 kb gene located on chromosome 8, comprising 48 exons that translate a 2750 residue peptide (Mendive et al., 2001). Mature hormone-containing Tg is located in the follicular lumen and constitutes the majority of the follicular colloid. To achieve this state, the immature Tg produced in the rough endoplasmic reticulum (RER) starts undergoing complex glycosylation that continues in the Golgi complex and where two Tg molecules combine to the final dimer form (Kim and Arvan, 1991; Kim et al., 1992; Kim and Arvan, 1995; Muresan and Arvan,

1997; Muresan and Arvan, 1998; Martin-Belmonte et al., 2000). Iodine is incorporated into Tg in the form of monoiodotyrosine (MIT) and diiodotyrosine (DIT) when the immature Tg arrives to the apical membrane in exocytotic vesicles from the Golgi. This process involves the oxidation of the iodide by thyroperoxidase (TPO) in the presence of H₂O₂ and the transfer of the oxidated iodide to the tyrosine group of Tg forming either MIT or DIT. The TPO is specifically expressed in the thyrocyte and two different cDNA's have been isolated in humans. Both enzymes possess a heme prosthetic group that is essential for enzyme activity (Ohtaki et al., 1982b; Ohtaki et al., 1982a). The H₂O₂ is generated in the apical membrane by a NADPH oxidase which requires Ca²⁺ (Corvilain et al., 1991; Bjorkman and Ekholm, 1992; Raspe and Dumont, 1995; Carvalho et al., 1996). Not all residues in Tg are iodinated and the molecules do not have more than 1% iodine. The subsequent step, hormone formation takes place in the apical microvilli of the thyrocyte. As iodination terminates the still immature Tg folds in such a way that certain MIT and/or DIT residues face each other (Fig. 1.6A). An oxidation process, involving TPO and H₂O₂ (Lamas et al., 1974; Cahmann et al., 1977; Deme et al., 1978; Virion et al., 1981; Virion et al., 1985) occurs which joins the opposing iodotyrosines and forms T₃, when a DIT couples to a MIT, or T₄, when two DIT couple together (Fig. 1.6B)(Gavaret et al., 1980; Gavaret et al., 1981). THs have to be released from mature Tg and liberated to the blood stream and this occurs in endosomes and lysosomes where digestive enzyme break it down (Ercson, 1981; Marino and McCluskey, 2000). In these digestive cellular compartments a series of sequential proteolytic enzymes free T₄ and T₃ (Rousset et al., 1990). These THs migrate towards the basal membrane and enter the circulation through an as yet unknown mechanism (Tietze et al., 1989; Andersson et al., 1990). In mammals, the thyroid secretes around 5 times more T₄ than T₃ (Dunn and Dunn, 2000).

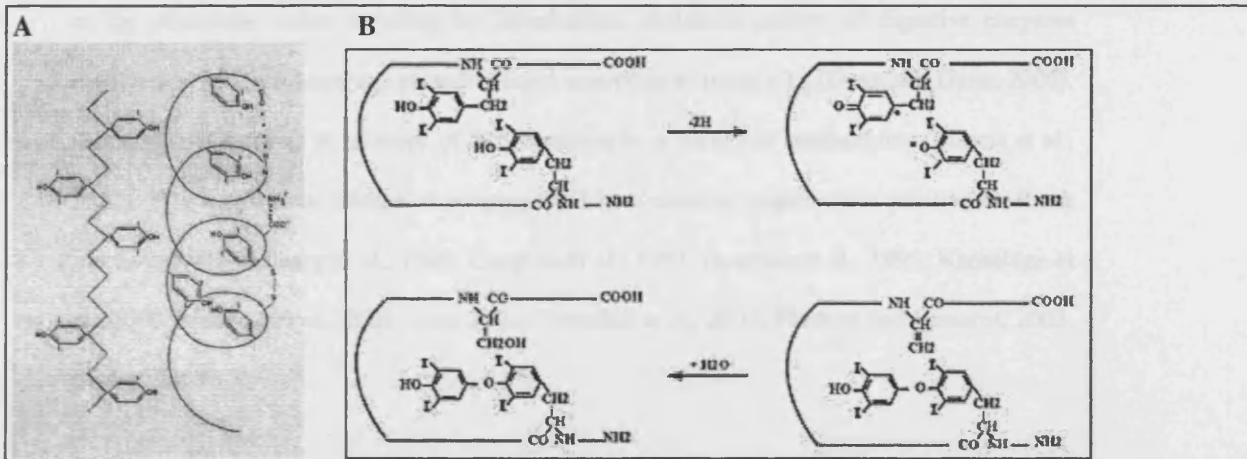


Figure 1.6. (A) Conformational changes of Tg necessary to permit the correct positioning of MIT and DIT residues for TH formation (www.thyroidmanager.org, 2003). (B) Proposed coupling reaction of iodotyrosines in Tg. The free radicals could combine to generate the iodothyronine residue (at the tyrosine acceptor site) and a dehydroalanine residue (at the tyrosine donor site), which in the presence of H₂O converts into a serine (Adapted from (Gavaret et al., 1980; Gavaret et al., 1981)).

1.2.1.2 Regulation of Thyroid Hormones Production

This hormone production process is controlled by the pituitary-thyroid axis and ultimately by available iodine levels and pituitary derived thyrotropin (TSH) (Dumont, 1971; Chambard et al., 1990; Bernier-Valentin et al., 1991; Nilsson et al., 1992; Deshpande and Venkatesh, 1999; Marino and McCluskey, 2000). Thyrotropin is involved in almost all steps of hormone production and release and acts through a G protein-coupled receptor, the TSH receptor (TSHR) that transmits and amplifies the signal via cAMP (Davies et al., 2002; Dremier et al., 2002; Szkudlinski et al., 2002; Chistiakov, 2003; Vassart et al., 2004). The presence of TSH in culture medium is necessary to maintain the differentiation status of thyrocytes *in vitro* and prolonged deprivation of the hormone leads to downregulation of thyroid-specific gene markers (Mascia *et al.*, 2002). Thyrotropin stimulates the expression and production of NIS (Saito et al., 1997; Lazar et al., 1999), TPO (Penel et al., 1998), H₂O₂ (Kimura et al., 1995; Raspe and Dumont, 1995; Dunn and Dunn, 2000) and Tg (Dunn and Dunn, 2000; van de Graaf et al., 2001), promotes glycosylation, decreases the ratio of T4/T3 formation in Tg, alters the priority of iodination and hormonogenesis in tyrosyls, increases formation of disulphide bounds

of Tg, stimulates iodine recycling by deionisation, stimulates activity of digestive enzymes involved in Tg breakdown and promotes rapid resorption of mature Tg (Dunn and Dunn, 2000). Overall, TSH controls of all steps of TH formation by a variety of mechanisms (Mascia et al., 2002). THs regulate the release of pituitary TSH by a classical negative and positive feedback mechanism (Hollenberg et al., 1995; Langlois et al., 1997; Gauthier et al., 1999; Kaneshige et al., 2000; Macchia et al., 2001; Yen, 2001; Tannahill et al., 2002; Flamant and Samarut, 2003; Brown, 2005).

1.2.1.3 Transport and Cellular Intake of TH

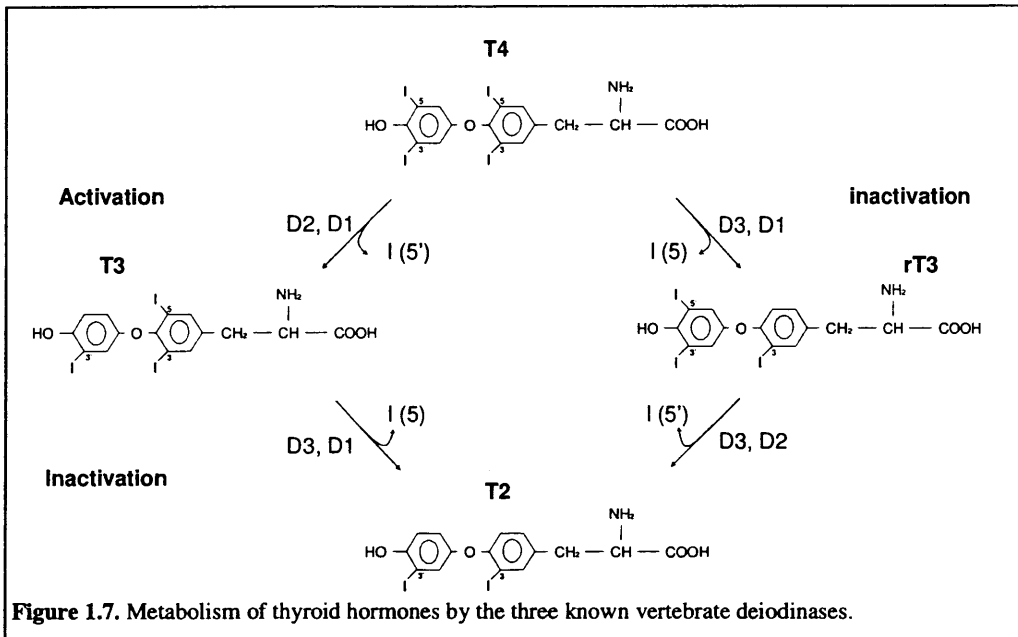
Thyroid hormones are generally transported in the serum by TH-binding serum proteins following their secretion from the thyroid follicles. There are several high density proteins and lipoproteins thought to be involved in TH serum transport but, thyroxine-binding protein (TBG), transthyretin (TTR) and serum albumin (SA) are the three major serum proteins involved in TH serum transport in vertebrates and other proteins show neither specific TH binding or a relevant physiological role (Bartalena and Robbins, 1993; Langsteger, 1997; Schussler, 2000). In higher vertebrates, TBG has the highest affinity for T4 followed by TTR which has 50-fold less affinity and by SA which has 7,000-fold less affinity for T4. For this reasons, TBG binds 75% of serum T4 and TTR and SA 20% and 5% respectively (Bartalena and Robbins, 1993; Langsteger, 1997; Schussler, 2000).

The process of transport of THs from the serum to the interior of the cell is the rate-limiting step on the subsequent metabolism in rats (Berry et al., 1991a; O'Mara et al., 1993; Maia et al., 1995; Salvatore et al., 1996). For many years, due to the lipophilic nature of THs, it was thought that cellular uptake of serum THs occurred by simple diffusion through the cell membrane but more recent evidence (Salvatore et al., 1996) suggests Na⁺-independent and –dependent transmembrane transporters and also amino acid transporters are involved (Abe et al., 2002; Mikkaichi et al., 2004; Friesema et al., 2005; Jansen et al., 2005; Maranduba et al.,

2006). It has been found that different TH transporters have different tissues specificities, thus suggesting that entry of THs into cells may be regulated in a tissue and possibly cell specific manner (Hsiang et al., 1999; Fujiwara et al., 2001; Pizzagalli et al., 2002).

1.3 Deiodination

The predominant form of circulating thyroid hormone is T4 but the biologically active form which is most able to bind to thyroid hormone receptors and transactivate gene expression, is T3. Moreover, 80% of T3 in the cells is converted locally from T4 with only 20% of T3 coming from the thyrocytes (Kohrle, 2000; Zhang and Lazar, 2000; Bianco et al., 2002; Harvey and Williams, 2002). T4 is subject to extensive tissue specific metabolism by a family of integral membrane enzymes belonging to the selenoprotein family of iodothyronine deiodinases that control local production and degradation of THs by deiodination. The deiodinases are transmembrane enzymes, either associated with the inner leaflet of the plasma membrane or with the cytosolic site of the endoplasmic reticulum (Kohrle, 2000; Bianco et al., 2002; Bianco and Larsen, 2005). Vertebrates have three different deiodinases that are differentially expressed in a developmental and tissue-specific manner. Deiodination reactions occur by outer ring deiodination (ORD) in the 5'-position of the phenolic ring or by inner ring deiodination (IRD) in the 5-position of the tyrosyl ring of T4. ORD of T4 generates T3 in peripheral tissues and alternative IRD of T4 yields the metabolite rT3. Further metabolism of T3 by IRD and rT3 by ORD results in the metabolite T2 (Fig. 1.7). All deiodinases are dependent on thiol cofactors for correct activity. Overall, the deiodinases act as gatekeepers that give T3 access to its intracellular receptors and regulate the cellular concentration of T4 and all other iodothyronines independent of nuclear receptors (Kohrle, 2000; Bianco et al., 2002).



1.3.1 Type I Deiodinase

Type I iodothyronine deiodinase (D1) is an enzyme with a high K_m and high V_{max} that prefers $rT3 \gg T4 > T3$ as substrate. It catalyses the ORD of rT3 more effectively and IRD of T4 and T3 is facilitated by sulphation (Visser, 1994; Kohrle, 2000; Bianco et al., 2002; Bianco and Larsen, 2005; Kuiper et al., 2005). D1 is found in rat liver associated with the endoplasmic reticulum and in the kidneys with the plasma membrane (Baqui et al., 2000; Kohrle, 2000; Bianco et al., 2002; Bianco and Larsen, 2005). The active enzyme is normally a homodimeric enzyme composed of two units of 27 kDa but it has recently been reported that the monomer also has catalytic activity (Toyoda et al., 1995a; Curcio-Morelli et al., 2003). The gene of D1 was assigned to chromosome 1p32-33 in humans and extends for 18 kb comprising four exons (Jakobs et al., 1997a). Each subunit of the active enzyme has a selenocysteine (Sec) encoded by a UGA codon (which normally acts as a terminator) in the mRNA. The mRNA possesses a selenocysteine-insertion sequence (SECIS) in the 3'UTR region that gives rise to a particular stem loop structure that specifies the insertion of a Sec residue instead of terminating translation at the UGA triplet (Berry et al., 1991a; Berry et al., 1991b; Kollmus et al., 1996;

Fagegaltier et al., 2000; Lambert et al., 2002). In *Fundulus heteroclitus* (Killifish) a cDNA for D1 of 1314 nt which encodes a 248 amino acid protein has been isolated and found to encode a functional D1 deiodinase (Orozco et al., 2003). A D1 cDNA has also been cloned in *Sparus auratus* (sea bream) and also has a TGA codon encoding a Sec aa followed by a SECIS element in the 3'UTR (Klaren et al., 2005). In contrast to *F. heteroclitus* and sea bream, in the Nile tilapia *Oreochromis niloticus* a D1 cDNA encoding a functional D1 protein possesses two tandem repeat SECIS elements in the 3'UTR (Sanders et al., 1997). Nevertheless, in all these teleost species a UGA encoding a Sec residue and at least one 3'UTR SECIS region is present indicating that, in common with mammals, teleost D1 enzymes are selenoproteins (Sanders et al., 1997; Orozco et al., 2003; Klaren et al., 2005).

The conversion of T4 to T3 by ORD and to rT3 by IRD mediated by D1 have similar efficiencies but, the sulphation of T4 enhances 200-fold the IRD of T4 and makes sulphated T4 ORD almost undetectable in rat (Bianco et al., 2002). Moreover, in humans and rats sulphation of T3 enhances 40-fold IRD of the hormone by D1 (Visser, 1994). Although sulphation causes no changes in ORD of rT3 by D1, in some species iodothyronine sulphation has an effect and either increases V_{max} or decreases K_m of D1. Moreover, sulphation of T2 also increases the ORD of this iodothyronine by D1 (Visser, 1994). Enzymatic activity of D1 suggests ping-pong type reaction kinetics where thiol cofactors play an important role in restoring the enzyme to its native form (Fig. 1.8). The Sec residue seems to be essential for correct enzymatic activity since substitution of this residue for a cysteine residue yielded a 100-fold decrease in D1 activity and substitution of the Sec residue by leucine inactivated the enzyme (Berry et al., 1991b). It is thought that the selenolate (Se-) groups of the enzyme work as acceptors of iodine thus catalysing its substitution for a proton in the hormone substrate giving rise to an enzyme intermediate (Fig. 1.8). The thiol cofactor, has a very high reactivity for sulphenyl iodide groups of proteins and is thought to reduce the Se-I group of the intermediate and restore the enzyme to its native form (Fig. 1.8)(Leonard and Köhrle, 2000; Bianco et al., 2002; Bianco and Larsen, 2005; Kuiper et al., 2005).

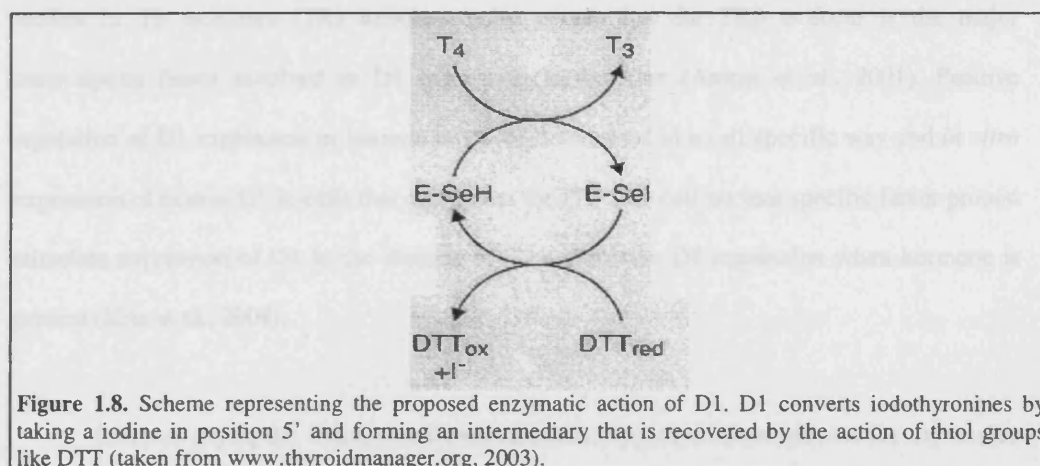


Figure 1.8. Scheme representing the proposed enzymatic action of D1. D1 converts iodothyronines by taking a iodine in position 5' and forming an intermediary that is recovered by the action of thiol groups like DTT (taken from www.thyroidmanager.org, 2003).

In adult mammals, D1 is mostly expressed in the liver, kidney, thyroid gland and intestine (Bates et al., 1999). In the liver, and to a lesser extent in the kidney, D1 expression and enzymatic activity are very high. In rats D1 is considered to be responsible for about 50% of serum T3 (Nguyen et al., 1998) but evidence from transgenic D1 knock-out mice suggests that D1 is principally involved in the production of T3 from T4 in the thyroid gland (Schneider et al., 2006). In addition, the thyroid gland D1 is implicated in the recycling of iodine by removal of the ion from MIT and DIT residues after Tg digestion and conversion of ~10% of T4 to T3 in the gland (Toyoda et al., 1992). Furthermore in D1 knock-out mice D1 seems to have a function in determining the amounts of T4 and T3 that are secreted in the thyroid gland into the circulation (Schneider et al., 2006). In humans D1 only account for 29% of peripheral serum T3 production (Maia et al., 2005) and in mice D1 assumes an important function in iodine recovery and recycling (Schneider et al., 2006). However, in euthyroid and hypothyroid mammals D1 seems to be the major factor involved in control and maintenance of TH serum homeostasis (Maia et al., 2005; Schneider et al., 2006).

In higher vertebrates, regulation of D1 occurs at the transcriptional level by action of T3 with stimulation of expression in hyperthyroidism and decreased expression in hypothyroidism (Kohrle, 2000). Moreover, Thyroid hormone Response Elements (TREs) have been identified in the upstream region of the D1 gene in humans (Toyoda et al., 1995b; Jakobs et al., 1997b) and

studies in T3 receptors (TR) knockout mice reveal that the TR β isoform is the major transcription factor involved in D1 expression in the liver (Amma et al., 2001). Positive regulation of D1 expression in humans might be determined in a cell specific way and *in vitro* expression of human D1 in cells that co-express the JTF JEG-cell nuclear specific factor protein stimulate expression of D1 in the absence of T3 and repress D1 expression when hormone is present (Kim et al., 2004).

Interestingly in the fish *Oreochromis niloticus*, hypothyroidism induces D1 expression in the liver and decreases expression in the kidney (Van der Geyten et al., 2001b) and in euthyroid *O. niloticus* no expression is detected in the liver and very little is detected in the kidney (Van der Geyten et al., 2001b). In contrast, in euthyroid trout (*Oncorhynchus mykiss*), turbot (*Scophthalmus maximus*) (Mol, 1998) and *F. heteroclitus* (Orozco et al., 2003) there are detectable levels of D1 activity in relation to *O. niloticus* (Orozco and Valverde-R, 2005; Van der Geyten et al., 2005). Also in *O. mykiss* maximal activity for rT3 ORD was observed in the intestine and the kidney whilst in *Clarias gariepinus* (African catfish) no rT3 ORD was detected in any tissue (Mol, 1998). The above observation suggest that D1 may not be the major enzyme responsible for T3 plasma levels in teleosts and that its expression is mostly concentrated in the kidney (Mol, 1998; Van der Geyten et al., 2001b). Nevertheless, the catalytic properties and activity of D1 in fish resemble those of mammals, with similar maximal velocities, affinities for the substrates, and optimum pH and temperature (Mol, 1998; Klaren et al., 2005). The major difference of D1 enzymes between fish and mammals appears to be their resistance in fish to 6-propyl-2-thiouracil (PTU), that in mammals inhibits all D1 activity (Mol, 1998; Kohrle, 2000; Van der Geyten et al., 2001b; Orozco et al., 2003).

1.3.2 Type II Deiodinase

Type II iodothyronine deiodinase (D2) acts by ORD at the 5' position of the phenolic ring but lacks IRD activity. In contrast to D1, D2 is a low K_m , low V_{max} enzyme that prefers T4

> rT3 as substrate and does not deiodinate sulphated T4 or rT3 (Kohrle, 2000; Bianco et al., 2002; Bianco and Larsen, 2005; Kuiper et al., 2005). In common with other deiodinases, D2 is located in cellular and intracellular membranes but is more abundant in the cytosolic face of the endoplasmic reticulum (Baqui et al., 2000; Kohrle, 2000; Bianco et al., 2002; Bianco and Larsen, 2005). The active enzyme complex is about 200 kDa and in rat seems to be composed of several subunits of the ~30 kDa protein encoded by D2 mRNA and by a 29 kDa (p29) subunit encoded by a different gene which is probably involved in cytoskeletal anchorage and substrate binding (Leonard et al., 2000) (Bianco et al., 2002). Recent reports suggest that *in vivo* monomers of D2 are active (Curcio-Morelli et al., 2003).

The human gene for D2 is located in chromosome 14q24.2-q24.3 and consists of 2 exons of 0.7 kb and 6.6 kb, with a SECIS sequence located ~5 kb from the coding region (Celi et al., 2000). In mouse a 5.8 kb cDNA for D2 has been cloned (Davey et al., 1999) and in mouse and human the D2 gene has a single intron separating 2 exons and the SECIS element in the mature mRNA is located ~5kb downstream of a coding region of only 798 bp (Davey et al., 1999). In *Rana catesbeiana* a D2 cDNA was isolated that is much shorter (1559 nt), than the mammalian sequence, and contains a UGA codon as well as the SECIS motif in the 3'UTR region of the cDNA (Davey et al., 1995). In the fish, *F. heteroclitus*, a ~4.6 kb cDNA coding D2 has been cloned, it has a SECIS sequence in the 3'UTR adjacent to the poly(A) tail of the mature mRNA, and has a conserved gene organisation with the human D2 sequence (Orozco et al., 2002). Some reports have supported the suggestion that D2 is not the product of a single gene, but that the mature active enzyme is in fact a complex of selenoproteins and non-selenoproteins, making D2 a very unusual deiodinase (Davey et al., 1999; Leonard et al., 2000). Nevertheless, the function of p29 in D2 enzymatic activity is still unknown (Bianco et al., 2002). Although in D2 as in D1 the Sec residue seems to be essential for proper enzymatic activity the two enzymes are thought to act by different mechanisms. Kuiper *et al.* (2002) have proposed a mechanism for deiodination by D2 in which the Se element of the active site of the enzyme acts as a nucleophile and attacks the iodine in the 5'-position of the either T4 or rT3

Huang et al., 2001; Schneider et al., 2001; Bianco et al., 2002). Strikingly, recent data in humans shows that D2 is responsible for 71% of peripheral T3 serum levels (Maia et al., 2005) and in rats and mice at least 50% of serum T3 is derived from D2 activity (Nguyen et al., 1998; Schneider et al., 2006). In fish the high levels of activity of D2 and the lack of D1 activity in the liver and kidney has led to the hypothesis that D2 is also the major contributor for T3 plasma levels (Mol, 1998; Orozco and Valverde-R, 2005; Van der Geyten et al., 2005). However, in rodents while D1 is involved in the rapid response to variations in TH serum levels, D2 is the major factor in long term control and regulation of thyroid status (Schneider et al., 2001; Bianco et al., 2002; Maia et al., 2005; Schneider et al., 2006).

The human D2 promoter has a TTF-1 consensus sequence, and in contrast to rat, this protein regulates D2 expression in the human thyroid gland (Gereben et al., 2002). In rat BAT it was found that catecholamines regulate D2 expression and that this enzyme is essential for thermogenesis in this tissue and essential to avoid death by hypothermia. In both teleost and tetrapods hyperthyroidism induces an decrease in D2 activity and transcription while the opposite is observed in hypothyroidism (Burmeister et al., 1997; Van der Geyten et al., 2001b; Garcia-G et al., 2004). The effect of T3 levels is thought to act via a mechanism which involves T3-binding nuclear receptors, although no TREs have been reported in the D2 promoter of any species. Hence T3 inhibition of D2 may be through intermediary pathways rather than TRs. In fact, T4 is involved in ubiquitination and subsequent degradation of D2 which increases with increasing turnover of the enzyme during its normal activity (Gereben et al., 2000; Bianco et al., 2002; Bianco and Larsen, 2005). D2 expression and activity is related to cAMP regulation and a cAMP-responsive element is present in the 5'UTR of the human gene (Bartha et al., 2000; Canettieri et al., 2000). Appropriate transport of the D2 protein and p29 subunit to the plasma membrane and correct assembly and activation of the multimeric selenoenzyme complex in the membranes of the cell involves cAMP signalling (Safran et al., 1996; Leonard et al., 2000). In this context, in human thyroid gland D2 is regulated at the transcriptional level through the TSH receptor-G_sα-cAMP regulatory cascade (Murakami et al., 2001).

In fish, D2 is the main selenoenzyme expressed in the liver and kidney whereas D2 mRNA or activity are undetectable in fish brain from a number of species (Mol, 1998; Orozco et al., 2000; Orozco et al., 2002; Van der Geyten et al., 2005). This contrasts to mammals and birds in which D2 is considered to be responsible for the majority of T3 in the brain as little or no uptake from the serum occurs (Bates et al., 1999; Darras et al., 2000; Kohrle, 2000; Bianco et al., 2002). This may indicate that in fish brain T3 levels are more dependent on serum concentration (Mol, 1998; Orozco et al., 2000; Orozco and Valverde-R, 2005). Although in fish the tissue distribution of D2 activity and mRNA expression is quite different from higher vertebrates, the enzymatic and physical properties of fish D2 are quite similar to its higher vertebrate counterparts (Mol, 1998; Orozco and Valverde-R, 2005; Van der Geyten et al., 2005).

1.3. 3 Type III Deiodinase

Inactivation of THs occurs by the action of type III iodothyronine deiodinase (D3), a low K_m , low V_{max} enzyme that prefers T3 > T4 as substrate. It acts exclusively as an IRD in mammals, birds and teleosts (Croteau et al., 1995; Salvatore et al., 1995; Mol, 1998; Hernandez et al., 1999; Sanders et al., 1999; Van der Geyten et al., 1999; Darras et al., 2000; Orozco et al., 2000; Bianco et al., 2002; Kuiper et al., 2003; Bianco and Larsen, 2005; Kuiper et al., 2005; Orozco and Valverde-R, 2005; Bres et al., 2006) but in *X. laevis* it was shown to also possess ORD activity, although its biological role is not clear (St Germain et al., 1994). Generally D3 inactivates TH by either converting T3 to T2 or by converting T4 into the iodothyronine rT3 through IRD at the 5-position of the tyrosine ring (Fig. 1.7). The putative vertebrate protein sequences known for D3 vary from 202 to 278 amino acids, with a predicted molecular weight varying from 20 to 31 kDa (St Germain et al., 1994; Croteau et al., 1995; Salvatore et al., 1995; Hernandez et al., 1999; Sanders et al., 1999). D3 acts exclusively as a homodimer with its active site located in the extracellular moiety (Curcio-Morelli et al., 2003; Bianco and Larsen, 2005) and it protects tissue from excessive T3 and controls the expression of T3-dependent

genes (St Germain et al., 1994; Becker et al., 1997; Richard et al., 1998; Bates et al., 1999; Galton et al., 1999; Huang et al., 1999a; Kohrle, 2000; Huang et al., 2003; Galton, 2005). In *X. laevis* D3 expression and activity in post-metamorphic frog tissues is essential for maintenance of adult phenotypes (Kawahara et al., 1999) and in mammals D3 is also necessary for correct function of the thyroid axis (Hernandez et al., 2006). Further evidence suggesting the role of D3 in protecting cells and tissues from excess of T3 is its cellular location *in vitro*, exclusively in the extracellular side of the plasma membrane, where it is closely associated with plasma membrane proteins and not endoplasmic reticulum proteins (Baqui et al., 2003; Bianco and Larsen, 2005).

The human (Salvatore et al., 1995), rat (Croteau et al., 1995), mouse (Hernandez et al., 1999), *X. laevis* (St Germain et al., 1994) and *O. niloticus* (Sanders et al., 1999) cDNAs for D3 with, respectively, 2.6 kb, 2.1 kb, 1.9 kb, 1.5 kb and 1.5 kb have been isolated. The human gene is localised on chromosome 14q31 and the mouse gene on chromosome 12F1 (Hernandez et al., 1999). Mouse D3 revealed sequence conservation at the protein level of 99% and 96% compared, respectively, with rat and human (Hernandez et al., 1999). At the nucleotide level, inclusion of the mouse 3'UTR still gives 86% conservation with human and rat; and in the three species the first 64 nucleotides 5' of the putative ATG start site are conserved suggesting conserved regulatory mechanisms (Hernandez et al., 1999). Analysis of all available cDNA sequences shows D3 to be a selenoenzyme with a highly conserved selenocysteine in its active site and SECIS motif in the 3'UTR of the mRNA (St Germain et al., 1994; Croteau et al., 1995; Salvatore et al., 1995; Mol, 1998; Hernandez et al., 1999; Sanders et al., 1999; Van der Geyten et al., 1999; Darras et al., 2000; Orozco et al., 2000; Bianco et al., 2002; Kuiper et al., 2003; Bianco and Larsen, 2005; Kuiper et al., 2005; Orozco and Valverde-R, 2005; Bres et al., 2006). The substitution in human and *X. laevis* D3 of the Sec residue by a cysteine residue results in a 2-fold and 6-fold decrease in turnover when T3 or T4 respectively is the substrate, whilst when the substitution was with an alanine residue or it was deleted the SECIS elements no activity was detected (St Germain et al., 1994; Kuiper et al., 2003). The relative insensitivity of D3 to

PTU as found for D2 may indicate that D3 acts through a similar sequential mechanisms to that observed for D2 and thiol cofactors are also important in restoring the enzyme to its native form (Fig. 1.9)(Kohrle, 2000; Bianco et al., 2002; Kuiper et al., 2005).

In the adult rat liver, thyroid, pituitary, BAT, skin and kidney little or no D3 mRNA expression is detected but in placenta, cerebral cortex and skeletal muscle considerable mRNA expression and enzymatic activity are found (Croteau et al., 1995; Bates et al., 1999; Galton et al., 1999; Galton, 2005). In humans, D3 expression is observed in the placenta and endometrial glands of nonpregnant human uteri (Huang et al., 2003). In salmonids, D3 activity is present in liver, gill and brain (Leatherland and Farbridge, 1992; MacLatchy and Eales, 1992; Morin et al., 1993) although in *O. mykiss* (Mol, 1998) no D3 activity is detected in the gills. D3 activity is detected in gill and skin of *O. niloticus*, liver and skin of *O. mykiss* and gill and kidney of *S. maximus* (Fenton et al., 1997; Mol, 1998; Van der Geyten et al., 2005). In the fish *O. niloticus* high levels of mRNA expression are observed in brain and gill although high enzymatic activity is measured in the brain (Sanders et al., 1999). However a more recent study seems to indicate that also in *O. mykiss* gills D3 activity is present (Van der Geyten et al., 2005) and in spleen and liver although D3 mRNA is of low abundance, enzymatic activity is higher than in the gills (Sanders et al., 1999; Van der Geyten et al., 2005). In the kidney and gut the mRNA expression and the enzymatic activity of D3 are at the same level and in muscle no expression or activity is observed in *O. niloticus* (Sanders et al., 1999; Van der Geyten et al., 2005). In both rat (Croteau et al., 1995) and *O. niloticus* (Sanders et al., 1999) several different size transcripts of D3 have been found which seem to have a tissue specific distribution. In *O. mykiss* two different D3 cDNAs have been found which result from alternative splicing and although the coding region is not involved it leads to differing SECIS elements and 3'UTR in the two transcripts (Bres et al., 2006). The biological significance of these observations in teleosts are unclear, but seem to highlight the importance of appropriate levels of D3 for maintaining T3 *status quo* and that the complex regulation of D3, in common with tetrapods, occurs both at the pre- and post-translational level (Kawahara et al., 1999; Hernandez et al., 2006).

The mouse and human promoter region of the D3 gene contain GC rich sequences although no TREs have been found in either species (Salvatore et al., 1995; Hernandez et al., 1999; Bianco et al., 2002). Nevertheless, in higher vertebrates hyperthyroidism and *in vitro* TH treatment induce D3 expression and activity to increase whereas hypothyroidism and cell culture without TH has an opposite effect (St Germain et al., 1994; Croteau et al., 1995; Pallud et al., 1999; Tu et al., 1999; Kohrle, 2000). Furthermore, T3, retinoic acid, the mitogen 12-*O*-tetradecanoyl phorbol 13-acetate (TPA) and basic fibroblast growth factor (bFGF) increase D3 mRNA expression and activity in rat astroglial cells cultured *in vitro* and different combinations of the same factors have a synergistic effect on D3 expression and activity (Pallud et al., 1999). Part of the response to these chemicals involves pre-translational mechanisms and two different responses occur: 1) TPA and bFGF, mediate their response through signalling at the cell surface and rapidly increase D3 mRNA and activity through MEK/Erk cascades (Pallud et al., 1999); and 2) T3 and retinoic acid, that act as ligands to its nuclear receptors, and provoke a lower, slower but long lasting increase in D3 mRNA and activity in cultured rat astroglial cells (Pallud et al., 1999). Studies in rat BAT also demonstrate *in vitro* enhancement and possible regulation *in vivo* of D3 expression by a number of growth factors (Hernandez et al., 1998; Hernandez et al., 1999). It is also proposed that T3 may be involved in increasing the extension of the poly(A) tail of D3 mRNA and hence its half-life, as in the cerebral cortex of rats treated with T3 the abundance of the 3.6 kb and 3.3 kb transcripts (larger than the expected D3 2.2kb transcript), are higher than in non-treated animals (Croteau et al., 1995). Although some differences exist between different fish species, overall, fish D3 expression and activity pattern either in eu-, hypo- or hyperthyroid animals resembles that observed in mammals (MacLachy et al., 1992; Mol, 1998; Finnson and Eales, 1999; Van der Geyten et al., 2001b). Taken together the evidence suggests that D3 regulation, as well as its physiological function, in fish is conserved when compared to mammals and other vertebrates although more studies are needed to evaluate D3 regulation in fish.

1.3.4 Deiodinases in development of vertebrates

Vertebrate deiodinases have an important role in thyroid axis function and maintenance of thyroid *status quo* in adult animals, but they also have an important role in tetrapod development. Moreover, it is the coordination and synergies between the expression and activity of the different deiodinases that brings about appropriate TH driven development (Becker et al., 1997; Van der Geyten et al., 1997; Richard et al., 1998; Bates et al., 1999; Huang et al., 1999a; Kawahara et al., 1999; Marsh-Armstrong et al., 1999; Callery and Elinson, 2000; Campos-Barros et al., 2000; Kohrle, 2000; Huang et al., 2001; Van der Geyten et al., 2001a; Shintani et al., 2002; Van der Geyten et al., 2002; Huang et al., 2003; Cai and Brown, 2004; Gereben et al., 2004; Kester et al., 2004; Ng et al., 2004; Brown, 2005; Galton, 2005). The complexity that deiodinases confer to the tissue and cellular action of THs gives these enzymes a crucial role in TH controlled processes. Moreover, normal embryonic development is only achieved after correct spatial and temporal expression of the iodothyronine deiodinases.

In mammals D1 has a relatively small role in development. It is present in liver and thyroid of humans and rat (Richard et al., 1998; Kohrle, 2000) and in rat kidney and intestine (Croteau et al., 1995; Bates et al., 1999) from foetus until adult stages where its expression and activity are more elevated and where its importance in serum T3 production and iodine recycling role has already been discussed. D3 in contrast is highly expressed and has high activity during rat foetal development with the exception of BAT, thyroid and pituitary, although expression and activity decrease sharply after birth and it becomes restricted to the brain cortex and skeletal muscle (Croteau et al., 1995; Bates et al., 1999). Furthermore, in rat retinal development it has been shown that TR are needed for retinal proliferation but it is D3 that determines which cells respond to T3 (Forrest et al., 2002). Also in rats, D3 activity increases in skin, testis and ovaries of newborn rats just before birth, together with an increase in serum T3, and is prolonged in first stages of lactation but in the adult tissues its activity and T3 levels diminish several fold (Croteau et al., 1995; Bates et al., 1999). In the development of

the rat cochlea the relevance of correct timing in expression and activity of D2 permits the T3-mediated postnatal development of this organ (Campos-Barros et al., 2000; Forrest et al., 2002; Ng et al., 2004). Interestingly in testis, an increase in either D2 mRNA or activity levels occurs at the same time as D3, suggesting coordination between the two enzymes so that appropriate intracellular levels of T3 are available (Bates et al., 1999). Further evidence in rat of the relationship between D3 and D2 for coordination in TH action on development is the observation of a sharp decrease of brain D3 expression and activity as intrauterine life terminates and the elevation of both D1 and D2 activity in the same developmental period (Bates et al., 1999).

In common with mammals, D3 appears to play a central role in development of chicken, however D1 has a much more prominent role in the development of chicken than in mammals in which D2 is more important (Van der Geyten et al., 2001a). In chicken D1 is expressed at almost constant levels through all embryonic development but D1 expression declines slightly in 1 day chicks (Van der Geyten et al., 1997; Van der Geyten et al., 2001a; Van der Geyten et al., 2002). In contrast with mammals D1 seems to have a much broader distribution in chicken development. Also in contrast to mammals, in chicken development D3 is expressed in all tissues including thyroid and the pituitary (Van der Geyten et al., 2001a). More reminiscent of mammals is the increase in D3 expression and activity near hatching followed by a sharp decrease immediately after birth of the chicks. The only exceptions are muscle, intestine and lung where an increase in expression and activity of D3 occurs as the chicks approach hatching and in hatched 1 day chicks (Van der Geyten et al., 2001a). In chicken development, and again in contrast to rat, the D2 tissue expression and activity is restricted to brain and it increase sharply just before hatching to decreases sharply in 1 day chicks (Van der Geyten et al., 2001a). Moreover, during embryonic development in chicken, D1 activity is positively correlated with plasma T3 whereas D3 is negatively correlated (Van der Geyten et al., 1997) suggesting their action may be coordinated.

In anuran metamorphosis (most extensively studied in *Rana catesbeiana* and *X. laevis*) the coordination of the action of different deiodinases brings about the correct developmental changes. In contrast to chicken and in common with mammals, D1 assumes a much less important, if not negligible, role in anuran metamorphosis whereas D2 and D3 seem to be the main selenoenzymes involved in the coordination of TH action during development (Becker et al., 1997; Huang et al., 1999a; Kawahara et al., 1999; Marsh-Armstrong et al., 1999; Huang et al., 2001; Shintani et al., 2002; Cai and Brown, 2004; Brown, 2005). During anuran metamorphosis different organs start developing at different stages where different serum T3 concentrations are present, illustrating the different sensitivities of the tissues to T3. An example of this is the coordination between tail regression and development of the limbs. In *R. catesbeiana* prometamorphosis, when T3 levels are still low and it is observed in the tail low D2 activity and high D3 activity, hind limb development is closely associated with an increase of D2 expression and activity in these tissues together with a low expression and activity of D3 (Becker et al., 1997). Hence TH-driven changes occur in limb but not tail. As metamorphosis approaches climax, and plasma T3 peaks, tail is D3 downregulated and its activity decreased at the same time that a sharp increase in D2 expression and activity is observed in the tail and fore limbs. These molecular changes result in a cascade of events that result in tail resorption and the completion of fore limb formation, so that at the end of metamorphosis the young frogs have a new and complete locomotion system (Becker et al., 1997). Moreover, the same tight coordination between D2 and D3 expression and activity occurs in *X. laevis*, suggesting that in anurans there is a dynamic mechanism that tightly controls intracellular T3 levels and hence action on gene transcription and morphogenetic processes (Marsh-Armstrong et al., 1999; Cai and Brown, 2004; Brown, 2005). (Becker et al., 1997; Cai and Brown, 2004; Brown, 2005). Furthermore, transgenic *X. laevis* that over-express D3 develop normally through embryogenesis and prometamorphosis but metamorphosis is retarded and most animals fail to achieve adulthood (Huang et al., 1999a). In particular, in *X. laevis* overexpressing D3 neural connections from the spinal cord to the new limb muscles that develop at metamorphosis did not form and frogs were tetraplegic (Marsh-Armstrong et al., 2004).

In fish, despite some reports of isolating, cloning and adult tissue distribution of the three deiodinases, only one study in the zebrafish *D. rerio*, has been made of deiodinase expression during development (Thisse et al., 2003). Moreover, in this single study only D2 and D1 expression were analysed. The results showed that D2 is already detected by *in situ* hybridisation in embryonic tissues after 24 hours post fertilization (hpf), more specifically in the retina and developing adenohypophysis cells in which D2 expression continues at least up until 5 days post-fertilization (dpf) (Thisse et al., 2003). By 36 hpf, *D. rerio* D2 expression begins in the developing intestinal bulb at the same time it starts to be downregulated in the retina (Thisse et al., 2003). By 5 dpf D2 expression in *D. rerio* larvae is only observed in the developing swim bladder and scattered adenohypophysis cells (Thisse et al., 2003). In the case of D1, expression is only detected after hatch in 72 hpf larvae and specifically in the gastrointestinal tract, liver and kidney (Thisse et al., 2003). Besides this one study in *D. rerio* no other reports exist that describe the role of deiodinases in any early life stage of teleosts.

1.4 Thyroid hormone receptors

Recently TH have been shown to have non-genomic cell action and TH signalling pathways have been found in the cell membrane, cytoplasm and mitochondria. These non-genomic actions involved the induction of cellular events by T3 by intracellular secondary messengers, calcium induction, cAMP and protein kinase pathways (Bassett et al., 2003; D'Arezzo et al., 2004) and also included the specific binding of TH to integrins (Bergh et al., 2005; Davis et al., 2005). However, the most prominent TH action is located in the cell nucleus. Thyroid hormones mediate their action by binding to nuclear receptors that act directly on target genes. These bind as heterodimers (with a retinoid-X receptor) to specific DNA sequences (Thyroid Response Elements - TRE), and activate or repress expression of the associated genes in the presence or absence of ligand, hence bringing about the cellular response to thyroid hormones (Fig. 1.10) (Tomic-Canic et al., 1992; Yen and Chin, 1994; Hollenberg et al., 1995; Tomic-Canic et al., 1996a; Radoja et al., 1997; Zhang and Lazar,

2000; Jho et al., 2001; Yen, 2001; Eckey et al., 2003; Jho et al., 2005; Yen et al., 2006). Thyroid hormone receptors (TRs) are members of the steroid-thyroid receptor superfamily that also includes receptors for ligands such as steroid hormones, retinoids, melatonin and vitamin D3 (Fig. 1.11) (Chin and Yen, 1997; Zhang and Lazar, 2000; Aranda and Pascual, 2001; Yen, 2001). In mammals, two *TR* genes were found and designated *TR α* (NR1A1) and *TR β* (NR1A2). *TR* genes code for proteins that act most frequently and efficiently as heterodimers with Retinoid X Receptors (RXRs - see Fig. 1.10). The action of TRs, as all nuclear receptors, is also highly dependent on the action of coactivators and corepressors activating or repressing transcription (Chin and Yen, 1997; Zhang and Lazar, 2000; Aranda and Pascual, 2001; Yen, 2001).

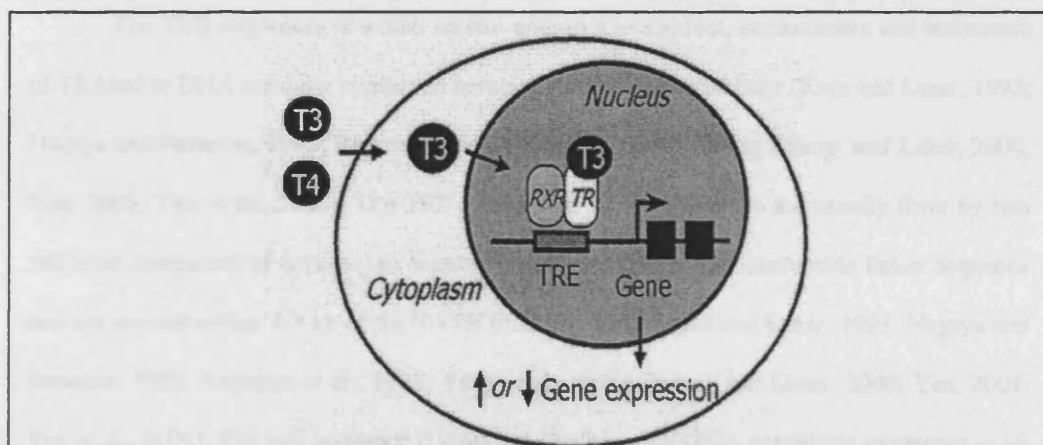
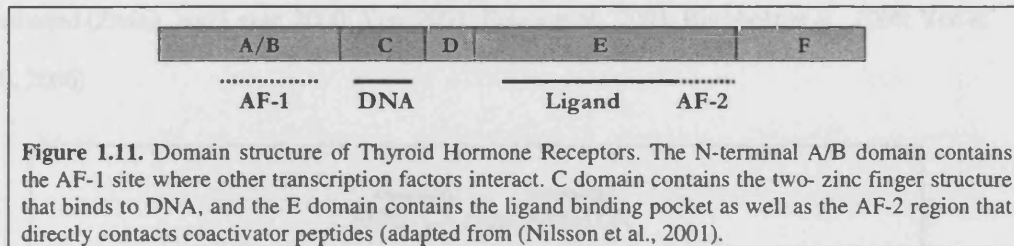


Figure 1.10. Proposed action of thyroid hormone receptors. The TR is bound to DNA in the TRE located upstream of the initiation site as a heterodimer with the RXR receptors. The plasma circulating T4 enters the cell, it is converted to T3 in the cytoplasm and enters the nucleus where it binds with TR. The binding of the hormone to its receptor causes conformational changes in the TR-RXR heterodimer and, depending of the target gene promoter context and other factors, will enhance or repress gene expression (adapted from www.thyroidmanager.org, 2003).

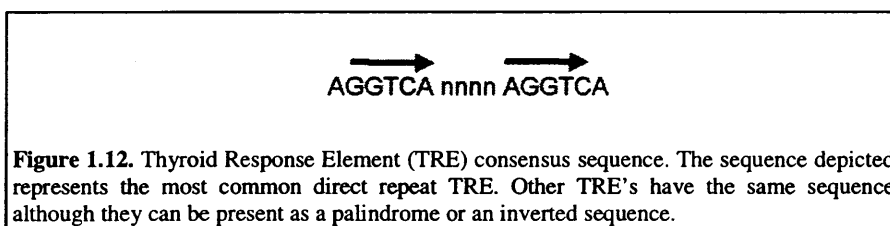
The TR proteins are composed at the N-terminal end by an A/B domains that interacts with other transcription factors, the C domain comprising two zinc fingers constitutes the DNA binding domain (DBD), the E-domain, also called the ligand binding domain (LBD), is involved in corepressor interaction, ligand binding, dimerisation and transactivation of gene expression; at the C-terminal end the F domain is responsible for corepressor and coactivator interaction (Fig. 1.11) (Chin and Yen, 1997; Zhang and Lazar, 2000; Aranda and Pascual,

2001; Yen, 2001). Both, TR α and TR β in all higher vertebrates have shown to express several isoforms generated by alternative splicing and/or different promoter usage that confer even more complex T3-target gene regulation (Weinberger et al., 1986; Hodin et al., 1989; Yaoita et al., 1990; Shi et al., 1992; Chassande et al., 1997; Williams, 2000; Gauthier et al., 2001)



The TRE sequences to which hetero- and, to a less extent, homodimers and monomers of TR bind to DNA are quite conserved between the various vertebrates (Katz and Lazar, 1993; Nagaya and Jameson, 1993; Reginato et al., 1996; Yang et al., 1996; Zhang and Lazar, 2000; Yen, 2001; Yen et al., 2006). The TRE elements to which TR binds are usually form by two half-sites composed of 6-base pair sequences separated by a four nucleotide linker sequence and are located within 2-3 kb of the TATA box (Fig. 1.12) (Katz and Lazar, 1993; Nagaya and Jameson, 1993; Reginato et al., 1996; Yang et al., 1996; Zhang and Lazar, 2000; Yen, 2001; Yen et al., 2006). The pair sequence is composed by two AGGTCA consensus sequences or by the higher affinity octamer sequence TNAGGTCA separated by a four nucleotides, and those sequences can be orientated as direct repeats (DR), palindromic sequences (Pal) or inverted palindrome sequences (Fig. 1.12) (Katz and Lazar, 1993; Nagaya and Jameson, 1993; Reginato et al., 1996; Yang et al., 1996; Zhang and Lazar, 2000; Yen, 2001; Yen et al., 2006). Furthermore, it seems that TR have a higher affinity for the 3'-half-site of the TRE, since it was shown that in TR-RXR heterodimers, the subunit TR binds preferentially to this half site (Yang et al., 1996; Farsetti et al., 1997). A proposed role for the differences observed in TREs is linked to the fact that these sequences are able to mediate DNA-TR interaction on the target genes, since the affinity of the DNA-heterodimer will influence the expression of the linked gene(s) (Katz and Lazar, 1993; Nagaya and Jameson, 1993; Reginato et al., 1996; Yang et al.,

1996; Zhang and Lazar, 2000; Yen, 2001; Yen et al., 2006). Functionally, two types of TREs have been identified. The first type is considered to be a positive TRE, where DNA-bound unliganded RXR-TR heterodimers inhibit gene expression and liganded heterodimers activate it, and a second type is denominated negative TREs, since in the presence of T3, DNA-bound RXR-TR heterodimers repress gene expression but in the absence of ligand gene expression is activated (Zhang and Lazar, 2000; Yen, 2001; Eckey et al., 2003; Buchholz et al., 2006; Yen et al., 2006)



A new class of negative TREs has been found with a different organisation and location in the promoter region of TH-target genes that induces expression of T3-target genes by TRs in the absence of T3 and downregulation in the presence T3. In the human keratin genes 5, 6, 14 and 17 such negative TREs were found to constitute a single half-site located 250 to 150 bp upstream of the TATA box (Tomic-Canic et al., 1996a; Radoja et al., 1997). Furthermore, in these TREs unligand TR α homodimer is able to induce expression of keratin genes but in the presence of T3 repression is strongly downregulated only by a TR α monomer (Tomic-Canic et al., 1996a; Radoja et al., 1997). Moreover, the same type of TREs were found in the human TRH gene but in this case one of the three TREs found is located at about 60 bp upstream of the TATA box whereas the second and third TRE half-site sequences are in the first 40 bp of exon 1 (Hollenberg et al., 1995). Recently it was found *in vitro* that co-transfection of human TRH promoter with either TR α or TR β isoforms respectively led to, repression or activation of transcription in the presence of T3 and vice-versa in its absence in culture (Guissouma et al., 2000). Furthermore, in case of human keratin genes it was found that when TR α was complexed to a negative TRE, known co-repressor proteins behaved like co-activators whereas proteins normally considered co-activators behaved as co-repressors (Jho et al., 2005). These

observations strongly suggest that the effect of TR is dependent on specific TREs and promoter context of target genes (Hollenberg et al., 1995; Tomic-Canic et al., 1996a; Radoja et al., 1997; Guissouma et al., 2000; Jho et al., 2005)

1.4.1 Role of TRs in mediating TH action in vertebrate development

In mammals, TR importance and action become more relevant in development and especially in post-natal and weaning periods, when an increase in TH levels occurs that decreases as the animals grow older (Forrest et al., 2002; Flamant and Samarut, 2003). Moreover, it was shown that specific TR isoforms are important in post-natal brain maturation (namely in neural and glial cell development), inner ear and retinal formation, intestine and bone proliferation and maturation as well as reproductive tissue maturation (Strait et al., 1992; Gauthier et al., 1999; Macchia et al., 2001; Plateroti et al., 2001; Forrest et al., 2002; Flamant and Samarut, 2003). It was further proposed that a surge in TR β 1 expression during embryonic development of mice controls proliferation and apoptosis of tissues in the face and limbs between stage 12.5F and 17.5F, with expression decreasing thereafter until 5 days post-natal (Nagasawa *et al.*, 1997). However, most surprisingly knock-out mice in which all possible isoforms of TR are absent appear to show normal embryonic development, thus suggesting that TH and TR are not essential for this process, although, these animals always present delayed growth, lower body temperatures and impaired learning ability (Strait et al., 1992; Gauthier et al., 1999; Macchia et al., 2001; Plateroti et al., 2001; Forrest et al., 2002; Flamant and Samarut, 2003).

In *Xenopus* and other amphibians there is a strong correlation between TH levels, TR expression and metamorphosis (Yaoita and Brown, 1990). Moreover, expression of TR is observed immediately after hatching of the embryos and found to be correlated to D2 expression in tissues undergoing metamorphic changes (Kawahara et al., 1999; Cai and Brown, 2004; Brown, 2005). TR α mRNA is found to increase through premetamorphosis until a peak

at prometamorphosis (onset of endogenous TH production by tadpole thyroid), falling at the climax of metamorphosis to very low levels in adult frogs (Yaoita and Brown, 1990). On the other hand, TR β mRNA is only found from prometamorphosis onwards, suggesting a T3-mediated induction of these receptors. This is further supported by a parallel increase in TH and TR β mRNA levels, both of which peak at metamorphic climax (Yaoita and Brown, 1990). In fact, it was recently shown that transgenic *X. laevis* with a dominant negative form of TR are unable to undergo metamorphosis (Buchholz et al., 2003). Moreover, when transgenic *X. laevis* tadpoles with a dominant-positive (i.e. constitutively active) TR under the control of a heat-shock promoter were reared in methimazol (an inhibitor of TH synthesis) animals were not able to undergo metamorphosis. However increasing the rearing temperature (and so activating the heat shock promoter) enabled the tadpoles to undergo metamorphosis even in the absence of TH further confirming that TR are necessary and sufficient to drive anuran metamorphosis (Buchholz et al., 2004; Buchholz et al., 2006).

In fish development TRs are present at least from mid-blastula transition, and increase at hatching until the transition from larvae to juvenile, before decreasing to the lower adult levels (Llewellyn et al., 1999; Liu et al., 2000; Nowell et al., 2001; Jones et al., 2002). In *D. rerio*, TR α was most abundant during embryonic development, with maternally derived transcripts being detected. TR β transcripts increase in level from the 16-cell stage onwards, although always at lower levels than TR α (Liu et al., 2000). Further studies with overexpression of TR α in *D. rerio* showed that TR receptors in fish embryogenesis might be fundamental for correct embryonic development in contrast with mammals, since these transgenic animals presented severe disruption of hindbrain formation, indicating a possible relation of TR with the retinoic acid receptor pathways and implications in Hox gene expression (Essner et al., 1999). In metamorphosing larvae of *H. hippoglossus* an increase in TR α expression was found from hatching onwards peaking at metamorphosis climax in parallel with what is observed in *Xenopus* (Yaoita and Brown, 1990; Llewellyn et al., 1999; Galay-Burgos et al., 2004). In fact, in halibut it was also found that TR α 1 (Llewellyn et al., 1999) and TR β (Sweeney, unpublished

results) have very low expression levels in pre-metamorphic larvae and in early metamorphic stages but as the animals reach climax the expression TR β , and to a much more limited extent TR α , peaks only to be reduced again immediately after metamorphosis. In turn, TR α 2 (Sweeney, unpublished results) is the most abundant TR in pre-metamorphosis and early metamorphic stages but as climax is reached its expression decreases several fold to a level that is maintained low thereafter (Galay-Burgos et al., 2004). These observations of TR expression during *H. hippoglossus* metamorphosis (Galay-Burgos et al., 2004) are reminiscent of *X. laevis* metamorphosis where TR α were shown to be more related to pre-metamorphic and early metamorphic T3 driven developmental events whereas TR β are more associated to late metamorphic events (Yaoita and Brown, 1990). In metamorphosis of the turbot *S. maximus* TR α upregulation was correlated with metamorphic climax instead of TR β and T3 treatment increased TR α expression but not TR β (Marchand et al., 2004). This contrasts with *D. rerio*, where T3 had no effect on TR α expression but up-regulated TR β (Liu and Chan, 2002). Nonetheless, the present evidence shows that TR are probably the most important mediators of TH action in teleosts even though little information is available about the functional aspect that these receptor display *in vivo*. A thorough analysis of TR and deiodinase expression and activity are required to better understand TH action in teleosts. Moreover, morphological and histological data needs to be combined with molecular data so that a more integrated image of TH action can be drawn in fish. Ultimately, transgenic analysis in a way similar to what was done in mice and *X. laevis* is needed to better understand these events and the interrelationship of all players involved in TH action in teleosts.

1.5 Molecular markers of fish metamorphosis

Molecular markers for metamorphosis are imperative for the study of metamorphosis in any animal system. They permit the researcher to determine the pre- and post-metamorphic stages in molecular terms as well as the metamorphic period, since the expression levels of such markers will vary (increasing or decreasing accordingly with the specific marker used) during

these stages. This change can arise from differential RNA splicing of the marker gene or by transcriptional repression or activation of such genes. In anuran metamorphosis, muscle tissue undergoes a dramatic change with the primary muscle lineage dying and a new secondary muscle lineage replacing it. In *X. laevis*, the death of the primary muscle lineage and the subsequent development of the adult muscle lineage is directly triggered by T3 (Chanoine and Hardy, 2003). In zebrafish (Liu and Chan, 2002), TH treatment makes muscle tissue less compact and in developing larvae of *Epinephelus coioides* (grouper) differences in locomotion between control and TH treated fish are observed (de Jesus et al., 1998). Furthermore, in *P. olivaceus*, Yamano and colleagues (1994b) showed that the 5',5'-dithio-bis-nitrobenzoic Myosin light chain (MLC) undergo a isoform switch from a pre- (larval) to post-metamorphic (adult) isoform. Importantly, in sea bream juveniles T4, but not T3, treatment increases myosin light chain 2 (MLC2) expression (Moutou et al., 2001). Taken together these studies indicate that muscle and muscle genes might be regulated by TH in teleost development.

Although skin development has been reported not to be affected by TH during development or by TH treatment in *D. rerio* (Brown, 1997; Liu and Chan, 2002), it has been shown in *D. rerio* (Le Guellec et al., 2004), *H. hippoglossus* (Ottensen and Olafsen, 1997), *Pseudopleuronectes americanus* (Murray et al., 2003) and *Pleuronectes platessa* (Roberts et al., 1973) that at the transition from larvae to juvenile the skin increased in thickness passing from a simple epithelia to a highly stratified tissue. Furthermore, the developmental events in teleosts at this stage of development are remarkably similar to the observed skin development of anurans at metamorphosis that has been shown to be under the control of TH (Kawai et al., 1994; Suzuki et al., 2001; Watanabe et al., 2001; Suzuki et al., 2002; Watanabe et al., 2002; Ishida et al., 2003). Overall this evidence seems to indicate that post-embryonic development of teleost skin might also be mediated by TH.

1.5.1 Troponin T

Troponin T (TnT) is the tropomyosin-binding subunit of the striated muscle troponin complex and plays a role in the Ca^{2+} -activation of contraction. In mammals and birds there are three different TnT genes that are expressed in a tissue specific manner as they are either fast, slow or cardiac muscle genes (Perry, 1998). In rat (Bucher et al., 1999) and mouse (Jin et al., 1998a) the fast skeletal TnT (fTnT) gene is composed of 18 exons and by 24 exons in quail (Bucher et al., 1999). The cardiac TnT (cTnT) in humans is composed of 17 exons (Farza et al., 1998) and in mouse by 16 exons (Jin et al., 2000a). In all species studied to date, multiple isoforms of fTnT and cTnT have been found. These multiple isoforms result from differential splicing of several exons in the N-terminal region of the protein, such that distinct embryonic isoforms are produced (Farza et al., 1998; Perry, 1998; Huang et al., 1999c; Huang et al., 1999d; Huang and Jin, 1999; Jin et al., 2000a). Furthermore, the fTnT gene of mouse and chicken, in contrast with the cTnT and the slow skeletal TnT (sTnT) genes, have two exons encoding part the C-terminal region of the protein that show mutually exclusive splicing (Jin et al., 1998b). The sTnT gene is composed by 14 exons in mouse (Huang et al., 1999d) and humans (Barton et al., 1999), produces far fewer splice variants than the fast and cardiac TnT genes and lacks embryonic specific isoforms (Perry, 1998). Despite these differences all three genes have exons with alternative internal acceptor sites that increase even more the isoform complexity (Barton et al., 1999).

In the only study of TnT expression during flatfish metamorphosis, in *P. olivaceus* pre-metamorphic larvae muscle was shown by SDS-PAGE to contain a high molecular weight muscle Troponin T (TnT) isoform that predominated over a smaller TnT isoform. However as metamorphic climax is reached the high molecular weight TnT band is totally repressed and a new intermediate molecular weight adult specific TnT isoform appears becoming the predominant TnT isoform in *P. olivaceus* muscle (Yamano et al., 1991a). Moreover, it was

found that T3 was able to induce these changes in TnT isoform expression whereas thiourea prevents from occurring at metamorphosis (Yamano et al., 1991a).

1.5.2 Epidermal keratin genes

In *X. laevis*, during T3 driven metamorphosis, the skin is one of the tissues that undergoes extensive remodelling, with the tadpole epidermis dying and the basal tadpole epidermis giving rise to the adult epidermis (Schreiber and Brown, 2003). Keratins are a member of a big family of intermediate filament proteins and are expressed differentially in various tissues including skin. Several keratin genes have been reported in vertebrates and subdivided in acidic (type I) and basic (type II) isoforms. It has been reported that the expression of a keratin gene in *X. laevis* is regulated by spontaneous and TH-induced skin metamorphosis (Mathisen and Miller, 1987; Mathisen and Miller, 1989). Moreover, it was also verified that T3 stimulated these changes in isolated and cultured larval epidermal cells (Shimizu-Nishikawa and Miller, 1991; Nishikawa et al., 1992; Shimizu-Nishikawa and Miller, 1992). Recently, other investigations revealed that novel epidermal keratins genes in *X. laevis* have a similar developmental expression pattern and that TH is essential for correct skin development at metamorphosis (Jonas et al., 1985; Nishikawa et al., 1992; Kawai et al., 1994; Suzuki et al., 2001; Watanabe et al., 2001; Suzuki et al., 2002; Watanabe et al., 2002; Ishida et al., 2003). Moreover, in humans it was shown that not only are several skin epidermal keratin genes are under direct regulation of TH but also that TH is a fundamental factor for skin development, function and homeostasis (Ellison et al., 1985; Tomic-Canic et al., 1992; Tomic-Canic et al., 1996a; Tomic-Canic et al., 1996b; Tomic-Canic et al., 1996c; Radoja et al., 1997; Tomic-Canic et al., 1998; Jho et al., 2001; Radoja et al., 2004; Jho et al., 2005).

CHAPTER 2

**MOLECULAR, CELLULAR AND
HISTOLOGICAL CHANGES IN SKIN
FROM A LARVAL TO AN ADULT
PHENOTYPE DURING HALIBUT
METAMORPHOSIS.**

2.1 Introduction

The skin is a complex epithelia and the most extensive interface between the animal and its external environment. In teleosts, skin houses sensory organs essential for survival and helps maintain body shape and protect against shock and infection. From an ontogenic perspective the epidermis is the major component of teleost embryonic and larval skin, the dermis is present as an acellular collagen lamella and the hypodermis is completely absent (Roberts et al., 1973; Ottensen and Olafsen, 1997; Murray et al., 2003; Le Guellec et al., 2004). As teleosts undergo metamorphosis skin differentiates into the adult structure and in common with the skin in other vertebrates is composed of the outermost epidermal layer, the dermis and the innermost hypodermis (Roberts et al., 1973; Ottensen and Olafsen, 1997; Murray et al., 2003; Le Guellec et al., 2004). Relatively little is known about the cellular and molecular events which accompany larval to adult skin differentiation in teleosts.

Pleuronectiformes represent an interesting group of teleosts in which to study metamorphosis as they undergo a dramatic morphological reorganisation during this process and change from a symmetrical larva to an asymmetric juvenile. In parallel with what occurs in anurans, thyroid hormones, and more specifically, T3 drive flatfish metamorphosis (Inui and Miwa, 1985; Tagawa et al., 1990a; Yamano et al., 1991b; Yamano et al., 1994a; Inui et al., 1995; Power et al., 2001; Liu and Chan, 2002). The way in which skin is modified during this process has yet to be described. In contrast to teleosts, anuran skin development at metamorphosis has been extensively studied.

The skin in anurans undergoes significant changes during metamorphosis and represents an interesting experimental model in which to study T3-driven changes. For example, in *Xenopus laevis*, the tadpole tail supra-basal epidermal layer undergoes apoptosis autonomously in response to T3 (Schreiber and Brown, 2003). In *Rana catesbeiana* epidermal basal cells undergo differentiation in such a way that pre-metamorphic tadpole basal skin cells give rise at climax to

larval basal skin cells which, after metamorphosis, become adult basal cells (Suzuki et al., 2002; Ishida et al., 2003). Distinct skin cell populations have been identified and characterised during anuran development using molecular, cellular and histological markers (Miyatani et al., 1986; Kawai et al., 1994; Suzuki et al., 2001; Watanabe et al., 2001; Suzuki et al., 2002; Watanabe et al., 2002; Ishida et al., 2003). Such studies reveal that changes in *X. laevis* skin prompted by spontaneous and TH-induced metamorphosis are accompanied by keratin protein isoform switching (Mathisen and Miller, 1987; Mathisen and Miller, 1989) and similar changes can also be induced by T3 in isolated larval epidermal cells *in vitro* (Shimizu-Nishikawa and Miller, 1991; Nishikawa et al., 1992; Shimizu-Nishikawa and Miller, 1992). Expression of different epidermal keratin cDNAs in *X. laevis* (Miyatani et al., 1986; Watanabe et al., 2001; Watanabe et al., 2002) and *R. catesbeiana* (Suzuki et al., 2001; Suzuki et al., 2002; Ishida et al., 2003) are regulated at metamorphosis and type II keratin genes expressed in larval anuran skin are downregulated late in metamorphosis and thereafter only adult skin type I keratins are expressed (Suzuki et al., 2001; Watanabe et al., 2001; Suzuki et al., 2002; Watanabe et al., 2002; Ishida et al., 2003).

Keratins are the most abundant proteins in tetrapod skin and belong to a large family of intermediate filament proteins. They are differentially expressed in all vertebrate epithelial tissues and constitute part of the cytoskeleton of every cell. In epidermal cells, keratin bundles associate with desmosomes and are important for tissue and cell integrity during mechanical stress and also for maintenance of epithelial cell architecture (Coulombe et al., 1991; Fuchs and Weber, 1994; Kouklis et al., 1994; Lloyd et al., 1995; Hutton et al., 1998). Numerous keratin genes have been reported in vertebrates and the putative proteins they encode are grouped into acidic (type I) and basic (type II) isoforms (Moll et al., 1982; Imboden et al., 1997; Conrad et al., 1998; Hesse et al., 2001; Suzuki et al., 2001; Watanabe et al., 2001; Schaffeld et al., 2002a; Schaffeld et al., 2002b; Zimek et al., 2003). The organisation of keratin genes in the genome of fish and mammals differs significantly - in mammals type I and II keratins are organised into two independent single-class gene clusters, while in fish they are randomly distributed throughout the genome (Hesse et al., 2001; Zimek et al., 2003). Recently, a comparison between keratin cDNA sequences isolated from

zebrafish (*Danio rerio*) and *Tetraodon nigroviridis* revealed that in zebrafish more type I keratin genes exist and that they seem to have resulted from tandem duplication events (Krushna Padhi et al., 2006), suggesting keratin I genes in teleost may have different evolutionary histories.

In teleost fish, several keratins have been described (Imboden et al., 1997; Chua and Lim, 2000; Martorana et al., 2001; Schaffeld et al., 2002a; Schaffeld et al., 2002b; Schaffeld et al., 2003) and the putative genes corresponding to all Fugu keratins have been identified *in silico* (Zimek et al., 2003). The expression profile of some of these teleost keratin genes have been analysed during zebrafish embryonic development (Imboden et al., 1997; Chua and Lim, 2000) but no information exists about keratin expression during the larval period or during the larval-juvenile transition or even in adult skin. Teleosts represent an interesting group in which to study skin as the entire adult body skin surface is covered in scales and the epidermis is composed of live cells and no layer of keratinized dead cells is present. This seems to be a specific adaptation of the teleostei since in the lungfish (*Protopterus aethiopicus*), skin has the same pattern of epidermal keratin deposition as seen in land vertebrates (Schaffeld et al., 2005).

In the present study, in order to understand the molecular and structural changes which occur in teleost skin during metamorphosis, skin development was studied from a molecular, cellular and histological perspective in a pleuronectiforme, the Atlantic halibut (*Hippoglossus hippoglossus*).

2.2 Materials and methods

2.2.1 cDNA isolation of an epidermal type I keratin – hhKer1

A halibut cDNA library made from pre-metamorphic larvae to post-metamorphosed juveniles (Llewellyn et al., 1998) was plated at a density of 5,000 plaque forming units (pfu) and nitrocellulose lifts performed to screen for *keratin* genes. An ~800 base pairs (bp) *Sparus aurata*

incomplete *keratin* cDNA clone (AF013284) labelled with ^{32}P -dCTP was used for screening. Labelled probe was hybridised with nitrocellulose membranes overnight at low stringency (55°C, 6xSSC, 5x Denhardt's solution, 10µg/ml tRNA, 0.1%SDS), and then washed twice for 30 minutes at room temperature (1xSSC and 0.1%SDS) followed by two washes of 30 minutes at low stringency (55°C in 1xSSC and 0.1%SDS). The membranes were exposed overnight at -80°C to Biomax MS film (Kodak). The positive plaques were isolated and automatically excised into pBluescript II SK+/- (Stratagene). The DNA was purified and cDNA clones sequenced to give 3-fold coverage using BigDye Version 3 (Perkin-Elmer, UK) chemistry and an ABI 3700 sequencer. *In silico* analysis using tBLASTx (Altschul et al., 1997) against the GeneBank database was carried out to establish the most probable identity of the halibut cDNA sequences. Further bioinformatics analysis of the deduced sequence of halibut keratin was carried out using ProDom (Bru et al., 2005) and STRING (von Mering et al., 2005) software in order to identify conserved type I keratin protein domains. The PRINTS software (Attwood et al., 2003) was then used to identify keratin type I motifs.

2.2.2 Phylogenetic analysis

To further confirm the identity of the halibut *keratin* cDNA a Clustal X analysis (Thompson et al., 1997) was performed using the predicted protein sequence of other vertebrate *keratin I* cDNA in GeneBank or protein sequence from SwissProt databases. The *Tetraodon nigroviridis* (Jaillon et al., 2004) and *Fugu rubripes* (Aparicio et al., 2002) sequences were retrieved from the respective genomic databases. Phylogenetic trees were generated using PAUP* Version 4.0b (Swofford et al., 2001) to identify maximum parsimony with 1000 bootstrap replicates (Fitch, 1971) and a range of vertebrate type I keratin protein sequences: *Homo sapiens* keratin 10 (P13645), hsKer10; *H. sapiens* keratin 12 (NP_000214), hsKer12; *H. sapiens* keratin 13 (X14640), hsKer13; *H. sapiens* keratin 14 (P02533), hsKer14; *H. sapiens* keratin 15 (NP002266), hsKer15; *H. sapiens* keratin 16 (S79867), hsKer16; *H. sapiens* keratin 18 (X12881), hsKer18; *H. sapiens* keratin 19 (NP_002267), hsKer19; *H. sapiens* keratin 20

(NP_061883), hsKer20; *H. sapiens* keratin 23a (NP_056330), hsKer23a; *H. sapiens* keratin 24 (NP_061889), hsKer24; *H. sapiens* keratin 25C (NP_853515), hsKer25C; *H. sapiens* keratin 25D (NP_853513), hsKer25D; *Mus musculus* keratin 17 (BC032161), mmKer17; *M. musculus* keratin 18 (BC020474), mmKer18; *Xenopus laevis* adult keratin-a (AB045600), XAK A; *X. laevis* adult keratin-b (AB045601), XAK B; *X. laevis* adult keratin C (AB086829), XAK C; *X. laevis* cytokeratin I (P05781), XCK 1; *X. laevis* larval keratin 81 (X04804), XK81; *Rana catesbiana* adult keratin (AB050955), RAK; *Oncorhynchus mykiss* keratin 10 (AJ272372), omKer10; *O. mykiss* keratin 11 (AJ272371), omKer12; *O. mykiss* keratin 12 (AJ427868), omKer12; *O. mykiss* keratin 13 (AJ427867), omKer13; *O. mykiss* keratin 18 (Y14289); *Fundulus heteroclitus* keratin 13 (CN984211), fhKer13; *F. heteroclitus* keratin 18 (CV821798), fhKer18; *F. heteroclitus* keratin 19 (CV824818), fhKer19; *Carassius auratus* keratin K48 (AAC38007), caK48; *C. auratus* keratin K49 (L09743), caK49; *C. auratus* keratin K50 (Q90303), caK50; *Danio rerio* (zebrafish) type I cytokeratin enveloping layer (NP571182), zfCKE; *D. rerio* cytokeratin CKI (NP571183), zfCKI; *D. rerio* keratin 18 (NP848524), zfKer18; *D. rerio* keratin 12 (NP001003445), zfKer12; *D. rerio* keratin 17 (NP001002383), zfKer17; *D. rerio* keratin type I c11b (NP998688), zfKert1c11b; *D. rerio* keratin type 1 c11d (NP001002392), zfKert1c11d; *D. rerio* keratin type 1 c6 (NP956862), zfKert1c6; *Tetraodon nigroviridis* keratin 1 (GSTENP00036759001), tnKer1; *T. nigroviridis* keratin type 1c (GSTENT00026404001), tn type1c; *T. nigroviridis* keratin type 1b (GSTENT00013816001), tn type1b; *T. nigroviridis* keratin type 1d (GSTENT00026403001), tn type1d; *T. nigroviridis* keratin type 1e (GSTENT00026405001), tn type1e; *T. nigroviridis* keratin type 1f (GSTENT00035830001), tn type1f; *T. nigroviridis* keratin type 1g (GSTENT00020008001), tn type1g; *Fugu rubripes* keratin 1 protein sequence (fgKer1) was deduced after assembly of cDNA clones EFRn051apsaF8 and BU806120; *Scyliorhinus stellaris* keratin 18 (Y14647), ssKer18. *D. rerio* type II keratin 8 (zfKer8; NM200080) was used as an outgroup since it is considered the nearest homologue of keratin type I genes and is present in all vertebrates species studied so far (Schaffeld et al., 1998; Schaffeld et al., 2002a; Schaffeld et al., 2002b; Schaffeld

et al., 2003; Zimek et al., 2003; Hesse et al., 2004; Schaffeld et al., 2004; Krushna Padhi et al., 2006).

2.2.3 Putative genomic organization

The genomic organisation of the isolated halibut *keratin* gene was predicted by comparison *in silico* with the *Tetraodon nigroviridis* genome database (Jaillon et al., 2004). The *Tetraodon* scaffolds giving the most significant hits with halibut keratin cDNA were extracted and pairwise alignment of halibut *keratin* cDNA and the corresponding *Tetraodon* scaffolds conducted using Spidey mRNA-to-genome software (Wheelan et al., 2001).

2.2.4 Animal and tissue sampling

Atlantic halibut at well-characterised ontogenic stages ranging from pre-metamorphic (stages 5, 6) and metamorphosing larvae (7, 8 and 9) to fully metamorphosed juveniles (stage 10, (Saele et al., 2004)) were obtained from Fiskey (Iceland). Five animals per stage were killed using an overdose of MS-222 (Sigma-Aldrich) and immediately collected into RNAlater (QIAgen, UK) and stored at -20°C until subsequent RNA extraction. A further five individuals per stage were killed by an overdose of MS-222 (Sigma-Aldrich) and immediately frozen in dry ice and used for thyroxine (T4) determination. An adult halibut (1 year old) was anaesthetised in MS-222 (Sigma) and killed by decapitation and the skin collected into RNAlater (QIAgen) and stored at -20°C.

Samples of Atlantic halibut larvae and adult skin for histology and *in situ* hybridisation were collected as outlined above but were fixed in paraformaldehyde (4% PFA) at 4°C overnight, washed twice for 5 minutes with Phosphate-triton buffer (PBT; Appendix I) and stored in 100% methanol at 4°C and decalcified in 0.5M EDTA pH 8 when necessary. Halibut

larvae and adult skin was embedded in paraffin Histosec (Merk, Darmstadt, Germany), and serial 5µm transverse section cut and mounted on APES coated slides.

All animals were sacrificed in accordance with European legislation for animal welfare.

2.2.5 Total RNA extraction

Total RNA was extracted from whole individual metamorphosing halibut larvae or 100mg of adult halibut tissue using Tri reagent (Sigma, UK) and following the manufacturers instructions. Total RNA suspended in sterile water was quantified by spectrophotometry (GeneQuant, Amersham Biosciences) and stored at -80°C until use.

2.2.6 Northern Blot

Total RNA from adult skin (3 µg) or from pools of five halibut of each stage (3 µg) was fractionated on a 1.5% agarose/5.5% formaldehyde gel which was run in 1x MOPS. RNA was transferred to nylon Hybond-N membranes (Amersham Biosciences) with 10x SSC overnight and cross-linked using UV light (Stratalinker, Stratagene). Membranes were hybridised overnight at high stringency (65°C in 6xSSC, 5x Denhardt's solution, 100µg/mL tRNA and 0.1%SDS) with a ³²P-dCTP-labeled 561bp DNA probe made from an *XhoI/SacI* digestion of the full-length halibut *keratin* cDNA clone that corresponded to C-terminal region of the putative protein and part of the 3'UTR. The membranes were then washed twice for 30 minutes at room temperature (1xSSC and 0.1%SDS) followed by two 30 minute high stringency washes (65°C in 1xSSC and 0.1%SDS) and exposed at -80°C to a Biomax MS film (Kodac, USA).

2.2.7 Semi-Quantitative RT-PCR analysis of halibut keratin expression during halibut metamorphosis

In order to determine the expression of the halibut *keratin* gene during metamorphosis a semi-quantitative RT-PCR assay was developed. For each sample 0.5µg of total RNA was treated with DNase following the protocol provided with the Ambion DNA Free kit (Ca, USA). DNase treated total RNA was used for first strand cDNA synthesis which was carried out in a 20µL volume using 0.05M Tris-HCl, pH8.3, 0.075M KCl, 3mM MgCl₂, 0.01M DTT, 1mM dNTP, 5pmol/µl random hexamer primers, 4U of RNase inhibitor (Promega, UK) and 10U of Superscript II reverse transcriptase (Invitrogen, UK). An iCycler thermocycler (Perkin Elmer) programmed for 10 minutes at 25°C followed by 50 minutes at 42°C and final heating for 2 minutes at 70°C was used for cDNA synthesis. Five individual cDNA synthesis reactions corresponding to five individual animals per stage were performed.

Initial experiments were conducted with halibut *keratin* specific primers to determine optimal cycle number to ensure that template amplification occurred in the logarithmic phase of the reaction. Normalisation of the total amount of cDNA introduced in each reaction was carried out using the expression of 18s ribosomal RNA (*rRNA*).

The halibut *keratin* gene RT-PCR analysis was carried out in a 25µl reaction volume containing ~20 ng of cDNA and 1.5 mM MgCl₂, 0.1 mM dNTP's, 1 pmol/µl of halibut keratin forward and reverse primer (respectively, CAGACTGGAGATGGAGATCG and CAGACAGAAGCTGTTGGTGG) and 0.6U *Taq* polymerase (Sigma-Aldrich). Primers were selected to amplify the 5' region of the cDNA which is the most variable region in vertebrate keratin genes and confers higher isoform specificity. The forward primer was located in the 5'UTR region of the isolated halibut keratin cDNA and the reverse primer in the coding region corresponding to the N-terminus of the putative protein. The PCR reactions were performed in an iCycler (Perkin Elmer) thermocycler, in the logarithmic amplification phase using the

following cycle; 1 minute at 95°C followed by 29 cycles of 30 seconds at 95°C, 1 minute at 56°C and 30 seconds at 72°C, followed by a final step of 1 minute at 72°C. Negative reactions without sample cDNA were also performed.

Transcripts of the *18s rRNA* gene were amplified in a 25µl reaction containing ~20ng of cDNA, 1 pmol/µl of forward and reverse primer (5'-TCAAGAACGAAAGTCGGAGG-3' and 5'-GGACATCTAAGGGCATCACA-3' respectively), 1.5 mM MgCl₂, 0.1 mM dNTP's and 0.6U of *Taq* polymerase (Sigma). The thermocycle utilised was: 1 minute at 95°C followed by 18 cycles of 30 seconds at 95°C, 1 minute at 56°C and 30 seconds at 72°C, followed by a final step of 1 minute at 72°C. All RT-PCR reaction products were fractionated on 2.5% agarose gels and analysed by densitometry using LabWorks version 4.5 software (Ultra-Violet Products Cambridge, UK). Results are expressed as the mean and standard error of five independent samples.

2.2.7 Radioimmunoassay for thyroid hormones

Whole body extracts of five individual animals per stage were prepared and used to assess T4 content of whole larvae by radioimmunoassay using a double-antibody method under equilibrium conditions as previously described (Einarsdóttir et al., 2006). In order to determine statistical differences in T4 levels at the different stages of halibut metamorphosis One Way Analysis of Variance was used and pair-wise comparisons were performed by using the Holm-Sidak method (HSM) for multiple comparison test. All statistical analysis were performed in the SigmaStat version 3 software (SPSS, Inc). Statistical significant differences were considered if $p < 0.05$.

2.2.8 Histology

In order to characterise halibut skin developmental ontogeny, sectioned larvae (n=5) were stained using Masson trichrome staining (Masson, 1929). Tissue sections were dewaxed and hydrated, stained in Mayer's haematoxylin for 5 min, rinsed in tap water and distilled water, followed by staining in 1% acetic acid containing 0.5% xylidine ponceau 2R and 0.5% acid fuchsin for 2 min. Subsequently, tissue sections were rinsed in distilled water, differentiated for 4 min in 1% aqueous phosphomolybdic acid, rinsed in distilled water and stained in light green 0.2% in 0.2% citric acid for 1.5 min. Finally, sections were rapidly rinsed in two changes of absolute alcohol, followed by xylene and mounted in DPX.

When exposed to blue light (460-490 nm) under a fluorescent microscope anuran basal skin cells from tissue sections double-stained with hematoxylin/eosin can be easily identified because the keratin bundles are fluorescent in tadpoles and larvae but not in adult basal cells (Kawai et al., 1994; Suzuki et al., 2002). A similar approach was taken to study halibut skin development during metamorphosis. Adjacent halibut sections were stained with Harris's hematoxylin and eosin (Stevens, 1990) and processed and mounted in DPX. Sections were analysed using a light and fluorescent microscope Leica DM 2000 coupled to a Leica DX430 digital camera for digital image analysis.

2.2.9 *In situ* hybridisation

The pattern of expression of halibut *keratin 1* mRNA in the skin of developing halibut larvae was investigated by *in situ* hybridisation. The 3'UTR of the halibut *keratin* cDNA, inserted in a pGemT vector (Promega) was linearized with *Sal I* (20 units, Promega) at 37°C for 1.5 h. The linearized vector was purified and *in vitro* transcription carried out using 20U of T7 RNA polymerase in transcription buffer (Promega) with 1 µl of digoxigenin-RNA labelling mix (Roche Diagnostics, Mannheim, Germany), for 1.5 h at 37 °C. The reaction was stopped with 2

μl of 0.2M EDTA. To further confirm the identity of the halibut skin cells which express *hhKer1*, *in situ* hybridisation was carried out using a 500 bp digoxigenin-labelled cRNA anti-sense probe of the 3'UTR region of *S. aurata Collagen 1a1* (*saColl1a1*) (accession number DQ324363), which shows a good conservation with other fish *collagen1a1* sequences. The probe was generated by linearising cDNA of *saColl1a1* cloned in pBlueScript (Stratagene) with *EcoRI* (20 units, Promega) for 1.5h at 37°C. *In vitro* transcription was then performed with the extracted linear vector as described previously. The digoxigenin labelled riboprobes were purified by lithium precipitation and resuspended in 25 μl of water. Riboprobe purity and concentration were determined by fractionation of reaction products on an agarose gel (1.5%).

For *in situ* hybridisation experiments tissue sections were dewaxed, rehydrated and then prehybridised at 58°C for 2h in hybridisation solution without probe (50% formamide, 4 \times SSC, 1 mg ml⁻¹ torula RNA, 0.1 mg ml⁻¹ heparin, 1 \times Denhardt's, 0.04% CHAPS). Tissues were then hybridised overnight in a humidified box at 58°C in 100 μl per section of hybridisation solution containing approximately 2 ng μl^{-1} of *hhKer1* or *saColl1a1* riboprobes. Controls were pretreated with RNase prior to hybridisation with riboprobes or the riboprobes were excluded from the hybridisations. The *in situ* hybridisations for *hhKer1* and *saColl1a1* riboprobes was carried out using adjacent sections.

Stringency washes were 3 \times 5 min at 58°C with 2 \times SSC and 5 min at 58°C in 1 \times SSC. Tissue sections were then washed 2 \times 5 min with 2 \times SSC:0.12% CHAPS at RT, followed by a wash for 5 min in 2 \times SSC:PTW (1:1, v/v) and finally 5 min in PTW. Blocking was performed by incubation in blocking reagent (Boehringer Mannheim, Germany) with 10% heat inactivated sheep serum, detection of hybridised probe was carried out using sheep anti-digoxigenin-alkaline phosphatase (AP) Fab fragments (1/600) (Roche, Lisbon, Portugal). The chromagens for colour detection were NBT (4-nitroblue tetrazolium chloride) and BCIP (5-bromo-4-chloro 3-indolylphosphate) and colour development was carried out over 2h at 38°C. Stained sections

were rinsed in PBS, fixed for 15 min in 4% formaldehyde at room temperature, rinsed in PBS and mounted in glycerol gelatine. Sections were analysed using a microscope (Olympus BH2) coupled to a digital camera (Olympus DP11) linked to a computer for digital image analysis.

2.3 Results

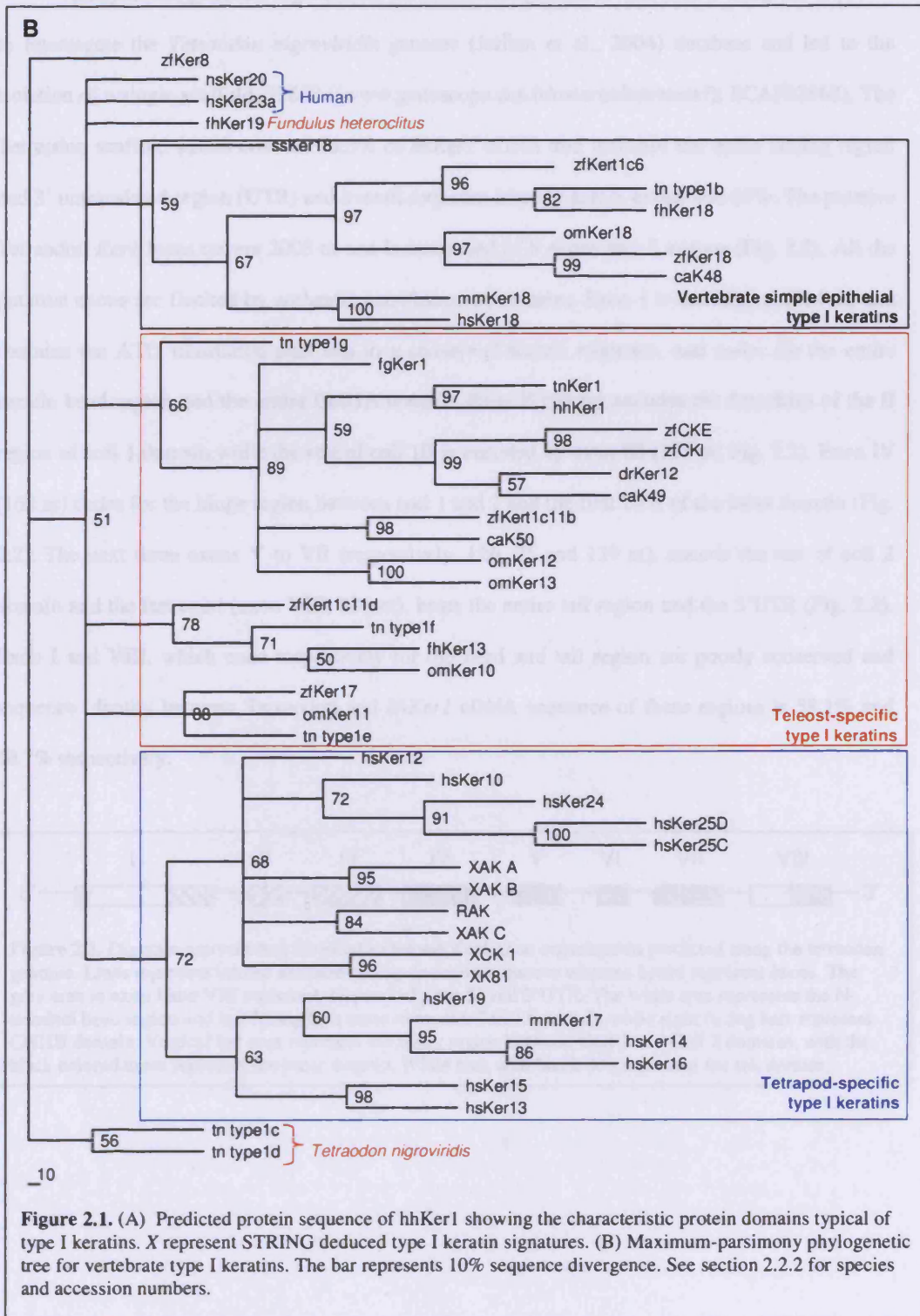
2.3.1 Halibut keratin 1 (*hhKer1*)

Analysis of the sequence of a cDNA clone isolated from a cDNA library prepared from metamorphosing halibut using tBLASTx searches of GenBank (Altschul et al., 1997) gave a highly significant match with teleost *type I keratin*, although no significant orthology relationships was identified. The cDNA clone designated *Hippoglossus hippoglossus keratin 1 (hhKer1; DQ364242)* is 1550 nucleotides (nt) and encodes a putative protein of 446 amino acids (aa) (Fig. 2.1A). The predicted pI of the putative hhKer1 protein is 5.11 and the predicted molecular weight is 47.81 kDa (Wilkins et al., 1998). Analysis of the predicted protein sequence of hhKer1 using ProDom (Bru et al., 2005) and STRING computational analysis (von Mering et al., 2005) revealed that it contains all the characteristic domains of vertebrate type I keratin. Namely, an N-terminal head and C-terminal tail region in addition to a central rod-like region (Fig. 2.1A). The head region (from aa 1 to aa 108; Fig. 2.1A) is very glycine rich and no domain related identification was possible in the ProDom database. The tail region of hhKer1 is small and comprises 30 residues, from aa 418 to 446 (Fig. 2.1A). The entire central α -helical rod domain extends from aa 109 to 417 and amino acids 109-250 and 278-417 encompass coil 1 and coil 2 respectively (Fig. 2.1A). Further computational analysis with PRINTS (Attwood et al., 2003) (X in Fig. 2.1A) identified five motifs in the predicted hhKer1 protein which are present exclusively in vertebrate epidermal type I keratins and are absent from simple epithelial keratins.

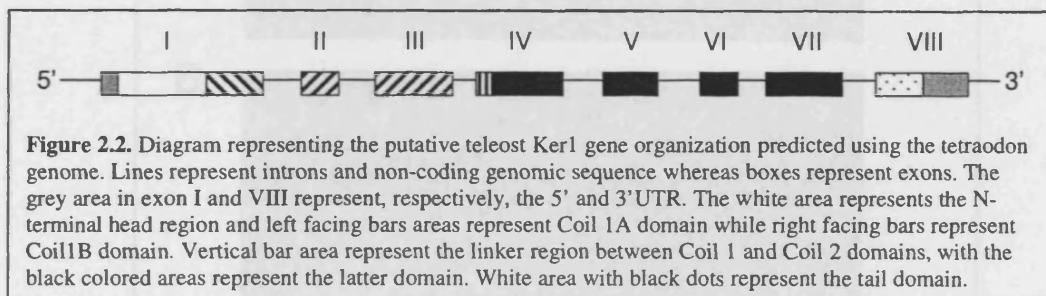
In silico analysis permitted the assignment of hhKer1 to the specific protein family of epidermal type I keratins (Fig. 2.1B). However, it was not possible to establish orthology

relationships with any of the previously described vertebrate *keratin* genes. Further tBLASTx analysis (Altschul et al., 1997) against the *Tetraodon nigroviridis* genome (Jaillon et al., 2004) was carried out in order to further explore the classification of the *hhKer1* cDNA isolated. The *Tetraodon* search gave a high match to scaffold, SCAF22868 that, in turn, matches the locus of *type I keratin 17* and *19* in human and mouse respectively in the Genewise IPI database. These results did not establish which vertebrate keratin genes are true orthologues of *hhKer1*.

Phylogenetic analysis of *hhKer1* and the predicted protein sequence of other vertebrate type I keratin genes by maximum-parsimony analysis (Swofford et al., 2001) using zebrafish type II keratin 8 protein sequence (*zfKer8*; Fig. 2.1B) as an outgroup, clustered the tetrapod and teleost keratin type I sequences in a super clade. The *T. nigroviridis* keratins *type1c* and *type1d* genes were the only keratin type I genes that did not cluster in the vertebrate keratin type I super clade (Fig. 2.1B). Within the keratin type I super clade the simple epithelial keratin 18 genes of the vertebrate species used clustered together and had a typical vertebrate topology (Fig. 2.1B). The non-simple epithelial keratin type I sequences formed four clades, one of which contained the tetrapod type I keratins with the exception of human Keratin 20 and 23a (Fig. 2.1B). In turn the remaining three clades are of teleost keratin type I sequences (Fig. 2.1B). The *hhKer1* sequence is located in the teleost specific clade containing the greatest number of sequences and closely clustered in a unique twig with the *T. nigroviridis* scaffold 22868 Genoscope-deduced (Jaillon et al., 2004) putative Ker1 protein (55% similarity; GSTENP00036759001; Fig. 2.1B). The zebrafish *zfCKE* (52.8% similarity with *hhKer1*), *zfCKI* (49.5% similarity with *hhKer1*) and *zfKer12* (54.8% similarity with *hhKer1*) and *C. auratus* *caK49* (54.5 similarity with *hhKer1*) also clustered closely with *hhKer1* but in a separate twig (Fig. 2.1B). The sequence similarity of the other teleost type I keratins which grouped with *hhKer1* varies from 48.9% (*omKer12*) to 45.8% (*fgKer1*; Fig. 2.1B). With all other vertebrate keratin type I protein sequences used in the phylogenetic analysis, *hhKer1* sequence similarity is always below 40%.



The putative genomic organization of the *hhKer1* gene was determined using the sequence to interrogate the *Tetraodon nigroviridis* genome (Jaillon et al., 2004) database and led to the isolation of a single scaffold, 22868 ((www.genoscope.cns.fr/externe/tetranew/); SCAF22868). The Tetraodon scaffold 22868 covered 99.5% of *hhKer1* cDNA and included the entire coding region and 3' untranslated region (UTR) and overall sequence identity across exons was 67%. The putative Tetraodon *Ker1* locus covers 2005 nt and is composed of 8 exons and 7 introns (Fig. 2.2). All the putative exons are flanked by authentic exon/intron boundaries. Exon I is the longest (514 nt) and contains the ATG translation start site in a conserved Kozak sequence, and codes for the entire keratin head region and the entire Coil1A domain. Exon II (83 nt) encodes the first third of the B region of coil 1 domain while the rest of coil 1B is encoded by exon III (157 nt; Fig. 2.2). Exon IV (162 nt) codes for the hinge region between coil 1 and 2 and the first 28% of the latter domain (Fig. 2.2). The next three exons V to VII (respectively, 126, 75 and 139 nt), encode the rest of coil 2 domain and the last exon (exon VIII, 286 nt), bears the entire tail region and the 3'UTR (Fig. 2.2). Exon I and VIII, which code respectively for the head and tail region are poorly conserved and sequence identity between Tetraodon and *hhKer1* cDNA sequence of these regions is 58.1% and 40.7% respectively.



2.3.2 *hhKer1* expression and *T4* levels during halibut metamorphosis

Expression of *hhKer1* during halibut metamorphosis and in adult skin was studied by northern blot (Fig. 2.3) and semi-quantitative RT-PCR (Fig. 2.4). Northern blot experiments using 3µg of a pool of five halibut per metamorphic stage and hybridised with a 3'UTR probe of *hhKer1* showed that a single transcript exists and that its expression is abundant in pre-metamorphic larvae up until stage 6 but as soon as halibut enter pro-metamorphosis (Stg 7) expression starts to decline. Thereafter *hhKer1* expression declines continuously through Stg 8 (beginning of metamorphosis) and Stg 9 (climax) and is barely detectable in Stg 10, fully metamorphosed juveniles (Fig. 2.3). In adult halibut skin *hhKer1* is undetectable (Fig. 2.3).

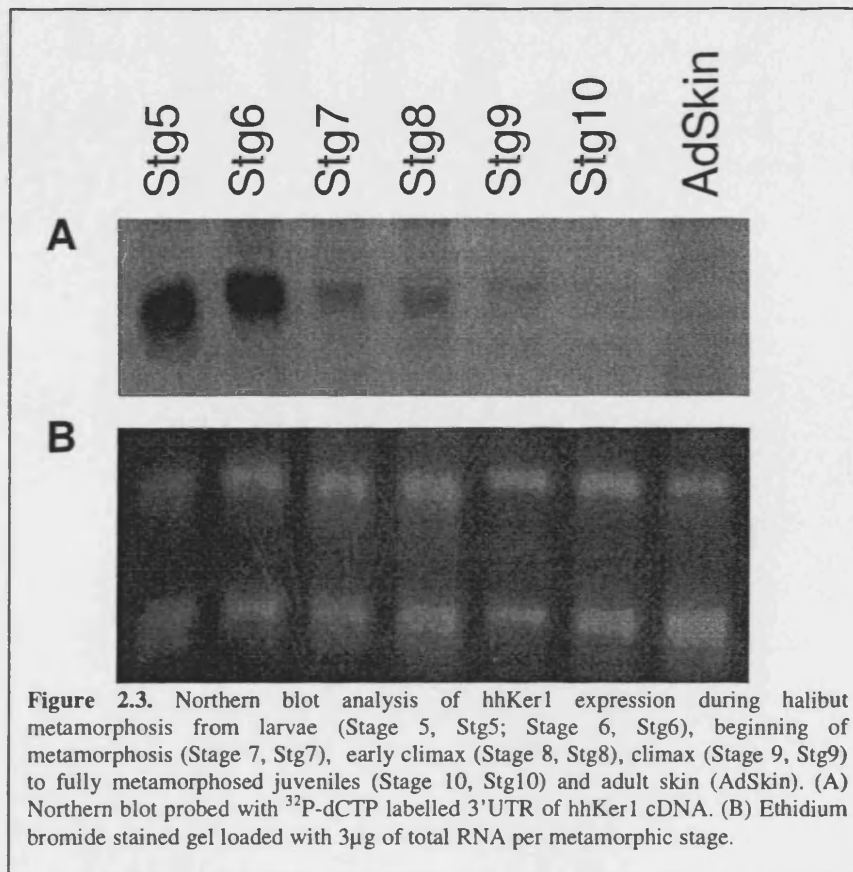


Figure 2.3. Northern blot analysis of *hhKer1* expression during halibut metamorphosis from larvae (Stage 5, Stg5; Stage 6, Stg6), beginning of metamorphosis (Stage 7, Stg7), early climax (Stage 8, Stg8), climax (Stage 9, Stg9) to fully metamorphosed juveniles (Stage 10, Stg10) and adult skin (AdSkin). (A) Northern blot probed with ^{32}P -dCTP labelled 3'UTR of *hhKer1* cDNA. (B) Ethidium bromide stained gel loaded with 3µg of total RNA per metamorphic stage.

The semi-quantitative RT-PCR of *hhKer1* confirmed the northern blot results (Fig. 2.3 and 2.4). The expression of *hhKer1* in pre-metamorphic larvae is very abundant but as metamorphosis approaches it starts to decline (Fig. 2.4). At the climax of metamorphosis, Stg 9, *hhKer1* expression is ~6-fold lower than any of the previous stages (Fig. 2.4). In fully metamorphosed juveniles (Stg 10) expression of *hhKer1* is ~16-fold lower than Stg 5 and ~3-fold lower than Stg 9 halibut (Fig. 2.4B). In adult halibut skin *hhKer1* is almost undetectable (Fig. 2.4B). Up until the beginning of climax (Stg8), T4 levels are fairly constant and no significant differences are found between the different stages of development (HSM, $p>0.05$; Fig. 2.4C). However, by stage 9 (climax of metamorphosis) T4 levels increase ~3-fold in relation to previous stages (HSM, $p<0.001$, Fig. 2.4C). In juveniles after metamorphosis (Stg10) T4 levels are significantly higher than all other previous stages (Stage 5 to 8, HSM, $p<0.001$; stage 9, HSM, $p=0.003$; Fig. 2.4C).

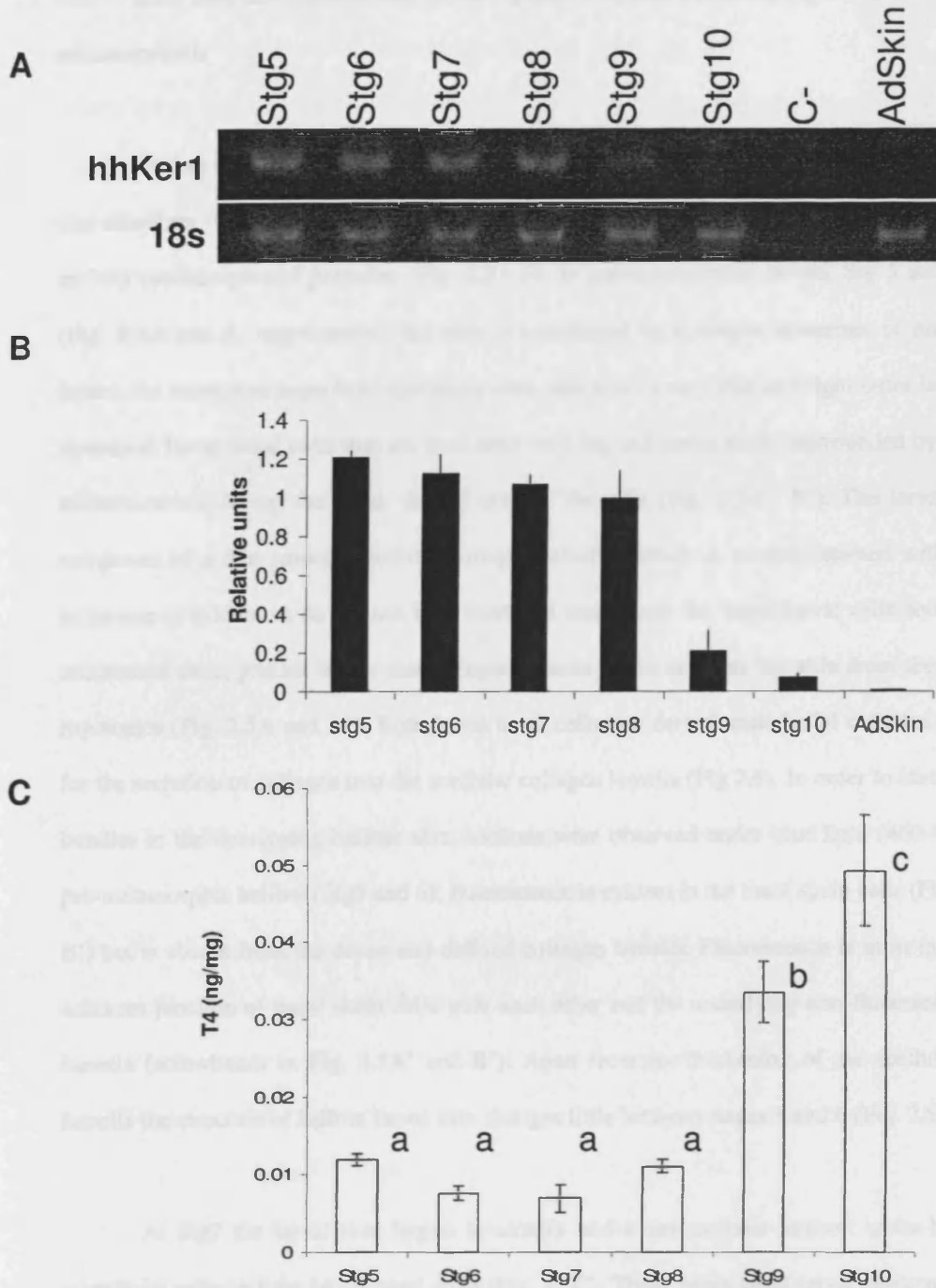


Figure 2.4. (A) RT-PCR analysis of expression of hhKer1 during halibut metamorphosis, and in adult halibut skin. The expression of 18s rRNA is also shown and used as an internal reference. (B) hhKer1:18s rRNA expression ratio during halibut metamorphosis, and in adult skin. C- control (no template). (C) Whole body T4 levels (ng T4/mg animal) during halibut metamorphosis. In Figure 3.4C "a" denotes no significant statistical differences observed (HSM, $p > 0.05$) in T4 levels between stages with the same letter; "b" denotes significant statistical differences between stage 9 (HSM, $p < 0.001$) T4 levels and all the other stages; and "c" denotes statistical significant differences between T4 levels of juveniles after metamorphosis (Stg10) and all other previous stages (Stage 5 to 8, HSM, $p < 0.001$; stage 9, HSM, $p = 0.003$). Bars represent standard error.

2.3.3 Skin development and hhKer1 spatial temporal pattern of expression during halibut metamorphosis

During the course of halibut metamorphosis skin undergoes a series of histological changes that transform the pre-metamorphic larval skin from a very thin epithelia to a highly stratified skin in fully metamorphosed juveniles (Fig. 2.5A-F). In pre-metamorphic larvae, Stg 5 and 6 animals (Fig. 2.5A and B, respectively), the skin is constituted by a simple epidermis of only two cell layers: the outermost superficial epithelial cells, that form a very thin and tight outer layer and the innermost larval basal cells that are oval with very big and dense nuclei surrounded by bundles of microfilaments facing the basal, dermal side of the cells (Fig. 2.5A', B'). The larval dermis is composed of a thin smooth acellular collagen lamella, which in sections stained with Masson's trichrome is evident as an intense blue band just underneath the basal larval cells and by dermal endothelial cells, present below the collagen lamella which separate the skin from the underlying myotomes (Fig. 2.5A and A'). Both larval basal cells and dermal endothelial cells are responsible for the secretion of collagen into the acellular collagen lamella (Fig 2.6). In order to identify keratin bundles in the developing halibut skin, sections were observed under blue light (460-490 nm). In pre-metamorphic halibut (Stg5 and 6), fluorescence is evident in the basal skin cells (Fig. 2.5B and B') but is absent from the dense and defined collagen lamella. Fluorescence is most intense at the adherent junction of basal skin cells with each other and the underlying non-fluorescent collagen lamella (arrowheads in Fig. 2.5A' and B'). Apart from the thickening of the acellular collagen lamella the structure of halibut larval skin changes little between stages 5 and 6 (Fig. 2.5B).

At Stg7 the larval skin begins to stratify and a new cellular stratum arises between the superficial cells and the larval basal cells (Fig. 2.5C). These supra-basal larval epidermal cells are pyramidal in shape and contain no microfilament bundles or cytoplasmic fluorescence around the nuclei (Fig. 2.5C and C'). As halibut enter metamorphosis, at Stg8, basal epidermal cells start to acquire a more cuboid morphology and in the dermis the collagen lamella continues to increase in thickness (Fig. 2.5D). At the climax of metamorphosis (Stg 9, Fig. 2.5E), the halibut skin starts to

acquire adult characteristics and the epidermis contains three clear strata; the outermost epithelial cells, the supra-basal epidermal cells and the basal, presumptive, adult cells (Fig. 2.5E), as well as, some mucous cells (* in Fig. 2.5E). Most of the deep epidermal cells have already acquired all the features of an adult cell and both basal and supra-basal cells are cube shaped and there is a total absence of microfilament bundles in the cytoplasm which coincides with the loss of fluorescence in these cells (Fig. 2.5E and E'). Nevertheless, some cytoplasmic fluorescence is still evident in a few scattered cells of the epidermis (Fig. 2.5E') suggesting that not all epidermal cells have undergone differentiation into an adult cell type. In the dermis, the collagen lamella starts to acquire a characteristic adult plywood-arrangement and fibroblast-like cells start to invade the acellular collagen lamella from its proximal side (arrowheads in Fig. 2.5E). Coincidentally, the collagen lamella becomes fluorescent indicating that structural modifications are occurring. Just underneath the dermis pigment cells start to appear (Arrowhead in Fig. 2.5E). The dermal endothelial cells become thinner and less evident but still form a continuous layer just underneath the collagen lamella (Fig. 2.5E).

In fully metamorphosed juvenile skin, the epidermis is composed of several layers and cell types (Fig. 2.5F). Mucous cells now intercalate the superficial epithelial cells and the supra-basal region of the epidermis has further stratified (Fig. 2.5F). All deep epidermal cells now have characteristics of adult cells and the adult basal cells form a contiguous layer of cuboidal cells (Fig. 2.5F). Notably, fluorescence is not detected in any cell types in halibut post-metamorphic juvenile skin (Fig. 2.5F and F') indicative of the absence of keratin filaments and keratinisation of halibut adult skin. In the dermis, fibroblast-like cells densely populate the collagen lamella that has intensified its plywood-like arrangement (Fig. 2.5F) and fluoresces slightly under blue light (Fig. 2.5F'). The dermal endothelial cells have proliferated and thickened, the hypoderm and pigment cells start to appear scattered both in the dermis and epidermis (Fig. 2.5F). At this stage, the first scales start to appear in the mid-line region of the body.

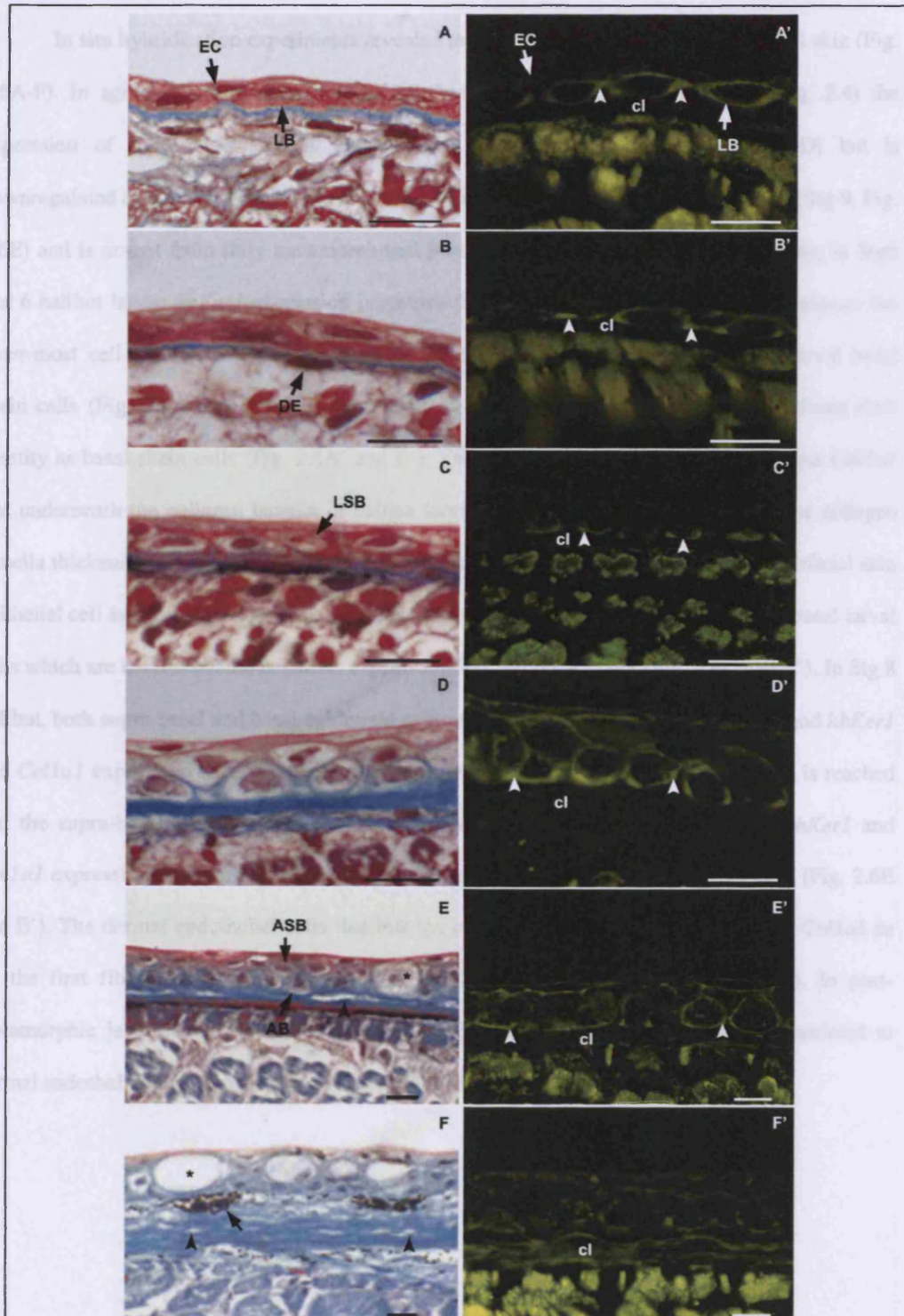
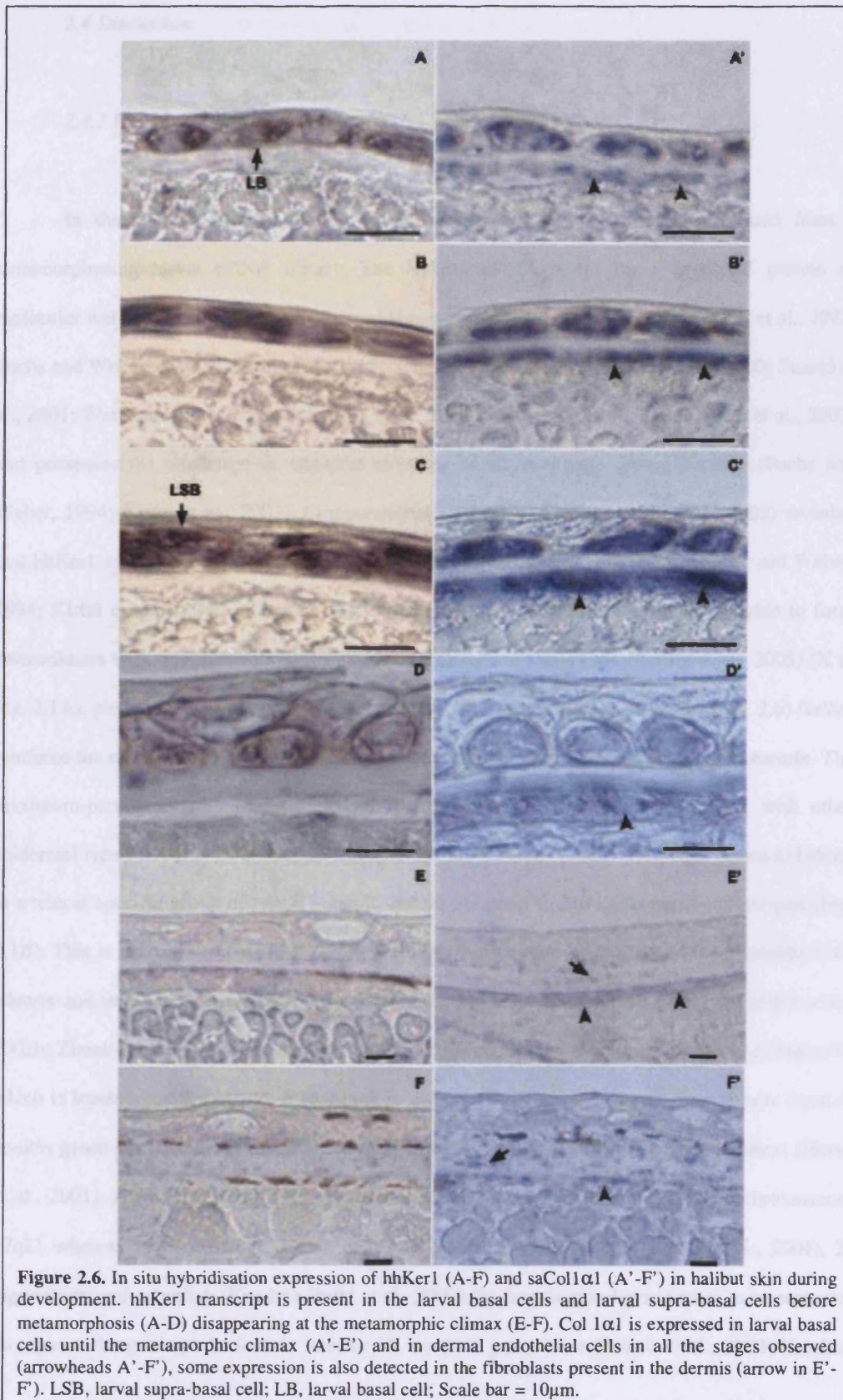


Figure 2.5. Masson trichrome staining (A-F) and detection of keratin filaments by fluorescence microscopy (A'-F') in halibut skin during development. EC, epithelial cells; LB, larval basal cells; DE, dermal endothelial cells; LSB, larval supra-basal cells; ASB, adult supra-basal cells; AB, adult basal cells; *, mucus cells; arrowheads in E,F indicate fibroblast-like cells in the collagen lamella; arrow in F denotes melanocyte; arrowheads in A'-E', indicate fluorescent keratin in basal cells and supra-basal cells; cl, collagen lamella. Note the fluorescent background on muscle fibers underlining the dermis. Scale bar = 10µm.

In situ hybridisation experiments revealed that *hhKer1* is specific to halibut larval skin (Fig. 2.6A-F). In agreement with the results of northern blot (Fig. 2.3) and RT-PCR (Fig. 2.4) the expression of *hhKer1* in skin is abundant up until metamorphosis (Fig. 2.6A-D) but is downregulated to almost undetectable levels in animals at the climax of metamorphosis (Stg 9, Fig. 2.6E) and is absent from fully metamorphosed juvenile skin (Stg 10, Fig. 2.6F). Notably, in Stg 5 and 6 halibut larvae *hhKer1* expression is restricted to a single cell population that constitutes the inner-most cell layer of the pre-metamorphic halibut larval epidermis, the putative larval basal skin cells (Fig. 2.6A and B'). The expression of *collagen 1a1* in this cell layer confirms their identity as basal skin cells (Fig. 2.6A' and B'). The dermal endothelial cells also express *Coll1a1* just underneath the collagen lamella of halibut larval skin and probably contribute to the collagen lamella thickening (Fig. 2.6A' and B'). No expression of *hhKer1* is observed in the superficial skin epithelial cell layer at any stage of halibut metamorphosis (Fig. 2.6). At Stg 7 the supra-basal larval cells which are keratin bundle negative, express *hhKer1* but not *Coll1a1* (Fig. 2.6C and C'). In Stg 8 halibut, both supra-basal and basal epidermal cells start to lose their larval morphology and *hhKer1* and *Coll1a1* expression is reduced (Fig. 2.6D and D'). As the climax of metamorphosis is reached and the supra-basal and basal epidermal cells achieve their final adult phenotype, *hhKer1* and *Coll1a1* expression is down regulated and only detectable in a few deep epidermal cells (Fig. 2.6E and E'). The dermal endothelial cells that line the collagen lamella continue to express *Coll1a1* as do the first fibroblasts that invade the collagen lamella (arrowheads in Fig. 2.6E'). In post-metamorphic juveniles no *hhKer1* expression is detected and *Coll1a1* expression is restricted to dermal endothelial cells and fibroblast-like cells of the collagen lamella (Fig. 2.6F').



2.4 Discussion

2.4.1 Halibut larval epidermal keratin type I gene – *hhKer1*

In the present study a halibut *type I epidermal keratin* gene was isolated from a metamorphosing larval cDNA library. The *hhKer1* cDNA codes for a predicted protein of molecular weight and pI within the expected values for vertebrate type I keratins (Moll et al., 1982; Fuchs and Weber, 1994; Conrad et al., 1998; Schaffeld et al., 1998; Chua and Lim, 2000; Suzuki et al., 2001; Watanabe et al., 2001; Schaffeld et al., 2002b; Watanabe et al., 2002; Ishida et al., 2003) and possesses the characteristic tripartite structure of all vertebrate type I keratins (Fuchs and Weber, 1994; Kirfel et al., 2003). Computational analysis in ProDom (Bru et al., 2005) revealed that *hhKer1* contains all the elements of a functional type I keratin (Fig. 2.1A) (Fuchs and Weber, 1994; Kirfel et al., 2003), indicating that *hhKer1* codes for a type I keratin that is able to form heterodimers with type II keratins. Results from STRING analysis (von Mering et al., 2005) (X in Fig. 2.1A), phylogenetic analysis (Fig. 2.1B) and *in situ* hybridisation experiments (Fig. 2.6) further reinforce the classification of the isolated halibut keratin cDNA as an *epidermal type I keratin*. The maximum-parsimony phylogenetic analysis performed (Fig. 2.1B) clusters *hhKer1* with other epidermal type I keratins from teleosts (Schaffeld et al., 2002b). Moreover, *hhKer1* seems to belong to a teleost specific group of type I keratins that do not seem to have a tetrapod counter-part (Fig. 2.1B). This is not unexpected since results from previous studies suggest that type I keratins from teleosts and tetrapods radiated and diversified independently (Hesse et al., 2001; Schaffeld et al., 2002b; Zimek et al., 2003; Krushna Padhi et al., 2006). With the exception of *keratin 18 (hsKer18)* which is located besides *keratin 8 (hsKer8)* in the type II keratin cluster, the human *type I* and *II keratin* genes are segregated on different chromosomes and form two independent clusters (Hesse et al., 2001). All human *keratin type I* genes are localised in a cluster of ~1Mb on chromosome 17q21 whereas in *F. rubripes* (Hesse et al., 2001; Zimek et al., 2003; Hesse et al., 2004), *T. nigroviridis* and zebrafish (Krushna Padhi et al., 2006) the *keratin type I* genes seem to be scattered throughout the genome. In fact, in teleosts 19 *keratin I* genes exist (Zimek et al., 2003; Krushna

Padhi et al., 2006) whereas in humans the number of non-hair *keratin type I* genes is 16 (Hesse et al., 2001; Hesse et al., 2004). In the present study the phylogenetic analysis performed resolved a tree (Fig. 2.1B) which in line with previous studies implies that independent radiation of keratin type I genes occurred between the tetrapods and teleosts (Hesse et al., 2001; Schaffeld et al., 2002a; Schaffeld et al., 2002b; Zimek et al., 2003). Phylogenetic analysis of type I keratins revealed that *hhKer1* has no tetrapod orthologue but in teleosts putative orthologues were found in *T. nigroviridis* (*mKer1*) and zebrafish (zfCKE, zfCKI and zfKer12; Fig. 2.1B). The three zebrafish *keratin type I* genes may have arisen from specific zebrafish gene duplication events. In fact, a comparative study of type I keratins in *F. rubripes*, *T. nigroviridis* and zebrafish showed the existence of different keratin type I gene duplication events between the pufferfishes and the zebrafish (Krushna Padhi et al., 2006). However, it remains to be established if the *hhKer1* putative homologues also have a similar temporal and cellular expression pattern in *T. nigroviridis* and zebrafish skin ontogeny.

In order to more fully characterise *hhKer1* the putative *in silico* genomic organization of the orthologue in *T. nigroviridis* was established (Fig. 2.2). The *Ker1* Tetraodon gene had a similar genomic organisation to other vertebrate *keratin type I* genes (Miyatani et al., 1986; Troyanovsky et al., 1992; Nishida et al., 1997). Due to the more compact genome of Tetraodon (Jaillon et al., 2004) the *Ker1* locus is the smallest vertebrate *epidermal keratin type I* gene described so far and spans only 2005 bp whereas the *X. laevis XK81*, and human *keratin 12* and *17* are bigger and are respectively, ~3.5, ~6 and ~5kb as a consequence of differences in intron size (Table 2.1)(Miyatani et al., 1986; Rosenberg et al., 1988; Troyanovsky et al., 1992; Nishida et al., 1997). The organisation of the tetraodon *Ker1* gene and the regions of the protein encoded by the exons is almost totally conserved between *X. laevis XK81* (Miyatani et al., 1986) and human *keratin 12* (*hsKer12*) (Nishida et al., 1997) and *17* genes (*hsKer17*) (Fig. 2.2 and Table 2.1)(Rosenberg et al., 1988; Troyanovsky et al., 1992). The results suggest that although independent evolution of *type I keratin* genes occurred in tetrapods and teleosts (Hesse et al., 2001; Schaffeld et al., 2002b; Zimek et al., 2003) there has been strong pressure to maintain *type I keratin* gene organisation in vertebrates.

Table 2.1. Exon size of epidermal type I keratin from the putative teleost *Ker1*, *X. laevis XK81* (Miyatani et al. 1986), *H. sapiens Ker12* (Nishida et al. 1997) and *Ker17* (Trojanovsky et al. 1992) genes.

Exon	Ker1 (nt)	XK81 (nt)	hsKer12 (nt)	hsKer17 (nt)
I	514	469	567	528
II	83	83	83	83
III	157	157	257	157
IV	162	162	162	162
V	126	126	126	126
VI	75	218	221	221
VII	139	47	71	47
VIII	286	208	457	229

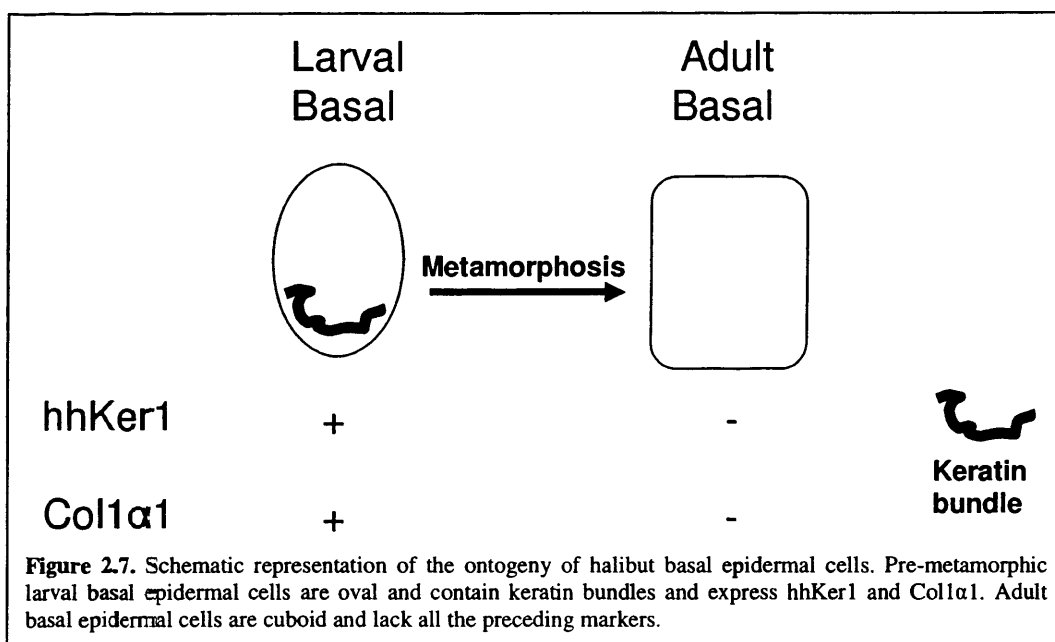
The halibut *Ker1* gene is downregulated at the climax of metamorphosis, making it a halibut larval-specific gene (Fig. 2.3, 2.4 and 2.6). Moreover, the downregulation of *hhKer* is negatively correlated with the increase in T4 levels that occurs at the climax of halibut metamorphosis (Fig. 2.4B and C). In common with other vertebrate *epidermal keratin* genes (Dale et al., 1985; Jonas et al., 1985; Suzuki et al., 2001; Watanabe et al., 2001; Suzuki et al., 2002; Watanabe et al., 2002; Ishida et al., 2003), *hhKer1* has a developmental specific pattern of expression. In both humans and anurans it has been shown that certain keratin genes are under the regulation of thyroid hormones (Ellison et al., 1985; Jonas et al., 1985; Nishikawa et al., 1992; Tomic-Canic et al., 1992; Tomic-Canic et al., 1996a; Tomic-Canic et al., 1996b; Radoja et al., 1997; Jho et al., 2001; Watanabe et al., 2001; Watanabe et al., 2002; Radoja et al., 2004; Jho et al., 2005). In humans, thyroid hormones appear to have a novel action on the *epidermal keratin* gene promoter (Tomic-Canic et al., 1992; Tomic-Canic et al., 1996a; Tomic-Canic et al., 1996b; Radoja et al., 1997; Jho et al., 2001; Radoja et al., 2004; Jho et al., 2005). Instead of gene activation via the classical thyroid hormone mechanism (Zhang and Lazar, 2000), activation of the *epidermal keratin* gene occurs in the absence of T3 as a consequence of the formation of homodimers of thyroid receptors while repression occurs by ligand-bound thyroid receptor monomers (Tomic-Canic et al.,

1992; Tomic-Canic et al., 1996a; Radoja et al., 1997). Moreover, when thyroid receptors are bound to the *keratin* promoter region in the presence of T3 typical thyroid receptor co-activator proteins behave like co-repressors and vice-versa in the absence of T3 (Jho et al., 2005). Notably, analysis of the -131bp and -83bp genomic region upstream of the presumed TATA-box (data not shown) of the Tetraodon *Ker1* gene revealed the existence of 3 putative TRE half-sites with the same sequence characteristics of human *epidermal keratin* promoters. These preliminary analysis in tetraodon may suggest that despite the differences in the overall genetic organization of epidermal keratin genes in teleosts and tetrapods (Hesse et al., 2001; Schaffeld et al., 2002b; Zimek et al., 2003), the regulatory elements that control epidermal keratin gene expression may be conserved. However, further experiments will be necessary to investigate this question.

2.4.2 Halibut metamorphosis and molecular and histological changes in skin

In several teleosts, whole-body levels of TH are correlated with metamorphosis (Inui and Miwa, 1985; Tagawa et al., 1990a; Yamano et al., 1991b; Yamano et al., 1994a; Inui et al., 1995; Power et al., 2001; Liu and Chan, 2002; Einarsdóttir et al., 2006) and are associated with changes in teleost larvae fish skin during natural and induced metamorphosis (de Jesus et al., 1998; Liu and Chan, 2002; Le Guellec et al., 2004). As halibut larvae progress to metamorphosis TH levels increase (Fig. 2.4C) and extensive differentiation in halibut skin accompanies this process (Fig. 2.5). During progression to metamorphosis halibut skin changes from simple epithelia composed of a thin epidermis formed by a superficial cell layer and larval basal epidermal cells supported by the dermis which is composed of an acellular collagen lamella and some scattered dermal endothelial cells, to a highly stratified post-metamorphic juvenile skin composed of epidermis, dermis and hypodermis (Fig. 2.5). The structural transformations observed in halibut skin during metamorphosis in the present study are in agreement with previous observation in halibut (Ottensen and Olafsen, 1997), zebrafish, winter flounder (*Pseudopleuronectes americanus*) and plaice (*Pleuronectes platessa*) skin (Roberts et al., 1973; Liu and Chan, 2002; Murray et al., 2003; Le

Guellec et al., 2004). Moreover, the structural changes that occur in halibut skin resemble the developmental changes observed in human (Dale et al., 1985) and anuran skin (Kawai et al., 1994; Suzuki et al., 2001; Watanabe et al., 2001; Suzuki et al., 2002; Watanabe et al., 2002; Ishida et al., 2003). In the present study the molecular and cellular modifications in skin are related to stage of skin differentiation in larvae or adults (Fig. 2.7).



In human skin, development-specific epidermal keratin pairs are expressed just before and during skin differentiation, implying that specific epidermal keratin genes are associated with different differentiation states of skin cells (Dale et al., 1985). In anuran metamorphosis specific *keratin* and *collagen 1* expression in a particular skin cell population at specific developmental stages has also been reported (Ellison et al., 1985; Jonas et al., 1985; Nishikawa et al., 1992; Suzuki et al., 2001; Watanabe et al., 2001; Suzuki et al., 2002; Watanabe et al., 2002; Ishida et al., 2003). In the halibut, the pre-metamorphic larval skin is constituted by a 2-cell layer in which the basal layer expresses keratin *hhKer1* and *Coll1α1* genes and the outermost epithelial layer is negative for both these genes (Fig. 2.6A and B, Fig. 2.7). Furthermore, the larval basal cells contain putative keratin microfilaments in their cytoplasm and strong fluorescence in the adherent junctions between

basal cells and at the basal side facing the collagen lamella (Fig. 2.5A and B). This cellular characteristic in anurans is indicative of the presence of epidermal keratin bundle bodies called “the figure of Ebert” (Kawai et al., 1994; Suzuki et al., 2002) and the results of the present study appear to suggest that a similar process occurs in larval halibut skin. In fact the presence of keratin bundles in basal epidermal cells at early stages of vertebrate skin development seems to be a common trend and scattered keratin bundles have also been reported in human embryonic skin basal epidermal cells (Dale et al., 1985). By using *Colla1*, previously reported in zebrafish (Le Guellec et al., 2004) and *R. catesbiana* (Suzuki et al., 2002) to be specific for pre-metamorphic skin epidermal basal cells, the present study demonstrates that halibut larval basal cells probably participate in the deposition of collagen on the dermal stroma before metamorphosis and up until climax and further confirms the nature of this cell population as halibut larval basal epidermal skin cells (Fig. 2.6A'-E'). In this way, halibut larval skin basal epidermal cells can be characterised as being positive for *Ker1*, *Colla1* and cytoplasmatic keratin-bundles. After metamorphosis juvenile/adult skin basal epidermal cell are negative for these three markers and clearly distinguishable from larval basal cells (Fig. 2.6 and 2.7). During halibut metamorphosis the larval basal cells seem to differentiate from a pre-metamorphic larval state to a post-metamorphic adult state and this differentiation is direct and no intermediate differentiation state occurs (Fig. 2.5, 2.6 and 2.7). In contrast, in anurans body skin basal skin cells are the only pre-metamorphic skin basal cells and at metamorphic climax they first differentiate into larval basal cells which in turn, after metamorphosis, finally differentiate into adult basal cells (Suzuki et al., 2001; Suzuki et al., 2002; Ishida et al., 2003).

The absence of keratinisation in halibut adult skin is in agreement with previous reports indicating that no keratins exist in adult fish skin apart from in specific structures prone to intense mechanical stress (Alibardi, 2002; Pinky et al., 2004). Moreover, in the present study despite extensive cDNA library screening and degenerate primer based PCR cloning strategies no adult-specific epidermal keratin was identified. The absence of keratinisation and the presence of dermal scales in fish is probably a specific adaptation to an aquatic environment. So while in humans at the end of skin development the outermost epithelial cells die and the cornified layer of keratinised cells

becomes the outermost skin cell layer of the newborn and adult (Dale et al., 1985), in the halibut the outermost epithelial cell layer does not appear to undergo any morphological changes. The absence of keratinisation in fish is probably a common phenomenon and in *C. auratus* adult skin neither a histidine-rich matrix material or loricrin or filaggrin, commonly associated with keratinisation in tetrapods, were found (Alibardi, 2002). Moreover, it was not possible to detect using immunocytochemistry epidermal keratins typical of keratinised tissues in adult skin of the teleosts *C. auratus*, *Tetractenos hamiltoni* and *Salmo gairneri* (Alibardi, 2002). Conversely, in the sarcopterygii fish *P. aethiopicus* (Schaffeld et al., 2005) and *Neoceratus auratus* (Alibardi, 2002), both of the same lineage as tetrapods, immunocytochemical detection of epidermal keratins occurred in adult skin with an expression pattern typical of tetrapod skin. From an evolutionary perspective it seems that keratinisation of the outermost cell layer of the epidermis might be a characteristic solely of the sarcopterygii lineage and an evolutionary event occurring early after the divergence of the actinopterygii and sarcopterygii. It would appear that in teleosts, skin, scales and mucus constitute the barrier against mechanical stress, infection and loss of body fluids with the same functional role as epidermal keratins and keratinized skin in tetrapods. Interestingly, the termination of differentiation of halibut adult skin at the end of metamorphosis coincides with the appearance of the first scales and mucus cells.

In conclusion, *hhKer1* a teleosts specific *epidermal type I keratin* has been cloned in the halibut and shown to be a stage specific skin cell marker. An inverse relationship is observed between the expression of *hhKer1* and the hormone T4 during metamorphosis. Preliminary analysis suggests that the teleosts *Ker1* gene promoter contains conserved motifs with human *epidermal type I keratin* genes which are known to be regulated by T3 (Tomic-Canic et al., 1992; Tomic-Canic et al., 1996a; Tomic-Canic et al., 1996b; Radoja et al., 1997; Jho et al., 2001; Radoja et al., 2004; Jho et al., 2005). Histological and molecular analysis indicate that the development of halibut skin is similar to that of anuran (Kawai et al., 1994; Suzuki et al., 2001; Watanabe et al., 2001; Suzuki et al., 2002; Watanabe et al., 2002; Ishida et al., 2003) and human skin (Dale et al., 1985). However,

the halibut adult skin is never keratinised and differentiation from larval basal cells to the adult state is direct (Fig. 2.7).

CHAPTER 3

TROPONIN T ISOFORM EXPRESSION IS MODULATED DURING ATLANTIC HALIBUT METAMORPHOSIS

3.1 Introduction

Troponin T (TnT) is a class of skeletal muscle specific proteins that are an important component of the thin-filament. TnTs are essential for correct assembly of the sarcomeres (Sehnert et al., 2002; Marco-Ferreres et al., 2005) and are responsible for anchoring of the Troponin complex to tropomyosin (Tm) and correct assembly and function of Troponin I and C (Perry, 1998; Jin et al., 2000b). In tetrapods, three TnT genes exist, fast, slow and cardiac, expressed respectively in white (fast-twitch and glycolytic), red (slow-twitch and oxidative) and cardiac muscle. However, recent studies indicate that in teleosts a greater number of genes exist and at least two fast TnT (fTnT) genes and two slow TnT (sTnT) exist as well as an apparently teleost specific intronless TnT (iTnT) gene (Hsiao et al., 2003; Campinho et al., 2005)(Chapter 5).

In terrestrial vertebrates, TnT genes are known to produce multiple protein isoforms by alternative splicing mechanisms (Gahlmann et al., 1987; Briggs and Schachat, 1993; Samson et al., 1994; Wang and Jin, 1997; Farza et al., 1998; Jin et al., 1998a; Perry, 1998; Barton et al., 1999; Bucher et al., 1999; Huang et al., 1999d; Jin et al., 2000b; Yonemura et al., 2000; Nakada et al., 2002; Wang et al., 2002; Yonemura et al., 2002; Campinho et al., 2005). A number of factors, such as contractile properties (Tobacman and Lee, 1987), intracellular pH (Nosek et al., 2004) in myofibres, calcium dependent modulation during cross-bridge cycling (MacFarland et al., 2002) and innervation patterns during development (Leeuw et al., 1994), are proposed to be associated with TnT isoform switching in cardiac and fast muscle of foetal and adult terrestrial vertebrates. In contrast, in terrestrial vertebrates, no developmental specific protein isoform changes occur with sTnT (Gahlmann et al., 1987; Samson et al., 1994; Jin et al., 1998a; Perry, 1998; Huang et al., 1999d; Yonemura et al., 2002), although in adults red-muscle-specific isoforms are detected (Jin et al., 2000b).

Studies in flatfish have indicated that changes occur in muscle during the thyroid hormone driven metamorphosis in which the bilaterally symmetrical larvae changes to an asymmetric juvenile. In pre-metamorphic pelagic larvae of the flatfish *Paralichthys olivaceus* (flounder) two fTnT immunoreactive proteins of 41.5 and 34 kDa are reported (Yamano et al., 1991a). However, when the larvae enter metamorphosis, to become a benthic flatfish, the 41.5 kDa protein is substituted by a new 33.5 kDa isoform. In post-metamorphosis juvenile fish only the 34 and 33.5 kDa isoforms of TnT are present (Yamano et al., 1991a). Similarly, during spontaneous metamorphosis, larval 5,5'-dithio-bis-nitrobenzoic acid (DTNB) light chain (myosin light chain 2, MLC2) is replaced by an adult specific isoform (Yamano et al., 1994b). Although it is evident that the changes that occur in muscle during metamorphosis are probably associated with changing functional requirements, surprisingly few molecular studies exist of this process. In the present study in order to analyse changes in skeletal muscle and in particular TnT gene expression during halibut (*Hippoglossus hippoglossus*) metamorphosis, cDNAs for slow and fast TnT were cloned and their expression and tissue distribution was studied in relation to changes in thyroid hormones (THs).

3.2 Materials and methods

3.2.1 TnT cDNA library screening

A lambda phage cDNA library made from metamorphosing larvae of halibut was plated in densities ranging from 1,000-5,000 plaque forming units (pfu). A probe was obtained for skeletal TnT by randomly isolating and sequencing 10 clones. A putative halibut fast TnT (hhfTnT) obtained in this way was used as a probe for cDNA library screening or alternatively a *Pst*//*EcoRI* digested cDNA fragment from a sea bream sTnT2 gene (sTnT2sb)(see Chapter 5) was utilised. In each screen using the halibut fTnT or the sTnT2sb probe, nitrocellulose membrane lifts were performed and membranes pre-hybridized for 2 hours, respectively, at 65°C or 60°C in hybridization solution (6xSSC, 0.1%SDS, 100µg/mL tRNA, 5x Denhardt's).

DNA probes were labelled with [³²P] by random priming (Megaprime, random labelling kit, Amersham Biosciences, UK) and purified on a sephadex column. Radioactively labelled probes were diluted in new hybridization mix and allowed to hybridize overnight with the membranes. Post-hybridisation stringency washes were carried out twice for ~30 minutes at room temperature (1xSSC, 0.1%SDS) followed by two 30 minute washes (1xSSC, 0.1%SDS) at 65°C or 60°C, respectively. Membranes were then exposed overnight at -80°C to Biomax MS film (Kodak, Palo Alto, CA, USA) and several positive plaques were isolated and automatically excised into pBluescript SK+/- (Stratagene), DNA purified and cDNA clones sequenced to give 3-fold coverage using BigDye Version 3 (Perkin-Elmer, UK) chemistry and an ABI 3700 sequencer.

3.2.2 Phylogenetic analysis

The identity of the diverse halibut TnT cDNA isolated was assigned by tBLASTx analysis (Altschul et al., 1990) against GenBank (www.ncbi.nlm.nih.gov) and the Medaka (*Oryzias latipes*) EST database (<http://medaka.lab.nig.ac.jp>). All tetrapod and teleost TnT cDNA sequences were retrieved and their deduced amino acid sequence compared to that of halibut TnTs using Clustal X software (Thompson et al., 1997). The phylogenetic relationship of halibut TnT genes with other vertebrate TnT genes was analysed using the maximum-parsimony method option of PAUP* version 4.0b software (Swofford et al., 2001) with 1000 bootstraps (Fitch, 1971) and TnT sequences available from databases (Table 4.1). *Caenorhabditis elegans* striated muscle TnT (GenBank accession no. NP_509076.1) was used as the outgroup. The sea bream sequences obtained in the present study, sTnT1sb, sTnT2sb and iTnTsb (Chapter 5) were also included in the analysis.

Table 3.1. Vertebrate TnT sequences used in phylogenetic analysis

Specie	Gene, abbreviation	Database, accession number
<i>Homo sapiens</i>	Slow TnT, sTnT hs	GenBank, AAB3027
	Fast TnT, fTnT hs	GenBank, NP_006748
	Cardiac TnT, cTnT hs	GenBank, NP_000355
<i>Gallus gallus</i>	Slow TnT, sTnT ck	GenBank, JC4970
	Fast TnT, fTnT ck	GenBank, AAA49100
	Cardiac TnT, cTnT ck	GenBank, BAA02369
<i>Coturnix coturnix japonicus</i>	Fast TnT, fTnT cj	GenBank, P06398
<i>Xenopus laevis</i>	Fast TnT, fTnT xl	GenBank, AAM55471
	Cardiac TnT, cTnT xl	GenBank, AAO33406
<i>Danio rerio</i>	Intronless TnT, iTnT zf	GenBank, NP_852476
	Slow TnT low MW isoform, sTnTLMW zf	GenBank, BQ259877
	Fast TnT a, fTnTa zf	GenBank, NP_571640
	Fast TnT b isoform 1, fTnTb zf1	GenBank, AF425741
	Fast TnT b isoform 2, fTnTb zf2	GenBank, BC065452
	Cardiac TnT, cTnT zf	GenBank, CAD59126
<i>Salmo salar</i>	Fast TnT, fTnT ss	GenBank, AAC24595
<i>Gadus morhua</i>	Fast TnT, fTnT gm	GenBank, AAM21701
<i>Salmo trutta</i>	Slow TnT 1S, sTnT 1s st	GenBank, AAB58912
<i>Fugu rubripes</i>	Putative slow TnT2, sTnT2 fg	HGMP, M001711
	Intronless TnT, iTnT fg	HGMP, M000253
<i>Ictalurus punctatus</i>	Slow TnT 1, sTnT1 ic	GenBank, CK412342
<i>Orizya latipes</i>	Slow TnT 2, sTnT2 md	Medaka EST, MF01FSA018J165
	Fast TnT isoform 1, fTnT md1	GenBank, BJ729852
	Fast TnT isoform 2, fTnT md2	GenBank, BJ728074
<i>Tetraodon nigroviridis</i>	Putative embryonic fast TnT isoform, efTnT tn	EMBL, CR660426
	Putative larval fast fTnT isoform, fTnT tn2	EMBL, CR658326
	putative adult fast TnT isoform, fTnT tn1	EMBL, CR658422
	Atypical fast TnT isoform 1, AfTnT tn1	EMBL, CR696067
	Atypical fast TnT isoform 2, AfTnT tn2	EMBL, CR675364
	Atypical fast TnT isoform 3, AfTnT tn3	EMBL, CR662746
	Atypical fast TnT isoform 4, AfTnT tn4	EMBL, CR727722
Atypical fast TnT isoform 5, AfTnT tn5	EMBL, CR673164	
<i>Sparus aurata</i>	Slow TnT1, sTnT1 sb	GenBank, AY684301
	Slow TnT2, sTnT2 sb	GenBank, AY684302
	Intronless TnT, iTnTsb	GenBank, AY953294
	Embryonic fast TnT isoform, efTnT sb	GeneBank, DQ473445
	Larval fast TnT isoform, LfTnT sb	GeneBank, DQ473444
	Adult fast TnT isoform, afTnT sb	GeneBank, DQ473443
<i>Caenorhabditis elegans</i>	striated muscle TnT, TnT ce	GeneBank, NP_509076

3.2.3 Putative genomic organisation of halibut TnT genes

The putative genomic organisation of isolated halibut TnT genes was established by *in silico* analysis carried out using the *Tetraodon nigroviridis* genome database (www.genoscope.cns.fr/externe/tetranew/). The *Tetraodon* scaffolds giving the most significant hit by tBLASTx analysis (Altschul et al., 1990) with the halibut TnT sequences were recovered. Pairwise alignment of halibut and *Tetraodon* TnT cDNA sequences with the selected *Tetraodon* scaffold using Spidey mRNA-to-genome software (www.ncbi.nlm.nih.gov) permitted identification of the putative exon/intron boundaries of the halibut and *Tetraodon* TnT genes.

3.2.4 Animal sampling

Atlantic halibut at different developmental stages (Saele et al. 2004) ranging from pre-metamorphic larvae to fully metamorphosed juveniles were obtained from Fiskey (Iceland). Animals (n = 10) were anesthetized in MS-222 (Sigma) and immediately collected for total RNA extraction by preservation in RNAlater (QIAgen, UK) according to the manufacturers instruction. An adult halibut was anesthetised in MS-222 (Sigma-Aldrich, UK) and killed by decapitation and white muscle, red muscle, heart and liver were immediately collected into RNAlater (QIAgen) according to the manufacturers instructions. Alternatively, for *in situ* hybridization and histology anesthetized halibut larvae and juveniles were fixed in paraformaldehyde (4% PFA) at 4°C overnight. Samples were subsequently washed twice for 5-10 minutes with PBT and stored in 100% methanol at 4°C. Samples were embedded in paraffin and 5µm post-anal transverse section were made from each animal.

For radioimmunoassay five individual samples were collected for each stage, anesthetised in MS-222 (Sigma) and immediately frozen in dry ice.

3.2.4 Total RNA extraction

Total RNA was extracted from whole-body metamorphosing larvae and 100mg of adult halibut tissue using Tri reagent (Sigma-Aldrich) according to the manufacturers instructions, quantified in a GeneQuant (Amersham Biosciences) spectrophotometer and stored at -80°C until use.

3.2.5 Northern Blot

Three micrograms of total RNA obtained from adult halibut white muscle, red muscle, heart and liver were fractionated on a 1.5% agarose /5.5% formaldehyde gel which was run in 1x MOPS. RNA was transferred to nylon Hybond-N membranes (Amersham Biosciences) with 10x SSC overnight and cross-linked using UV light (Stratalinker, Stratagene). Hybridisations were carried out using 3'UTR probe prepared from each cloned halibut TnT gene (~10µg) by digestion for 2 hours at 37°C with 10U of appropriate restriction enzyme (Promega) and 1x buffer (Table 3.2). The resulting DNA for probes was purified by electrophoresis followed by extraction of DNA using the GFX gel band extraction kit (Amersham Biosciences).

Table 3.2. Restriction enzymes used to produce 3'UTR probes for northern blot hybridization.

Gene	Restriction enzyme	Probe size (bp)
fTnThh	<i>PstI/XhoI</i>	492
AfTnThh	<i>PstI</i>	364
sTnT2hh	<i>BtgI/EcoRV</i>	276

Individual membranes were hybridized overnight at high stringency (65°C in 6xSSC, 5x Denharts solution, 100µg/mL tRNA and 0.1%SDS) with its respective ³²P-dCTP-labeled halibut TnT probe. The membranes were then washed twice for 30 minutes at room temperature (1xSSC and 0.1%SDS) followed by two 30 minute high stringency washes (65°C in 1xSSC and 0.1%SDS) and exposed at -80°C to Biomax MS film (Kodak, USA).

3.2.6 Semi-Quantitative RT-PCR analysis of TnT expression during halibut metamorphosis

In order to determine expression of halibut TnT genes during metamorphosis a semi-quantitative RT-PCR assay was developed as follows. Total RNA (0.5µg) was treated with DNase using an Ambion DNA Free kit (Ca, USA), and used for first strand cDNA synthesis which was carried out in a 20µL volume using 0.05M Tris-HCl, pH8.3, 0.075M KCl, 3mM MgCl₂, 0.01M DTT, 1mM dNTP, 5pmol/µl random hexamer primers, 4U of RNase inhibitor (Promega, UK) and 10U of Superscript II reverse transcriptase (Invitrogen, UK). Synthesis reactions were carried out in an iCycler thermocycler (Perkin Elmer) for 10 minutes at 25°C followed by 50 minutes at 42°C and 2 minutes at 70°C to terminate synthesis. Five individual cDNA synthesis reactions corresponding to five individual animals per stage were performed.

Initial RT-PCR amplifications with primers specific for each halibut TnT gene were conducted to determine optimal cycle number and ensure that amplification occurred in the logarithmic phase of the reaction. The expression of 18s ribosomal RNA (rRNA) was used as an internal standard for normalisation.

RT-PCR analysis of halibut TnT genes was carried out in a 25µl reaction volume containing ~20 ng of cDNA for each sample and 1.5 mM MgCl₂, 0.1 mM dNTP's, 1 pmol/µl of halibut specific TnT gene forward and reverse primer (Table 3.3) and 0.6U *Taq* polymerase (Sigma-Aldrich). Primers for all the halibut TnT genes analysed were selected to amplify the entire N-terminal region, which in terrestrial vertebrates (Perry, 1998) and sea bream (Chapter 5) (Campinho et al., 2005) undergoes alternative splicing. The forward primer was located in the 5'UTR region of the isolated halibut TnT cDNAs. The reverse primer was designed in a constitutively expressed region of the halibut TnT cDNAs.

Table 3.3. Primer sequence and concentration used for RT-PCR analysis of fTnThh, AfTnThh and sTnT2hh during halibut metamorphosis.

Gene	Forward Primer	Reverse Primer
fTnThh	TCTCAGGTTGCAAAGTCCAC	GACGCTTCTCAATCCTGTCC
AfTnThh	CTCTGAGGTGTGAAGTCTG	CTCGACGCTTCTCAATTCGATC
sTnT2hh	ATCTTGCTGAGCTCATTCAT	ACGCTGATCCTCCATCTCC

The PCR reactions were performed in an iCycler (Perkin Elmer) thermocycler, using the following cycle; 1 minute at 95°C followed by 27 cycles, for fTnThh and sTnT2hh, or 28 cycles, for AfTnThh of; 30 seconds at 95°C, 1 minute at 56°C and 30 seconds at 72°C, followed by a final step of 1 minute at 72°C. Negative reactions without sample cDNA were also performed.

Amplification of the housekeeping gene 18s rRNA used for normalisation was carried out as described above using 1 pmol/μl of forward and reverse primer (5'-TCAAGAACGAAAGTCGGAGG-3' and 5'-GGACATCTAAGGGCATCACA-3' respectively). The thermocycle utilised was: 1 minute at 95°C followed by 16 cycles of 30 seconds at 95°C, 1 minute at 56°C and 30 seconds at 72°C, followed by a final step of 1 minute at 72°C. All RT-PCR reaction products were fractionated on 2.5% agarose gels and analysed by densitometry using LabWorks software, version 4.5 (Ultra-Violet Products Cambridge, UK). Results are expressed as the mean and standard error of five independent samples.

3.2.7 *In situ* hybridisation

The spatial-temporal expression pattern of halibut fTnT gene, and its efTnT isoform, sTnT2 and AfTnThh in metamorphosing halibut larvae and post-metamorphosed juveniles was investigated by *in situ* hybridisation using specific digoxigenin riboprobes. For *in situ* analysis of the fTnThh gene a 492 bp riboprobe for the conserved 3'UTR region in all fTnThh isoforms was generated using the same restriction enzymes used for generation of the northern blot

fTnThh 3'UTR probe (Table 3.2). The expression of efTnThh isoform was established by generating a riboprobe complementary to the embryonic/larval exon (aa 12 to 68) and extracted using a restriction digest with *HaeII/SfcI* (10U each enzyme; Promega) according to the manufacturers instructions. AfTnThh gene expression was established using a 364 bp riboprobe complementary to the constitutive 3' coding region and the 3'UTR of the AfTnThh and identical to the probe used for northern blot (Table 3.2). The restriction digest reactions were carried out at 37°C for 1.5h and fraction in a 0.8% agarose gel. The desired DNA bands for each probe were collected by gel band extraction using an Amersham GFX gel band extraction kit following the manufacturers instructions. The bands were then cloned into pGemT-easy vector (Promega) overnight with T4 DNA ligase. The 3'UTR fTnThh and AfTnThh vectors were linearised using *PstI* (10U; Promega) and for efTnThh and sTnT2hh the cDNA was digested with *EcoRI* (10U; Promega) in appropriate buffer for 1.5h at 37°C. The linearised vectors were extracted with phenol (pH 8) and precipitated in 3M sodium acetate (pH 5) and ethanol overnight at -20°C.

Specific riboprobes were generated by *in vitro* transcription using the linearized vector (10µg) as template and 20U of RNA polymerase in transcription buffer (Promega) with 1 µl of digoxigenin-RNA labelling mix (Roche Diagnostics, Mannheim, Germany), for 1.5 h at 37 °C. The reaction was stopped with 2 µl of 0.2M EDTA. The digoxigenin labelled riboprobes were purified by lithium precipitation and resuspended in 25 µl of water. Riboprobe purity and concentration were determined by fractionation of reaction products on an agarose gel (1.5%). To assess potential cross hybridization between probes and target sequences dot blots were performed. Each digoxigenin labeled riboprobe was hybridized individually with each of the halibut TnT target mRNA sequence, no cross hybridization reactions were detected and each probe was found to be specific for its target template.

For *in situ* hybridisation experiments adjacent transverse tissue sections of halibut larvae were dewaxed, rehydrated and then prehybridised at 58°C for 2h in hybridisation solution without probe (50% formamide, 4× SSC, 1 mg ml⁻¹ torula RNA, 0.1 mg ml⁻¹ heparin, 1× Denhardt's, 0.04% CHAPS). Tissues were then hybridised overnight in a humidified box at 58°C in 100 µl per section of hybridisation solution containing approximately 2 ng µl⁻¹ of the riboprobes. Control sections were pretreated with RNase prior to hybridization with riboprobes or the riboprobes were excluded from the hybridizations.

Stringency washes were carried out as follows; 3× 5 min at 58°C with 2× SSC and 5 min at 58°C in 1× SSC. Tissue sections were then washed 2× 5 min with 2× SSC:0.12% CHAPS at RT, followed by a wash for 5 min in 2×SSC:PTW (1:1, v/v) and finally 5 min in PTW. Blocking was performed by incubation in blocking reagent (Boehringer Mannheim, Germany) with 10% heat inactivated sheep serum. Detection of hybridised probe was carried out using sheep anti-digoxigenin-alkaline phosphatase (AP) Fab fragments (1/600) (Roche, Lisbon, Portugal). The chromagens for colour detection were NBT (4-nitroblue tetrazolium chloride) and BCIP (5-bromo-4-chloro 3-indolylphosphate) and colour development was carried out over 2h at 38°C. Stained sections were rinsed in PBS, fixed for 15 min in 4% formaldehyde at room temperature, rinsed in PBS and mounted in glycerol gelatine. Sections were analysed using a microscope (Olympus BH2) coupled to a digital camera (Olympus DP11) linked to a computer for digital image analysis.

3.2.8 Radioimmunoassay for thyroid hormones

Larval extracts were used to assess T4 and T3 content of whole larvae by radioimmunoassay (RIA) using a double-antibody method under equilibrium conditions. Frozen larvae (n = 8 per stage) were extracted individually in 50µl methanol, 200µl chloroform and 100µl barbital buffer, centrifuged (3,000 rpm for 30 min at 4°C) and the upper phase removed,

lyophilized, reconstituted in assay buffer, heat denatured (75°C for 2 hours) and assayed. Standard curves were prepared with T4 or T3 standards (Sigma-Aldrich) dissolved in 0.1N NaOH and diluted to appropriate concentrations in assay buffer. T3 and T4 assays were conducted in barbital buffer (0.07M, pH 8.6) and Tris buffer (0.1M, pH 7.4), respectively, and contained 0.1% BSA and 0.1% sodium azide. In both RIA, either 100µl of standard or larval extract was added. For both hormones, the total assay volume was 300µl and included 100µl of ¹²⁵I-T3 (Amersham Biosciences, Buckinghamshire, UK) or ¹²⁵I-T4 and 100µl T3 antisera (1:15,000, Sigma-Aldrich) or T4 antisera (1:10,000, Sigma-Aldrich). Antisera were added to all tubes apart from those to determine total count (cpm) and non-specific binding. The T3 and the T4 assays were incubated for 16-24 h at 4°C and subsequently, the free hormone was separated from the bound hormone using precipitation with a secondary antibody (Rotllant et al., 2003). Two-way analysis of variance (ANOVA) was performed in order to determine if significant differences in the concentration of T4 or T3 detected at different metamorphic stages occurred. If the two-way ANOVA detected significant differences in T4 or T3 between stages a Holm-Sidak (HSM) multiple comparison analysis was performed to determine which stages have different T4 or T3 levels. Both T4 and T3 concentration values were transformed using a logarithmic function before statistical analysis. Significance was considered if $p < 0.05$. All statistical analysis was performed using SigmaStat version 3 software (SPSS Corp.)

3.3 Results

3.3.1 Halibut TnT genes

Five cDNAs corresponding to different skeletal muscle TnT genes (Fig. 3.1) were isolated from a cDNA library of metamorphosing halibut larvae. In tBLASTx analysis (Altschul et al., 1990) against the GeneBank database, three cDNAs gave a highly significant match with teleost, fTnT genes. From the analysis it was determined that the fTnThh cDNAs isolated correspond to a putative embryonic/larval halibut fTnT (denominated efTnThh) and two

different adult isoforms (denominated fTnThh-1 and fTnThh-2). The efTnThh cDNA is a full-length clone with 965 nucleotides (nt) encoding a 286 amino acids (aa) protein from nt 62 to 919. The size of the deduced protein is 34.6 kDa and the predicted pI is 5.27 (Fig. 3.1)(Wilkins et al., 1998). The fTnThh-1 isoform is a 752 bp complete cDNA which encodes a protein of 232 aa from nt 22 to 717 (Fig. 3.1). The deduced fTnThh-1 protein has a predicted molecular weight of 27.89 kDa and a pI of 9.42 (Wilkins et al., 1998). The cDNA of the third isoform, denominated fTnThh-2, is 1,020 bp long and encodes a putative protein of 229 aa from nt 70 to 756 (Fig. 3.1). The predicted molecular weight and pI for the fTnThh-2 protein isoform is respectively 27.5 kDa and 9.55 (Wilkins et al., 1998).

In silico characterisation of the deduced halibut fTnT proteins using ProDom (Bru et al., 2005) and PRINTS (Attwood et al., 2003) software confirmed that they possess all the characteristics of fully functional fTnT proteins. ClustalX (Thompson et al., 1997) multiple alignment analysis of these putative halibut fTnT cDNAs and their deduced protein sequence indicates that they are the products of alternative splicing of the halibut fTnT gene (Fig. 3.1). Isoform efTnThh shares 80% sequence identity with fTnThh-1 and -2 isoforms, whereas isoforms fTnThh-1 and -2 are 99% similar. The differences between the halibut TnT cDNA isolated are due to the presence of an insert in efTnThh (aa 12 to 68) and fTnThh-1 (aa 12 to 14) which is lacking in the fTnThh-2 isoform (Fig. 3.1).

A further 1,107 bp cDNA was also cloned and tBLASTx analysis (Altschul et al., 1990) suggests that it most closely resembles an fTnT gene and gave the most significant hit to *D. rerio* fTnTa gene and it was tentatively designated as an atypical fast TnT cDNA (AfTnThh). The predicted protein product encoded by AfTnThh cDNA was 289 aa with a pI of 5.07 and molecular weight of 34.21 kDa (Fig. 3.1)(Wilkins et al., 1998).

A halibut cDNA homologous to a previously reported teleost specific sTnT2 gene was also cloned. This cDNA, designated sTnT2hh, is 980 bp long and encodes a deduced protein of

246 aa (Fig. 3.1) with a predicted molecular weight of 29 kDa and a pI of 9.24 (Wilkins et al., 1998). It was not possible, despite extensive cDNA library screening to isolate a cDNA that was the product of a halibut sTnT1 gene.

Clustal X multiple sequence alignment (Thompson et al., 1997) of the deduced amino acid sequence of halibut TnT genes show that efTnThh shares 69% and 52% sequence identity, respectively, with AfTnThh and sTnT2hh. Comparison of the other halibut fTnT-1 and -2 isoforms with AfTnThh and sTnT2hh reveal they share ~59% sequence identity while, AfTnThh and sTnT2hh share 50% identity.

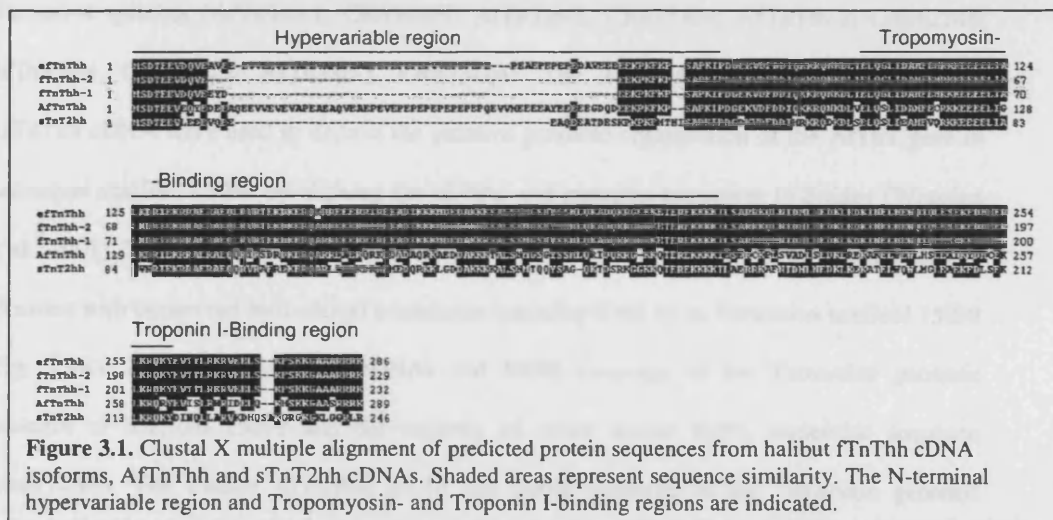


Figure 3.1. Clustal X multiple alignment of predicted protein sequences from halibut fTnThh cDNA isoforms, AfTnThh and sTnT2hh cDNAs. Shaded areas represent sequence similarity. The N-terminal hypervariable region and Tropomyosin- and Troponin I-binding regions are indicated.

3.3.2 Putative genomic organization of halibut skeletal TnT genes

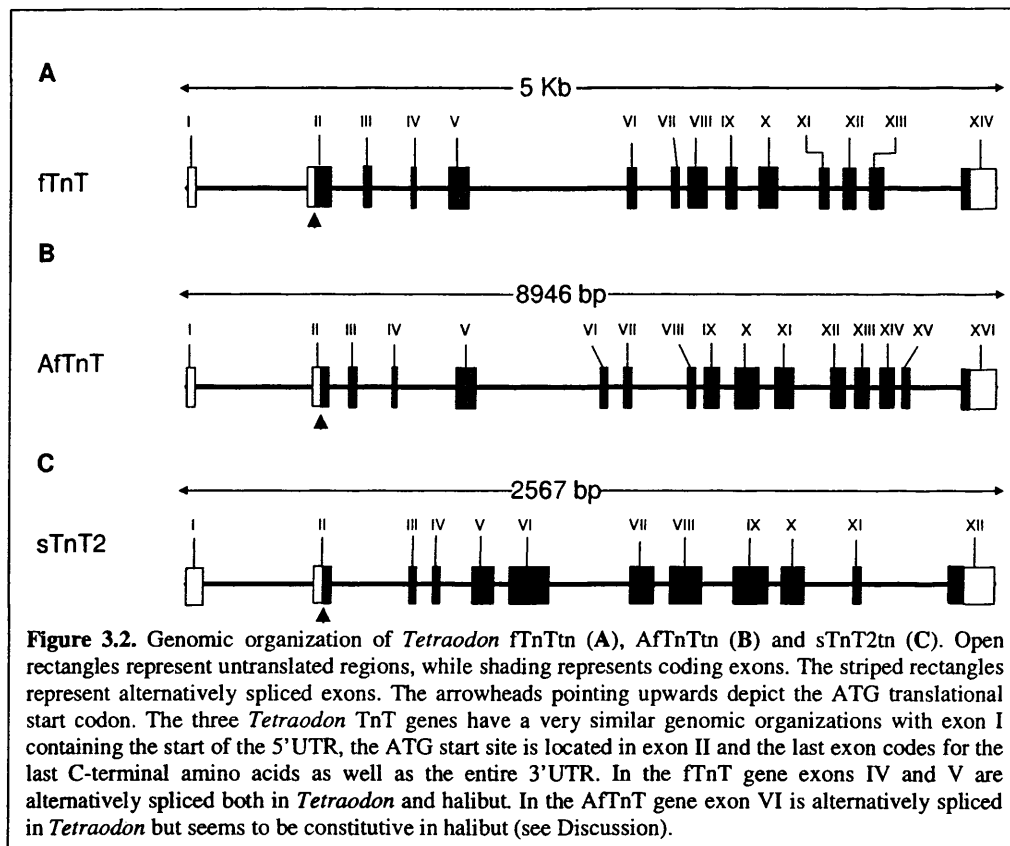
In silico tBLASTx analysis (Altschul et al., 1990) using halibut fTnT cDNA sequences gave a highly significant hit to *Tetraodon* genomic scaffold 7217 (SCAF7217). The putative *Tetraodon* and deduced halibut fTnT gene is composed of 14 exons (Fig. 3.2A) as described for the sea bream (Chapter 5). The efTnThh isoform is composed of exons I to III and V to XIV (Fig. 3.2A). Isoform fTnThh-1 is composed of all exons except exon V, which codes for the highly acidic peptide containing a glutamic acid (E), proline (P) repeat (Fig. 3.1 and 3.2A). In the isoform fTnThh-2 mRNA, exons IV and V are spliced out (Fig. 3.2A) which results in the

loss of 9 nt in relation to fTnThh-1 (Fig. 3.1). The ATG transcription start signal is located in exon II and exon I only bears the beginning of the 5'UTR (Fig. 3.2A). The 3'UTR and the 5'-end of the coding region are located in exon XIV. Overall coverage of the fTnThh cDNA sequences was 97% and overall identity between it and the *Tetraodon* fTnT gene sequence was 82%.

The halibut AfTnThh gene used in tBLASTx analysis led to the identification of the putative *Tetraodon* AfTnT locus in scaffold 15099 (SCAF15099) as well as five different *Tetraodon* AfTnT cDNA isoforms (numbered 1 to 5) which seem to be the product of alternative splicing (AfTnTtn-1, CR696067; AfTnTtn-2, CR675364; AfTnTtn-3, CR662746; AfTnTtn-4, CR727722; AfTnTtn-5, CR673164). The *Tetraodon* AfTnT cDNA and the AfTnThh cDNA were used to deduce the putative genomic organization of the AfTnT gene in *Tetraodon* scaffold 15099 by aligning the cDNAs and genomic sequences in Spidey (Wheelan et al., 2001). The analysis revealed that the *Tetraodon* AfTnT gene (AfTnTtn) is composed of 16 exons with conserved intron/exon boundaries spanning 8946 bp in *Tetraodon* scaffold 15099 (Fig. 3.2B). *Tetraodon* AfTnTtn cDNAs had 100% coverage in the *Tetraodon* genomic sequence of scaffold 15099 and the majority of exons shared 100% nucleotide sequence conservation. The halibut AfTnThh cDNA had 100% coverage in the *Tetraodon* genomic sequence of scaffold 15099 and shared 79% overall sequence identity. Exon I bears part of the 5'UTR while exon II contains the remainder and the ATG translation start site. Exon III is composed of 13 nt and constitutes together with exons I and II the N-terminal constitutive exons present in all *Tetraodon* AfTnT cDNAs identified. Exon II and III share 77% sequence identity between the *Tetraodon* genomic sequence and halibut AfTnThh cDNA, while exon I shares only 58% identity. Exon IV which codes for 3 acidic residues both in *Tetraodon* and halibut is the first N-terminal alternatively spliced exon in *Tetraodon* cDNAs, and shares 75% sequence identity between *Tetraodon* genomic and halibut AfTnThh cDNA sequence. Exon V is the largest alternatively spliced N-terminal exon in *Tetraodon* and is the most divergent between the *Tetraodon* genomic sequence and halibut AfTnT cDNA. In this exon the sequence identity is

only 52% and a 41 nt insertion in the third quarter of the *Tetraodon* genomic sequence renders this exon bigger in *Tetraodon* than in halibut. However, the 5' and 3' regions of the *Tetraodon* sequence are well conserved with the corresponding halibut AfTnT sequence. Exons VI and VII are highly conserved (94%) between the *Tetraodon* genomic sequence and halibut AfTnT cDNA sequence and are alternatively spliced in *Tetraodon*. Exons VIII to XVI encode the C-terminal constitutive region present in all vertebrate TnT genes and sequence conservation between the *Tetraodon* and halibut was always greater than 85% and no splice variants of this region were observed in *Tetraodon*. Exon XVI codes for the last 11 amino acid residues of the protein and the entire 3'UTR. Although exon XVI shares only 47% sequence identity between *Tetraodon* and halibut the sequence divergence was in the 3'UTR rather than the coding region (86% sequence identity).

The genomic organization of halibut sTnT2 gene in *Tetraodon* was also determined (Fig. 3.2C). Using the sTnT2hh sequence in tBLASTx analysis (Altschul et al., 1990) of the *Tetraodon* genome database (Jaillon et al., 2004) a single hit with *Tetraodon* scaffold 15000 (SCF15000) was found. A single cDNA transcript (CR734482) arising from *Tetraodon* sTnT2 gene (SCF15000) was isolated and introduced in Spidey aligning software (Wheelan et al., 2001) along with the halibut sTnT2 cDNA sequence to determine the putative genomic organization of sTnT2. The putative *Tetraodon* sTnT locus is composed of 12 exons and spans 2567 nt in the *Tetraodon* genomic sequence (Fig. 3.2C). Exon I bears the first three-quarters of the 5'UTR and the beginning of the coding region is located in exon II. Exon XII contains the 5'-end of the coding region as well as the 3'UTR (Fig. 3.2C). The halibut sTnT2hh cDNA sequence had 86% coverage in the *Tetraodon* genomic sequence and shared 82% sequence identity.



3.3.3 Tissue specificity of halibut TnT genes

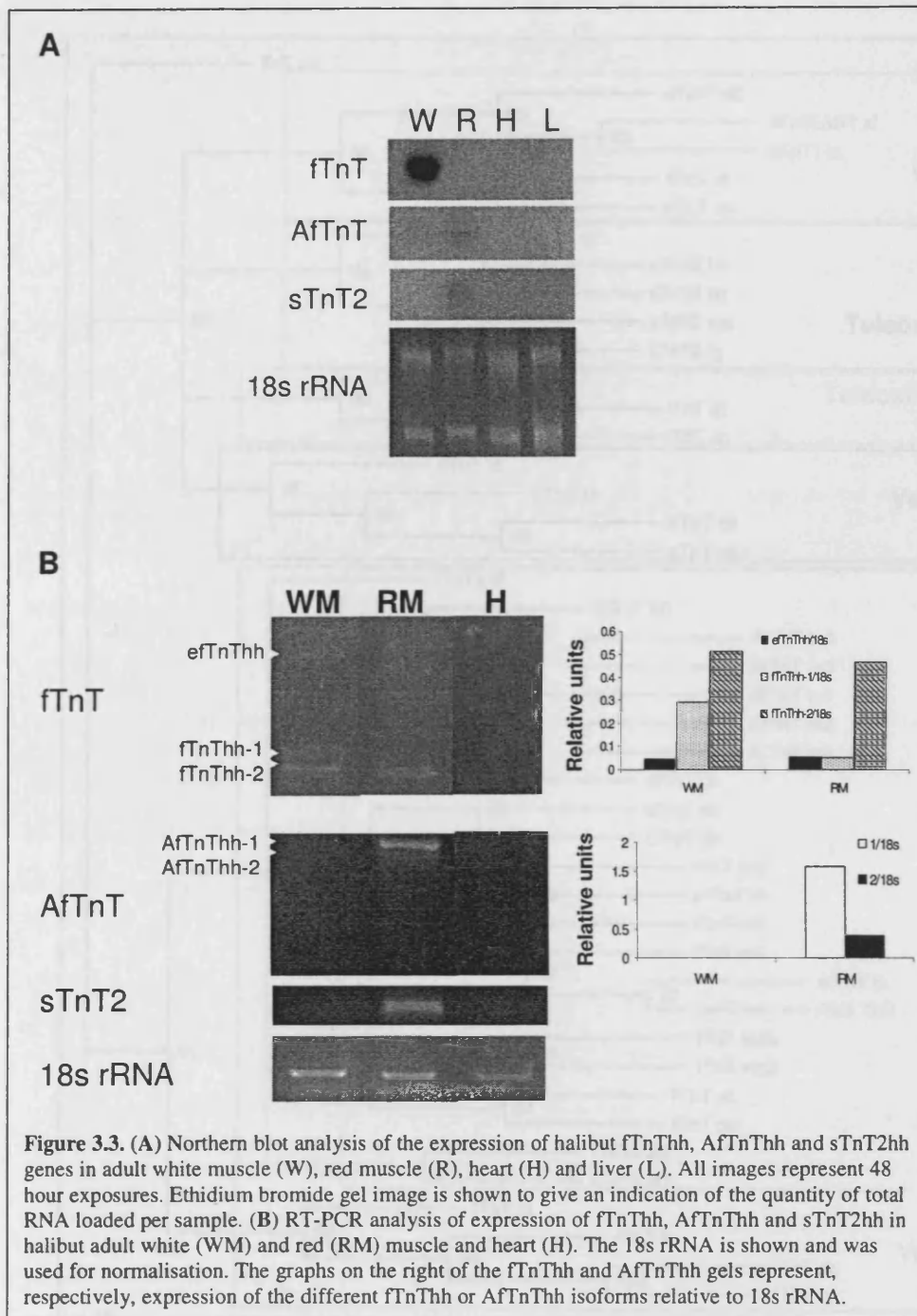
Northern blot and RT-PCR analysis were carried out in order to determine tissue specificity of the halibut TnT genes isolated. The northern results in Figure 3.3A show that the fTnThh as expected is expressed in adult halibut white (fast) muscle and is absent from red muscle, cardiac muscle and liver. However, the more sensitive RT-PCR technique revealed that fTnThh is also expressed in halibut adult red muscle tissue (Fig. 3.3B). The tBLASTx and phylogenetic analysis of AfTnThh classified this cDNA as the product of a fast TnT gene. However, analysis by Northern blot (Fig. 3.3A) show that its expression is red (slow) muscle specific and it is not detected in halibut adult white (fast) muscle, cardiac muscle or liver. The halibut sTnT2 gene is exclusively expressed in halibut adult red muscle (Fig. 3.3A). The red muscle tissue specificity of AfTnThh and sTnT2hh was further confirmed by RT-PCR (Fig. 3.3B).

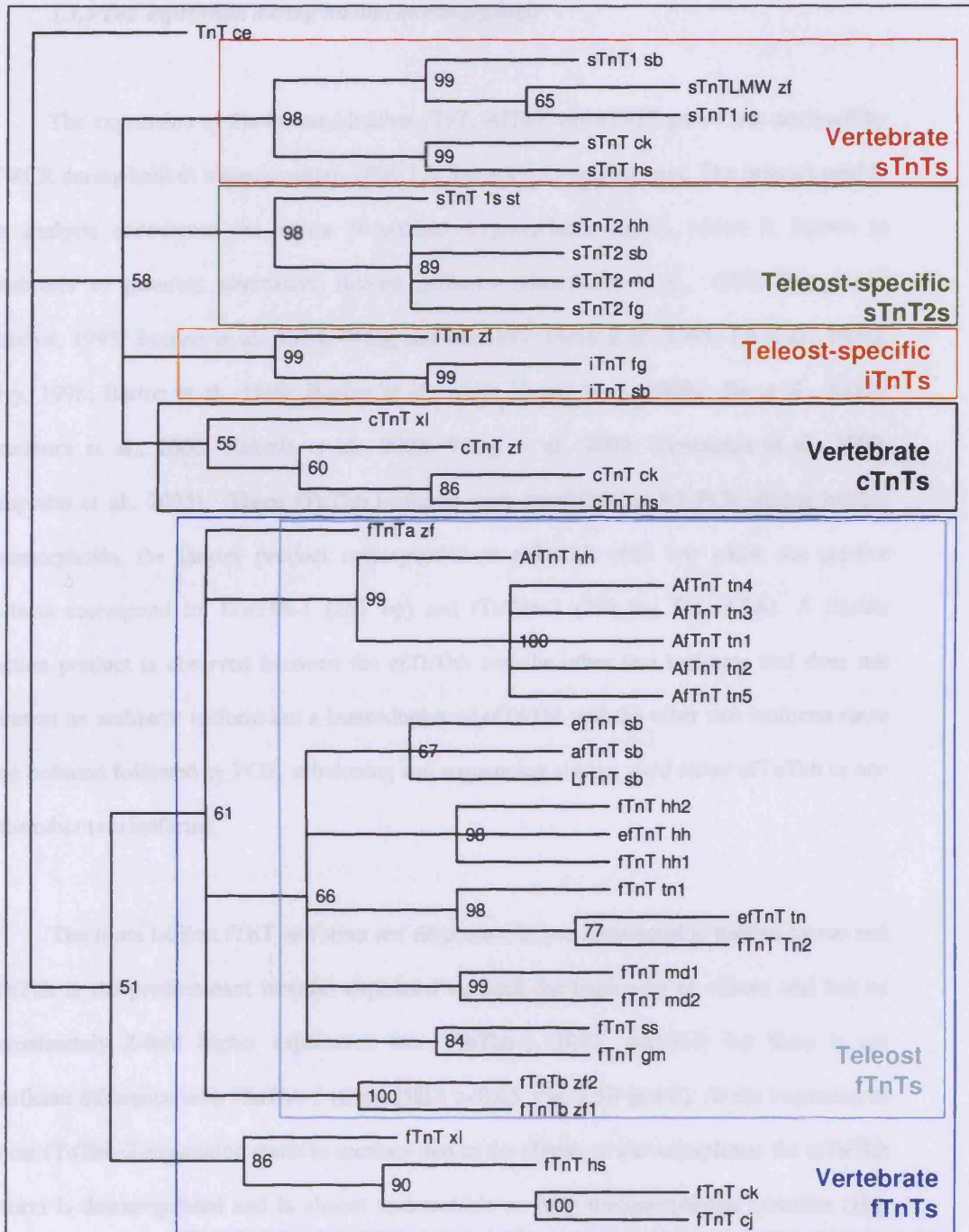
3.3.4 Phylogenetic analysis of Halibut TnT genes

Clustal X multiple sequence alignment (Thompson et al., 1997) of the deduced protein sequence of halibut TnT and several vertebrate TnT protein sequences and striated muscle TnT from *C. elegans* was performed and the resulting phylogenetic relationships were determined in PAUP* version 4.0b software (Swofford et al., 2001) using the maximum-parsimony method with 1000 bootstraps (Fitch, 1971) and *C. elegans* TnT as an outgroup.

The phylogenetic tree shows that the vertebrate fTnTs form a single clade and that within it the tetrapod fTnTs cluster apart from the fish fTnTs (Figure 4.4). Moreover, efTnThh, fTnThh-1 and fTnThh-2 cluster with highly significant bootstrap values with other teleost fTnT genes. Within the main fTnT clade, AfTnThh and *Tetraodon* AfTnTtn isoforms clustered together and formed a separate group and this topology was supported by highly significant bootstrap values (Fig. 3.4).

Two principal clades were found for sTnT which corresponded to sTnT1 and sTnT2 (Fig. 3.4). The halibut sTnT2hh clusters with other teleost specific sTnT2 genes (Fig. 3.4) and forms a group apart from tetrapod sTnT and sTnT1, which clustered together.





10

Figure 3.4. Maximum parsimony phylogenetic tree using the predicted protein sequence of the different halibut TnT cDNA isolated and that of other vertebrates (table 3.1) retrieved from Genebank and the Medaka EST database (see Materials and Methods). The bar in the bottom left-hand corner represents 10% sequence divergence. The abbreviations are described in Table 3.1.

3.3.5 TnT expression during halibut metamorphosis

The expression of the isolated halibut fTnT, AfTnT and sTnT2 genes was analysed by RT-PCR during halibut metamorphosis (Fig. 3.5, 3.6 and 3.7, respectively). The primers used in this analysis encompass the entire N-terminal hypervariable region which is known in vertebrates to generate alternative spliced isoforms (Gahlmann et al., 1987; Briggs and Schachat, 1993; Samson et al., 1994; Wang and Jin, 1997; Farza et al., 1998; Jin et al., 1998a; Perry, 1998; Barton et al., 1999; Bucher et al., 1999; Huang et al., 1999d; Jin et al., 2000b; Yonemura et al., 2000; Nakada et al., 2002; Wang et al., 2002; Yonemura et al., 2002; Campinho et al., 2005). Three fTnThh isoforms were amplified by RT-PCR during halibut metamorphosis, the largest product corresponded to efTnThh (423 bp) while the smaller products correspond to, fTnThh-1 (261 bp) and fTnThh-2 (252 bp; Fig. 3.5A). A further reaction product is observed between the efTnThh and the other two isoforms that does not represent an authentic isoform but a heteroduplex of efTnThh and the other two isoforms since band isolation followed by PCR, subcloning and sequencing always yield either efTnThh or one of the other two isoforms.

The three halibut fTnT isoforms are all present in pre-metamorphic halibut larvae and efTnThh is the predominant isoform expressed up until the beginning of climax and has an approximately 2-fold higher expression than fTnThh-1 (HSD, $p < 0.001$) but there is not significant difference with fTnThh-2 (Stg8; HSD, $p < 0.05$; Fig. 3.5B and C). At the beginning of climax fTnThh-2 expression starts to increase and at the climax of metamorphosis the efTnThh isoform is downregulated and is almost undetectable in fully metamorphosed juveniles (Fig. 3.5A and B). In parallel fTnThh-2 becomes the most highly expressed fThThh isoform and increases ~3-fold in juveniles (Fig. 3.5B and C). Prior to and after metamorphosis fTnThh-1 expression does not change significantly (Fig. 3.5A and B).

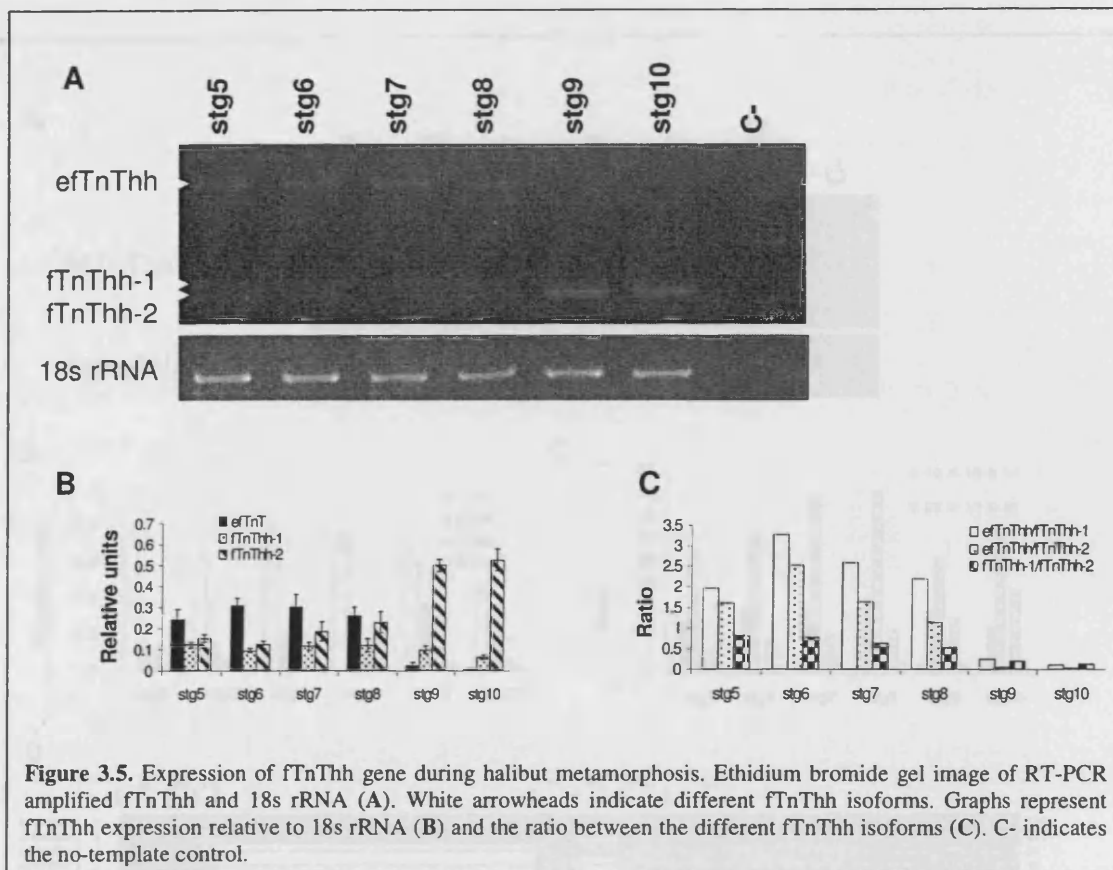
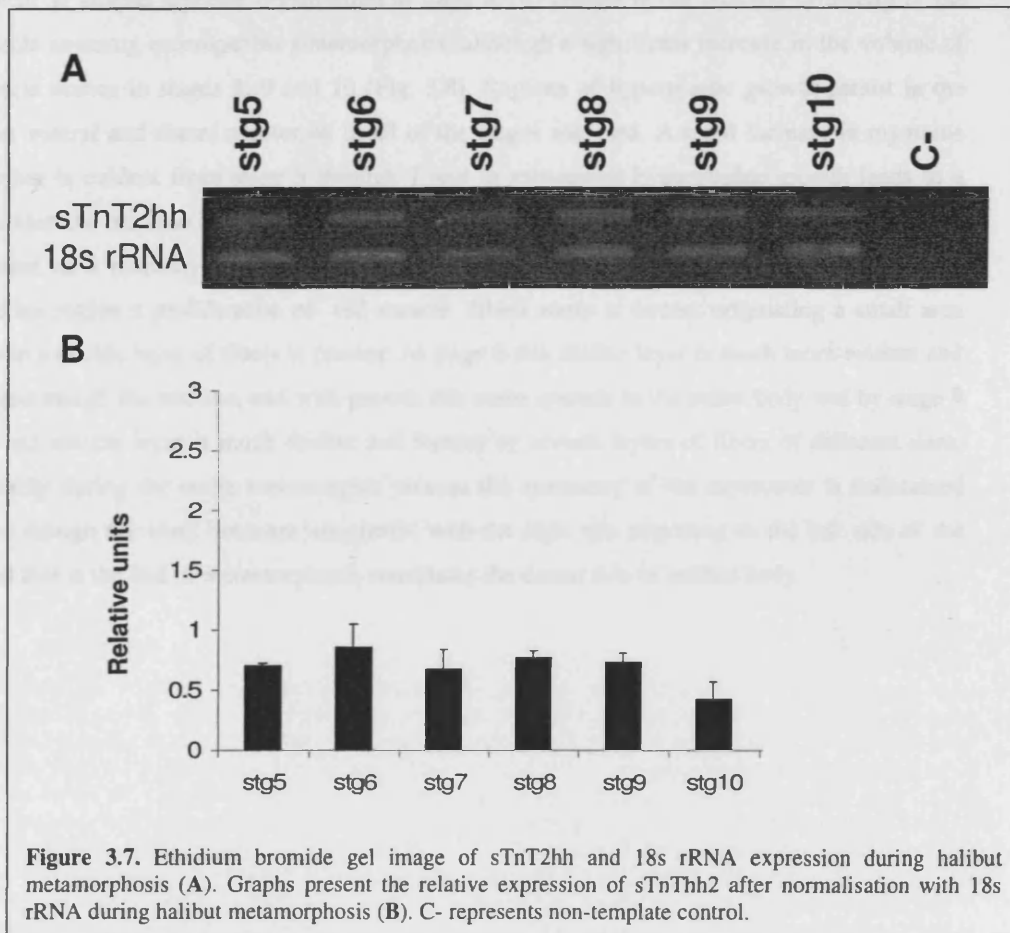


Figure 3.5. Expression of fTnThh gene during halibut metamorphosis. Ethidium bromide gel image of RT-PCR amplified fTnThh and 18s rRNA (A). White arrowheads indicate different fTnThh isoforms. Graphs represent fTnThh expression relative to 18s rRNA (B) and the ratio between the different fTnThh isoforms (C). C- indicates the no-template control.

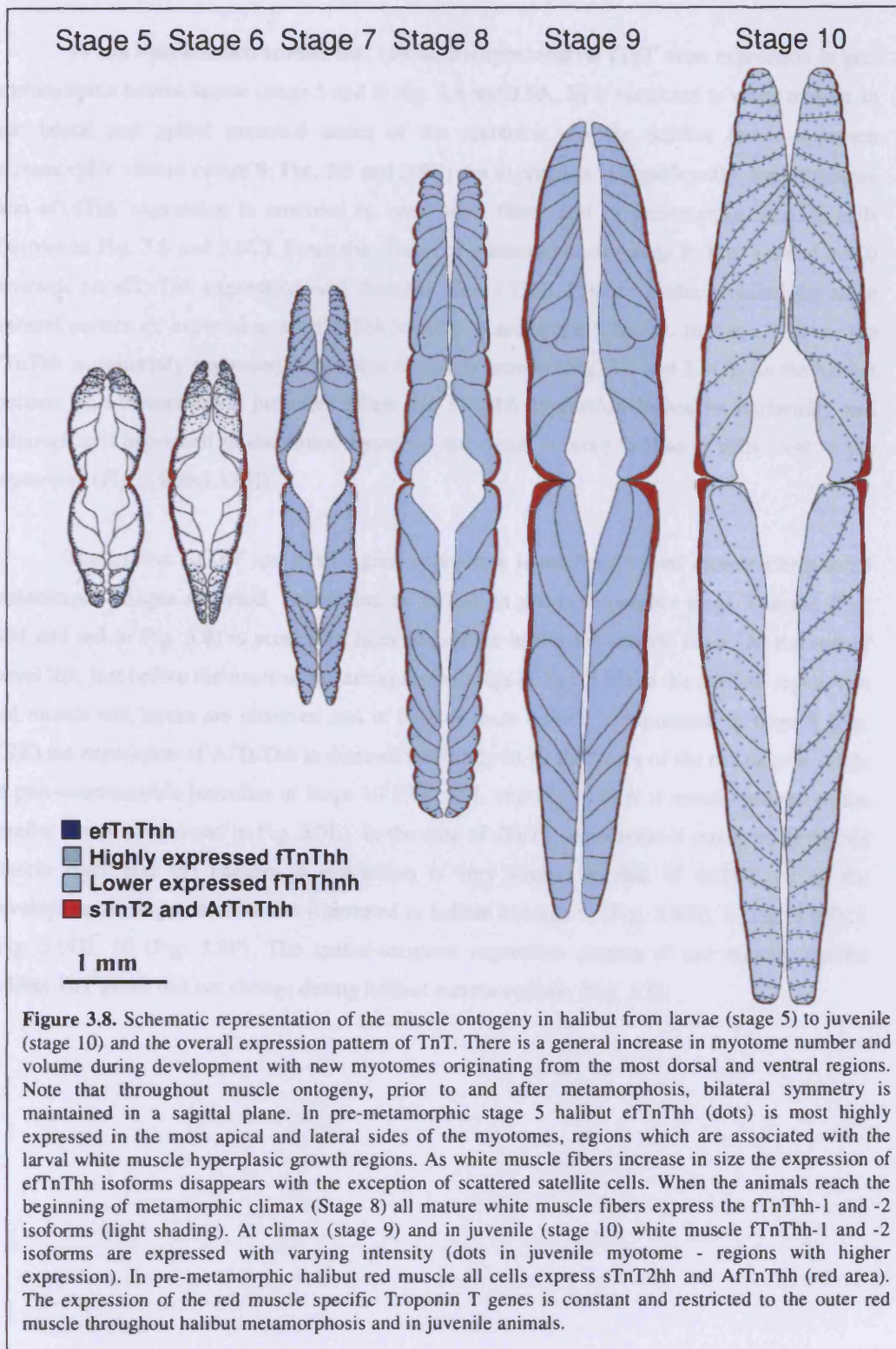
Analysis of the expression of fTnT isoforms in adult halibut muscle confirmed the same general pattern of expression as encountered by northern blot (Fig. 3.3A). However, the more sensitive RT-PCR technique permitted detection of fTnThh isoforms in halibut adult red muscle (Fig. 3.3B). In halibut adult white muscle low expression of efTnThh (~14-fold lower than fTnThh-2) is observed, fTnThh-2 continues to be the predominant isoform although fTnThh-1 expression has increased and is now about half of fTnThh-2 expression (Fig. 3.3B). The ratio of the different isoforms of fTnThh gene in red muscle differs from white muscle since fTnThh-2 is ~10-fold more expressed than efTnThh and fTnThh-1 which are almost undetectable (Fig. 3.3B).

AfTnThh-1 is the predominantly expressed isoform throughout the halibut's life. In turn, AfTnThh-2 is the second most abundant isoform and its expression increases after climax (HSD, $p < 0.006$; Fig. 3.6A and B). However, in adult red muscle the ratio of the two isoforms is identical to pre-metamorphic Stg5 animals (Fig. 3.6A and C and 3.3B). The AfTnThh-3 and -4 isoforms have identical (HSD, $p > 0.05$), very low expression (Fig. 3.6A-C) and their expression and ratio in relation to other isoforms never changes during metamorphosis (HSD, $p > 0.05$; Fig. 3.6A-C). Moreover, in adult red muscle these low molecular weight isoforms are not expressed (Fig. 3.3B).



3.3.6 Muscle Growth and Ontogeny

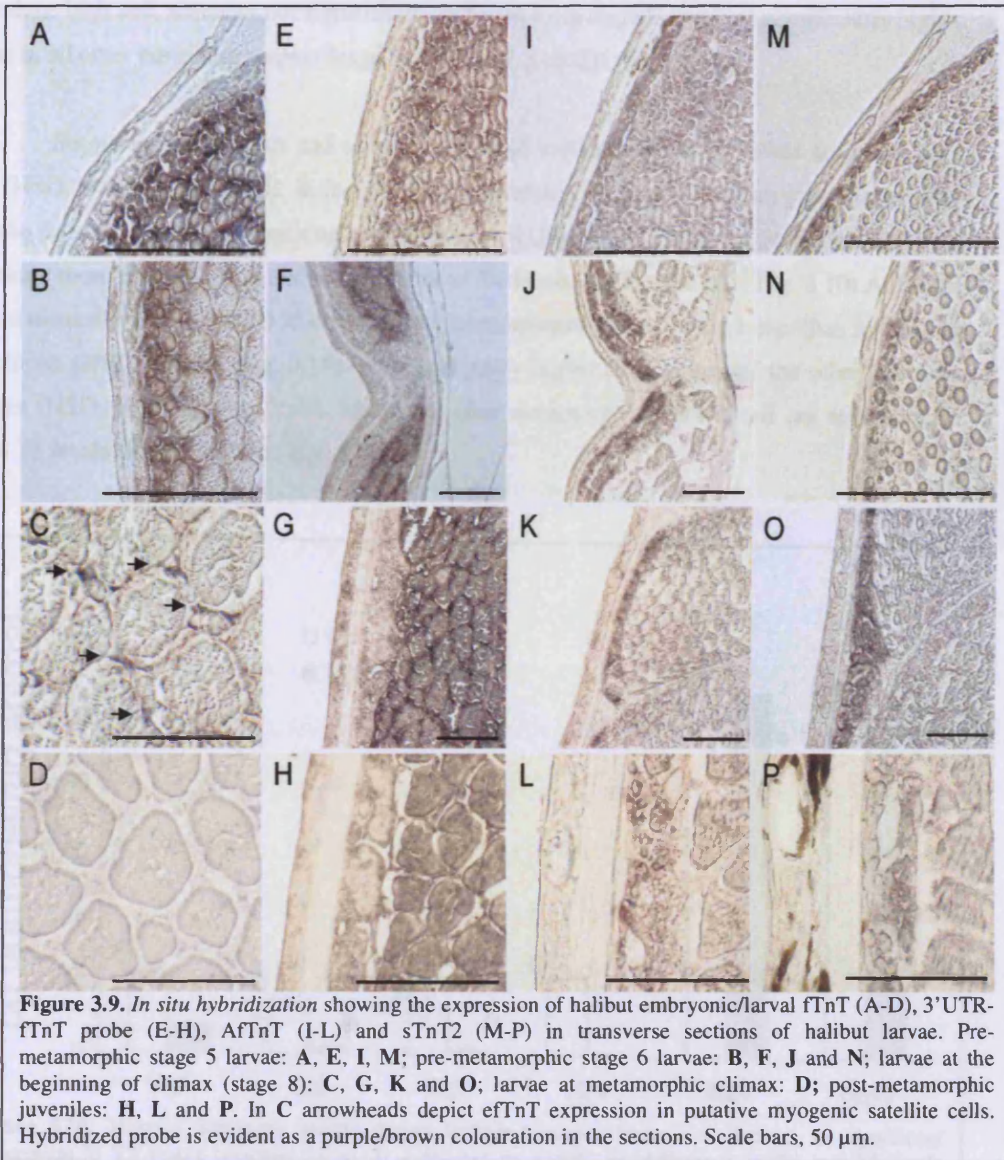
The larval stages studied all correspond to free swimming larvae which feed exogenously. In such larvae two distinct muscle layers are evident, an inner white and superficial red muscle layer (Fig. 3.8). In stage 5 halibut the anatomical organisation of the white muscle is very simple with a v shaped myomere and is composed of several block-like myotomes bounded by a septum which are bilaterally symmetrical. The extreme dorsal and ventral myotomes and the lateral region of the myotomes close to the red muscle is characterized by the presence of numerous small rounded fibres, characteristic of germinal zones, while the deeper region of the larger myotomes, fibres are much larger, more block-like and are closely packed. In subsequent stages myotome number increases and they take on the typical W shaped myomer organisation in stage 6. No change in the bilateral symmetry of the muscle anatomy accompanies metamorphosis, although a significant increase in the volume of muscle occurs in stages 8, 9 and 10 (Fig. 3.8). Regions of hyperplastic growth persist in the most ventral and dorsal myotomes in all of the stages analysed. A rapid increase in myotome number is evident from stage 5 through 7 and in subsequent hypertrophic growth leads to a considerable increase in myotome and overall muscle volume. In stage 5 the red muscle layer is present as a monolayer of fibers present at the outermost regions of the myotomes, at the midline region a proliferation of red muscle fibers starts to occur originating a small area where a double layer of fibers is present. At stage 6 this double layer is much more evident and spread through the midline, and with growth this event spreads to the entire body and by stage 9 the red muscle layer is much thicker and formed by several layers of fibers of different sizes. Notably during the entire metamorphic process the symmetry of the myotomes is maintained even though the skull becomes asymmetric with the right eye migrating to the left side of the head that at the end of metamorphosis constitutes the dorsal side of halibut body.



3.3.7 Spatial-temporal expression pattern of halibut TnT genes during metamorphosis

In situ hybridisation reveals that halibut embryonic/larval fTnT exon expression in pre-metamorphic halibut larvae (stage 5 and 6; Fig. 3.8 and 3.9A, B) is restricted to white muscle, in the lateral and apical germinal zones of the myotome. As the halibut larvae approach metamorphic climax (stage 8; Fig. 3.8 and 3.9C) the expression is significantly downregulated and efTnThh expression is confined to very small fibres and to presumptive satellite cells (arrows in Fig. 3.8 and 3.9C). From the climax of metamorphosis (stage 9; Fig. 3.8 and 3.9D) onwards no efTnThh expression was detected. The 3'UTR fTnThh probe revealed the same general pattern of expression as efTnThh in stage 5 and stage 6 larvae. In stage 8 larvae the fTnThh is uniformly expressed throughout the white muscle (Fig. 3.8 and 3.9G). As the halibut become post-metamorphic juveniles (stage 10) fTnThh expression loses its uniformity and although still expressed in the entire myotome, the signal is more intense in cells close to the myoseptra (Fig. 3.8 and 3.9H).

The halibut AfTnT and sTnT2 gene expression is confined to red muscle fibres in all metamorphic stages analysed. Expression of AfTnT in pre-metamorphic stage 5 larvae (Fig. 3.9I and red in Fig. 3.8) is present in high abundance in the red muscle layer. At the end of larval life, just before the onset of metamorphosis, (stage 6; Fig. 3.9J) in the midline region two red muscle cell layers are observed and in both of them AfTnT is expressed. In stage 8 (Fig. 3.9K) the expression of AfTnThh is detected uniformly in all the fibres of the red muscle, while in post-metamorphic juveniles at stage 10 (Fig. 3.9L and Fig. 3.8) it is mostly present in the smaller fibres (arrowhead in Fig. 3.9L). In the case of sTnT2, expression is restricted to the red muscle layer and the pattern of expression is very similar to that of AfTnT, in all the developmental stages studied and illustrated in halibut at stage 5, (Fig. 3.9M), 6 (Fig. 3.9N), 8 (Fig. 3.9O), 10 (Fig. 3.9P). The spatial-temporal expression pattern of red muscle specific halibut TnT genes did not change during halibut metamorphosis (Fig. 3.8).

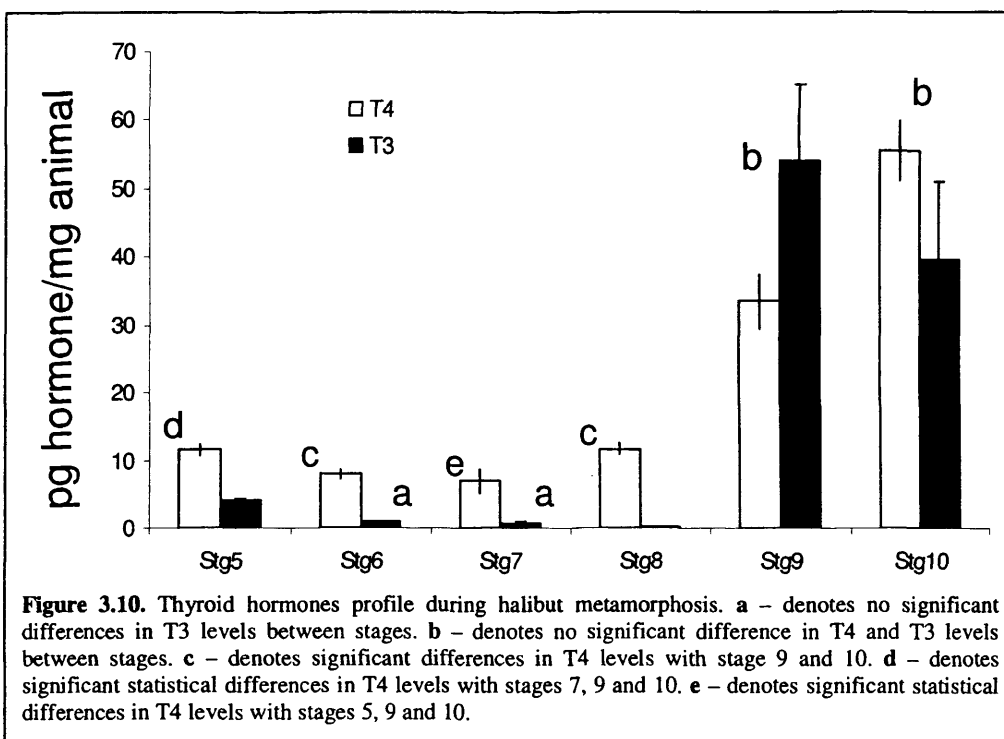


3.3.8 TH levels in metamorphosing halibut

At the beginning of metamorphosis and up until the beginning of climax (Stg8), T4 levels remain low with no significant differences observed between the stages 5, 6 and 8 of (HSM, $p > 0.05$; Fig. 3.10). In fact in larvae at the beginning of metamorphosis (stage 7) T4 levels are lower than in stage 5 pre-metamorphic larvae (HSD, $p < 0.05$). At the climax of metamorphosis (Stg9), whole-body T4 content increases about 3-fold in relation to all the

previous stages (HSM, $p < 0.005$, Fig. 3.10). In post-metamorphic juveniles (Stg10) T4 levels continue high and, although not significantly different from stage 9, they are significantly higher than in all other preceding stages (Stage 5 to 8, HSM, $p < 0.001$; Fig. 3.10).

Before metamorphosis and up until climax of metamorphosis T3 levels are lower than T4 (HSD, $p < 0.001$; Fig. 3.10). In fact, T3 levels decrease concomitantly from pre-metamorphic larvae up until animals approaching climax at stage 8 (Fig. 3.10). However, at climax T3 levels increase more than 200-fold and are higher than T4 levels (HSD, $p < 0.001$; Fig. 3.10). Although not statistically significant T3 levels in fully metamorphosed juveniles are lower than in animals at climax (HSD, $p > 0.05$; Fig. 3.10) but significantly higher than in any of the other previous stages (HSD, $p < 0.001$; Fig. 3.10). Moreover, after metamorphosis T4 levels are again higher than T3 levels (HSD, $p < 0.001$; Fig. 3.10).



3.4 Discussion

3.4.1 Halibut TnT genes

We have isolated cDNAs from three different striated muscle TnT genes in the halibut one of which is white muscle specific while the other two are red muscle specific. Alternative splicing of the fTnThh gene gives rise to three alternative splice variants which encode three proteins varying only in the N-terminal region (Fig. 3.1). The halibut fTnT cDNAs isolated are the product of a single fTnT gene that is an orthologue of tetrapod fTnT genes confirmed both by phylogenetic analysis (Fig. 3.4) and their predominant expression in white muscle (Fig. 3.3). As observed for the fTnT gene of *S. auratus* (a perciform; see Chapter 5), halibut fTnT is also expressed in adult red muscle. In fact, the expression of teleost fast-specific genes in red muscle seems to be a common feature in teleost species (Mascarello et al., 1995; Chauvigne et al., 2006). In relation to fTnThh-1 (predicted M_R 27.89 kDa and pI 9.42) and fTnThh-2 (predicted M_R 27.5 kDa and pI 9.55), the putative efTnThh protein isoform is bigger (M_R 34.6 kDa) and more acidic (pI 5.27) and the difference arises as a consequence of splicing in of exon V (Fig. 3.2A), in a way similar to that previously reported in *S. auratus*, a perciform and also in other vertebrates (Chapter 5) (Briggs et al., 1984; Breitbart et al., 1985; Hastings et al., 1985; Briggs et al., 1987; Briggs et al., 1988; Briggs and Schachat, 1989; Briggs and Schachat, 1993; Morgan et al., 1993; Wu et al., 1994; Jin, 1996; Jin et al., 1996; Wang and Jin, 1997; Jin et al., 1998a; Ogut and Jin, 1998; Perry, 1998; Bucher et al., 1999; Bastide et al., 2002; Jozaki et al., 2002). In the halibut the number of alternatively spliced fTnT isoforms is the same as that found in *Tetraodon* and *S. auratus* (Chapter 5). In common with *Tetraodon* efTnT, exon V is spliced in and exon IV is spliced out (Fig. 3.1 and 3.2A). This is in contrast to efTnT in *S. auratus* in which exon IV is also spliced in along with exon V (Chapter 5) suggesting that in the halibut and *Tetraodon* exons IV and V are mutually exclusively expressed (Fig. 3.2A). Although no data is available about the specific biochemical characteristics of muscle fibres in halibut, *S. aurata* or *Tetraodon* larvae, the present study indicates that differences probably exist between

teleost species and these differences are probably an adaptation to their differing ecologies and locomotive strategies.

In rat, human and mouse it has been reported that some fTnT isoforms predominate over others due to the specific biochemical characteristics of different fibres types (Briggs and Schachat, 1996). In these mammals acidic, fetal fTnT isoforms predominate in mainly glycolytic fibres whereas more basic isoforms are predominant in mainly oxidative fibres (Briggs and Schachat, 1996). However, there are clear differences between teleost and tetrapod fTnT genes. In tetrapods alternative splicing of the fTnT gene generates several N-terminal protein isoforms through the use of a greater number of alternatively spliced exons (Perry, 1998; Bucher et al., 1999) whereas in teleosts it seems that only two exons undergo alternative splicing (Fig. 3.2A; Chapter 5). Although the fetal/embryonic exon is bigger in teleosts than in tetrapods they have similar biochemical characteristics and it encodes an acidic peptide containing multiple glutamic acid residues (present chapter, Chapter 5) (Briggs and Schachat, 1993). No fTnT cDNA isoforms representing 3' spliced variants and therefore proteins with differing C-terminal sequences are observed in halibut, *Tetraodon* or *S. auratus*. Curiously, the deduced C-terminal amino acid sequence of all halibut fTnT isoforms share greatest identity to tetrapod isoforms containing the embryonic specific exon 17 (Wang and Jin, 1997; Jin et al., 1998b; Perry, 1998; Jozaki et al., 2002). Together with a previous study in teleosts (Chapter 5) the present data in halibut seem to reinforce the idea that the occurrence of alternative spliced exons in the C-terminal region of the fTnT gene is a characteristic exclusive to terrestrial vertebrates. Nonetheless, the genomic organization of fTnT genes in teleosts is identical to tetrapods (Bucher et al., 1999) and from an evolutionary perspective, it seems likely that alternative splicing to generate N-terminal protein variants of the fTnT gene in vertebrates already occurred before the divergence between the actinoperigii and sarcopterigii vertebrate lineages.

An unexpected observation arising from the present study was the identification of a large (predicted Mw 34.21 kDa), highly acidic (predicted pI 5.07) halibut skeletal muscle TnT (AfTnT) gene that in tBLASTx analysis (Altschul et al., 1990) had highest sequence identity to *D. rerio* fTnTa gene (Hsiao et al., 2003). A homologue of this TnT gene was found in *Tetraodon* together with five splice variants and despite its unusual characteristics it had a similar organization to other vertebrate TnT genes (Briggs et al., 1984; Breitbart et al., 1985; Hastings et al., 1985; Briggs et al., 1987; Briggs et al., 1988; Briggs and Schachat, 1989; Briggs and Schachat, 1993; Morgan et al., 1993; Wu et al., 1994; Jin, 1996; Jin et al., 1996; Wang and Jin, 1997; Jin et al., 1998a; Ogut and Jin, 1998; Perry, 1998; Bucher et al., 1999; Bastide et al., 2002; Jozaki et al., 2002; Hsiao et al., 2003). The highly acidic nature of the protein isoforms encoded by this gene is a consequence of splicing in of exon V which encodes a very acidic stretch (~50 aa) of amino acids. Regardless of the fact that both sequence similarity and phylogenetic analysis categorise the putative AfTnThh protein as a fast TnT the tissue expression analysis (Fig. 3.3) indicates that the AfTnT is a red muscle specific gene in halibut. This is the first time to our knowledge that a gene presumed on the basis of its sequence to be fast muscle specific is found in a vertebrate to be exclusively expressed in red muscle. The present observation in halibut and zebrafish (Hsiao et al., 2003) indicate that despite the apparent anatomical simplicity of striated skeletal muscle in teleosts, at the molecular level they have completely novel adaptations that probably underline species-specific control mechanisms of muscle development.

The sTnT2hh cDNA sequence is highly conserved when compared to other teleost sTnT2 genes and in the halibut it is exclusively expressed in red muscle (Fig. 3.3 and 3.9A-E and A'-E'). Moreover, in common with what occurs in *S. auratus* (Chapter 5) a single cDNA was found in halibut suggesting that the sTnT2 gene does not undergo alternative splicing. Species specific differences occur in the N-terminal region and 5 and 6 additional amino acids (EAQEE and EEAQEE respectively) are found in *Tetraodon* and halibut compared to *Fugu* and *S. auratus* and make the former putative sTnT2 proteins more acidic. The localisation in teleosts

of modifications in the N-terminal region of sTnT2 highlights the probable existence of species-specific differences in the modulation of muscle contraction an observation that is supported by the importance of this region in fine-tuning contraction in mammals (Perry, 1998; Jin et al., 2000b).

3.4.2 Halibut TnT genes expression during metamorphosis

The expression of AfTnThh and sTnT2hh does not appear to change at climax of metamorphosis; however changes in the expression of fTnT gene isoforms do coincide with this developmental stage in halibut. The higher molecular weight band bearing the larval/embryonic exon (efTnThh) is the predominant fTnT isoform up until the start of metamorphosis (Fig. 3.5). At climax of metamorphosis, the efTnThh isoform is downregulated and fTnThh-2 becomes the predominant fTnThh isoform and this expression pattern is maintained even in adult white muscle (Fig. 3.5). Apparently, fTnThh-1 isoform expression is not affected at metamorphosis but in adult white muscle it increases slightly (Fig. 3.5). When the transition in expression of the different fTnThh isoforms is observed in light of TH levels a correlation is found between the increase in whole-body T3 and T4 levels and the downregulation of efTnThh. In turn, TH levels correlate positively with the increase in expression of fTnThh-2 (Fig. 3.5, 3.9 and 3.10). A similar situation also occurs in *Paralichthys olivaceus* (Yamano et al., 1991a) and at the climax of metamorphosis an acidic 41.5 kDa efTnT isoform is downregulated and two lower molecular weight and more basic isoforms are upregulated, and detected in juvenile and adult white muscle. While in *Solea solea*, *Scophthalmus maximus* (Focant et al., 2003) and the halibut the lowest molecular weight isoform, fTnThh-2 predominates in white muscle after metamorphosis, in *P. olivaceus* an intermediate molecular weight isoform is more abundant (Yamano et al., 1991a).

Comparison of fTnT isoform expression in flatfish reveals a very similar pattern of expression across species, although notably in the only study of a round fish, *S. auratus*, the

fTnT gene isoform expression profile is very different and seems to be more complex as each *S. auratus* fTnT isoform predominates at different life stages (Chapter 5). While in the halibut (present chapter) and *P. olivaceus* (Yamano et al., 1991a) the acid high molecular weight isoform is only downregulated at metamorphosis, in *S. auratus* this occurs immediately after hatching (Chapter 5). Moreover, in *S. auratus* the lowest molecular weight protein is predominant in larval stages but in adult white muscle the intermediate isoform predominates. These data about fTnT isoform expression in different teleosts during development argue in favour of the hypothesis that different larval and adult muscle developmental programs exist in order to respond to species-specific functional requirements.

In fact, adult muscle regeneration after injury in *S. auratus* and *D. rerio* differs and involves different populations of myoblasts suggesting alternative mechanisms of post-embryonic muscle development occur in these two teleosts (Rowlerson et al., 1997). Moreover, in *S. auratus* red muscle grows by stratified hyperplasia of the germinal zones beneath the red muscle layer and the white muscle myotome when the animals are well into the juvenile stage (Rowlerson et al., 1995). In contrast, in *Clupea harengus* larvae new red muscle fibres are added at the superficial layer of the red muscle by a distinct cell population (Johnston et al., 1998). It seems likely that in teleosts alternative splicing of TnT genes as well as increased TnT gene number are involved in species specific muscle adaptations at the molecular level.

The changes in fTnT isoform expression in different teleost (present study, Chapter 5) (Yamano et al., 1991a; Focant et al., 2003) are reminiscent of what occurs in tetrapods in which fetal acidic fTnT isoforms are downregulated immediately after birth and are substituted by basic adult isoforms (Yao et al., 1992; Wang and Jin, 1997; Wang et al., 2001). The transition from acidic to a basic isoforms in fTnT genes seems to be a common trend in vertebrates and represent a physiological, mechanistic and functional adaptation of developing striated muscle (Wang and Jin, 1997; Jin et al., 2000b; MacFarland et al., 2002; Nosek et al., 2004). This strong conservation suggests that the same factors responsible for fTnT isoform transition during

development are common throughout vertebrates and may be a trait acquired long before the divergence of the actinoperigii and sarcopterigii vertebrate lineages. In fact, teleost muscle and tetrapod muscle face similar physiological and biochemical changes during development. Foetal mammalian muscle grows by hyperplasia up until birth and muscle fibres are mainly glycolytic while the mainly oxidative adult muscle fibres, that differentiate after birth, express predominantly basic fTnT isoforms (Briggs and Schachat, 1996). In teleosts, the muscle fibres also change their biochemical and physiological characteristics during development and up until metamorphosis white muscle is the major respiratory surface of the larvae and fibres are mainly aerobic and rich in mitochondria whereas the adult muscle fibres are mainly anaerobic what is opposite to the observed in tetrapod muscle fibres (Osse, 1990; Johnston, 1994; Koumans and Akster, 1995; Johnston et al., 1997; Patruno et al., 1998; Osse and van den Boogaart, 1999; Watabe, 1999). However, it has been suggested in teleosts that the change in muscle protein isoforms during development is more related to increase energy utilization efficiency and appropriate contraction characteristic of muscle (Koumans and Akster, 1995). In fact it was shown in tetrapods that embryonic fast and cardiac TnT isoforms present lower cooperative with Tm, TnI and TnC in contrast to adult isoforms and that this resulted in differences more efficient contraction of adult isoforms (Jin et al., 2000b). Nonetheless, the fact that the fTnT gene alternatively spliced 5' exons from teleosts to mammals show similar codon splitage combinations implying similar alternative splicing mechanisms (Chapter 5)(Bucher et al., 1999) further reinforces the hypothesis that alternative splicing of the fTnT gene occurs in order to cope with similar developmental demands on muscle in all vertebrates and that the molecular mechanism by which this change occurs might be conserved.

As shown by others, and in contrast to tetrapod post-embryonic muscle development, in teleost species of large size, like the halibut, post-embryonic muscle development takes place in two steps in which hyperplasia is the main mechanism of muscle growth (Johnston, 1994; Koumans and Akster, 1995; Mascarello et al., 1995; Patruno et al., 1998; Stoiber et al., 1999; Mommsen, 2001). The first hyperplastic phase of post-embryonic muscle development in large

size teleost larvae is characterised by proliferative epaxial and lateral areas of the myotome and as animals reach the juvenile stage these regions are depleted and a second stage of hyperplastic growth continues in scattered myogenic cells throughout the myotome. Notably, the efTnThh isoform is mainly found at the most epaxial and lateral zones of halibut pre-metamorphic larval white muscle myotome, especially in small diameter white muscle fibres (Fig. 3.8 and Fig. 3.9A-E and A'-E'). The early differentiated halibut larvae white-muscle myoblasts appear to first express predominantly efTnT and as they mature and are incorporated in the myotome expression is downregulated and other fTnT isoforms take their place. In vertebrates the embryonic to adult fTnT isoforms pattern of change is related to alterations in cellular pH, metabolic and physiological characteristics of maturing muscle fibres (Wang and Jin, 1997; Jin et al., 2000b; MacFarland et al., 2002; Nosek et al., 2004). The transition from acid to basic pH fTnT isoforms in developing halibut muscle may be associated with the transition from proliferative small diameter muscle cells to more basic larger white muscle fibres. In fact, in *S. auratus* it was found that larval small diameter myoblast cells located in the hyperplastic lateral and epaxial region of the larval myotome contain acid mATPase activity whereas mature large diameter muscle fibres have mild alkali mATPase activity (Mascarello et al., 1995). Together with the downregulation of expression of efTnThh at halibut metamorphosis these hyperplastic proliferative areas of the myotome are gradually depleted just as metamorphosis starts and totally absent in animals entering climax (Fig. 3.8 and Fig. 3.9A-E and A'-E'). This resembles the situation in *S. auratus* where at the end of larval life the same lateral and apical hyperplastic white muscle germinative areas are depleted (Rowlerson et al., 1995).

The relationship between THs and change in fTnT isoform expression has yet to be directly demonstrated in teleosts. However, in rats T3 increased the expression of Ca²⁺ ATPase specifically in white muscle fibres and the increase in relaxation rate of post-embryonic white muscle was strictly dependent on THs (Everts, 1996). Moreover, in mammals THs are necessary to complete development of skeletal muscle (Vadaszova et al., 2004). However, in *S. auratus* juveniles (Chapter 5) T3-treatment has no effect on fTnT isoform transition during

development, although T4 treatment in *S. auratus* juveniles increased myosin light chain 2 expression (Moutou et al., 2001). The results from experiments in teleosts suggest that various post-embryonic muscle development mechanisms exist and are probably also different from tetrapods. This is further emphasized by the fact that in mammals (Everts, 1996; Soukup and Jirmanova, 2000) and *S. auratus* (Chapter 5) slow muscle seems to be more sensitive to THs than white muscle, whereas in halibut expression of the slow-muscle specific genes sTnT2hh and AfTnThh does not alter during metamorphosis when endogenous T4 levels rise (Fig. 3.6, 3.7 and 3.10).

Together with previous studies in teleost TnT genes (Yamano et al., 1991a; Focant et al., 2003; Hsiao et al., 2003; Campinho et al., 2005)(Chapter 5) the present work shows that teleost muscle, although apparently simpler and having a smaller number of specialized muscles in comparison to tetrapods (Perry, 1998; Jin et al., 2000b) shows remarkable genetic heterogeneity and species-specific regulation. The diversity of TnT forms in teleost muscle arise from alternative splicing but also from a new teleost specific TnT gene and this heterogeneity contributes to better adapt the musculature to the specific functional demands of different teleost species. In common with other flatfish, but in contrast to the round fish *S. auratus* (Chapter 5), the halibut fTnT gene isoform expression profile is apparently regulated at metamorphosis by THs. However, the halibut red muscle specific genes do not seem to be regulated at metamorphosis and are insensitive to THs. The data present in this paper seem to suggest that flatfish muscle have different THs responsiveness to round fish muscle. In general the present work seems to suggest that white muscle in the flatfishes is more TH sensitive than red muscle whereas in round fish the opposite seems to occur (Chapter 5).

CHAPTER 4

**DEIODINASES PRESENT A
COORDINATED PATTERN OF
EXPRESSION THROUGHOUT
HIPPOGLOSSUS HIPPOGLOSSUS
(ATLANTIC HALIBUT)
METAMORPHOSIS**

4.1 Introduction

The predominant form of circulating thyroid hormone is T4 (thyroxin) but the biologically active form of thyroid hormone (TH), which is most able to conjugate with thyroid hormone receptors and transactivate gene expression, is T3 (triiodothyronine) (Kohrle, 2000; Zhang and Lazar, 2000; Bianco et al., 2002; Harvey and Williams, 2002). In order to exert its biological effect T4 must be converted to T3 which occurs by the action of a family of selenocysteine protein enzymes, the deiodinases. These enzymes are involved in the maintenance of serum TH levels but they are also likened to gatekeepers as they control conversion of T4 into T3 and in this way access to nuclear receptors (Kohrle, 2000; Bianco et al., 2002). Iodothyronine deiodinases control local production and degradation of THs by deiodination. Deiodination reactions occur by outer ring deiodination (ORD) in the 5'-position of the phenolic ring or by inner ring deiodination (IRD) of the 5-position on the tyrosyl ring of T4. ORD of T4 generates T3 in peripheral tissues and IRD of T4 yields the inactive metabolite rT3. Further metabolism of T3 by IRD and rT3 by ORD results in the metabolite T2 (Kohrle, 2000; Bianco et al., 2002).

In vertebrates (St Germain et al., 1994; Croteau et al., 1995; Croteau et al., 1996; Valverde et al., 1997; Davey et al., 1999; Hernandez et al., 1999; Sanders et al., 1999; Leonard et al., 2000; Orozco et al., 2002; Orozco et al., 2003; Sutija et al., 2003; Klaren et al., 2005; Bres et al., 2006) three iodothyronine deiodinase genes have been identified: deiodinase 1 (D1); deiodinase 2 (D2); and deiodinase 3 (D3). The selenocysteine residue present in all vertebrate deiodinases identified so far (St Germain et al., 1994; Croteau et al., 1995; Croteau et al., 1996; Valverde et al., 1997; Davey et al., 1999; Hernandez et al., 1999; Sanders et al., 1999; Leonard et al., 2000; Orozco et al., 2002; Orozco et al., 2003; Sutija et al., 2003; Klaren et al., 2005; Bres et al., 2006) is encoded by an in-frame UGA codon with a SElenoCysteine Insertion Sequence (SECIS) RNA secondary structure downstream in the 3' untranslated region (UTR) of the mRNA which is recognised by a selenocysteine-tRNA (Kollmus et al., 1996; Buettner et al., 1998; Fagegaltier et al., 2000; Lambert et al., 2002).

Type I iodothyronine deiodinase, D1, is an enzyme with a high K_m , high V_{max} that prefers rT3 >> T4 > T3 as substrate. It catalyses preferentially ORD of rT3 and IRD of T4 and T3 is facilitated by sulphation (Visser, 1994; Mol, 1998; Bianco et al., 2002). Type II iodothyronine deiodinase, D2, causes ORD at the 5' position of the phenolic ring, lacks IRD activity and is a low K_m , low V_{max} enzyme that prefers T4 > rT3 as substrate and does not deiodinate sulphated T4 or rT3 (Mol, 1998; Kohrle, 2000; Bianco et al., 2002). Inactivation of THs occurs principally by the action of type III iodothyronine deiodinase, D3, a low K_m , low V_{max} enzyme that prefers T3 > T4 as substrate. It acts exclusively as an IRD in mammals and fishes (Croteau et al., 1995; Salvatore et al., 1995; Mol, 1998; Hernandez et al., 1999; Sanders et al., 1999). D3 inactivates THs by either converting T3 to T2 or by converting T4 into the iodothyronine rT3 through IRD of the 5-position of the tyrosine ring.

In mammals D1 does not appear to be important during development. It is present from foetus to adults in human and rat liver and thyroid (Richard et al., 1998; Kohrle, 2000) and also in rat kidney and intestine (Croteau et al., 1995; Bates et al., 1999). The broad expression pattern and activity of D3 decreases sharply after birth and it becomes restricted to the brain cortex and skeletal muscle (Croteau et al., 1995; Bates et al., 1999). In the development of the rat cochlea D2 plays a pivotal role and is the most important factor in T3-mediated postnatal development of this organ (Forrest et al., 2002). The coordinated expression of D3 and D2 and/or D1 during development is essential to ensure the spatial and temporal coordination of TH actions during development. In anurans, and especially in *Rana catesbeiana* and *X. laevis* metamorphosis, coordination of the action of different deiodinases brings about the correct developmental changes. In contrast to chicken and in common with mammals, D1 has a negligible role in anuran metamorphosis whereas D2 and D3 seem to be the main selenoenzymes involved in the coordination of TH action during metamorphosis (Becker et al., 1997; Huang et al., 1999b; Shintani et al., 2002). Furthermore, transgenic *X. laevis* over-expressing D3 develop normally through embryogenesis and pro-metamorphosis but fail to achieve an adult stage (Huang et al., 1999b).

In fish, even though three deiodinases have been cloned and adult tissue distribution characterised, no studies exist of these key enzymes in any early life stages apart from the limited analysis of zebrafish D1 and D2 described in chapter 1 (Thisse et al., 2003). In flatfish, which have a TH driven metamorphosis (Miwa et al., 1988; Miwa and Inui, 1991; Yamano et al., 1991a; Miwa et al., 1992; Yamano et al., 1994a; Yamano et al., 1994b; Power et al., 2001), the lack of information about deiodinases is striking. For this reason in the present study, in order to better understand the importance of deiodinases in flatfish metamorphosis, partial cDNA clones of halibut (*Hippoglossus hippoglossus*) D1, D2 and D3 were obtained. The spatial-temporal expression pattern of halibut D1, D2 and D3 has been determined during halibut metamorphosis by Taqman quantitative RT-PCR and *in situ* hybridisation. Halibut metamorphosis is accompanied by significant changes in skin and muscle morphology and gene expression (Chapters 3 and 4). In the present study the tissues responses to thyroid hormones proposed in chapters 3 and 4 are further explored by analysis of deiodinase expression during halibut metamorphosis.

4.2 Material and Methods

4.2.1 cDNA isolation of halibut D1 and D3

For isolation of halibut deiodinases, 1,000,000 clones from an halibut cDNA library made from pre-metamorphic larvae to post-metamorphosed juveniles (Llewellyn et al., 1998) were plated at a density of 50,000 plaque forming units (pfu) per plate and nitrocellulose lifts performed to screen for deiodinase genes. The complete cDNA clone of *Sparus aurata* D3 (Sweeney, unpublished results) labelled with ^{32}P -dCTP was used for screening. Labelled probe was hybridised with nitrocellulose membranes overnight at low stringency (60°C, 6xSSC, 5x Denhardt's solution, 10µg/ml tRNA, 0.1%SDS), and then washed twice for 30 minutes at room temperature (1xSSC and 0.1%SDS) followed by two washes of 30 minutes at low stringency (55°C in 1xSSC and 0.1%SDS). The membranes were exposed overnight at -80°C to Biomax MS film (Kodak). The positive plaques were isolated and a second round of screening was performed as described above.

Single positive clones were selected and automatically excised into pBluescript SK+/- (Stratagene). The DNA was purified and cDNA clones sequenced to give 3-fold coverage using BigDye Version 3 (Perkin-Elmer, UK) chemistry and an ABI 3700 sequencer. *In silico* analysis using tBLASTx (Altschul et al., 1990) against the GenBank database was carried out to establish the most probable identity of the halibut cDNA sequences. In order to better characterise putative halibut deiodinase cDNA clones the presence of SECIS elements in the 3'UTR was assessed using SECISearch 2.19 software (Kryukov et al., 2003).

4.2.2 RT-PCR cloning of halibut D2

It was not possible to isolate a clone for halibut D2 using cDNA library screening and so an RT-PCR strategy with degenerate primers was instead utilised. Degenerate primers, using modified nucleotides, were designed to conserved regions of D2 identified after multiple nucleotide sequence alignment (Clustal X, (Thompson et al., 1997) of cDNA sequences retrieved from GenBank. The following primers were designed: F1, CGNTCCATMTGGAAYAGYTT; F2, TTYGGYTCGGCMACCTGACC; F3, CAYCCYTCTGAYGGNTGGGT; R1, GGTCAGGTKGCCGANCCRAA; R2, ACCCAWCCRTCAGANGGRTG; R3, GCATTGTTRTCCATRCARTC; R4, CCGTARSTSWKYTCCAGCCA. The primer combinations used were F1/R1, F1/R2, F1/R3, F1/R4, F2/R2, F2/R3, F2/R4, F3/R3 and F3/R4. The PCR reactions were performed using Sigma 2xReadyMix, 1.5 mM of MgCl₂ and 1 mM of each primer. The reactions were performed in a 20µl volume using 1µl of 1/1000 dilution of the halibut cDNA library or ~20ng of cDNA from whole-body halibut larvae at the climax of metamorphosis (see below) as the template. Amplification was carried out in a Techne TC-512 thermocycler with the following program: 5 minutes at 95°C followed by 35 cycles of 45 seconds at 95°C, 1 minute and 15 seconds at 55°C and 45 seconds at 72°C and a final extension time of 5 minutes at 72°C.

4.2.3 Phylogenetic analysis

To further characterise the putative halibut deiodinases cDNAs isolated, maximum-parsimony phylogenetic analysis with 1000 bootstraps (Fitch, 1971) was performed using PAUP 4.0b software (Swofford et al., 2001). All available vertebrate deiodinase sequences were retrieved from GenBank or SwissProt databases: *Homo sapiens* D1, BC107170, hsD1; *H. sapiens* D2, AAD45494, hsD2; *H. sapiens* D3, BC017717, hsD3; *Mus musculus* D1, NM_007860; *M. musculus* D2, AAD11422, mmD2; *M. musculus* D3, NM_172129, mmD3; *Rattus norvegicus* D2, P70551, rnD2; *R. norvegicus* D3, P49897, rnD3; *Gallus gallus* D1, Y11110, ggD1; *G. gallus* D2, AAD33251, ggD2; *G. gallus* D3, Y11273, ggD3; *Xenopus laevis* D1, DQ098656, xlD1; *X. laevis* D2, AAK40121, xlD2; *X. laevis* D3, BC106400, xlD3; *Rana catesbeiana* D2, AAC42231, rcD2; *Danio rerio* (zebrafish) D1, AAO65268, zfD1; *D. rerio* D2, AAO065269, zfD2; *Fundulus heteroclitus* D1, AAO31952, fhD1; *F. heteroclitus* D2, AA262449, fhD2; *Scophthalmus maximus* D2, AAQ05027, smD2; *Oncorhynchus mykiss* D2, AAL25715, omD2; *Oreochromis niloticus* D1, CAA71995, onD1; *O. niloticus* D3, CAA71997, onD3; *Sparus aurata* D1, AJ619717, saD1 and with the isolated halibut cDNA sequences D1 (hhD1- DQ856302), D2 (hhD2, DQ856304) and D3 (hhD3, DQ856303) were submitted to phylogenetic analysis with the ascidian *Halocynthia roretzi* iodothyronine deiodinase (hrDio, AAR25890) protein sequence as an outgroup. Before computational calculation of the maximum-parsimony tree all the vertebrate cDNA sequences were translated to the predicted protein using BioEdit software and a Clustal X (Thompson et al., 1997) multiple protein alignment was performed.

4.2.4 Animal and tissue sampling

Well-characterised Atlantic halibut larvae and juveniles ranging from pre-metamorphic (stages 5, 6) and metamorphosing larvae (7, 8 and 9) to fully metamorphosed juveniles (stage 10,) were obtained from Fiskey (Iceland). Halibut at different stages (n=5 per stage) were killed with an overdose of MS-222 (Sigma-Aldrich) and immediately collected into RNAlater

(QIAGEN, UK) and stored at -20°C until subsequent RNA extraction. For histology and *in situ* hybridisation experiments, Atlantic halibut at different stages were fixed in paraformaldehyde (4% PFA) at 4°C overnight, washed twice for 5 minutes with PBT and stored in 100% methanol at 4°C and decalcified in EDTA pH 8 when necessary. Fixed halibut (n=6) were embedded in paraffin Histosec (Merk, Darmstadt, Germany), and serial 5µm transverse section cut and mounted on APES coated slides. For radioimmunoassay five individual samples were collected for each stage, anaesthetised in MS-222 (Sigma) and immediately frozen. All animals were sacrificed in accordance with European legislation for Animal welfare.

4.2.5 Total RNA extraction

Total RNA was extracted from whole individual metamorphosing halibut larvae using Tri reagent (Sigma, UK) and following the manufacturers' instructions. Total RNA suspended in sterile water was quantified by spectrophotometry (GeneQuant, Amersham Biosciences) and stored at -80°C until use.

4.2.6 Quantitative Taqman RT-PCR analysis

Individual total RNA samples were then treated with DNase using the DNase Free kit (Ambion) according to the manufacturers' instructions. First strand cDNA synthesis reactions were performed as described previously (Chapter 2).

The previously isolated partial cDNA sequences for halibut D1, D2 and D3 were introduced in the PrimerExpress V2 software (Perkin-Elmer) and qPCR probes and primers were designed (Table 4.1). Primers and probes were selected based upon a Primer Express software (Perkin-Elmer) penalty gap score below 100. The probes were labelled at the 5'-end with FAM and at the 3'-end with TAMRA-6-FAM (OPERON). 18s rRNA was used as an internal standard using the primers and probes previously described (Burgos et al., 2004). qPCR

reactions for halibut deiodinases were performed using the Eurogentec qPCR mastermix and ~20ng of sample cDNA with the primers and probe conditions (Table 4.1) or 1 μ L of 1/10000 dilution of sample cDNA for 18s rRNA. All reactions were carried out in 25 μ L volumes and a preliminary assay was performed to determine optimal primer and probe concentration.

Table 4.1. Quantitative RT-PCR primers and Taqman probes sequences and respective concentration used to analyse halibut D1, D2 and D3 expression normalised with 18s rRNA expression. The PCR efficiencies are also given.

Gene	Sequence Forward Primer qPCR Concentration (nM)	Sequence Taqman probe qPCR Concentration (nM)	Sequence Reverse Primer qPCR Concentration (nM)	PCR efficiency
D1	GCGACGTGGCTGACTTCCT 30	TGGTCTACATCGCAGAGGCTCATTCAACA 100	TGGTGAAGGCCCAACCAT 90	76%
D2	AGTGATGTGGCGGACTTCCT 90	TTGGGTACATTGACGAAGCTCACCCA 300	GGCCACCCAGCCATCAG 90	73%
D3	GACATCGCAGACTCTGTAGTTGTGTA 90	ATTGAGGAAGCGCACCCCTCC 100	CGCGTCTGTGCTCATCCA 90	70%
18s	GCATGCCGGAGTCTCGTT 90	TTATCGGAATTAACCAGACAAATCGCTCCA 100	TGCATGGCCGTTCTTAGTTG 90	70%

Taqman quantitative RT-PCR was performed and analysed using, respectively, an ABI 7700 qPCR thermocycler and software (Perkin-Elmer). The qPCR thermocycle program utilised was 10 minutes at 95°C followed by 40 cycles of 15 seconds at 95°C followed by 1 minute at 60°C.

Quantification was carried out using the standard curve method with 1/10 serial dilutions (1ng/ μ L to 1fg/ μ L) of cDNA plasmid of target genes in each experiment. To normalise the quantity of halibut deiodinase amplicons obtained per reaction they were divided by 18s rRNA absolute values. Results are presented as a mean of five individual samples per stage and the bars represent standard error. In order to compare expression between halibut deiodinase genes in the different metamorphic stages, analysis of variance between the standard curves for each halibut deiodinase gene was determined. If standard curves of the halibut deiodinases had less than 5% variation the expression in each metamorphic stage was compared. The existence

of significant differences in expression of halibut deiodinase genes during halibut metamorphosis was assessed by 2-Way analysis of variance (2-Way ANOVA) followed by Holm-Sidak post-hoc test (HSM) if significant differences were found. Significant statistical differences were considered if $p < 0.05$. All statistical analysis was performed using SigmaStat3 software (SPSS Inc.).

4.2.7 Radioimmunoassay for T4 and T3

Frozen whole-body halibut larvae were extracted in 50 μ l methanol, 200 μ l chloroform and 100 μ l barbital buffer using a mechanical homogeniser. The extracts were centrifuged (3,000 rpm for 30 min at 4°C) and the upper phase removed, lyophilized and reconstituted in assay buffer for analysis of either T4 or T3. Determination of the concentration of T4 and T3 was performed by using standard curves prepared with T4 or T3 standards (Sigma-Aldrich) dissolved in 0.1N NaOH and diluted to appropriate concentrations in assay buffer. Prior to radioimmunoassay (RIA) extracted samples were heat treated (65°C for 2h). RIA for T3 and T4 were then performed as previously described (Einarsdottir et al., 2006). Statistical analysis was performed by 2-Way analysis of variance (2-Way ANOVA) followed by Holm-Sidak post-hoc test (HSM) if significant differences were found ($p < 0.05$) using SigmaStat3 software (SPSS Inc.).

4.2.8 *In situ* hybridisation

The pattern of expression of halibut D1, D2 and D3 in tissue of developing halibut larvae were investigated by *in situ* hybridisation. Digoxigenin riboprobes with sizes ranging 270-750 bp were prepared from cDNA of hhD1, hhD2 and hhD3 and the corresponding region in the cloned cDNA are indicated in Figure 5.1. Riboprobe production was carried out as previously described (Chapter 3 and 4). In order to prepare the cRNA probes the cDNA clone hhD1 and hhD3 were digested, respectively, with *Sall* (Promega) and *Eco0109I* (Promega) in

appropriate buffer accordingly to the manufacturers instructions for 1.5h. The band with the vector and the desired halibut deiodinase sequence to use as a probe was extracted from an agarose gel (Amersham GFX gel extraction kit) and 10U of T4 DNA ligase (Promega) used to recircularise the DNA by incubation at 4°C overnight in appropriate buffer. Ligated DNAs were used to transform competent cells and the recombinant plasmid DNA purified using the Promega Wizard kit accordingly to the manufacturers instructions. The hhD2 fragment obtained from degenerative RT-PCR and cloned in PGem-Teasy (Promega) was used directly to produce the hhD2 cRNA probe. All the cloned deiodinase cDNA were linearised at 37° C for 1.5 h with appropriate enzymes to generate sense and anti-sense riboprobes. To this end D1 cDNA was linearised with *Sal I* (1.5 U/μl; Promega) or *EcoRI* (0.6 U/μl; Promega); D2 cDNA with *Sac II* (1.2 U/μl; Promega) or *Sal I* (1.5 U/μl; Promega); and D3 cDNA with *Eco0109I* (2 U/μl; BioLabs inc.) or *EcoRI* (Promega). The linearised DNAs were purified and *in vitro* transcription was carried out with 1 U/μl of the appropriate RNA polymerase. The sense probe for D1 and the anti-sense probes for D2 and D3 were transcribed with T7 RNA polymerase (Promega); the sense probe for D3 and the anti-sense probe for D1 were transcribed with T3 RNA polymerase (Roche); and the sense probe for D2 was transcribed with SP6 RNA polymerase (Promega). *In vitro* transcription were carried out with linearised plasmid, ~10μg template, 1 U/μl of appropriate RNA polymerase (Promega) in 1x transcription buffer (Promega) with 1 μl of digoxigenin – RNA labelling mix (Roche Diagnostics, Mannheim, Germany) for 1.5 h at 37° C. Reactions were stopped with 2 μl of 0.2M EDTA and riboprobes were purified by lithium precipitation and resuspended in 25 μl of sterile nuclease free water (Sigma-Aldrich) and purity and approximate concentration determined by fractionation of the reaction product (1μl) on an agarose gel (1%).

Tissue sections were dewaxed, rehydrated and prehybridised at 56° C for 2 h with hybridisation solution (50% formamide, 4× SSC, 1 mg ml⁻¹ torula RNA, 0.1 mg ml⁻¹ heparin, 1× Denhardt's, 0.04% CHAPS). For hybridisation, tissues were covered with 2 μl of each probe

in 100 µl of hybridisation solution overnight at 56° C in a humidified box. In control hybridisations, riboprobes were excluded or the hybridisation was carried out with the sense probes. Post-hybridisation high stringency washes were carried out at 56° C for 2x 5 min with 2x SSC; 1x 5 min with 1x SSC; and 2x 5 min with 0.2x SSC. Tissue sections were then washed at room temperature for 2x 5 min with 2x SSC/0.12% CHAPS, followed by a 5 min wash with 2x SSC/PTW (1/1, v/v) and finally with PTW for 5 min. The blocking step was performed by incubation in 2% blocking reagent (Boehringer Mannheim, Germany) with 10% heat inactivated sheep serum for 2 h at room temperature. Detection of hybridised probe was carried out with anti-Digoxigenin–Alkaline Phosphatase (AP) Fab fragments (1/600; Roche) in 1% blocking reagent (Boehringer Mannheim, Germany) overnight at 4° C and colour development carried out at 37°C using the chromagens NBT and BCIP (Roche) according to the manufacturer's instructions. Stained sections were rinsed for 5 min in 1x PBS and then fixed for 15 min in 4% PFA at room temperature, rinsed 2x 5 min with 1x PBS and mounted in pre-warmed glycerol-gelatine (Sigma-Aldrich). Riboprobe localisation was analysed using a microscope (Olympus BH2) coupled to a digital camera (Olympus DP11) linked to a computer for digital image analysis.

4.3 Results

4.3.1 Halibut deiodinase genes

Several clones encoding two different cDNAs were isolated from the metamorphosing halibut cDNA library. Analysis by tBLASTx (Altschul et al., 1990) of the two cDNA revealed they shared highest homology with vertebrate deiodinase type 1 (hhD1) and type 3 (hhD3) genes, respectively. The hhD1 and hhD3 cDNAs had full-length 3' untranslated regions (UTR), most of the coding sequence but lacked the 5' UTR. The hhD1 cDNA is 1660 nucleotide (nt) long (Fig. 4.1A) and the hhD3 cDNA is 942 nt long (Fig. 4.1B). The hhD1 cDNA codes for a 204 amino acid (aa; from nt 3 to 615, Fig. 4.1A) protein while the hhD3 cDNA codes for a 125

aa protein (from nt 2 to 376, Fig. 4.1B). The hhD1 cDNA did not contain the ATG translation start codon or the sequence encoding the first putative 43 N-terminal aa, but contained a TGA Selenocysteine (Sec; nt 246) insertion codon (double underlined in Fig. 4.1A) as well as a consensus ATTAAA polyadenylation signal 12 nt upstream of the poly(A) tail (nt 1625 to 1630, underline in Fig. 4.1A). Moreover, analysis with SECISearch 2.19 software (Kryukov et al., 2003) revealed a consensus type I SECIS element in the 3'UTR (nt 1213 to 1305; in bold in Fig. 4.1A) and further supports the classification of the cloned hhD1 cDNA as a vertebrate type I deiodinase cDNA. The hhD3 cDNA contains a AATAAA polyadenylation signal (nt 907-912; underlined in Fig. 4.1B) 12 nt upstream of the poly(A) and in the 3'UTR from nt 743 to 843 (in bold in Fig. 4.1B, 1B') a SECIS element with greatest resemblance to a type 2 form was identified using SECISearch 2.19 software (Kryukov et al., 2003). The hhD3 cDNA is incomplete and lacks the entire 5'UTR and half of the protein coding region including the TGA Sec codon (Fig. 4.1B). Nonetheless, the tBLASTx analysis (Altschul et al., 1990) together with the identification of a type 2 SECIS element in the 3'UTR of the cDNA indicates the most probable identity of the isolated cDNA is a type III deiodinase.

A 277 nt cDNA product amplified using degenerate RT-PCR primers (combination F2/R3) was cloned from a dilution of a metamorphosing halibut cDNA library and from cDNA of whole-body stg9 (climax of metamorphosis) halibut (Fig. 4.1C). The PCR fragment obtained included a TGA Sec insertion codon (double-underlined in Fig. 4.1C) and gave highest sequence homology to other vertebrate D2 sequences in tBLASTx analysis (Altschul et al., 1990). This hhD2 fragment encoded a 91 aa peptide that corresponded to the third quarter of other vertebrate D2 proteins. Conservation was high, 85.9%, between the hhD2 peptide fragment and the corresponding D2 cDNA isolated from *Fundulus heteroclitus*, *Danio rerio* and *Scophthalmus maximus*. Comparison of the predicted aa sequence of hhD2 to tetrapod D2 revealed they share 71.8% sequence identity. Moreover, 61 aa (out of 91) are identical to other vertebrate D2 proteins in the deduced hhD2 peptide. This includes the highly conserved phenylalanine (F) and serine (S) residues that precede the Sec (U) and followed by two prolines

(P) and F residue (boxed in Fig. 4.1C) that are considered to be essential for correct enzymatic activity (Bianco et al., 2002; Bianco and Larsen, 2005; Kuiper et al., 2005).

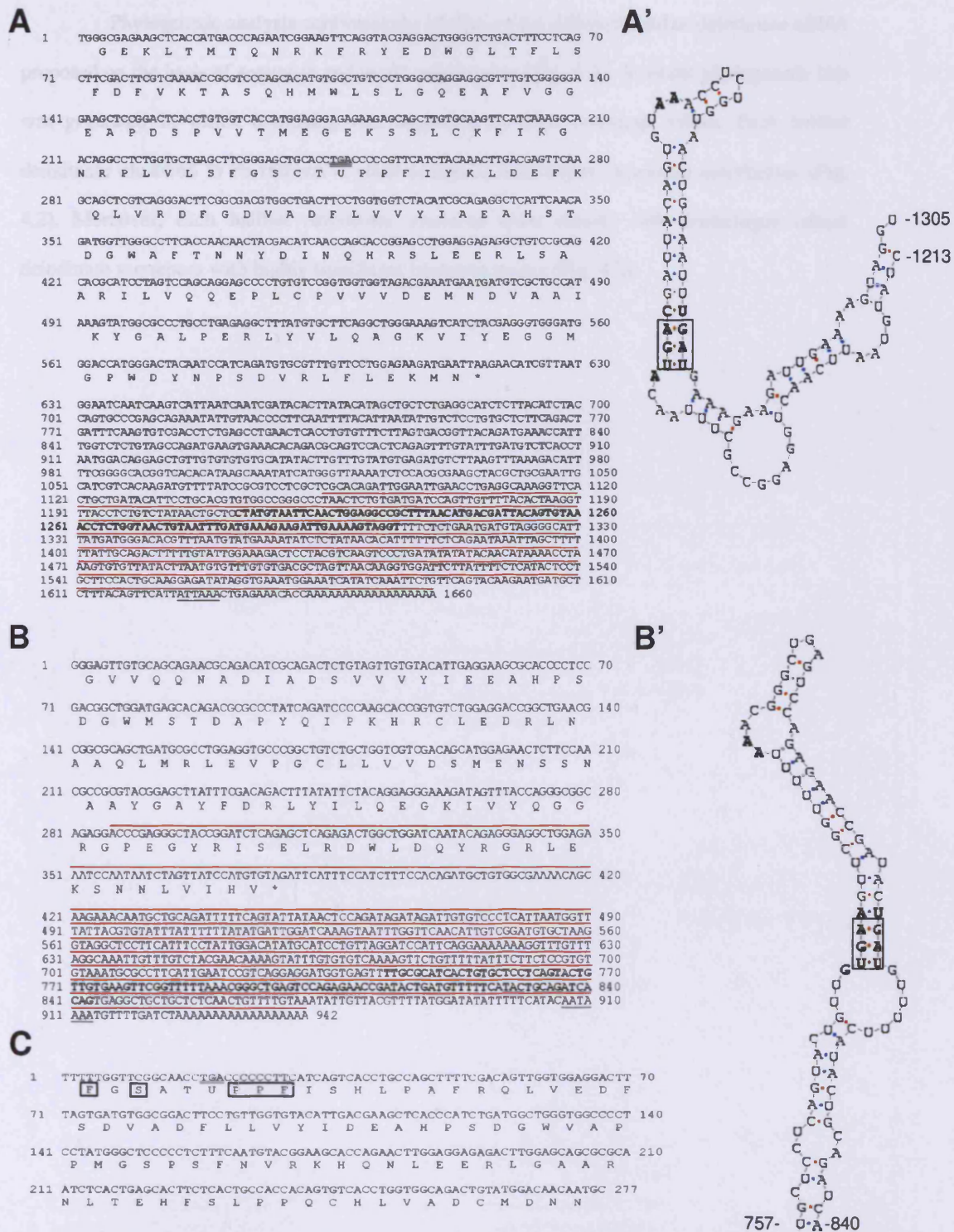


Figure 4.1. Halibut D1 (A) and D3 (B) cDNA sequences and predicted protein sequences. The double underline in (A) represents the TGA Sec insertion codon. In (A) and (B) the single underline represent the putative polyadenylation signal, the sequences in bold the SECISearch predicted SECIS element and the (*) denotes the termination codon. SECISearch predicted hhd1 (A') and hhd3 (B') SECIS element. The boxed region in (A') and (B') represent the SECIS core while the bold letters represent conserved SECIS nucleotides. Halibut D2 RT-PCR isolated nucleotide and predicted peptide sequences (C). The double underline in (C) represents the TGA Sec insertion codon and the boxed amino acids conserved vertebrate D2 amino acids. Red lines in (A) and (B) above sequences indicate hhd1 and hhd3 digoxigenin-labelled cRNA probes template sequence used for in situ hybridizations. In the case of hhd2 the entire DNA sequence isolated was used.

Phylogenetic analysis confirmed the identity of the different halibut deiodinase cDNA proposed on the basis of sequence and motif conservation (Fig. 4.2). A robust phylogenetic tree was generated in which branching was supported by high bootstrap values. Each halibut deiodinase clustered in its respective clade alongside homologue vertebrate deiodinases (Fig. 4.2). Moreover, each halibut deiodinase clustered more closely with homologue teleost deiodinase sequences with highly significant bootstrap scores (Fig. 4.2).

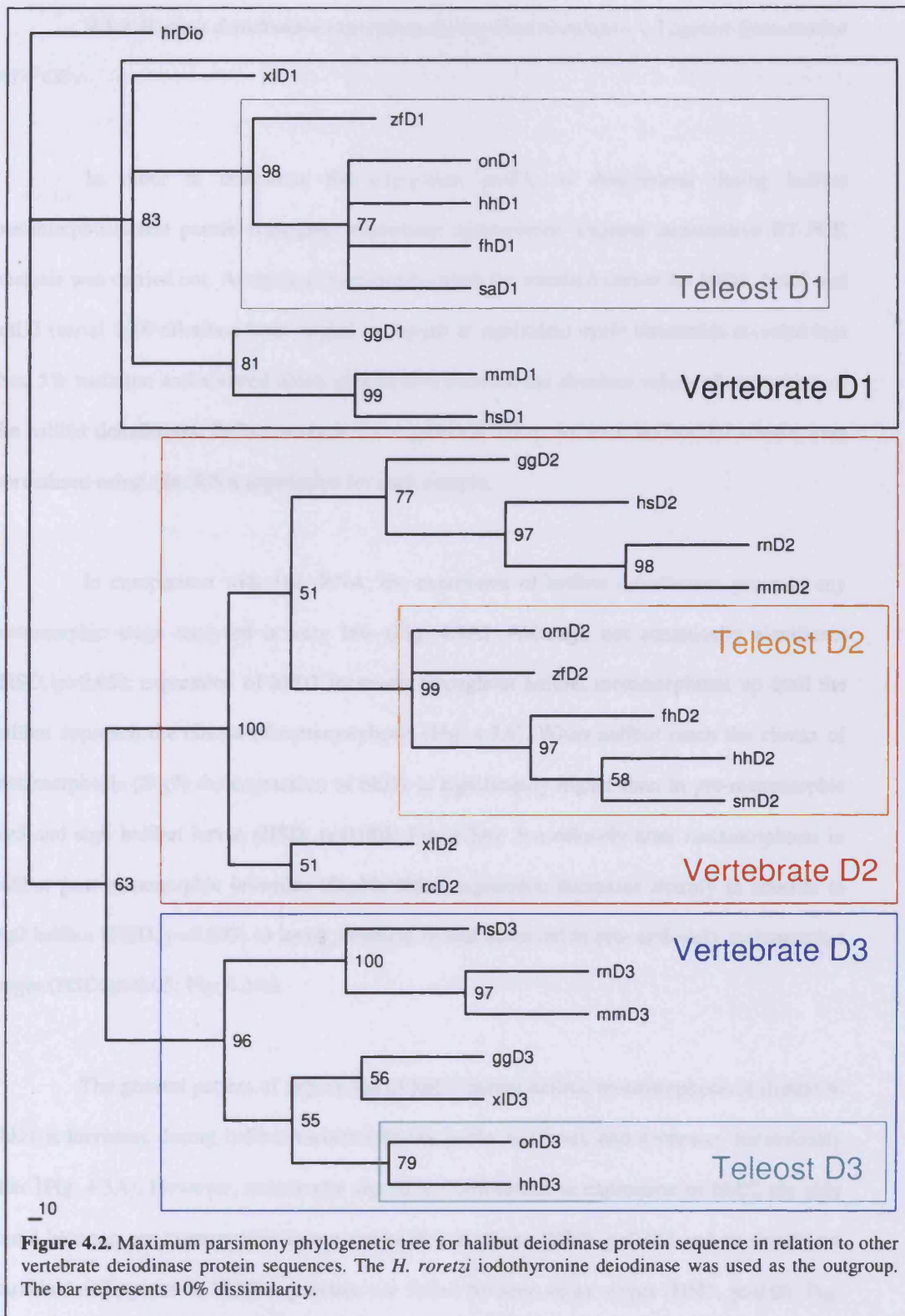


Figure 4.2. Maximum parsimony phylogenetic tree for halibut deiodinase protein sequence in relation to other vertebrate deiodinase protein sequences. The *H. roretzi* iodothyronine deiodinase was used as the outgroup. The bar represents 10% dissimilarity.

4.3.2 *Halibut deiodinases expression during metamorphosis – Taqman Quantitative RT-PCR*

In order to determine the expression profile of deiodinases during halibut metamorphosis and permit inter-gene expression comparisons Taqman quantitative RT-PCR analysis was carried out. Analysis of variance between the standard curves for hhD1, hhD2 and hhD3 (serial 1/10 dilutions from 1ng/ μ l to 1fg/ μ l) at equivalent cycle thresholds revealed less than 5% variation and allowed direct comparison between the absolute values of expression of the halibut deiodinases. Before analysis the expression values for each halibut deiodinase were normalised using 18s rRNA expression for each sample.

In comparison with 18s rRNA, the expression of halibut deiodinases genes in any metamorphic stage analysed is very low (Fig. 4.3A). Although not statistically significant (HSD, $p>0.05$), expression of hhD1 increases throughout halibut metamorphosis up until the halibut approach the climax of metamorphosis (Fig. 4.3A). When halibut reach the climax of metamorphosis (Stg9) the expression of hhD1 is significantly higher than in pre-metamorphic stg5 and stg6 halibut larvae (HSD, $p=0.005$; Fig. 4.3A). Immediately after metamorphosis in halibut post-metamorphic juveniles (Stg10) hhD1 expression decreases sharply in relation to stg9 halibut (HSD, $p=0.007$) to levels identical to that observed in pre- and early metamorphic stages (HSD, $p>0.05$; Fig. 4.3A).

The general pattern of expression of hhD2 during halibut metamorphosis is similar to hhD1 it increases during halibut metamorphosis, peaks at climax and decreases immediately after (Fig. 4.3A). However, statistically significant differences in expression of hhD2 are only found between pre-metamorphic larvae and halibut at climax (HSD, $p<0.05$) and no significant statistical differences in hhD2 expression are found between other stages (HSD, $p>0.05$; Fig. 4.3A).

The expression of hhD3 did not change significantly from pre-metamorphic halibut larvae throughout the entire metamorphic period (stgs 5-8, HSD, $p>0.05$), although in juvenile halibut (stg 10) hhD3 expression was significantly higher (stgs 5-8; HSD, $p\leq 0.01$; Fig. 4.3A). However, no statistical differences in hhD3 expression occur between individuals at climax (stg 9) and juvenile halibut (stg 10, HSD, $p>0.05$, Fig. 4.3A).

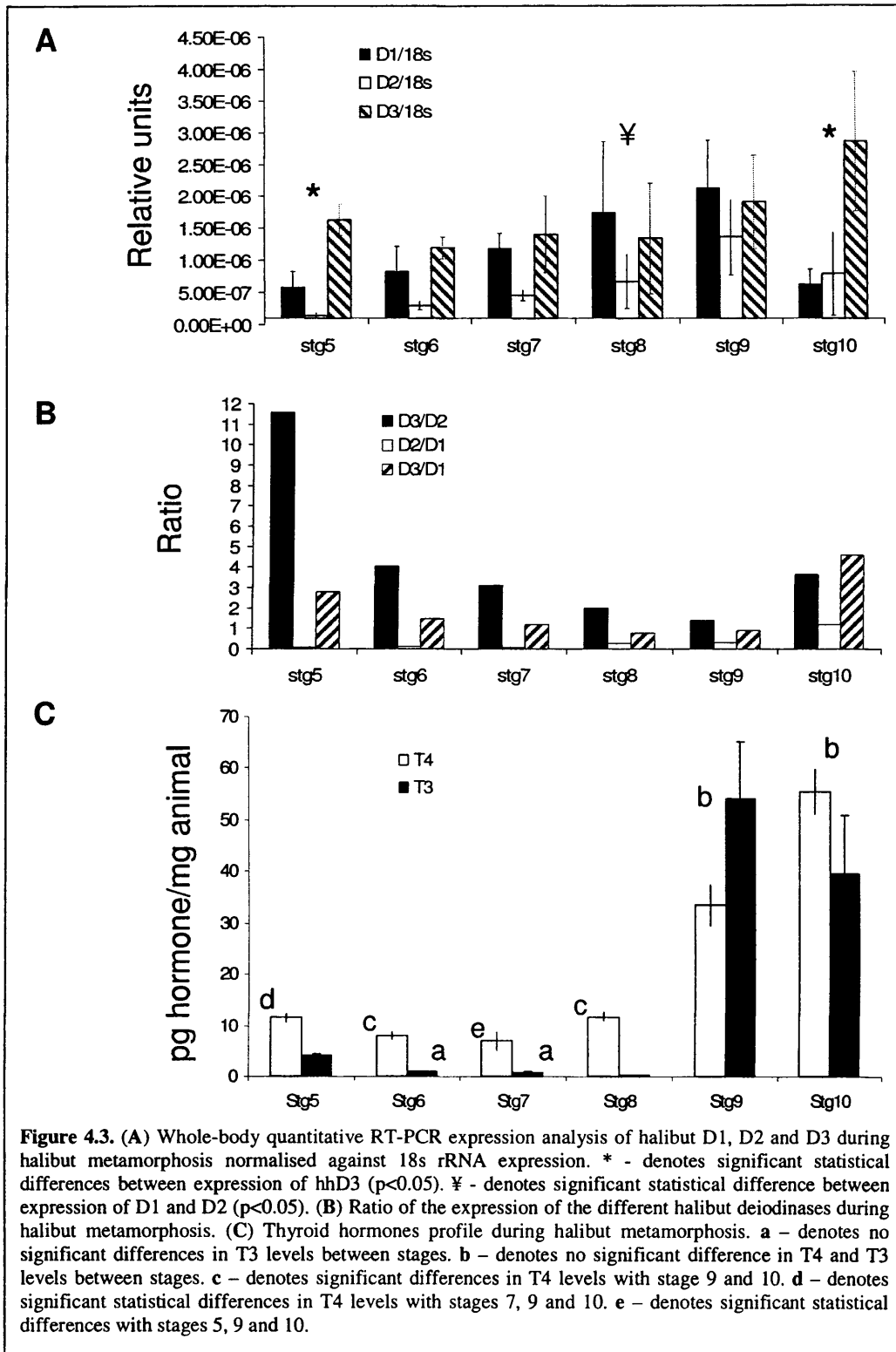
In pre-metamorphic halibut larvae (Stg5) hhD3 is the most highly expressed deiodinase (Fig. 4.3A; HSD, $p<0.05$) while hhD2 expression is at the limit of detection (Fig. 4.4A). However, no significant statistical difference between hhD1, hhD2 or hhD3 expression occurs in stage 5 halibut (Fig. 4.3A). As the halibut reach the end of larval life but just before the start of metamorphosis (Stg6) hhD3 expression diminishes while hhD1 and hhD2 expression start to increase (Fig. 4.3A) although this change is not statistically significant (Fig. 4.3A; HSD, $p>0.05$). From this stage onwards the expression of hhD1 and hhD2 increase concomitantly up until the climax of metamorphosis (Stg9) when they reach their highest expression value (Fig. 4.3A). In contrast, hhD3 expression is unaltered from stage 6 up until metamorphic climax (Stg9; Fig. 4.3A). At metamorphic climax the expression of the three deiodinases is very similar and not significantly different (Fig. 4.4; HSD, $p>0.05$). However, in post-metamorphic halibut juveniles (Stg10) hhD3 expression increases slightly while hhD1 and hhD2 expression decreases sharply (Fig. 4.3A). Notably, after metamorphosis the three halibut deiodinases have expressions values close to those of pre-metamorphic halibut larvae (Fig. 4.3A).

Comparison of the ratio between the expression of different halibut deiodinases, reveals hhD3 is highly expressed in pre-metamorphic halibut larvae in comparison to hhD1 and hhD2 (Fig. 4.3B). As development progresses and halibut enter metamorphosis (stg7), the ratio between the expression of hhD3: hhD1 and hhD2 approaches 1 (Fig. 4.3B). At the climax of metamorphosis, hhD3 reaches its lowest expression level compared to the other two halibut deiodinases and its expression is 1.4-times that of hhD2 and 0.9-times that of hhD1 (Fig. 4.3B). However, in post-metamorphic halibut juveniles the ratio between hhD3:hhD1 and hhD3:hhD2

increases sharply. The expression levels of hhD1 and hhD2 in the developmental stages studied are very similar (Fig. 4.3). Even though there is no statistical difference between hhD1 and hhD2 expression during metamorphosis, from pre-metamorphoses up until climax expression of hhD1 is always slightly higher than hhD2 but after metamorphosis hhD2 seems to be more highly expressed than hhD1 (Fig. 4.3).

4.3.3 T4 and T3 profile during halibut metamorphosis

During halibut metamorphosis T4 and T3 hormone levels vary significantly (2-Way ANOVA, $p < 0.001$; Fig. 4.3C). Before metamorphosis (Stage 5 and 6) T4 levels are around 10 pg/mg and higher than T3 levels (HSD, $p < 0.001$; Fig. 4.3C). At the beginning of metamorphosis (stage 7) T4 levels are at their lowest levels (HSD, $p < 0.05$; Fig. 4.3C) but are still higher than T3 (HSD, $p < 0.001$) which continues to drop to its lowest levels up until the beginning of climax (stage 8; HSD, $p < 0.001$; Fig. 4.3C). At climax, T4 increases ~3-fold whereas T3 increases ~230-fold in relation to the previous stage (Fig. 4.3C; HSD, $p < 0.002$) becoming the most abundant thyroid hormone at this time (Fig. 4.3C; HSD, $p < 0.001$). In fully metamorphosed juveniles T4 levels, although not significantly different (HSD, $p > 0.05$) are higher than at climax and T4 becomes again the most abundant thyroid hormone (Fig. 4.3C; HSD, $p < 0.001$). Conversely, halibut juvenile T3 concentrations decrease in relation to climax, although this decline is not statistically significant (Fig. 4.3C; HSD, $p > 0.05$), but is still ~170-fold higher than in stage 8 halibut at the beginning of climax (Fig. 4.3C; HSD, $p < 0.001$).



4.3.4 Deiodinase expression in skin during halibut metamorphosis

In pre-metamorphic larval halibut skin hhD2 expression is only encountered in larval basal epidermal cells and is at the limits of detection (Fig. 4.4A). Although more highly expressed than hhD2 expression, hhD3 transcripts are present in low abundance in the basal larval skin cells that constitute part of the epidermis, and are absent from the epithelial cells that constitute the outermost layer of the skin (Fig. 4.4A'). As the halibut reach the end of larval life just before metamorphosis (Stg6), hhD2 expression in skin increases slightly but only in larval basal epidermal cells (Fig. 4.4B). Halibut D3 expression in skin becomes more highly expressed as halibut larvae approach the end of larval life, and hhD3 is still the most expressed halibut deiodinase in skin (Fig. 4.4B and B'). In the dermis the first dermal endothelial cells start to be clearly observable and they too express hhD2 and hhD3 (Arrowheads in Fig. 4.4B and B'). The expression of both deiodinases is almost identical in skin epidermal basal cells of halibut approaching the climax of metamorphosis (Stg8; Fig. 4.4C and C'). At this time expression has also increased in dermal endothelial cells (Arrowheads in Fig. 4.4C and C') and hhD2 and hhD3 expression is, for the first time, detectable in the outermost epithelial cells (Arrows in Fig. 4.4C and C'). When metamorphosing halibut reach the climax of metamorphosis (Stg9) hhD3 expression in skin epidermis is downregulated and present in low abundance in a few scattered cells (Fig. 4.4D'). Although hhD2 expression ceases in the outermost epithelial skin cell layer its expression continues both in basal and supra-basal epidermal skin cells (Fig. 4.4D). Notably, in dermal endothelial cells hhD2 and hhD3 are still expressed although at much lower levels (Arrowheads in Fig. 4.4D and D'). However, in fully metamorphosed juvenile skin (Stg10), hhD2 expression is totally downregulated in adult basal epidermal skin cells (Fig. 4.4E) and in the epidermis is only observed in some scattered adult epidermal supra-basal cells and always at the limit of detection (Small arrows in Fig. 4.4E). Moreover, hhD2 expression is also absent in dermal endothelial cells but is now detectable in the fibroblast that have invaded the dermal collagen lamella (Arrowheads in Fig. 4.4E). Conversely, hhD3 expression restarts in both adult

epidermal basal and supra-basal cells but is absent in epithelial cells and in the dermal endothelial cells hhD3 expression has increased (Fig. 4.4E').

Despite extensive *in situ* hybridisation experiments performed with hhD1 no expression was ever found in halibut skin during the entire metamorphic period.

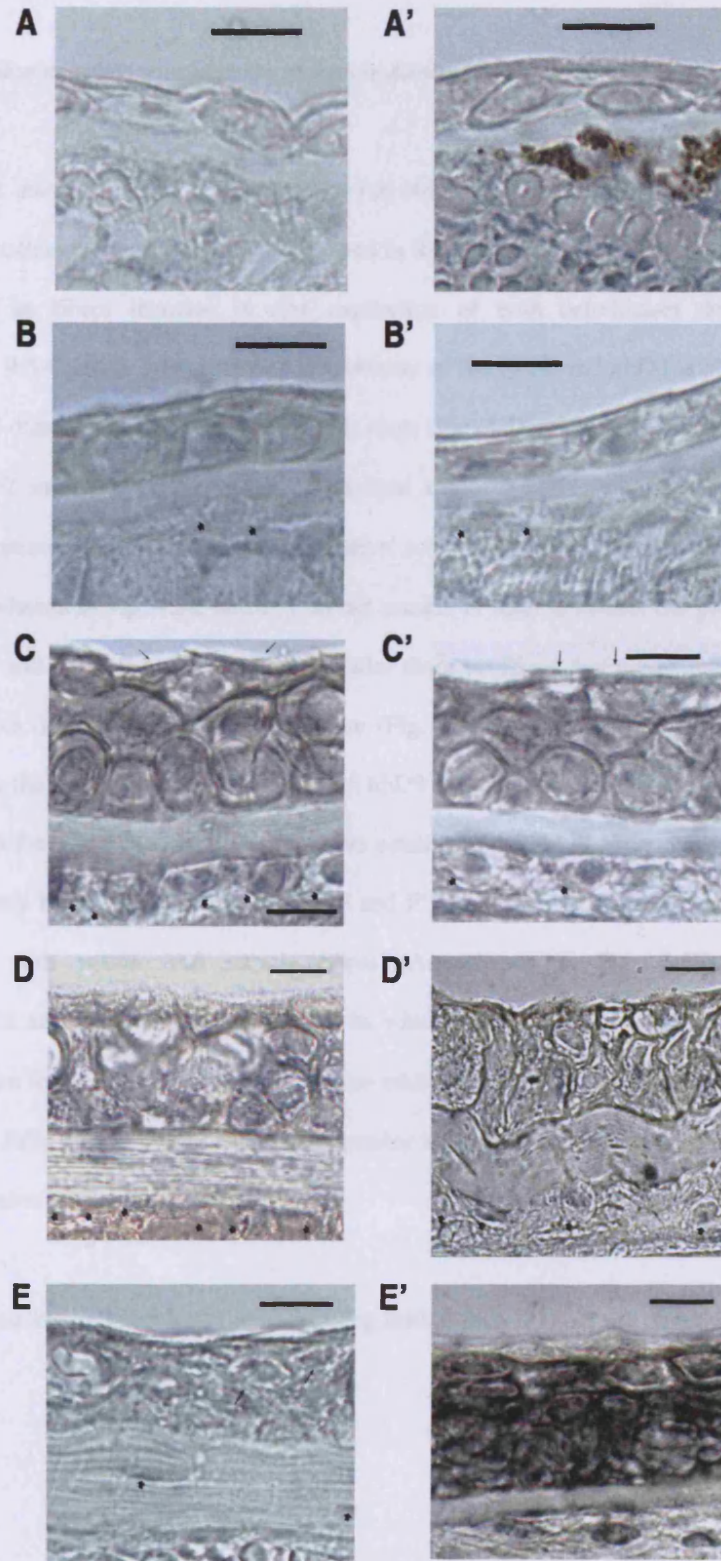


Figure 4.4. *In situ* expression of hhD2 (A- E) and hhD3 (A'-E') in halibut skin during metamorphosis. Stage 5, A and A'; Stage 6 B and B'; Stage 8 C and C'; Stage 9 D and D' and; Stage 10 E and E'. Arrowheads in B, B', C, C', D and D' denote dermal endothelial cells while in E denote collagen bound fibroblast-like cells. Small arrows in C and C' denote the outermost epithelial cells of the epidermis. The bar represents 10 μ m.

4.3.5 Halibut deiodinase expression in muscle during halibut metamorphosis

In halibut muscle, in pre-metamorphic larvae hhD2 and hhD3 are detected in low abundance in the smallest white muscle fibres localised in the most epaxial and lateral zones of the myotome, but as fibres increase in size expression of both deiodinases decreases concomitantly (Fig. 4.5A and A', respectively). Expression of the hhD3 and hhD2 is absent in the superficial small diameter red muscle fibres at this stage (Fig. 4.5B and B'). This expression pattern of both hhD2 and hhD3 continues up until halibut approach climax (Stg8), when both deiodinases are expressed at similar levels in putative satellite cells scattered in the white muscle fibres (arrowheads in Fig. 4.5C and C'). In red muscle in stage 8 halibut the pattern of expression of hhD2 and hhD3 is restricted to the smaller diameter fibres that are abundant and the expression of both deiodinases seems to be similar (Fig. 4.5D and D'). When halibut reach metamorphic climax the expression of both hhD2 and hhD3 continues but only in the scattered cells that intersperse the white muscle fibres (putative satellite cells, Fig. 4.5E and E'). In red muscle, at climax only hhD2 is expressed (Fig. 4.5F and F') and solely in scattered oval cells closely associated with mature red muscle fibres (Arrowheads in Fig. 4.5F). After metamorphosis hhD2 and hhD3 expression pattern in white muscle remains localised in the scattered cells that are found associated with the mature white muscle fibres (Fig. 4.5G and G'). In red muscle from fully metamorphosed halibut juveniles hhD2 expression is not detected as well as hhD3 expression (Fig. 4.5H and H').

It was not possible to detect hhD1 in developing halibut muscle by *in situ* experiments.

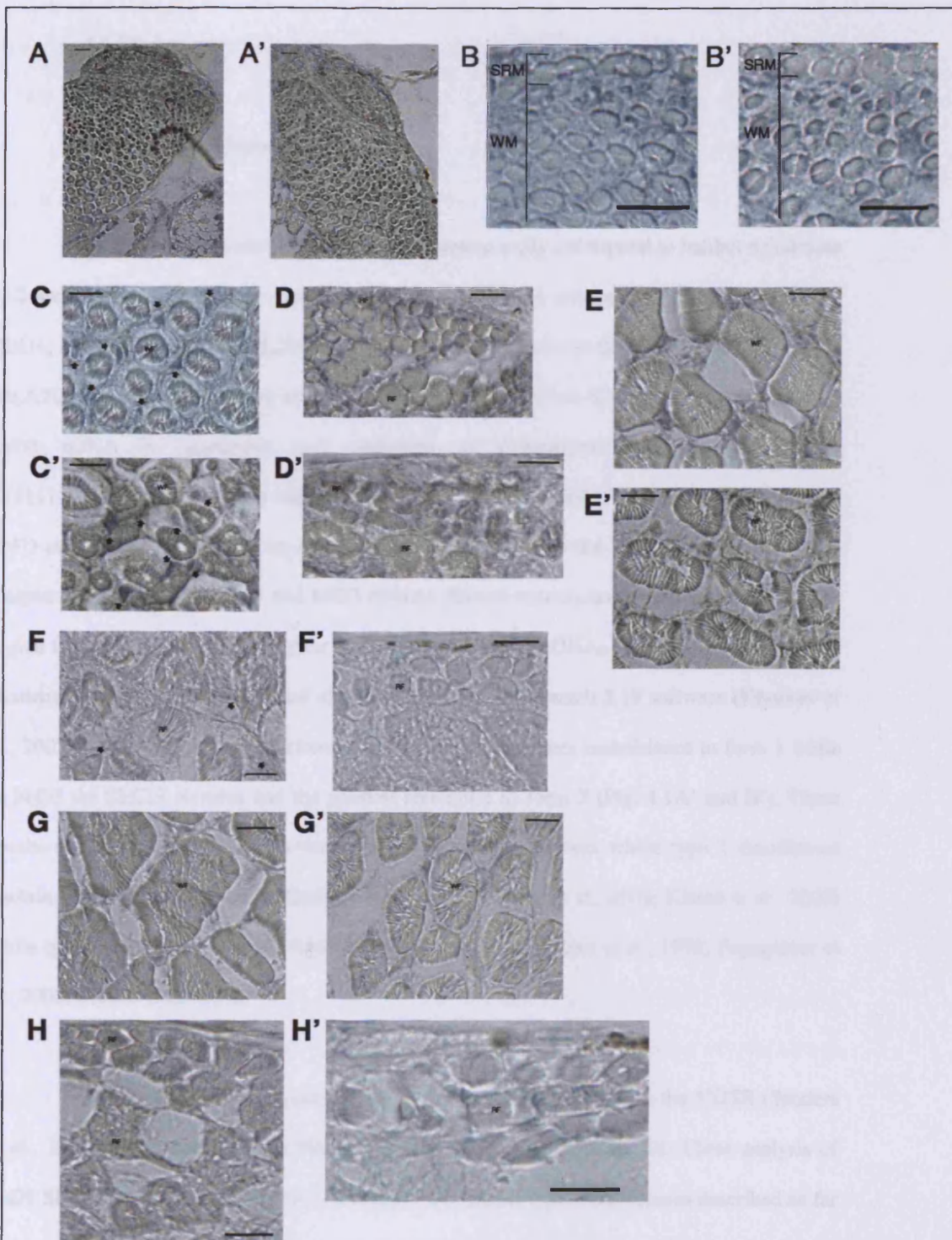


Figure 4.5. In situ expression of hhD2 (A-H) and hhD3 (A'-H') in halibut white (A, A', C, C', E, E', G and G') and red (B, B', D, D', F, F', H and H') muscle during halibut metamorphosis. Stage 5, A, A', B and B'; Stage 8 C, C', D and D'; Stage 9 E, E', F and F' and; Stage 10 G, G', H and H'. Arrowheads in B and B' denote cells that are closely associated with mature white muscle fibres. Arrowheads in F denote cells associated with mature red muscle fibres. SRM- superficial red muscle cells; WF- white muscle fibre; RF – red muscle fibre. The bar represents 10 μ m.

4.4 Discussion

4.4.1 Halibut deiodinase genes

The three cDNA clones isolated in the present study correspond to halibut deiodinase 1, 2 and 3 (Fig. 4.1A and B). Comparison to the nucleotide sequence of *Sparus auratus* D1 (SaD1; AJ619717)(Klaren et al., 2005) indicates hhD1 cDNA lacks the entire 5'UTR as well as the ATG translation start codon and the sequence coding the first 42aa of the N-terminus. The hhD3 cDNA is incomplete and compared to *Oreochromis niloticus* D3 mRNA (Y11111)(Sanders et al., 1999) only codes for the C-terminal third of the D3 protein. Thus, the hhD3 cDNA does not include the ATG translation start codon or the TGA Sec insertion codon. Despite the fact that the hhD1 and hhD3 cDNAs did not encompass the entire protein coding region they contain the 3'UTR region of the hhD1 and hhD3 cDNAs including putative SECIS elements (Fig. 4.1A' and B') found after analysis with SECISearch 2.19 software (Kryukov et al., 2003). Moreover, the SECIS element in hhD1 had the greater resemblance to form 1 while in hhD3 the SECIS element had the greatest resembles to form 2 (Fig. 4.1A' and B'). These results are in agreement with previous reports in other vertebrates where type 1 deiodinases contain form 1 SECIS elements (Sanders et al., 1997; Orozco et al., 2003; Klaren et al., 2005) while type 3 deiodinases contain form 2 SECIS elements (Sanders et al., 1999; Fagegaltier et al., 2000; Bianco et al., 2002).

O. niloticus D1 cDNA, contains two tandem SECIS elements in the 3'UTR (Sanders et al., 1997), while only a single SECIS element was found in halibut D1. Close analysis of hhD1 SECIS element reveals that in contrast to other teleost type 1 deiodinases described so far and in common with other vertebrate selenoprotein genes (Sanders et al., 1997; Sanders et al., 1999; Orozco et al., 2003; Klaren et al., 2005) the SECIS core of hhD1 (boxed region in Fig. 4.1A') is preceded 5' by adenine and not guanine (Fig. 4.1A'). In contrast, the SECIS core of hhD3 contains a guanine 5' and not adenine (boxed region in Fig. 4.1B'). These results in the

halibut are in conflict with the suggestion that a 5' guanine preceding the teleost deiodinase SECIS core is a feature of teleost deiodinase genes (Klaren et al., 2005). Although a guanine preceding the SECIS core is rare, substitution of adenine in that position for any nucleotide besides cytosine does not bring any functional changes to the SECIS element (Fagegaltier et al., 2000). For this reason it seems likely that these differences probably reflect species-specific differences. Moreover, although two D3 cDNA that encode identical proteins but diverge in the 3'UTR and contain different SECIS elements occur in *O. mykiss* (Bres et al., 2006), in the halibut only a single D3 cDNA was ever found. The two alternative SECIS elements of *O. mykiss* D3 are most like form 1 SECIS (Bres et al., 2006) in contrast to the majority of other vertebrate D3 SECIS elements which resemble form 2 SECIS (Sanders et al., 1999; Fagegaltier et al., 2000; Bianco et al., 2002), further supporting the idea that in teleosts, species specific differences in deiodinase transcripts might be a common feature.

4.4.2 Deiodinase in coordination of halibut metamorphosis

A coordinated expression pattern of D1, D2 and D3 occurs during halibut metamorphosis (Fig. 4.3A and B). Notably, hhD3 the T3-degrading deiodinase is the predominant expressed deiodinase before and after halibut metamorphosis while during metamorphosis the three halibut deiodinases had converged in their expression (Fig. 4.3A and B). Moreover, in halibut metamorphosis the decrease in expression of hhD3 T3-degrading deiodinase and the increase in expression of the T3-producing hhD1 and hhD2 deiodinases are highly correlated with the increase in whole-body levels of TH that culminate at climax (Fig. 2). This pattern of deiodinase expression during halibut metamorphosis serves to highlight the putative role of D1 and D2 in converting serum T4 to cellular T3 thus generating the general increase in T3 levels that surpass T4 levels. These observations in the halibut are reminiscent of what occurs during anuran metamorphosis and also TH-driven tetrapod development where it has been shown that until the precise moment of TH-action, D3 is the prevailing deiodinase. The reduction in D3 expression and activity levels is tightly regulated and associated with a rise

in D2 and in some cases D1 to give high, locally generated T3 levels that bring about the correct developmental changes in a particular tissue or cell type (Becker et al., 1997; Van der Geyten et al., 1997; Richard et al., 1998; Bates et al., 1999; Kawahara et al., 1999; Shepherdley et al., 2002; Van der Geyten et al., 2002; Cai and Brown, 2004; Kester et al., 2004; Brown, 2005; Galton, 2005). The present data indicates that as demonstrated in other vertebrates, coordination between the expression of the different halibut deiodinases and TH levels ensure appropriate timing of developmental changes necessary to permit the pelagic halibut larvae to become a benthic juvenile flatfish.

In post-metamorphic *Xenopus* (Kawahara et al., 1999) and in adult mice (Hernandez et al., 2006) D3 has been shown to be one of the most important factors for proper maturation and function of the thyroid axis and tissue homeostasis after TH-driven ontogenetic events. The fact that after halibut metamorphosis, hhD3 becomes again the most expressed deiodinase suggests that, as in anurans and mammals, D3 might have a pivotal role not only in the regulation and correct maturation of the thyroid axis in halibut after metamorphosis but also in the preservation of tissue-specific differentiation status after metamorphosis. Taken together, the present results strongly argue that the molecular mechanism by which deiodinases intervene in thyroid hormone metabolism and action during development and also in adult halibut fish may be conserved from teleosts to mammals.

The increase in halibut D2 expression at the same time that D3 is downregulated as halibut metamorphosis approached climax was not unexpected due the large body of information already available in tetrapods. What is remarkable, is that halibut D1 is strongly upregulated up until climax in parallel with D2 expression and increasing TH levels and opposite to D3 (Fig. 4.3A and B). This observation is quite intriguing since D1 is considered to have no role in anuran metamorphosis and in mammalian development its action is confined to kidney, liver, lung, eye and intestine (Richard et al., 1998; Bates et al., 1999; Bianco and Larsen, 2005; Galton, 2005). However, in chicken development D1 has a more widespread

tissue expression and a more prominent role than D2, which is restricted to the brain and controls local T3 levels together with D3 to give rise to the specific TH driven developmental changes (Van der Geyten et al., 1997; Van der Geyten et al., 2002; Gereben et al., 2004). The present halibut D1 expression data might suggest that, as for chicken, D1 may have a greater role in coordinating local T3 levels, together with D2 and D3, during halibut metamorphosis. An alternative explanation is that the increase in whole-body hhD1 expression is related to its tissue localisation. If in metamorphosing halibut larvae, as in zebrafish D1 is expressed in kidney, liver and in the gut (Thisse et al., 2003), then the increase in halibut D1 expression may be a consequence of the increase in the relative contribution of these tissues to the pool of mRNA. However, as the *in situ* hybridisation experiments with hhD1 in the present study were not successful it was not possible to establish tissue distribution of D1 in any stage of halibut development. Whole-mount *in situ* hybridisation is the probably the best strategy to more accurately determine local and tissue specific expression of hhD1 during halibut metamorphosis. Notably, the levels of halibut D1 gene expression were positively correlated with T3 levels during halibut metamorphosis which resembles the known effect of T3 in D1 expression in hyperthyroid rats, mice and humans (Berry et al., 1990; Berry et al., 1991a). Further studies will be required in halibut to better characterise tissue specific changes particularly as deiodinase TH-regulation during vertebrate development can be temporal and tissue or cell specific (Becker et al., 1997; Bates et al., 1999; Kawahara et al., 1999; Marsh-Armstrong et al., 1999; Campos-Barros et al., 2000; Shintani et al., 2002; Cai and Brown, 2004; Kim et al., 2004; Ng et al., 2004; Brown, 2005).

In anuran tissues that undergo change late during metamorphosis, the synergy between the increase in expression of D2 and TR β , and a decrease in D3 expression, together with higher T3 levels, are needed to bring about correct metamorphic development (Yaoita and Brown, 1990; Becker et al., 1997; Berry et al., 1998; Huang et al., 1999a; Kawahara et al., 1999; Huang et al., 2001; Brown, 2005). Conversely, in *X. laevis* TR α isoforms are found in early metamorphosing tissues, like the brain and limb buds, and correlate with the localised increase

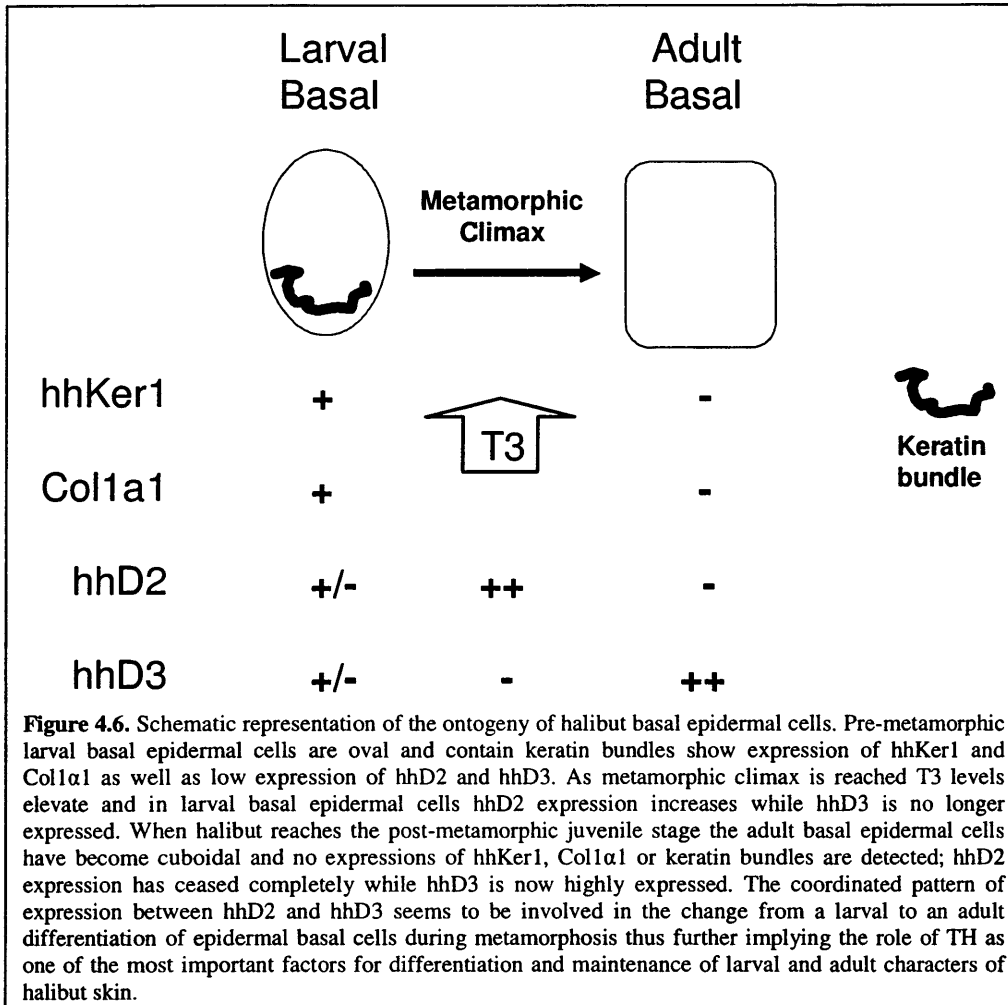
in D2 expression and decrease in D3 expression prior to the metamorphic climax when these tissues remodel (Cai and Brown, 2004; Brown, 2005). Similar relationships between TR and deiodinase expressions have been found in mouse during cochlear development between post-natal day 7 and 10. This is strictly dependent on TH and occurs before TH levels increase in neonates, serum T4 is converted to T3 in the bony labyrinth cells that express D2 only, but not TRs, which afterwards segregate, in a paracrine-manner, T3 into the adjacent TR β positive sensory epithelium (Campos-Barros et al., 2000; Ng et al., 2004; Galton, 2005). The complementary D2 and TR β expression correlate positively with each other and with the development of the cochlea suggesting that in tetrapods TH action also involves the coordinated action of deiodinases and TRs. During halibut metamorphosis a similar relationship between TH-levels, deiodinase expression and TR isoform expression is observed. In the halibut thyroid hormone receptors (TR α 1, TR α 2 and TR β) are already expressed in pre-metamorphic larvae (Galay-Burgos et al., 2004). Halibut TR α 1 and TR β expression (Galay-Burgos et al., 2004) show a profile very similar to that of T3 levels and halibut D2 and D1 deiodinases which progressively increase during metamorphosis to peak at climax but to sharply decrease immediately after, while TR α 2 in pre- and early metamorphic stages is the most abundant TR isoform when TH levels are very low and D3 the predominantly expressed deiodinase (Fig. 4.3). Taken together, these data strongly suggests that TR α 1 and TR β during halibut metamorphosis are associated with tissues that change late in halibut metamorphosis and that TR α 2 might be more related to early metamorphic changes or TH tissue-specific regulation that occurs during the larval period (Galay-Burgos et al., 2004).

4.4.3 Deiodinase expression in skin and muscle during halibut metamorphosis

The halibut D2 and D3 expression pattern in metamorphosing skin basal and supra-basal cells is coordinated with the downregulation of halibut larval Keratin 1 (hhKer1), collagen1 α 1 and disappearance of keratin bundles in the cytoplasm of larval cells as they undergo differentiation into adult type cells at climax (Chapter 2; Fig. 4.6). The differential

expression of both D2 and D3 in epidermal basal and supra-basal cells at early stages of halibut metamorphosis suggest that appropriate T3 levels are important for maintenance of the epidermis in halibut larvae and also for the transition from a larval to an adult differentiation state. In fact, during *X. laevis* metamorphosis T3 has been shown to have a dose dependent action on D3 and TR β expression and only high levels of T3 are able to induce high expression of TR β , by auto-induction, and drive metamorphic change in those tissues (Yaoita and Brown, 1990; Kawahara et al., 1999). The fact that in halibut adult inner epidermal cells only D3 is expressed is striking and suggests that in common with *X. laevis* D3 might have a protective role on T3 action after metamorphosis and maintain the proper differentiation state of those tissues (Kawahara et al., 1999). Further studies will be required in halibut to clarify this question. In anuran skin, coincident with the peak in TH at the climax of metamorphosis, fibroblast invade the acellular collagen lamella and start to express collagen1 α 1 (Watanabe et al., 2001; Suzuki et al., 2002; Watanabe et al., 2002; Ishida et al., 2003). A similar process occurs during halibut skin development (Chapter 2) and in halibut skin, fibroblasts express hhD2, but not hhD3 suggesting that TH may be involved in the migration and settlement of the fibroblast cells in the dermal collagen lamella. The results of the present study suggest that T3 is a key factor in halibut skin development during metamorphosis but that deiodinases might also be important for the homeostasis of fully developed halibut adult skin epidermis. The expression of both hhD3 and hhD2 in the same cell types in pre-metamorphic halibut stages strongly suggests that the action of TH in halibut skin may already be influencing skin development at late larval stages before metamorphosis starts. Moreover, the spatial-temporal expression pattern of hhD2 and hhD3 in other cell types may suggest the role of THs is not be solely restricted to the deep epidermal cells (Chapter 2). The regulation of halibut skin development by THs resembles observations in mammals (Tomic-Canic et al., 1992; Tomic-Canic et al., 1996a; Tomic-Canic et al., 1996b; Radoja et al., 1997; Bates et al., 1999; Sinha et al., 2000; Radoja et al., 2004) and anurans (Mathisen and Miller, 1987; Mathisen and Miller, 1989; Warshawsky and Miller, 1995; Suzuki et al., 2001; Watanabe et al., 2001; Suzuki et al.,

2002; Watanabe et al., 2002; Ishida et al., 2003) in which TH has been shown to be one of the most important factors regulating skin development, differentiation and homeostasis.

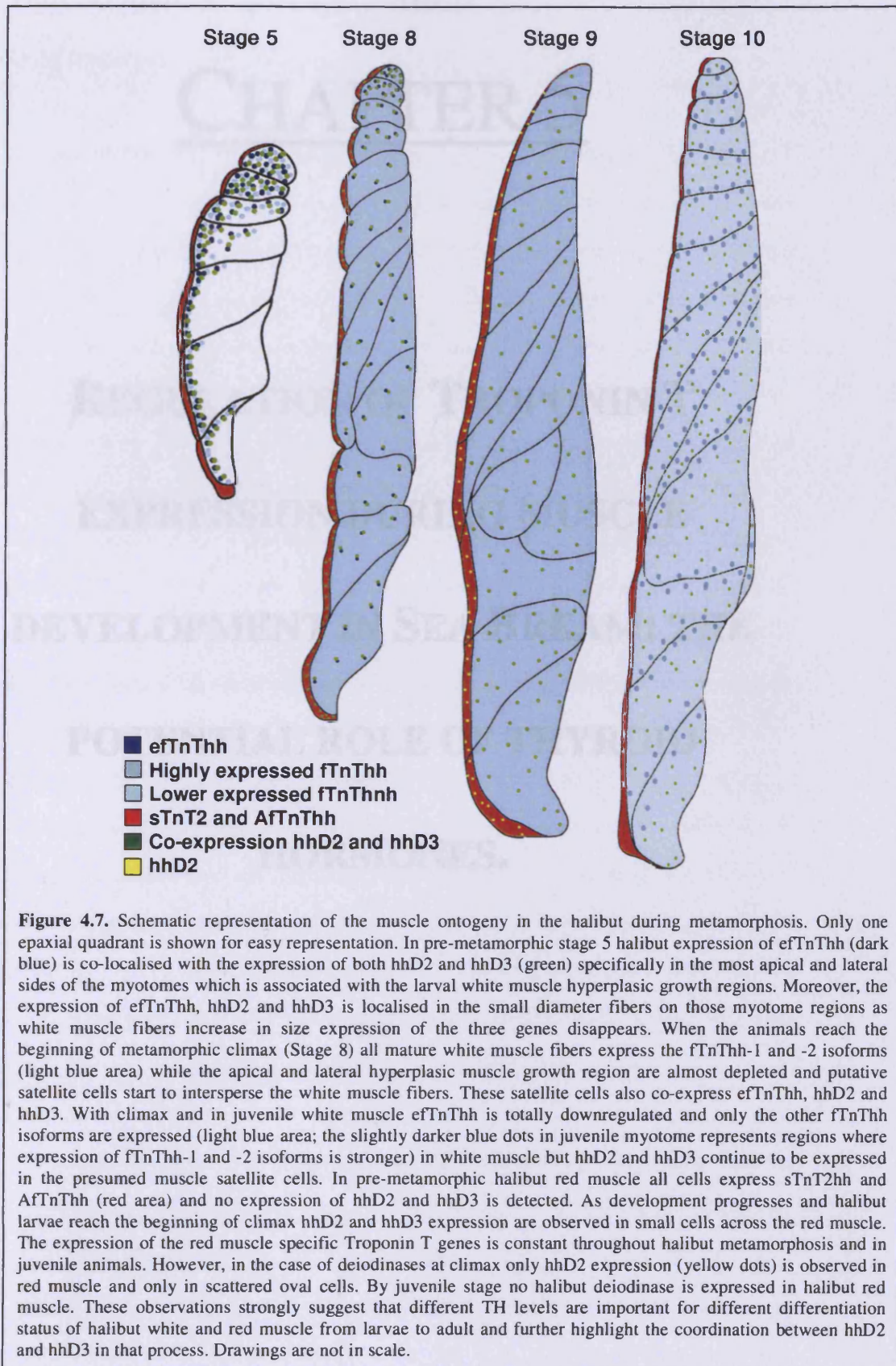


THs seem to be important in larval and post-metamorphic development of muscle in halibut in common with the Japanese flounder in which they are responsible for the transition of expression of embryonic to adult fTnT and myosin light chain proteins (Yamano et al., 1991a; Yamano et al., 1994b). Relatively little is known about the role of THs in muscle development in mammals, although both T4-ORD and T3-IRD activity have been measured in rat fetal muscle (Huang et al., 1988; Zacharova et al., 1999; Vadaszova et al., 2004). Strikingly, in larval halibut white muscle hhD2 and hhD3 are most abundant in the small diameter fibres localised at

the most apical and lateral areas of the myotome that constitute the hyperplastic growth region (Fig. 4.5A, C, A' and C') that also express primarily the embryonic isoform of fTnThh (efTnThh; Chapter 3)(Fig. 4.7). In fact hhD2 and hhD3 have the same spatial-temporal pattern of expression as efTnThh (Chapter 3, Fig. 4.5 and 4.7) throughout halibut metamorphosis. The co-localisation of deiodinase transcripts with fTnT in developing muscle suggest that appropriate TH levels are essential for muscle development and may influence fTnT isoform expression through an as yet unstudied process.

In red muscle hhD2 and hhD3 expression is observed mainly in the small red muscle fibres and is restricted to these fibres up until climax when only hhD2 is expressed (Fig. 4.5). These results suggest that THs are involved in red muscle development at least from late larval stages to metamorphic climax, when intracellular levels of T3 probably increase as only hhD2 is expressed. It is intriguing that even though hhD2 and hhD3 have an expression profile that seems to suggest TH-driven developmental events in halibut red muscle no changes in the expression of halibut red muscle specific TnT genes is observed suggesting THs may influence other genes (Chapter 3). Nevertheless, in common with rats (Zacharova et al., 1999; Vadaszova et al., 2004), TH seems to be important also for red muscle development in halibut and possibly other teleosts.

In conclusion, the present study in the halibut suggests that THs regulate metamorphosis and the associated tissue specific changes in halibut. Moreover, specific tissue specific regulation of THs during development through the coordinated action of the deiodinases D2 and D3 probably occurs in a similar fashion in teleosts and tetrapods (Yaoita and Brown, 1990; Becker et al., 1997; Berry et al., 1998; Huang et al., 1999a; Kawahara et al., 1999; Campos-Barros et al., 2000; Huang et al., 2001; Cai and Brown, 2004; Ng et al., 2004; Brown, 2005; Galton, 2005).



CHAPTER 5

**REGULATION OF TROPONIN T
EXPRESSION DURING MUSCLE
DEVELOPMENT IN SEA BREAM: THE
POTENTIAL ROLE OF THYROID
HORMONES.**

5.1 Introduction

Thyroid hormones (THs), important regulatory factors during development, are known to be important in post-natal muscle development in vertebrates. It has been shown that in rats full differentiation of skeletal muscle phenotype is only achieved with appropriate thyroid hormone levels (Vadaszova et al., 2004). Moreover in rats, T3 treatment significantly changes the muscle contractile properties and myosin heavy chain (MHC) isoform expression in both fast and slow muscle types (Larsson et al., 1994; Larsson et al., 1995; Adams et al., 1999; Soukup and Jirmanova, 2000). In both thyroidectomised and thiourea treated chick embryos prolonged expression of slow MHC and myosin light chains (MLC) and inhibition of neonatal fast MHC isoforms occurs in the fast *posterior latissimus dorsi* muscle, whereas in the slow *anterior latissimus dorsi* muscle slow muscle differentiation is delayed, expression of embryonic fast MHC isoforms persists and there is induction of fast MLCs (Gardahaut et al., 1992). During amphibian metamorphosis, larval muscle fibres die and give place to newly formed adult fibres and associated MHC isoform switching which seems to be under the control of THs (Chanoine and Hardy, 2003). In zebrafish (Liu and Chan, 2002), TH treatment makes muscle tissue less compact and in developing larvae of *Epinephelus coioides* differences in locomotion between control and TH treated fish are observed (de Jesus et al., 1998). TH-induced and spontaneous metamorphosis of the flounder (*Paralichthys olivaceus*), causes biochemical changes in muscle proteins. In particular, different protein isoforms of fast troponin T (fTnT), the tropomyosin-binding subunit of the striated muscle troponin complex, are present in muscle from pre- and post-metamorphic larvae (Yamano et al., 1991a).

Troponin T (TnT) is the tropomyosin-binding subunit of the troponin complex in striated muscle and plays a role in Ca^{2+} -activation of contraction. In addition to anchoring the troponin complex to tropomyosin, TnT is necessary for the correct assembly and functioning of Troponin C and I, and hence correct Ca^{2+} -driven muscular activity. TnT also has a modulatory effect on myosin ATPase activity (Perry, 1998; Jin et al., 2000b). *TnT* genes are best

characterised in mammals and birds, where three *TnT* genes have been identified which are restricted in expression to either slow (red) skeletal muscle (*sTnT*), fast (white) skeletal muscle (*fTnT*) or cardiac muscle (*cTnT*) respectively (Perry, 1998). All three *TnT* genes produce multiple N-terminal isoforms which result from alternative splicing and the tetrapod *fTnT* and *cTnT* also present alternative splicing of the C-terminal region (Gahlmann et al., 1987; Briggs and Schachat, 1993; Samson et al., 1994; Wang and Jin, 1997; Farza et al., 1998; Jin et al., 1998a; Perry, 1998; Barton et al., 1999; Bucher et al., 1999; Huang et al., 1999d; Jin et al., 2000b; Yonemura et al., 2000; Nakada et al., 2002; Wang et al., 2002; Yonemura et al., 2002).

The evidence from mammals and birds provides a possible explanation for the switch in expression of *fTnT* isoforms in embryonic/larval and juvenile fish muscle. However, in the only molecular study of TnTs in fish (excepting those on halibut described in chapter 3), although two *fTnT* genes with a similar organisation to higher vertebrate *fTnT* genes were identified in zebrafish no evidence of alternative splice variants was reported (Hsiao et al., 2003). The present study reports for the first time in a teleost, the sea bream (*Sparus auratus*), cloning and characterisation of three different cDNA encoding different *fTnT* isoforms which are the product of a single gene. Alternative splicing of a single gene appears to give rise to the three isoforms identified, one of which is a larval specific isoform and generates a putative protein with markedly different biochemical characteristics. Moreover, cDNAs for two different *sTnT* genes, one of which presents developmental expression of alternatively spliced isoforms, were also identified. In comparison to the flounder and halibut, the sea bream undergoes a less radical metamorphosis raising questions about the potential role of THs in isoform switching during the larval/juvenile transition of this species. In order to assess the involvement of THs in regulation of TnT gene transcription, the ontogeny of isoform switching was related to thyroid hormone levels in developing sea bream. In addition, to further assess the effect of THs on TnT expression, experiments were performed in which T3 and methimazol (an anti- thyroidogenic compound in mammals) were administered to sea bream larvae and juveniles and the expression of slow TnT (*sTnT*) and *fTnT* isoforms was analysed.

5.2 Materials and Methods

5.2.1 Sea bream *fTnT* cDNA Library Screen

A lambda phage cDNA library made from sea bream larvae aged 20-100 days post-hatch (dph; (Nowell et al., 2001)) plated at a density of 1,000 plaque forming units (pfu) was screened at low stringency with a 891-bp partial clone of AfTnThh muscle from *Hippoglossus hippoglossus* (Chapter 3). Nitrocellulose membranes containing plaque DNA were prehybridised for 2 hours at 50°C in hybridisation solution alone (6xSSC, 0.1% SDS, 100 µg/ml tRNA, 5x Denhardt's) and then overnight at low stringency (50°C) in hybridisation solution to which [³²P]-labelled putative skeletal muscle sTnT probe prepared by random priming (Megaprime, random labelling kit, Amersham Biosciences, UK) had been added. Low stringency washes were carried out, by washing membranes twice for 30 minutes at room temperature in 1xSSC/0.1% SDS solution, followed by two washes of 30 minutes at 50°C in 1x SSC, 0.1% SDS. The membranes were then exposed overnight at -80°C to Biomax MS film (Kodak, Palo Alto, CA, USA). Positive plaques were isolated, automatically excised into pBluescript SK+/- (Stratagene, La Jolla, CA, USA), DNA purified and cDNA clones sequenced to give 3-fold coverage using BigDye Version 3 (Perkin-Elmer, Berkshire, UK) chemistry and an ABI 3700 sequencer.

5.2.2 Strategy for cDNA library screening for sea bream *sTnT* genes

Since a whole larval sea bream cDNA library was used (Nowell et al., 2001), clones representing *fTnTs* are much more prevalent than those representing *sTnTs* due to the far greater abundance of fast muscle in the larvae. A modified screening strategy was therefore utilised to obtain clones of sea bream *sTnT*. Two probes were used simultaneously to screen a sea bream larval cDNA library; a halibut *fTnT* probe corresponding to a region conserved in all *TnTs*, and

a 3'UTR probe for the sea bream *fTnT* gene. Differential selection of positive plaques with the two different probes allowed the isolation of non-fast *TnT* cDNAs.

The library was plated out at a density of 50,000 plaque-forming units (pfu) per plate and three lifts were taken per plate using nitrocellulose filters (Pall Life Sciences, UK). The first two membranes were hybridised overnight at low stringency (50°C, 6xSSC, 100 µg/ml tRNA, 5x Denhardt's solution, 0.1% SDS) with a 891bp [α -³²P]-dCTP labelled halibut fast *TnT* cDNA probe (Megaprime, random labelling kit, Amersham Biosciences, UK) generated by *EcoRI* digestion of a partial clone of a putative skeletal muscle *fTnT* isolated from halibut (unpublished data). It was expected that under the low stringency conditions utilised, this probe would hybridise to all forms of sea bream *TnT*. The third membrane was hybridised overnight under high stringency conditions (65°C, 6xSSC, 100 µg/ml tRNA, 5x Denhardt's solution, 0.1% SDS) with a 301bp [α -³²P]-dCTP labelled probe corresponding to the 3'UTR of a sea bream larval *fTnT* gene (unpublished data). After hybridisation the duplicate membranes were probed with the 891bp fragment of halibut *AfTnT* and were washed twice at room temperature with 1xSSC/0.1%SDS for 30 minutes per wash. Membranes were then subject to a low stringency wash at 50°C in 1xSSC/0.1%SDS for 30 minutes. Membrane 3, probed with the 301bp 3' UTR fragment of sea bream *fTnT* was also washed twice at room temperature as described above but was then subject to a high stringency wash in 1xSSC/0.1%SDS for 2 x 30 minutes at 65°C. The membranes were then exposed to Biomax MS film (Kodak, Palo Alto, CA, USA) in cassettes with intensifying screens at -80°C overnight. The films were developed and the positive plaques present on membranes 1 and 2, but not on membrane 3, were selected and subject to a further round of screening and selection as described above to permit isolation of single plaques. Positive plaques were automatically excised into pBluescript SK+/- (Stratagene) and sequenced to give 3-fold coverage using the BigDye Version 3 (Perkin-Elmer, UK) chemistry and an ABI 3700 sequencer.

5.2.3 RT-PCR cloning of the sea bream intronless *TnT* gene (*iTnTsb*)

In order to isolate the sea bream orthologue of the zebrafish intronless *TnT* gene (Hsiao et al., 2003) PCR cloning with degenerate primers was employed. Primers were designed after alignment in ClustalX (Thompson et al., 1997) of the zebrafish *iTnT* gene (GenBank accession no. NP_852476) and the putative *Fugu iTnT* gene sequence deduced from mayfold 253 (HGMP accession no. M000253). The primers were: F1: ATGTCNGACTCYGARGARWT; F2: GAGAAGGTGGAYTTTGAYGA; F3: CAGAAGGTGGAYCAGAAGAA; R1: GGTCRTCAAARTCCACCTTCTC; R2: CARTTTVGCSCCTCYTCYTC; R3: TTCTTCTGRTCCACYTTYTG; R4: CTTCMRGGAGCCRGCYTT. The following primer combinations were used: F1/R1, F1/R2, F1/R3, F1/R4, F2/R2, F2/R3, F2/R4 and F3/R4. All PCR reactions contained 2.5mM MgCl₂ and either sea bream genomic DNA or cDNA prepared from RNA extracted from sea bream embryos collected at 43 hours post fertilisation (hpf). The thermocycle program was as follows, 5 minutes at 95°C followed by 40 cycles of 2 minutes at 95°C, 2.5 minutes at annealing temperatures ranging from 50°C-59°C, and 2 minutes at 72°C before a final step of 2 minutes at 72°C. PCR products of the expected size were gel purified, subcloned into pGEM-T (Promega), and sequenced.

5.2.4 Animal and Tissue Sampling

Adult sea bream, maintained at the Marine research station of the Centre of Marine Sciences (CCMAR, University of the Algarve, Portugal) were anaesthetized in MS-222 (125mg/l, Sigma-Aldrich, Madrid, Spain) and killed by decapitation in accordance with National legislation for the welfare of animals. White muscle, red muscle, heart and liver were collected immediately into RNAlater reagent (Sigma-Aldrich, Madrid, Spain) and stored at -20°C until RNA extraction.

Pools of sea bream eggs ($n = 3$) were collected at 30% epiboly (12 hours post fertilisation - hpf), 90% epiboly (18 hpf), 2 somite stage (24 hpf) and when the most posterior somites had formed (36 hpf). Larvae ($n = 3$) were collected at hatching (1 day post hatch - dph) and at 4, 15, 46, 64, 75 and 89 dph. The small size of the sea bream larvae meant that several different pools composed of several larvae (50-100mg) of the same age were collected for each sample point until 46 dph and thereafter individual larvae were collected and analysed. Larvae were anaesthetized in MS-222 (125mg/l, Sigma-Aldrich, Madrid, Spain) before being snap frozen in liquid Nitrogen and stored at -80°C until use.

5.2.5 Total RNA extraction

Total RNA was extracted from 100 mg of adult sea bream striated white muscle, red muscle, heart and liver from 3 different individuals using Tri reagent (Sigma-Aldrich, Madrid, Spain) and following the manufacturer's instructions. Tri reagent was also used to extract total RNA from triplicate samples of 50-100 mg of pooled sea bream embryos and larvae up until 46 dph and from triplicate samples of individual larvae of 64, 75 and 89 dph.

5.2.6 Northern blot

Total RNA (3 μg) from white muscle, red muscle, heart and liver was fractionated on a 1.5% agarose /5.5% formaldehyde gel which was run in 1x MOPS. RNA was transferred to nylon Hybond-N membranes (Amersham Biosciences, Buckinghamshire, UK) with 10x SSC and cross-linked using UV light (Stratalinker, Stratagene, La Jolla, CA, USA). A 3'UTR DNA probe was prepared for northern blotting by digesting the putative sea bream larval *fTnT* cDNA isolated in the library screening with *XhoI* and *SacI* (0.1 U/ μl , Promega, Madison, WI, USA). This probe should hybridise all the isoforms arising from the sea bream *fTnT* gene. For sea bream *sTnT* genes northern blotting was carried out using DNA probes generated by PCR using primers specific for the 3'UTR region of the two forms of sea bream *sTnT* isolated by library

screening. The PCR reactions were carried out in a 50µl volume with ~1µg of plasmid DNA, 0.1mM dNTPs, 1pmol/µl of forward and reverse primers (*sTnT1sb*, GAGGAAGCGTATAGGAACTG and GACGTCATCACATAATGCATC respectively, and *sTnT2sb* GTTTGACCTCAGTGAGAAAC and ACAGAGAAATGGACATCCTGC respectively) and 0.6U of *Taq* polymerase (Sigma-Aldrich). The PCR products were gel purified using the Quiagen gel extraction kit and kept at -20°C until use. The individual membranes were hybridised overnight using high stringency conditions (65°C in 6xSSC, 0.1% SDS, 100 µg/ml tRNA, 5x Denhardt's solution) with either fTnTsb, sTnT1sb or sTnT2sb [³²P]dCTP labelled 3'UTR DNA probes. The membranes were subsequently washed using high stringency conditions (65°C in 1x SSC, 0.1% SDS for 30 minutes) and exposed for several hours or overnight at -80°C to Biomax MS film (Kodak, Palo Alto, CA, USA).

5.2.7 Identification in silico of fTnT variants in other teleosts

Sea bream fTnT cDNA sequences were used to identify and retrieve presumptive homologues of sea bream fTnTs in other teleosts using tBLASTX (Altschul et al., 1990) and a number of databases: GenBank (www.ncbi.nlm.nih.gov), zebrafish (www.ncbi.nlm.nih.gov/genome/seq/DrBlast.html), Medaka (*Oryzias latipes*) (Medaka_EST_database), *Fugu* (*Fugu rubripes*) (<http://Fugu.hgmp.mrc.ac.uk>¹) and *Tetratodon nigroviridis* (www.genoscope.cns.fr/externe/tetranew/). Full length cDNA were retrieved, translated using BioEdit and protein multiple alignments performed in ClustalX (Thompson et al., 1997). A Pearson multiple comparison analysis was performed to establish similarity between the sea bream fTnT isoforms and the fTnT sequences retrieved from the databases.

¹ Current address: <http://www.fugu-sg.org/>

5.2.8 Phylogenetic analysis of sea bream TnT genes

The probable identity of the cDNA sequences isolated was determined by searching against GenBank (www.ncbi.nlm.nih.gov) using tBlastX (Altschul et al., 1997). Comparison between the sea bream sTnT deduced protein sequence and that of other species was performed using Clustal X software (Thompson et al., 1997). Phylogenetic trees were generated using PAUP* Version 4.0b (Swofford et al., 2001) to identify maximum parsimony with 1000 bootstrap replicates (Fitch, 1971) and a range of TnT sequences (Table 5.1). All the sequences obtained during this study have been submitted to EMBL/GenBank data library (see Table 5.1).

Table 5.1. Vertebrate TnT sequences used in phylogenetic analysis

Specie	Gene, abbreviation	Database, accession number
<i>Hippoglossus hippoglossus</i>	Slow TnT 2, sTnT2 hh	GenBank, DQ680172
	Embryonic fast TnT isoform, efTnT hh	GenBank, DQ680173
	Fast TnT isoform 1, fTnT hh1	GenBank, DQ680174
	Fast TnT isoform 2, fTnT hh2	GenBank, DQ680175
	Atypical fast TnT isoform 1, AfTnT hh-1	GenBank, DQ680176
<i>Homo sapiens</i>	Slow TnT, sTnT hs	GenBank, AAB3027
	Fast TnT, fTnT hs	GenBank, NP_006748
	Cardiac TnT, cTnT hs	GenBank, NP_000355
<i>Gallus gallus</i>	Slow TnT, sTnT ck	GenBank, JC4970
	Fast TnT, fTnT ck	GenBank, AAA49100
	Cardiac TnT, cTnT ck	GenBank, BAA02369
<i>Coturnix coturnix japonicus</i>	Fast TnT, fTnT cj	GenBank, P06398
<i>Xenopus laevis</i>	Fast TnT, fTnT xl	GenBank, AAM55471
	Cardiac TnT, cTnT xl	GenBank, AAO33406
<i>Danio rerio</i>	Intronless TnT, iTnT zf	GenBank, NP_852476
	Slow TnT low MW isoform, sTnTLMW zf	GenBank, BQ259877
	Fast TnT a, fTnTa zf	GenBank, NP_571640
	Fast TnT b isoform 1, fTnTb zf1	GenBank, AF425741
	Fast TnT b isoform 2, fTnTb zf2	GenBank, BC065452
	Cardiac TnT, cTnT zf	GenBank, CAD59126
<i>Salmo salar</i>	Fast TnT, fTnT ss	GenBank, AAC24595
<i>Gadus morhua</i>	Fast TnT, fTnT gm	GenBank, AAM21701
<i>Salmo trutta</i>	Slow TnT 1S, sTnT 1s st	GenBank, AAB58912
<i>Fugu rubripes</i>	Putative slow TnT2, sTnT2 fg	HGMP, M001711
	Intronless TnT, iTnT fg	HGMP, M000253
<i>Ictalurus punctatus</i>	Slow TnT 1, sTnT1 ic	GenBank, CK412342
<i>Orizya latipes</i>	Slow TnT 2, sTnT2 md	Medaka EST, MF01FSA018J165
	Fast TnT isoform 1, fTnT md1	GenBank, BJ729852
	Fast TnT isoform 2, fTnT md2	GenBank, BJ728074
<i>Tetraodon nigroviridis</i>	Putative embryonic fast TnT isoform, efTnT tn	EMBL, CR660426
	Putative larval fast fTnT isoform, fTnT tn2	EMBL, CR658326
	putative adult fast TnT isoform, fTnT tn1	EMBL, CR658422
	Atypical fast TnT isoform 1, AfTnT tn1	EMBL, CR696067
	Atypical fast TnT isoform 2, AfTnT tn2	EMBL, CR675364
	Atypical fast TnT isoform 3, AfTnT tn3	EMBL, CR662746
	Atypical fast TnT isoform 4, AfTnT tn4	EMBL, CR727722
	Atypical fast TnT isoform 5, AfTnT tn5	EMBL, CR673164
<i>Sparus aurata</i>	Slow TnT1, sTnT1 sb	GenBank, AY684301
	Slow TnT2, sTnT2 sb	GenBank, AY684302
	Intronless TnT, iTnTsb	GenBank, AY953294
	Embryonic fast TnT isoform, efTnT sb	GeneBank, DQ473445
	Larval fast TnT isoform, LfTnT sb	GeneBank, DQ473444
	Adult fast TnT isoform, afTnT sb	GeneBank, DQ473443
<i>Caenorhabditis elegans</i>	striated muscle TnT, TnT ce	GeneBank, NP_509076

5.2.9 Putative genomic organisation of sea bream TnT gene

In order to establish the putative genomic organisation of sea bream TnT genes *in silico* analysis was carried out using the puffer fish (*Fugu rubripes*) and *Tetraodon nigroviridis* genomes (Aparicio et al., 2002; Jaillon et al., 2004). The *Fugu* and *Tetraodon* scaffolds giving the most significant hit by tBLASTx analysis (Altschul et al., 1990) with the sea bream fTnT sequences were retrieved. Pairwise alignment of sea bream fTnT cDNA sequences with the selected *Fugu* and *Tetraodon* scaffolds using Spidey mRNA-to-genome software (Wheelan et al., 2001) permitted identification of the putative exon/intron boundaries of the sea bream gene.

5.2.10 First strand cDNA synthesis

First strand cDNA (20 µl total reaction volume) was synthesised using 0.5µg total RNA of the different sea bream embryonic, larval and juvenile stages and adult tissues. Before cDNA synthesis all samples were treated with DNase using the DNA free kit (Ambion, Austin, TX, USA) and following the manufacturer's instructions. cDNA synthesis was carried out in 0.05M Tris-HCl, pH8.3, 0.075M KCl, 3mM MgCl₂, 0.01M DTT, 1mM dNTP, 5pmol/µl random hexamer primers, 4U of RNase inhibitor (Promega, Madison, WI, USA) and 10U of Superscript II reverse transcriptase (Invitrogen, Carlsbad, CA, USA). Synthesis reactions were carried out in an iCycler thermocycler (Perkin-Elmer, Berkshire, UK) for 10 minutes at 25°C followed by 50 minutes at 42°C and synthesis was terminated by heating for 2 minutes at 70°C. cDNA corresponding to three independent pools (50-100mg/extract) of sea bream larvae were prepared for each developmental stage and for samples of adult sea bream white muscle, red muscle, heart and liver.

5.2.11 Developmental expression of sea bream TnT genes - Semi-Quantitative RT-PCR analysis

A semi-quantitative RT-PCR strategy was employed to analyse the developmental expression of *fTnT*, *sTnT1*, *sTnT2* and *iTnT* genes in sea bream. Initial experiments were conducted with TnT genes to determine optimal cycle number and ensure that amplification occurred in the logarithmic phase of the reaction. The internal standard selected to normalise the results was the expression of 18s ribosomal RNA (rRNA).

Amplification of *fTnTsb* was carried out in a 25µl reaction volume containing ~20 ng of cDNA for each of the samples described and 1.5 mM MgCl₂, 0.1 mM dNTP's, 1 pmol/µl of sea bream specific *fTnT* forward and reverse primer (5'-ACAAGTCCACTCTCACCATG-3' and 5'-TCTCAATCCTGTCTTGAGG-3', respectively) and 0.6U *Taq* polymerase (Sigma-Aldrich, Madrid, Spain). Primers were selected to amplify the entire N-terminal region of the *fTnTsb* protein which in terrestrial vertebrates undergoes alternative splicing (Perry, 1998). The forward primer was located in the 5'UTR region of the isolated sea bream *fTnT* cDNAs (forward pointing arrow in Fig. 5.1D). The reverse primer was designed in a constitutively expressed region of the sea bream *fTnT* cDNAs (backwards pointing arrow in Fig. 5.1D).

Amplification of *sTnT1sb* was performed in a 25µl reaction volume containing ~20 ng of cDNA for each of the samples described and 1.5 mM MgCl₂, 0.1 mM dNTP's, 1 pmol/µl of forward and reverse primer (5'-ACGAGGCTCTTGTGTCTGGTG-3'; and 5'-CTCTTTCTCTGCTCAAAGTGG-3', respectively) and 0.6U *Taq* polymerase (Sigma-Aldrich). The same reaction mix was used for *sTnT2sb* with the exception of the forward and reverse primers (5'-GGCTCACAGAGCTCATCCAT-3' and 5'-CACTGTACTGCTGGGTCAGT-3' respectively) and concentration of MgCl₂ (2.5mM). The amplification reaction mix for *iTnTsb* was identical to that described for *sTnT1sb* with the exception of the primers (F2 and R3 as described for the isolation of the *iTnTsb* gene).

The PCR reactions were performed in an iCycler (Perkin-Elmer, Berkshire, UK) thermocycler, using the following cycle; 1 minute at 95°C followed by 28 cycles of 30 seconds at 95°C, 1 minute at 56°C and 30 seconds at 72°C, followed by a final step of 1 minute at 72°C. The thermocycles used for *sTnT1sb* and *sTnT2sb* were identical to *fTnTsb* except that the cycle number were, respectively, 27 and 32 cycles. The thermocycle for *iTnTsb* was 1 minute at 95°C, followed by 30 cycles of 30 seconds at 95°C, 1 minute at 58°C, and 30 seconds at 72°C, followed by a final extension step of 1 minute at 72°C. Negative reactions without sample cDNA were also performed. The identity of RT-PCR products was confirmed by sequencing.

The housekeeping gene 18s, was amplified in each sample in a 25µl reaction containing ~20ng of cDNA, 1 pmol/µl of forward and reverse primer (5'-TCAAGAACGAAAGTCGGAGG-3' and 5'-GGACATCTAAGGGCATCACA-3' respectively), 1.5 mM MgCl₂, 0.1 mM dNTP's and 0.6U of *Taq* polymerase (Sigma-Aldrich, Madrid, Spain). The thermocycle utilised was; 1 minute at 95°C followed by 16 cycles of 30 seconds at 95°C, 1 minute at 56°C and 30 seconds at 72°C, followed by a final step of 1 minute at 72°C. RT-PCR reaction products were fractionated on a 2.5% agarose gel and analysed by densitometry using LabWorks version 4.5 software (Ultra-Violet Products, Cambridge, UK). Results are expressed as the mean and standard error of three independent samples.

5.2.12 Experiments - T3 and Methimazol treatment

The experiments described comply with the Guidelines of the European Union Council (86/609/EU) and Portuguese National legislation. Larvae were acclimated to sea water in three 125 L aquaria (100-150 larvae/tank) for at least 2 weeks in an open system (38 p.p.t. salinity, 1162 mOsm/kg H₂O) with a water temperature of 19°C ± 1°C and under natural photoperiod for February in the Algarve. Larvae were fed twice daily on dry food (grade 10 fish pellets, Anivite, Alverca, Portugal).

The objective of the experiments was to alter TH balance in the sea bream larvae and to this end the diet was supplemented with T3 (Sigma-Aldrich, Madrid, Spain) or a blocker of TH production in mammals, methimazol (Sigma-Aldrich, Madrid, Spain). Experiments lasted for 31 days and started when larvae were 57 days post hatch (dph), tank conditions were maintained and each vessel contained approximately 100 larvae and represented a different experimental group (T3 treatment, methimazol treatment and control). Larvae were fed as previously with the exception that food was pre-treated with either T3 dissolved in ethanol (10 mg/g dry food), methimazol dissolved in ethanol (10 mg/g dry food) or was treated with the vehicle (ethanol) alone (control). No mortality was detected in any of the experimental groups during the experiment. Preliminary trials were conducted to optimise the dose, duration and route of hormone/blocker administration.

Larval samples were collected from each experimental group before feeding, after 7 (64 dph larvae), 14 (74 dph larvae) and 31 days (89 dph larvae) of treatment. Larvae were killed with an overdose of MS222 (Sigma-Aldrich, Madrid, Spain) and larvae (n=12) were snap frozen in liquid nitrogen or fixed (n=3) in 4% paraformaldehyde (PFA; Sigma-Aldrich, Madrid, Spain) at 4°C overnight. Frozen samples were used for either RT-PCR or to determine TH content by radioimmunoassay (RIA). Fixed samples were washed twice for 5 minutes with Phosphate Buffer with 5% Tween-20 (Sigma-Aldrich, Madrid, Spain) and stored in 100% methanol at 4°C. The heads of fixed sea bream were removed and embedded in paraffin and serial 8µm longitudinal sections were cut and mounted on APES coated slides.

*5.2.13 Sea bream TnT genes in T3 and Methimazol-treated animals - Semi-Quantitative**RT-PCR analysis*

Expression of the sea bream fTnT, sTnT1, sTnT2 and iTnT genes gene was determined by semi-quantitative RT-PCR as described above. The amount of cDNA included in RT-PCR reactions was assessed using amplification of 18s rRNA. Reaction products were quantified by densitometry and analysed using LabWorks version 4.5 software (Ultra-Violet Products, Cambridge, UK). The results are presented as mean and standard error of three individual samples and and statistical differences were assessed by two-way analysis of variance (ANOVA) as described below.

5.2.14 TH extraction and Radioimmunoassay

The T4 and T3 content in T3- and methimazol-treated and control animals was extracted and assessed by RIA. Five frozen individual animals per each sampling time of each experimental group were extracted in methanol and centrifuged at 3,000 rpm for 30 min at 4°C. Then, the upper phase was removed, lyophilised, reconstituted in assay buffer (0.01 M PBS, pH 7.6), heat treated at 65°C for 60 minutes and assayed.

Assays for both T3 and T4 were highly specific and reproducible and were performed as previously described (Einarsdóttir et al., 2006) under equilibrium conditions using T2777 anti-T3 (<0.01% cross-reactivity with T4; Sigma-Aldrich) and T2652 anti-T4 polyclonal sera (~3% cross-reactivity with T3; Sigma-Aldrich, Madrid, Spain). Results are presented as means and standard error of five individuals and the existence of significant statistical differences are assessed by two-way analysis of variance (ANOVA) as described below.

5.2.15 Thyroid follicular activity analysis

In order to analyse thyroid follicle activity the sectioned animal heads were dewaxed in xylene (2 x 10 minutes), rehydrated through an alcohol series (90%, 70%, 50%), washed in phosphate buffered saline (PBS, 1.7mM KH₂PO₄, 5.2mM Na₂HPO₄, 150mM NaCl) and then stained with Eosin/Haematoxylin for 5 minutes. Slides were rinsed in deionised water and mounted in PBX. Follicle number and thyrocyte cell height were determined at the end of the vomer bone in all animals so that comparative analysis could be performed. Cell height of four different thyrocytes per follicle lying 90° from one another were measured and a total of four different follicles per animal were analysed. Mean thyrocyte cell height was measured using a direct method (Kalishnik et al., 1977) without applying any correction factor for shrinkage. The results are expressed as mean of 16 measurements per animal, with 3 individual animals at each time point for each treatment analysed. Results are reported as mean and standard error and a two-way ANOVA is used to test for statistical differences as described below.

5.2.16 Statistical analysis

The data arising from semi-quantitative RT-PCR of *fTnT* developmental ontogeny, *TnT* genes in T3 and Methimazol-treated fish; thyroid hormone concentrations and follicle parameters were each assessed by two-way analysis of variance (ANOVA). If statistically significant differences were detected between treatments, a Tukey (HSD) multiple comparison test was applied. All the statistical analysis was performed using Sigma Stat software version 3 (SPSS, Chicago, IL, USA). Differences were considered statistically significant at $p < 0.05$.

5.3 Results

5.3.1 Characterization of sea bream fast TnT isoforms

Three different full-length cDNAs for sea bream fast TnT gene (fTnTsb) were isolated from a sea bream larval library and their identity assigned after tBLASTx analysis (Altschul et al., 1990) and developmental expression, as sea bream embryonic (efTnTsb; DQ473445), larval (LfTnTsb; DQ473444) and adult (afTnTsb; DQ473443) fast TnT respectively (Fig. 5.1 and 5.8). ClustalX nucleotide (nt) sequence analysis (Thompson et al., 1997) indicated that all sea bream fTnT clones isolated most likely result from alternative splicing of the same gene (Fig. 5.1D). An additional tBLASTx search (Altschul et al., 1990) performed against the *Fugu* database (<http://Fugu.hgmp.mrc.ac.uk>) using all sea bream fTnT sequences gave a highly significant match with a single mayfold, M0001617 (<http://Fugu.hgmp.mrc.ac.uk>). In the Unigene database, mayfold M0001617 gave the most significant hit with the human fTnT locus.

The efTnTsb cDNA is 1,107 bp and contains a 39 base pair (bp) 5' untranslated region (UTR) and a 193 bp 3'UTR. The ATG translation start site (bold in Fig. 5.1A) is located at nucleotide (nt) 40 and spans a coding region of 860 nt terminating in a TAG termination codon at nt 900 (bold in Fig. 5.1A). The cDNA encodes a putative protein of 287 amino acids (aa) (Fig. 5.1A) with a predicted molecular weight of 33.8 KDa and a pI of 5.16 (Wilkins et al., 1998). The cDNA contains a well-conserved Kozak sequence (underlined in Fig. 5.1A) as well as a putative consensus polyadenylation signal just before the beginning of the poly(A) tail (double underlined in Fig. 5.1A).

The presumptive adult afTnTsb cDNA is 973 bp and contains a coding region that spans 695 bp from the ATG translation start site at nt 68 until the TGA termination codon at nt 763 (bold in Fig. 5.1B). The afTnTsb encodes a putative 232 aa protein (Fig. 5.1B) with a predicted molecular weight of 27.8 kDa and a pI of 9.39 (Wilkins et al., 1998). The 5'UTR of afTnTsb

has 67 nt and the 3'UTR of 193 nt is identical in sequence and length to the 3'UTR of efTnTsb (Fig. 5.1B and D). The sea bream cDNA LfTnTsb is 1006 bp and includes a 5'UTR region of 108 nt, and a 3'UTR region of 193 nt identical in size and sequence to the two other sea bream fTnT cDNAs isolated (Fig. 5.1C and D). The LfTnTsb cDNA has a presumptive coding region of 686 nt starting at an ATG translation start site at nt 109 until the TGA termination codon at nt 795 (bold in Fig. 5.1C) and encodes a predicted protein of 229 aa with a molecular weight of 27.2 kDa and pI of 9.57 (Wilkins et al., 1998).

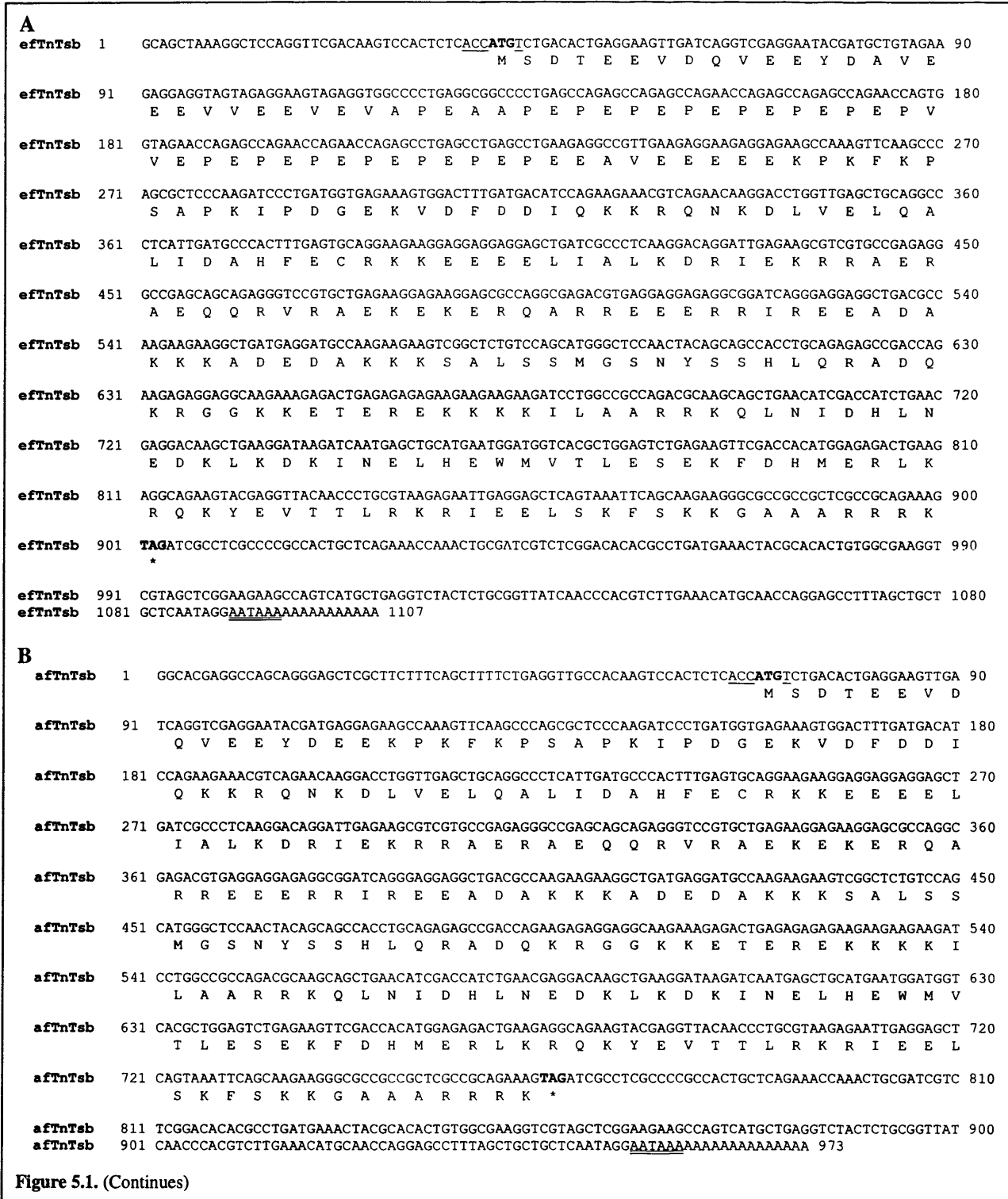


Figure 5.1. (Continues)

Figure 5.1. Nucleotide sequence and deduced protein sequence of the sea bream fTnT isoforms isolated. Putative isoform efTnTsb (A), isoform afTnTsb (B) and LfTnTsb (C) are shown. The ATG translation initiation codon is shown in bold as well as the TAG STOP codon, which is also represented by an asterisk (*). The Kozak consensus sequence is underlined and the double underline indicates the polyadenylation signal. (D) Clustal X (Thompson et al., 1997) multiple nucleotide sequence alignment of sea bream fTnT cDNAs. The position of Forward and Reverse primers used for RT-PCR expression analysis are indicated by arrows.

Clustal X multiple sequence alignment (Thompson et al., 1997) of the isolated sea bream fTnTs revealed that efTnTsb cDNA shared 78% and 82% nt sequence conservation, respectively, with LfTnTsb and afTnTsb. The isoforms afTnTsb and LfTnTsb shared 95% sequence similarity. Sequence comparison of the deduced sea bream fTnT proteins revealed that efTnTsb shared 80 and 81% sequence identity respectively with LfTnTsb and afTnTsb (Table 5.2) and that the latter two deduced proteins shared 99% sequence identity. The differences in sequence conservations between the sea bream fTnT cDNA arise as a consequence of localised insertions or deletions as the remainder of the sequence is 100% conserved, indicating the different forms are generated by alternative splicing (Fig. 5.1D). The efTnTsb cDNA contains an insertion of 146 bp that corresponds to a putative embryonic exon encoding 55 amino acids, of which 27 residues are glutamic acid accounting for the significantly lower pI of the deduced protein (Fig. 5.1A and 5.4). The efTnTsb cDNA shares an additional 9 nt putative exon with afTnTsb but not with LfTnTsb (Fig. 5.1D). This putative exon is located just before the putative embryonic exon in efTnT and is in-between the region identical in all fTnTsb isoforms (Fig. 5.1D) and encodes three amino acids, EYD (Fig. 5.4). The differences observed between the three different fTnTsb cDNAs are not solely located in the coding region. Although the nt sequence of the 5'UTR of afTnTsb and LfTnTsb are identical (Fig. 5.1D), in efTnTsb only nts 23 to 49 which precede the ATG translation start site are identical.

Table 5.2. Protein sequence identity matrix after ClustalX (Thompson et al., 1997) multiple alignment. Sea bream sequences are shown in light grey.

	efTnTsb	afTnTsb	LfTnTsb	efTnTtn	LfTnTtn	afTnTtn	fTnTmd-2	fTnTmd-1	fTnTss	fTnTgm	fTnTazf	fTnTbzf-2	fTnTbzf-1
efTnTsb	1.00	0.81	0.780	0.88	0.74	0.75	0.72	0.73	0.68	0.71	0.67	0.67	0.68
afTnTsb		1.00	0.99	0.75	0.91	0.93	0.89	0.90	0.84	0.88	0.83	0.83	0.84
LfTnTsb			1.00	0.76	0.92	0.92	0.90	0.89	0.84	0.89	0.83	0.84	0.83
efTnTtn				1.00	0.82	0.81	0.73	0.72	0.65	0.70	0.66	0.68	0.67
LfTnTtn					1.00	0.98	0.88	0.87	0.79	0.85	0.80	0.82	0.81
afTnTtn						1.00	0.88	0.89	0.80	0.84	0.80	0.81	0.82
fTnTmd-2							1.00	0.99	0.80	0.86	0.83	0.82	0.81
fTnTmd-1								1.00	0.80	0.85	0.83	0.81	0.82
fTnTss									1.00	0.86	0.78	0.79	0.78
fTnTgm										1.00	0.81	0.81	0.80
fTnTazf											1.00	0.834	0.83
fTnTbzf-2												1.00	0.98
fTnTbzf-1													1.00

5.3.2 Characterization of cloned sea bream *sTnT* and *iTnT* genes

The differential screening strategy employed led to the isolation of two independent sea bream cDNA clones which shared only 43% nucleotide sequence identity and represented distinct *sTnT* genes. The *sTnT1sb* cDNA is 1257 bp and possesses a 45 bp 5'UTR region and a 357 bp 3'UTR (GenBank accession number AY684301). It has an ATG translation start site located within a well-conserved Kozak sequence. An in frame TAA termination codon is located at nt 852 of the cDNA and the only polyadenylation consensus signal is located 18bp before the poly(A) tail. *sTnT1sb* encodes a putative protein of 268 amino acids (Fig. 5.2) with a predicted molecular weight of 32kDa and an isoelectric point of 5.72 (<http://au.expasy.org>; Wilkins et al., 1998).

The *sTnT2sb* cDNA is 1,024 bp long and has a 35 bp 5'UTR and 226 bp 3'UTR (GenBank accession number AY684302). The ATG start site is located within a well-conserved Kozak consensus sequence. The 3'UTR of the cDNA includes an atypical polyadenylation signal (AATTAAA) 14 bp upstream of the poly(A) tail, and additional putative polyadenylation sequences at nucleotides 891 and 958. *sTnT2sb* encodes a putative 240 amino acid protein (Fig. 5.2), which has a predicted molecular weight of 28.4 kDa and an isoelectric point of 9.31.

Interrogation by tBLASTX (Altschul et al., 1990) of GenBank (www.ncbi.nlm.nih.gov) using *sTnT1sb* gave a very high match with other vertebrate *sTnTs* and it has thus been assigned as an orthologue of higher vertebrate *sTnT* genes. In contrast, *sTnT2sb*, although identified as a *TnT* after tBLASTX analysis against GenBank, gave a high probability match with both *sTnT* and *cTnT* sequences. Hence sequence data alone was not sufficient to assign putative gene identity.

No apparent orthologue of the intronless *TnT* gene previously described in zebrafish (Hsiao et al., 2003) was obtained from the library screens. To establish if such an orthologue exists in the sea bream a PCR cloning strategy was devised in which an alignment of *iTnTzf* and its deduced putative homologue in the *Fugu* (*iTnTfg*) was used to design degenerate primers. PCR reactions using the primers combinations F1/R3, F2/R4, F2/R3 and F1/R4 generated fragments of the expected sizes both with a 43 hpf cDNA sample and with sea bream genomic DNA (data not shown). Sequencing of the RT-PCR reaction products revealed they were identical to those derived from genomic DNA, showing that an intronless *TnT* gene exists in the sea bream also. Moreover, tBlastX analysis (Altschul et al., 1997) of these fragments gave a highly significant match only with *iTnTzf*. Sequence assembly of PCR products allowed the complete putative iTnTsb protein sequence to be deduced: it is 274 amino acids (Fig. 5.2) and has a predicted pI of 5.46 and a molecular weight of 35.6kDa.

<i>sTnT2sb</i>	1	MSDTEEVLEE-----EVQDG-----EDESKP--KPKFMTNI	29
<i>iTnTsb</i>	1	...S..IV..YEEEEVEEEEEVEEEEE.E..NETEKKEEQ.E...RH.TTYVP..	60
<i>sTnT1sb</i>	1	...V..EY..QAEAEAEQAEPEQE-EEAEQ.EEDAGEQQEYQ.ERP.----KPMVQL	56
<i>sTnT2sb</i>	30	SAPKIPDGEKVDFFDDIHRKRQEKDLSELQSLIEAHFIQRKKEEELIALVNRIEKRRRAER	89
<i>iTnTsb</i>	61	AP..L.....L....V...FND.....V..SS.Q.....RS...R...D.	120
<i>sTnT1sb</i>	57	AP....E.DR.....M....L..HT..DV..E...RD.....S.KD...R..S..	116
<i>sTnT2sb</i>	90	AEQQRVRETEREKERQARLAEKERKEQEEQRKKYDDDAKKKKALSNTQQYSAGQKSESR	149
<i>iTnTsb</i>	121S.QDR...T.Q...RA.R.E.AAKLRAEEE...AIFT.KS--FGGYLQKVDQ	178
<i>sTnT1sb</i>	117	..I....A.K..D..N.I...RH...E..AK..A.....V..G.GANFGGFLAKAES	176
<i>sTnT2sb</i>	150	KGGKKQTEREKKKKILADRRKALNVDHLNEDKLKEKASELWQWLMGLEAEKFDLSEKLR	209
<i>iTnTsb</i>	179	.K..L.A.E...A.M..K.P..I...QE..A...QD.....HQ.H....E.A.....	238
<i>sTnT1sb</i>	177	RR..RL.GK.IR..T..E..QP.GI.N.R..G..QR.Q.M.NSIYQ..S....FI.HM.H	236
<i>sTnT2sb</i>	210	QKYDINQLLARVQDHQ-----SAKGRGKGMAGRLR	240
<i>iTnTsb</i>	239YV.RN..S...RGSKA.KTS..AKGK..S.K	274
<i>sTnT1sb</i>	237	.R.E.IV..N.I.HA.K----FK.VH....VG..WK	268

Figure 5.2. Multiple sequence alignment of the deduced amino acid sequence of sea bream *sTnT1*, *sTnT2* and *iTnT*. Identical amino acids are denoted by a dot, gaps introduced to maximise similarity are indicated by hyphens.

ClustalX multiple sequence alignment revealed that *sTnT1sb* and *sTnT2sb* cDNAs are dissimilar and the deduced proteins share only 48% amino acid sequence identity (Table 5.3, Fig 6.2). Amino acid sequence identity between *iTnTsb* and *sTnT1sb* and *sTnT2sb* is respectively 43% and 50% which is consistent with the notion that each protein is encoded by a different gene. *iTnTsb* and *sTnT1sb* have longer and more acidic N-terminal regions than *sTnT2sb* (Fig. 5.2). Amino acid sequence conservation between the three sea bream TnT proteins increases after the first third of the sequence onwards, as a consequence of the conserved binding domains for tropomyosin, troponin C and I, and actin which are located in the central and C-terminal end of the TnT proteins (Perry, 1998; Jin et al., 2000b). Compared to *sTnT2sb*, the N-terminal domains of *sTnT1sb* and *iTnTsb* have 26 and 27 additional amino acid residues respectively (Fig. 5.2). The abundance of glutamate in this region (13 in *sTnT1sb* and 21 in *iTnTsb*) contributes to the low isoelectric points of the putative proteins. Comparison of the amino acid sequence of *sTnT1sb* with other species reveals that it shares the greatest similarity with human *sTnT* (61%) and less with human *cTnT* (53%) and *fTnT* (48%), consistent with its designation as slow TnT (Table 5.3). A similar comparison between the amino acid sequence of *sTnT2sb* and other species is inconclusive and it shares a similar level of sequence similarity to human *sTnT* (47%), fast TnT (52%) and cardiac TnT (51%), making its identity more difficult to assign. However, expression analysis (see below) showed that it corresponds to a slow *TnT*. Comparison of the amino acid sequence of *sTnT2sb* with other fish *sTnT* reveal it shares 86% identity with *Fugu* and Medaka, and 56% identity with *sTnT* from with *Salmo. trutta* (Table 5.3), suggesting that this teleost specific *TnT* has diverged most from the ancestral gene possibly as a consequence of specific functional constraints. *iTnTsb* showed higher identity with *iTnTfg* (86%) and *iTnTzf* (66%) and had less than 50% identity with the other TnT sequence used in the analysis (Table 5.3).

Table 5.3. Amino acid identity matrix derived after ClustalX (Thompson et al., 1997) multiple alignment. Sea bream results are shown in light grey.

	sTnTISb	sTnTLMZf	sTnTIC	sTnT_Hs	sTnT2Sb	sTnT2Fg	sTnT2Md	sTnT_1sSt	fTnT_Ss	fTnT_Gm	fTnTazf	fTnTbzf	fTnT_Hs	iTnT_Zf	cTnT_Hs	cTnT_Zf	iTnTsb	iTnTFg
sTnTISb	1.00	0.50	0.65	0.61	0.48	0.48	0.47	0.45	0.45	0.43	0.45	0.46	0.48	0.43	0.53	0.48	0.43	0.43
sTnTLMZf	---	1.00	0.41	0.43	0.35	0.35	0.36	0.28	0.34	0.33	0.34	0.36	0.34	0.29	0.33	0.31	0.29	0.29
sTnTIIc	---	---	1.00	0.53	0.40	0.42	0.38	0.38	0.39	0.39	0.40	0.41	0.44	0.40	0.44	0.44	0.41	0.41
sTnT_Hs	---	---	---	1.00	0.47	0.46	0.44	0.41	0.45	0.45	0.48	0.48	0.52	0.46	0.51	0.48	0.45	0.48
sTnT2Sb	---	---	---	---	1.00	0.86	0.86	0.64	0.56	0.56	0.56	0.58	0.53	0.46	0.54	0.49	0.48	0.50
sTnT2Fg	---	---	---	---	---	1.00	0.79	0.60	0.54	0.55	0.53	0.56	0.53	0.44	0.52	0.46	0.47	0.47
sTnT2Md	---	---	---	---	---	---	1.00	0.62	0.51	0.52	0.52	0.55	0.51	0.44	0.51	0.47	0.47	0.47
sTnT_1sSt	---	---	---	---	---	---	---	1.00	0.43	0.43	0.44	0.45	0.47	0.48	0.52	0.45	0.43	0.47
fTnT_Ss	---	---	---	---	---	---	---	---	1.00	0.87	0.80	0.78	0.59	0.43	0.45	0.44	0.42	0.43
fTnT_Gm	---	---	---	---	---	---	---	---	---	1.00	0.81	0.80	0.58	0.44	0.44	0.43	0.43	0.42
fTnTazf	---	---	---	---	---	---	---	---	---	---	1.00	0.83	0.60	0.44	0.44	0.45	0.45	0.46
fTnTbzf	---	---	---	---	---	---	---	---	---	---	---	1.00	0.61	0.46	0.47	0.47	0.46	0.45
fTnT_Hs	---	---	---	---	---	---	---	---	---	---	---	---	1.00	0.49	0.51	0.44	0.49	0.52
iTnT_Zf	---	---	---	---	---	---	---	---	---	---	---	---	---	1.00	0.53	0.52	0.66	0.65
cTnT_Hs	---	---	---	---	---	---	---	---	---	---	---	---	---	---	1.00	0.62	0.47	0.47
cTnT_Zf	---	---	---	---	---	---	---	---	---	---	---	---	---	---	---	1.00	0.48	0.49
iTnTsb	---	---	---	---	---	---	---	---	---	---	---	---	---	---	---	---	1.00	0.86
iTnTFg	---	---	---	---	---	---	---	---	---	---	---	---	---	---	---	---	---	1.00

5.3.3 Northern blot analysis

The 3'UTR probe of efTnTsb cDNA used for northern blotting hybridises with all fTnT isoforms identified in sea bream. In northern blot no fTnT transcripts are detected in adult heart or liver and in red muscle transcripts are present in low abundance and are only detected after overnight exposure of films (Fig. 5.3, lane 2). Comparison of the relative abundance of fTnT transcripts in sea bream white and red muscle reveals that transcripts are most abundant in the former tissue (Fig. 5.3). This agrees with results in tetrapods in which fTnT is exclusive to white muscle.

The specific probes used for detection of *sTnT1sb* and *sTnT2sb* by northern blot corresponded to the 3'UTR of each gene and did not cross hybridise with each other or with other *TnT*'s. Northern blotting gave a single low abundance transcript (~1260 nucleotides) of *sTnT1sb* in adult sea bream red muscle, which is similar in size to the cDNA isolated from the library screening. No *sTnT1sb* transcripts are present in adult white muscle, heart or liver (Fig. 5.3). *sTnT2sb* gave a single, high abundance transcript of ~1000 nucleotides in adult red muscle and even after prolonged exposure (48h) of the autoradiograph no transcripts were observed in the heart or fast muscle (Fig. 5.3, data not shown). The results of northern blotting confirm the classification of *sTnT1sb* and *sTnT2sb* as striated red (slow) muscle *TnT* genes. The expression of *iTnT* was not assessed by northern blotting since only a clone of the coding region was available which may cross-hybridise with other *TnT* isoforms.

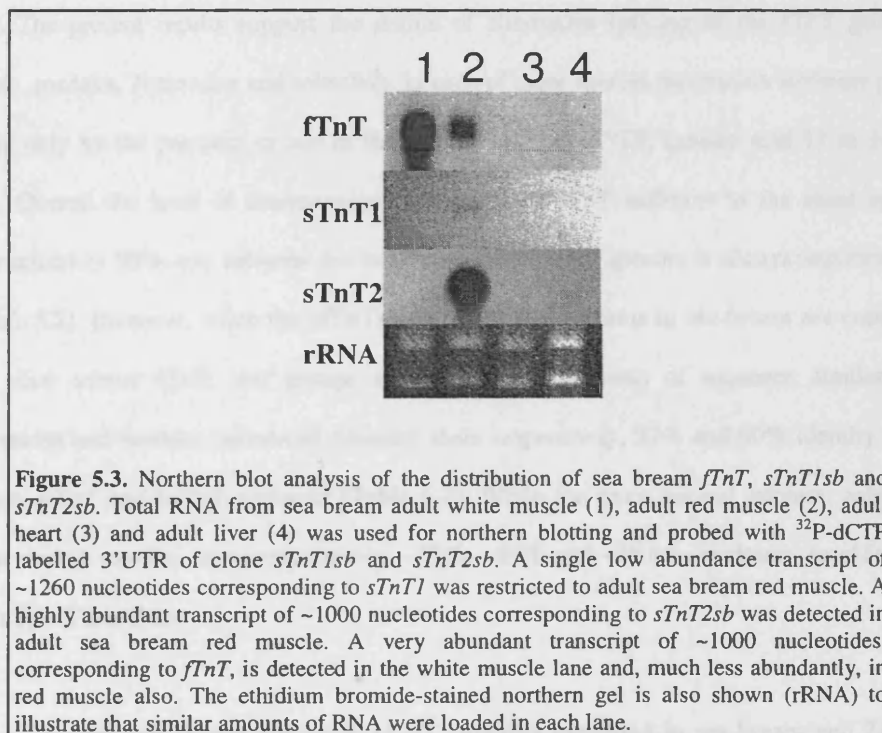


Figure 5.3. Northern blot analysis of the distribution of sea bream *fTnT*, *sTnT1sb* and *sTnT2sb*. Total RNA from sea bream adult white muscle (1), adult red muscle (2), adult heart (3) and adult liver (4) was used for northern blotting and probed with ^{32}P -dCTP labelled 3'UTR of clone *sTnT1sb* and *sTnT2sb*. A single low abundance transcript of ~1260 nucleotides corresponding to *sTnT1* was restricted to adult sea bream red muscle. A highly abundant transcript of ~1000 nucleotides corresponding to *sTnT2sb* was detected in adult sea bream red muscle. A very abundant transcript of ~1000 nucleotides, corresponding to *fTnT*, is detected in the white muscle lane and, much less abundantly, in red muscle also. The ethidium bromide-stained northern gel is also shown (rRNA) to illustrate that similar amounts of RNA were loaded in each lane.

5.3.4 *In silico* identification of fTnT variants in other teleosts

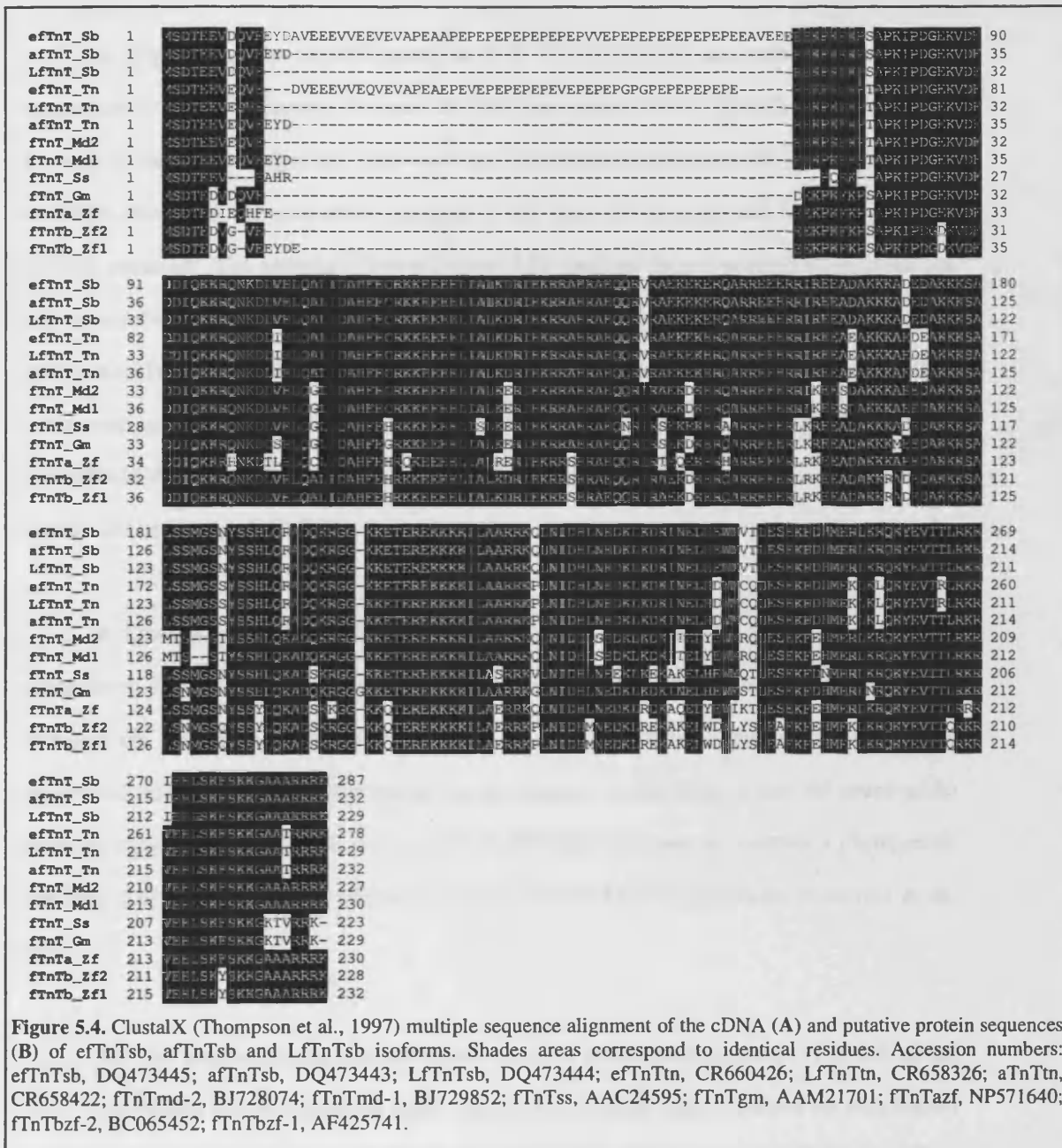
Sequences homologous to the sea bream fTnT cDNAs exist in zebrafish, cod (*Gadus morhua*), Atlantic salmon (*Salmo salar*), medaka (*Oryzias latipes*) and *Tetraodon nigroviridis* (Fig. 5.4). Multiple sequence alignment of the predicted amino acid sequence of the retrieved fTnT cDNAs demonstrated that fTnT isoforms also occur in other teleosts (Fig. 5.4). In zebrafish a second fTnT gene was identified confirming previous reports (Hsiao et al., 2003).

Tetraodon is the only teleost in which 3 isoforms matching the 3 sea bream fTnT cDNAs are identified. In the medaka (fTnTmd-1 and -2) and zebrafish (fTnTbzf-1 and -2) two isoforms are found that seem to correspond respectively to afTnTsb and LfTnTsb cDNAs (Fig. 5.4). The present results support the notion of alternative splicing of the fTnT gene in sea bream, medaka, *Tetraodon* and zebrafish. In each of these species the protein isoforms predicted differ only by the presence or not of the peptide EYD or EYDE (amino acid 11 to 14 in Fig. 5.4). Overall the level of conservation between these fTnT isoforms in the same species is approximately 98% and between the two forms in different species is always superior to 83% (Table 5.2). However, when the afTnTsb and LfTnTsb isoforms in sea bream are compared to the other teleost fTnT, two groups are evident on the basis of sequence similarity. The *Tetraodon* and medaka (advanced teleosts) share respectively, 92% and 90% identity with sea bream afTnT and LfTnT isoforms (Table 6.2). While the more ancient teleosts, zebrafish, *S. salar* and *G. morhua* share respectively, ~82%, ~83% and ~86.6%, similarity to afTnTsb and LfTnTsb (Table 5.2).

Comparison of the embryonic fTnT isoforms identified in sea bream and *Tetraodon* reveal they share 87.8% identity and are most dissimilar in the embryonic specific exon which is 54 aa long in sea bream and 47 aa in *Tetraodon* (Fig. 5.4). The embryonic specific exon in both species encodes a proline and glutamic acid rich sequence and this causes a change from basic to acidic of the predicted pI of fTnT and presumably causes a change in protein function.

The sea bream embryonic specific exon (encodes amino acid 15 to 69; Fig. 5.4) is longer than the same region in the *Tetraodon* (amino acid 12 to 59, Fig. 5.4) and encodes a unique C-terminal sequence (EAVEEEE, amino acid 64 to 69, Fig. 5.4). An additional difference is that sea bream efTnT has the alternatively spliced peptide EYD while in the *Tetraodon* all the clones identified coding efTnT did not possess this peptide (Fig. 5.4). Interspecies comparison of sea bream and *Tetraodon* efTnT isoforms to the presumed adult fTnT sequences revealed around 74% amino acid identity (Table 5.2). Likewise, the sea bream and *Tetraodon* efTnTsb share ~73% amino acid identity with the presumed adult and larval fTnT in medaka and ~70% when compared to zebrafish, *G. morhua* and *S. salar* fTnT proteins (Table 5.2).

Comparison of the C-terminal region of the deduced teleost fTnT proteins with the same region of avian and mammalian fTnT reveals that the teleost fTnTs are most like tetrapod fTnT isoforms that include exon 17.



5.3.5 Phylogenetic analysis of sea bream TnT genes

A frequent problem in phylogenetic analysis of teleost genes and proteins is the limited representation of fish sequences. In order to carry out a more robust phylogenetic analysis, the genome of the model organism *Fugu rubripes* (<http://fugu.hgmp.mrc.ac.uk>) was searched as described above and the nucleotide sequence of the *Fugu sTnT2* gene and the intronless *TnT* (*iTnTfg*) extracted. The Medaka (*Oryzias latipes*) EST database (<http://medaka.lab.nig.ac.jp>) was also searched using both sea bream sTnT cDNAs, leading to the identification of two principal groups of ESTs. *sTnT1sb* cDNA matched Medaka ESTs MF01FSA041P13 and MF01FSA035G24, which were not full length and coded 185 amino acids of the putative protein. Medaka EST clones MF01FSA015N09 and MF01FSA018J16, were full length, coded for a putative protein of 240 amino acids and matched sTnT2sb.

A ClustalX multiple alignment (Thompson et al., 1997) of the predicted amino acid sequences of sTnT1sb, sTnT2sb and iTnTsb, together with TnT sequences from other vertebrates, including the deduced protein sequences of sTnT2 and iTnT from *Fugu* and medaka (Clone MF01FSA018J165), and a zebrafish partial protein sequence (comprising the last 165 amino acids) for a low molecular weight sTnT isoform (sTnTLMW ZF), was used to construct a phylogenetic tree (Fig. 5.5) using maximum parsimony analysis with PAUP* 4.0 software (Swofford et al., 2001).

The two putative sTnTs from sea bream clustered in independent groups (Fig. 5.5) as did iTnT. This division was supported by highly significant bootstrap values obtained for each branch of the tree. None of the sea bream slow troponins described in this manuscript (sTnT1sb, sTnT2sb and iTnTsb) grouped with the vertebrate fTnT or cTnT sequences used in this analysis. The sTnT1sb sequence clustered with tetrapod sTnT sequences and the extracted sequence for the low molecular weight sTnT isoform from zebrafish and African catfish (*Ictalurus punctatus*) troponin T

slow type isoform 1. Within this sTnT group the teleost sequences cluster apart from the tetrapod sequences (Fig. 5.5).

All fish sTnT2 sequences used, including the sTnT2sb isolated in the present study, the extracted *Fugu* and Medaka sTnT2 protein sequences (sTnT2 Fg and sTnT2 Md, respectively), and the *S. trutta* 1s slow TnT (sTnT 1s St), clustered together constituting a new, previously unidentified sTnT group which appears to be teleost specific (Fig. 5.5). Moreover, in agreement with predicted evolutionary relationships the sequence of sTnT2 from sea bream, *Fugu* and medaka, all of which are perciforms, grouped closely together.

The intronless iTnTsb, iTnTzf and iTnTfg sequences did not group with the clades containing sTnT1 or sTnT2 in the phylogenetic tree. Instead they formed an independent cluster, distinct from all other vertebrate TnT sequences used in the analysis (Fig. 5.5, Table 5.3) and constituted another previously undescribed vertebrate TnT group. These intronless TnT genes may have arisen as a result of a reverse transcription event that occurred in the teleost lineage before the divergence of perciforms (sea bream and *Fugu*) and cyprinids (zebrafish).

Finally the sea bream fTnT sequences isolated all clustered together with all other vertebrate fTnT but more closely with other teleost fTnT sequences (Fig. 5.5)

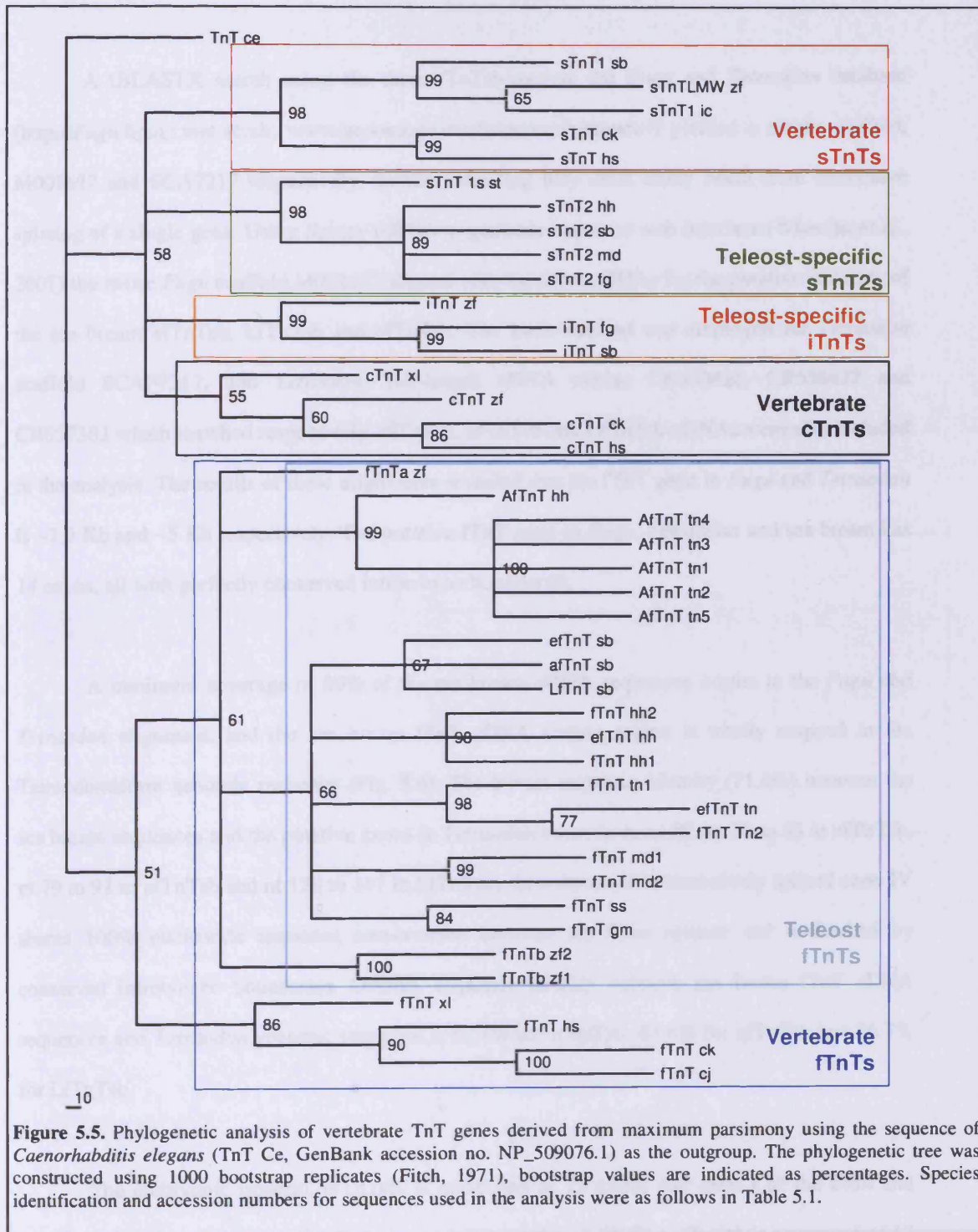


Figure 5.5. Phylogenetic analysis of vertebrate TnT genes derived from maximum parsimony using the sequence of *Caenorhabditis elegans* (TnT Ce, GenBank accession no. NP_509076.1) as the outgroup. The phylogenetic tree was constructed using 1000 bootstrap replicates (Fitch, 1971), bootstrap values are indicated as percentages. Species identification and accession numbers for sequences used in the analysis were as follows in Table 5.1.

5.3.6 Putative genomic organisation of the sea bream fTnT gene

A tBLASTX search using the three fTnTsb against the *Fugu* and *Tetraodon* database (<http://Fugu.hgmp.mrc.ac.uk>; www.genoscope.cns.fr/externe/tetranew/) yielded a single scaffold, M001617 and SCA7217 respectively, further indicating they most likely result from alternative splicing of a single gene. Using Spidey mRNA to genomic sequence web interface (Wheelan et al., 2001) the entire *Fugu* scaffold M001617 aligned with the three cDNAs for the putative isoforms of the sea bream afTnTsb, LfTnTsb and efTnTsb. The same method was employed for *Tetraodon* scaffold SCA7217, and *Tetraodon* full-length cDNA clones CR660426, CR658422 and CR657382 which matched respectively, efTnTsb, afTnTsb and LfTnTsb cDNAs were also included in the analysis. The results of these alignments revealed that the fTnT gene in *Fugu* and *Tetraodon* is ~7.5 Kb and ~5 Kb respectively. The putative fTnT gene in *Fugu*, *Tetraodon* and sea bream has 14 exons, all with perfectly conserved intron/exon boundaries.

A minimum coverage of 80% of the sea bream cDNA sequences occurs in the *Fugu* and *Tetraodon* alignment, and the sea bream fTnT cDNA coding region is totally mapped in the Tetraodontiform genomic sequence (Fig. 5.6). The lowest sequence identity (71.4%) between the sea bream sequences and the putative exons in *Tetraodon* occur in exon III (nt 70 to 83 in efTnTsb, nt 79 to 91 in afTnTsb and nt 128 to 141 in LfTnTsb). In contrast, the alternatively spliced exon IV shares 100% nucleotide sequence conservation between the three species and is flanked by conserved intron/exon boundaries. Overall, sequence identity between sea bream fTnT cDNA sequences and *Tetraodon* genomic sequence is 87.4% for efTnTsb, 87.8% for afTnTsb and 86.7% for LfTnTsb.

The embryonic isoform, efTnTsb, is composed of 13 exons and exon I of the adult and larval isoforms is missing but all other exons are present (Fig. 5.6). The afTnTsb is composed of 13 exons, exons I to IV and VI to XIV, while LfTnTsb is composed of 12 exons, exons I to III and VI to XIV (Fig. 5.6). Comparison of afTnTsb and LfTnTsb isoforms reveals that the 3 additional

amino acids (EYD) in the isoform afTnTsb are the results of alternative splicing of exon IV (Fig. 5.6). Embryonic exon, V, is absent from adult and larval fTnT isoforms (Fig. 5.6).

The nucleotide sequence of the putative embryonic exon in the tetraodontiform genomic sequences and sea bream cDNA is highly conserved (84.2%). However 18 additional nucleotides encoding 6 amino acid residues (EAVEEE) are present in the sea bream embryonic exon (exon V). The putative *Tetraodon* embryonic exon is flanked by consensus intron/exon boundaries and an in frame TGA stop codon is located 5 nucleotides downstream of the 3' exon/intron boundary. This suggests that the truncation in the 3'-end of the tetraodontiform embryonic exon is authentic and specific to *Fugu* and *Tetraodon* and that the differences between the sea bream and tetraodontiforms are species specific.

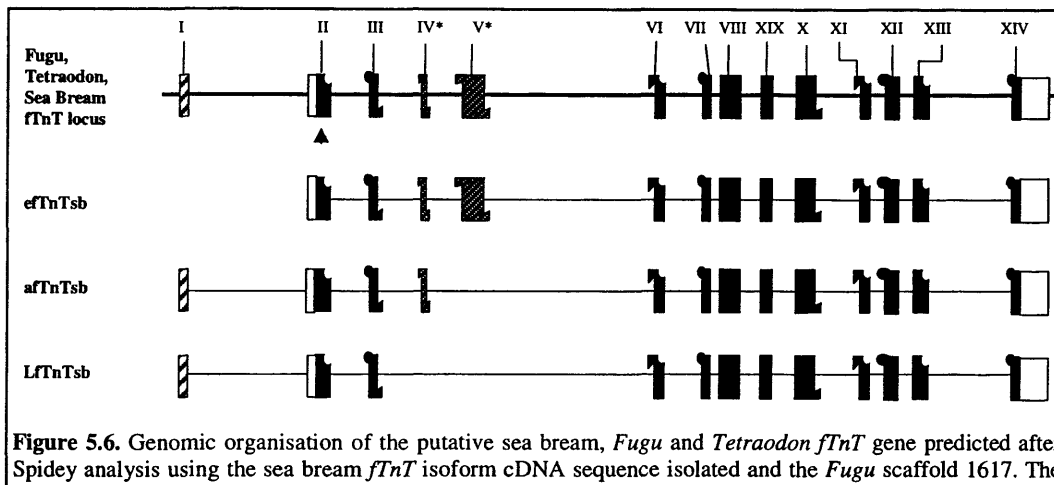


Figure 5.6. Genomic organisation of the putative sea bream, *Fugu* and *Tetraodon* *fTnT* gene predicted after Spidey analysis using the sea bream *fTnT* isoform cDNA sequence isolated and the *Fugu* scaffold 1617. The same analysis was carried out using the sea bream *fTnT* isoforms isolated and *Tetraodon* scaffold SCAF7217, but including also the *Tetraodon* full-length cDNA clones CR660426, CR658422 and CR657382. The black boxed areas represent constitutive protein coding regions while the empty boxes represent untranslated regions. White blocks bearing black diagonal lines represent alternatively spliced untranslated exons, while black blocks bearing white diagonal lines represent protein coding alternatively spliced exons. Exon II contains the ATG initiation codon (arrowhead) and is composed of part of the 5'UTR and the start of the coding region. The sea bream, *Fugu* and *Tetraodon* *fTnT* locus has 14 exons from which exon I, and XIV represent untranslated exons. The exon numbers represented with an asterisk denote alternatively spliced exons. Exon V represents the larval specific exon. Flush junction boundaries in exons indicate that they start or end in intact codons; saw tooth boundaries indicate that the upstream exon donates one nt to the codon while the other two are contributed by the downstream exon; concave/convex exon boundaries indicate that codon splitage takes place by the upstream exon donating two nt while the downstream exon contributes with one. The *efTnTsb* isoform results from the incorporation of all exons except exon I. The *afTnTsb* isoform results from splicing of exons I-IV and VI-XIV while in the *LfTnTsb* isoform exons I-III and VI-XIV are spliced. Both, *afTnTsb* and *LfTnTsb*, have an extra 5'UTR exon, exon I, which is absent from the *efTnTsb*. Sequence conservation between this region (exon I) of the presumed adult sea bream *fTnT* cDNAs and the genomic sequence of *Tetraodon* was higher than 88%.

5.3.7 Putative genomic organization of fish *sTnT* genes and *iTnT*

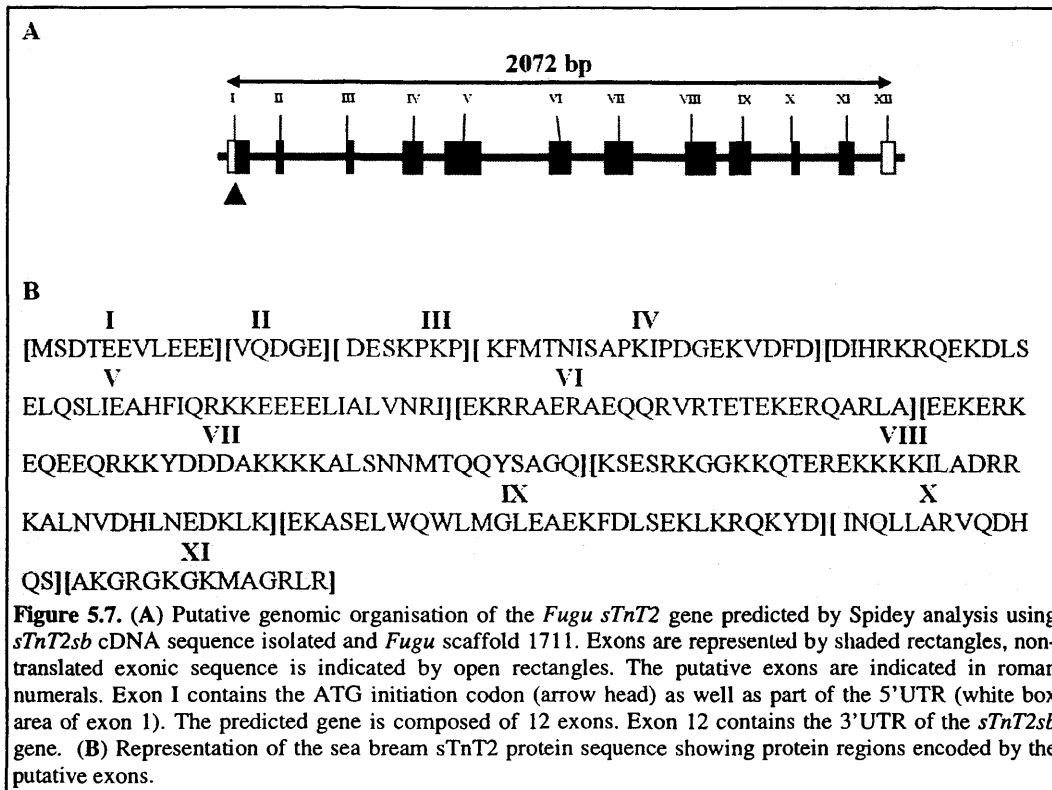
In order to assess the putative genomic organisation of *sTnT1sb* and *sTnT2sb*, the cDNA sequences were used to interrogate the *Fugu* database using tBLASTx. Two mayffolds, M001511 and M000824 gave a highly significant match with *sTnT1sb*, mayffold M001711 gave a highly significant match with *sTnT2sb*, and mayffold M000253 gave a highly significant match with *iTnTsb*. Comparison of the *Fugu* mayffolds matching *sTnT1sb*, *sTnT2sb* and *iTnTsb* revealed they were significantly different, supporting the notion that these mRNAs are coded for by different genes.

No contiguous mayffold spanned the entire *sTnT1sb* cDNA. Alignment of *sTnT1sb* with M001511 and M000824 revealed that the 5'-region (nucleotide 41 to 373) of *sTnT1sb* cDNA matched M001511 while the 3' region (nucleotide 373 to 853) matched M000824. An overlapping region in the two *Fugu* mayffolds identified spanned nucleotide 196 to 373 of the *sTnT1sb* cDNA. However the sequence similarity between the overlapping region in *Fugu* M001511 and M000824 was only 70% and the size of one of the introns differed. The failure to identify a single mayffold spanning *sTnT1sb* and the differences between the 2 scaffolds identified meant the genomic organisation of *Fugu* and sea bream *sTnT1* gene could not be deduced with confidence. Consequently it was not possible to define the potential origin of the additional *sTnT1sb* isoform identified by RT-PCR (Fig. 5.9). However, taking into consideration the structure derived from the two *Fugu* mayffolds it seems likely that in seabream that this gene is composed of at least 12 exons and has a similar overall genomic organisation to the tetrapod *sTnT* genes (Gahlmann et al., 1987; Perry, 1998; Barton et al., 1999; Huang et al., 1999d; Yonemura et al., 2000).

Alignment of *sTnT2sb* with M001711 using Spidey software indicated that the *sTnT2* gene in *Fugu* and sea bream is composed of 12 putative exons and, in *Fugu*, encompasses 2,072 bp (Fig. 5.7). The overall identity of the *Fugu* and sea bream coding sequence is 82.4% and the entire coding region of the sea bream cDNA was mapped on the *Fugu* mayffold. The ATG start codon in

Fugu and sea bream *sTnT2* is located in exon I and within a Kozak consensus sequence (Fig. 5.7).

Fugu mayfold M000253 includes a single-exon TnT gene with 82% sequence similarity to *iTnTsb*.



5.3.8 Developmental analysis of sea bream *fTnT* – semi-quantitative RT-PCR

The RT-PCR co-amplified the three forms of *fTnTsb* (*efTnTsb* – 411bp; *afTnTsb* – 245bp; *LfTnTsb* – 236bp) as primers are localised in the common 5'-region of the cDNAs (Arrows in Fig. 5.1D). Expression of the *fTnT* gene in sea bream commences at 36 hpf (Fig. 5.8), and is detected in all subsequent stages and in adult white and red muscle but is absent from heart and liver (in agreement with the results from northern blot (Fig. 5.3 and 5.8A)). The expression of *LfTnTsb* in adult white muscle is very low, although overall *fTnT* is highly expressed as a result of the high *afTnTsb* transcript abundance. The overall expression of *fTnT* in sea bream adult red muscle is extremely low and only *efTnTsb* and *afTnTsb* transcripts are expressed (Fig. 5.8A and B).

Noticeable, is the fact that efTnT is highly expressed in relation to other isoforms in adult red muscle but it has only a residual expression in adult white muscle (Fig. 5.8C). Furthermore, efTnTsb and afTnTsb have an overlapping expression and both are present in adult red muscle and in embryos before hatch (Fig. 5.8B).

The expression pattern of sea bream fTnT isoforms changed with hatching and from larval stages to adulthood (Fig. 5.8C). efTnTsb and afTnTsb are the only isoforms detected in embryonic stages at 36 hpf (Fig. 5.8A and B) and LfTnTsb only after hatching, although in all subsequent stages analysed LfTnTsb is abundant (Fig. 5.8). efTnTsb is the most abundant isoform before hatching but is strongly downregulated after hatching and by 64 dph onwards is undetectable (Fig. 5.8C). Immediately after hatching, and in all larval and juvenile stages analysed, LfTnTsb is the most abundant isoform of fTnT and the ratio afTnTsb:LfTnTsb is always lower than 1 (Fig. 5.8C). The ratio of the two isoforms starts to change at 89 dph and in adult white muscle there is a ~10-fold inversion in the relative abundance of the two isoforms (Fig. 5.8C).

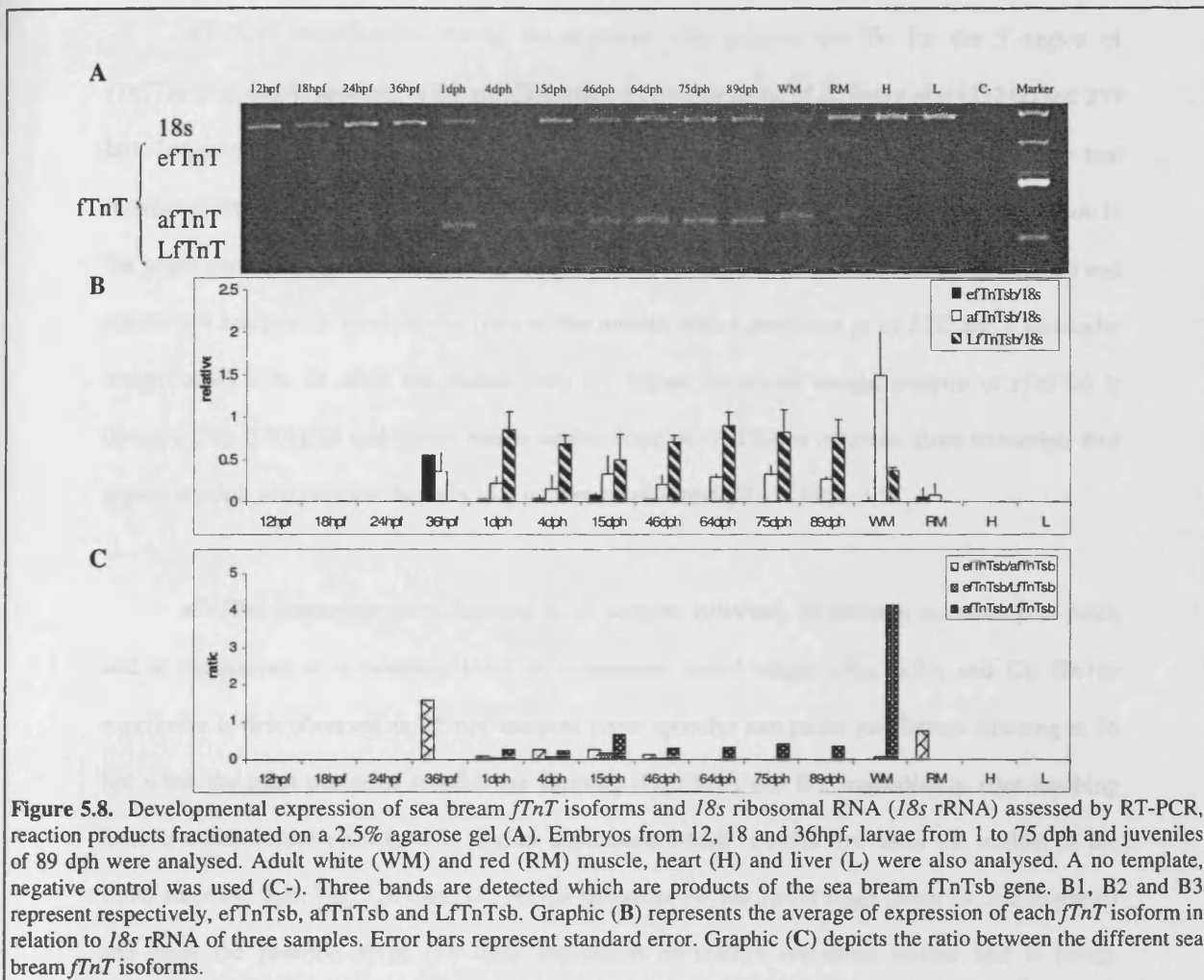


Figure 5.8. Developmental expression of sea bream *fTnT* isoforms and *18s* ribosomal RNA (*18s* rRNA) assessed by RT-PCR, reaction products fractionated on a 2.5% agarose gel (A). Embryos from 12, 18 and 36hpf, larvae from 1 to 75 dph and juveniles of 89 dph were analysed. Adult white (WM) and red (RM) muscle, heart (H) and liver (L) were also analysed. A no template, negative control was used (C-). Three bands are detected which are products of the sea bream *fTnTsb* gene. B1, B2 and B3 represent respectively, efTnTsb, afTnTsb and LfTnTsb. Graphic (B) represents the average of expression of each *fTnT* isoform in relation to *18s* rRNA of three samples. Error bars represent standard error. Graphic (C) depicts the ratio between the different sea bream *fTnT* isoforms.

5.3.9 Tissue specific and developmental expression of *sTnT1sb*, *sTnT2sb* and *iTnTsb* – semi-quantitative RT-PCR

The RT-PCR results for *sTnT1sb* and *sTnT2sb* in adult tissue are in agreement with the results observed with northern blotting - their expression is confined to the red skeletal muscle and even with the much more sensitive method of RT-PCR, it is not possible to detect *sTnT1sb* or *sTnT2sb* in adult sea bream white muscle, heart or liver (Fig. 5.9). Surprisingly *iTnTsb* expression is highest in adult white muscle and barely detectable in adult red muscle (Fig. 5.9A and D).

RT-PCR amplification during development with primers specific for the 5'-region of *sTnT1sb* (Fig. 5.9A) resulted in the amplification of two fragments of different size (332 bp and 353 bp). Sequencing of the amplified products and alignment with ClustalX revealed that the two fragments were identical to the *sTnT1sb* cDNA with the exception of a 21 bp nucleotide insertion in the larger product (Fig. 5.9E). This insert encodes seven additional amino acids (DQDAQEE) and results in a marginally more acidic form of the protein with a predicted pI of 5.42 and a molecular weight of 33 kDa. In adult red muscle only the higher molecular weight isoform of *sTnT1sb* is detected (Fig. 5.9A). In embryonic stages neither form of *sTnT1sb* is detected. Both transcripts first appear at 4dph and increase linearly to a maximum at 75dph (Fig. 5.9B).

sTnT2sb transcripts were detected in all samples collected. Expression increases post-hatch and is maintained at a constant level in subsequent larval stages (Fig. 5.9A and C). *iTnTsb* expression is first observed in 18 hpf samples (90% epiboly) and peaks just before hatching at 36 hpf when the most posterior somites are forming (Fig. 5.9A and D). Immediately after hatching there is a substantial reduction in *iTnTsb* expression which remains low until the middle of the larval stage (46 dph; Fig. 5.9A and D). As the fish enter the last larval stage (from 64 dph onwards) and enter the juvenile stage (89 dph) expression of *iTnTsb* decreases further and is barely detectable.

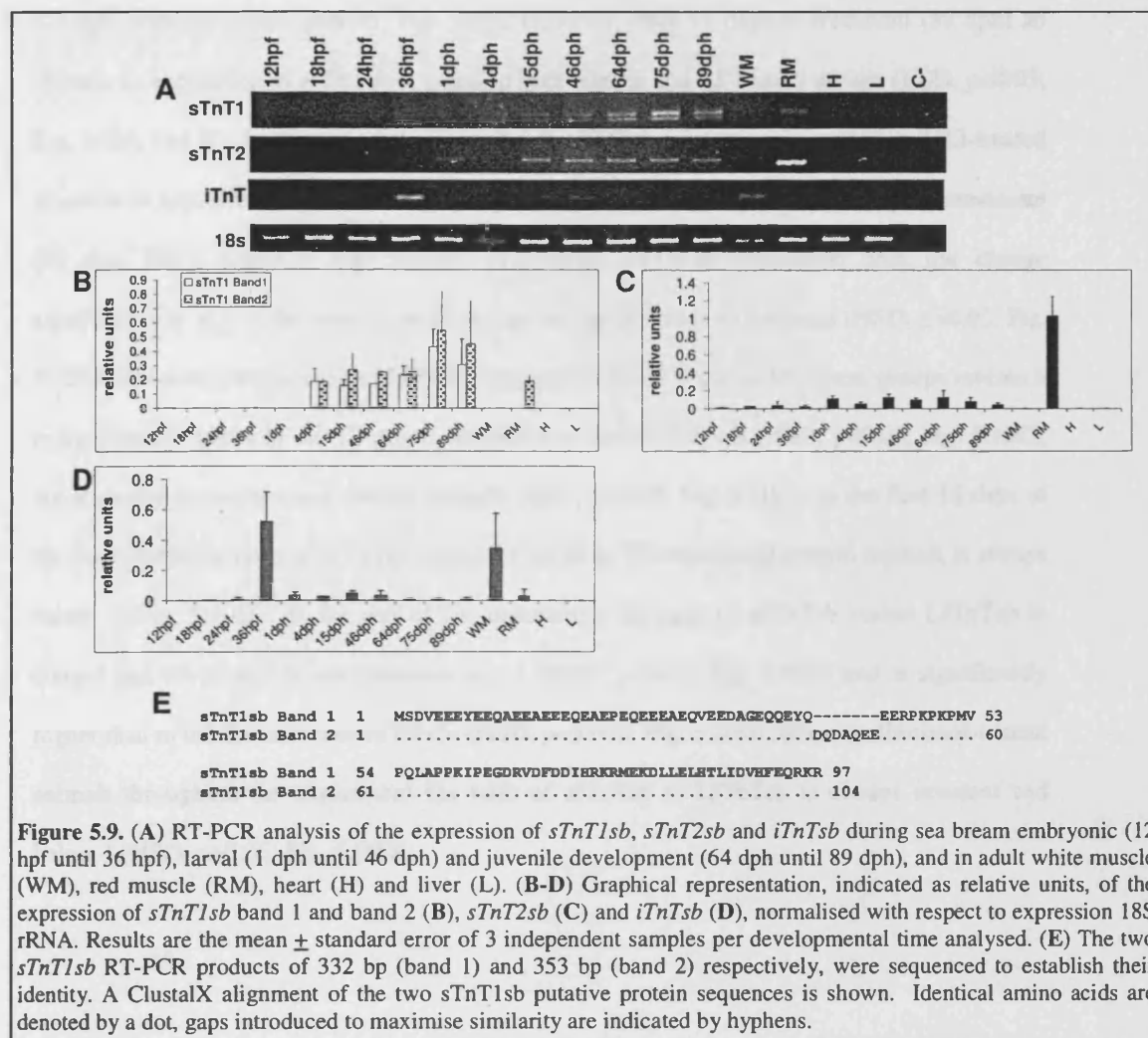


Figure 5.9. (A) RT-PCR analysis of the expression of *sTnT1sb*, *sTnT2sb* and *iTnTsb* during sea bream embryonic (12 hpf until 36 hpf), larval (1 dph until 46 dph) and juvenile development (64 dph until 89 dph), and in adult white muscle (WM), red muscle (RM), heart (H) and liver (L). (B-D) Graphical representation, indicated as relative units, of the expression of *sTnT1sb* band 1 and band 2 (B), *sTnT2sb* (C) and *iTnTsb* (D), normalised with respect to expression 18S rRNA. Results are the mean \pm standard error of 3 independent samples per developmental time analysed. (E) The two *sTnT1sb* RT-PCR products of 332 bp (band 1) and 353 bp (band 2) respectively, were sequenced to establish their identity. A ClustalX alignment of the two sTnT1sb putative protein sequences is shown. Identical amino acids are denoted by a dot, gaps introduced to maximise similarity are indicated by hyphens.

5.2.10 T3 and Methimazol treatments – sea bream TnT expression

The efTnTsb isoform was not detected in any of the samples collected from control, T3 and methimazol experiments (Fig. 5.10A and B). In methimazol treated juveniles there is no significant change in the expression of afTnTsb at any time during the 31 days of methimazol treatment and expression throughout the experiment is significantly lower than in control and T3-treated animals (HSD, $p \leq 0.005$, Fig. 5.10B). No significant difference is observed in the expression of afTnTsb and LfTnTsb isoforms in control juveniles or those treated for 18 days

(75 dph) with T3 (HSD, $p>0.05$; Fig. 5.10). However, after 31 days of treatment (89 dph) an increase in expression of afTnTsb is noted in both control and T3-treated groups (HSD, $p<0.05$; Fig. 5.10A and B). At the end of the experiment, afTnTsb expression in control and T3-treated juveniles is approximately 3- and 2-fold higher respectively than that after 18 days of treatment (75 dph; HSD, $p<0.001$; Fig. 5.10B). In contrast, LfTnTsb expression does not change significantly in any of the experimental groups during the entire experiment (HSD, $p>0.05$; Fig. 5.10C). However, comparison of LfTnTsb expression levels between treatment groups reveals it is significantly lower in the T3 group compared to control animals (HSD, $p<0.05$, Fig. 5.10C), but is similar to methimazol treated animals (HSD, $p>0.05$; Fig. 5.10C). In the first 18 days of the experiment the ratio of afTnTsb versus LfTnTsb in T3-treated and control animals is always below 1 (Fig. 5.10D). At the end of the experiment the ratio of afTnTsb versus LfTnTsb in control and T3-treated larvae increases to ~1 (HSD, $p<0.05$; Fig. 5.10D) and is significantly higher than in methimazol treated larvae (HSD, $p<0.002$; Fig. 5.10D). In the methimazol-treated animals throughout the experiment the ratio of afTnTsb to LfTnTsb is always constant and below 1 (HSD, $p>0.05$; Fig. 5.10D).

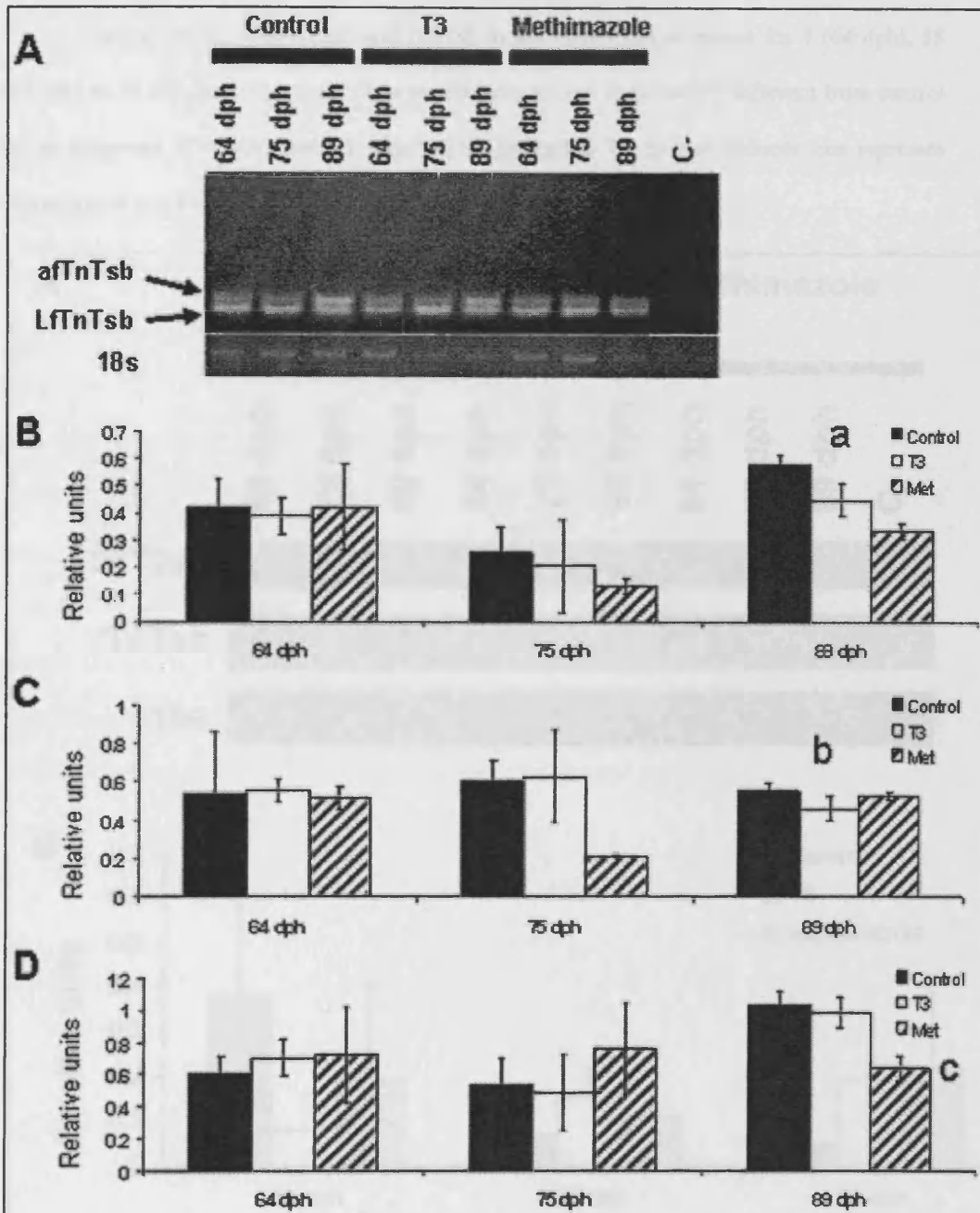
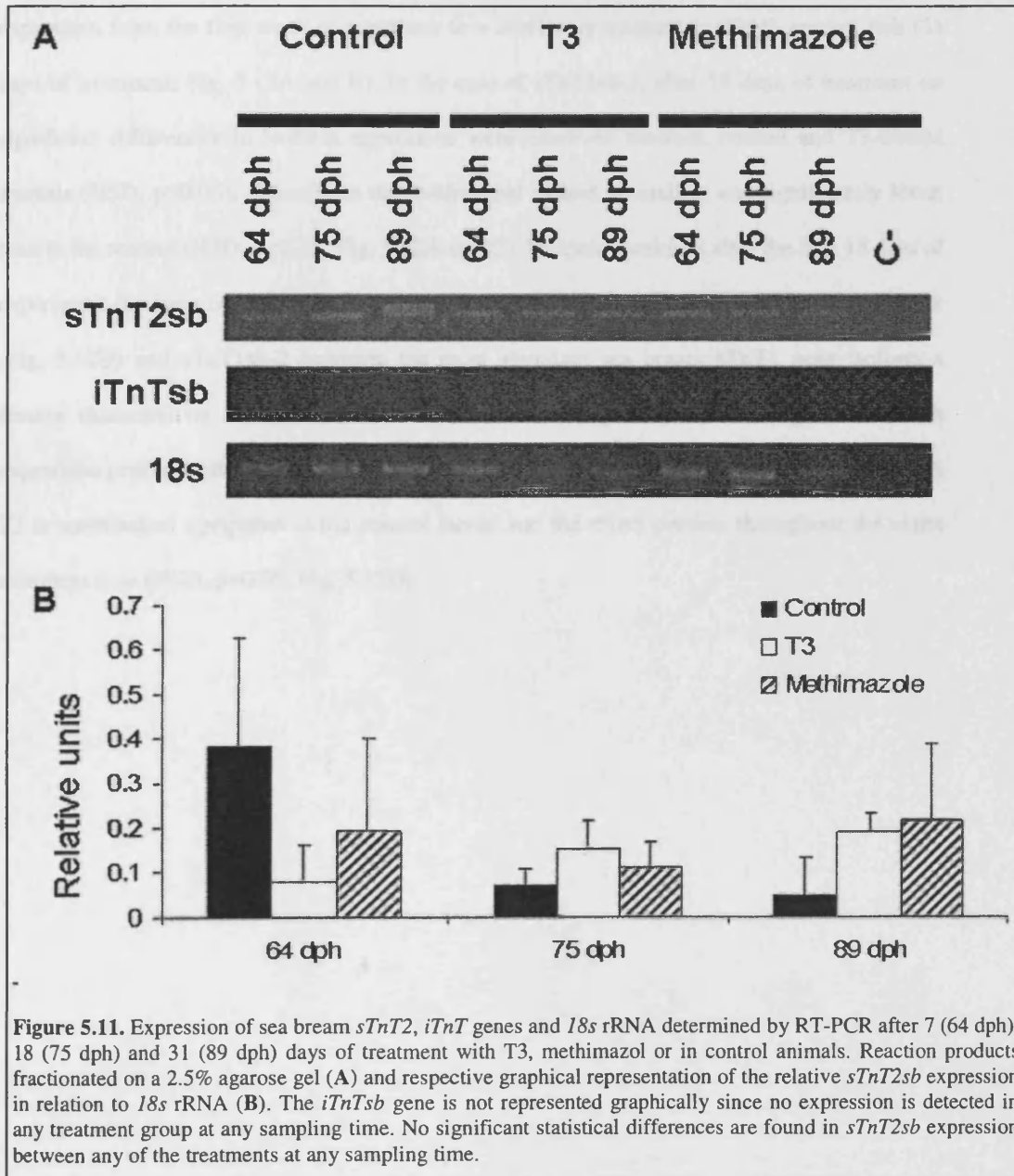
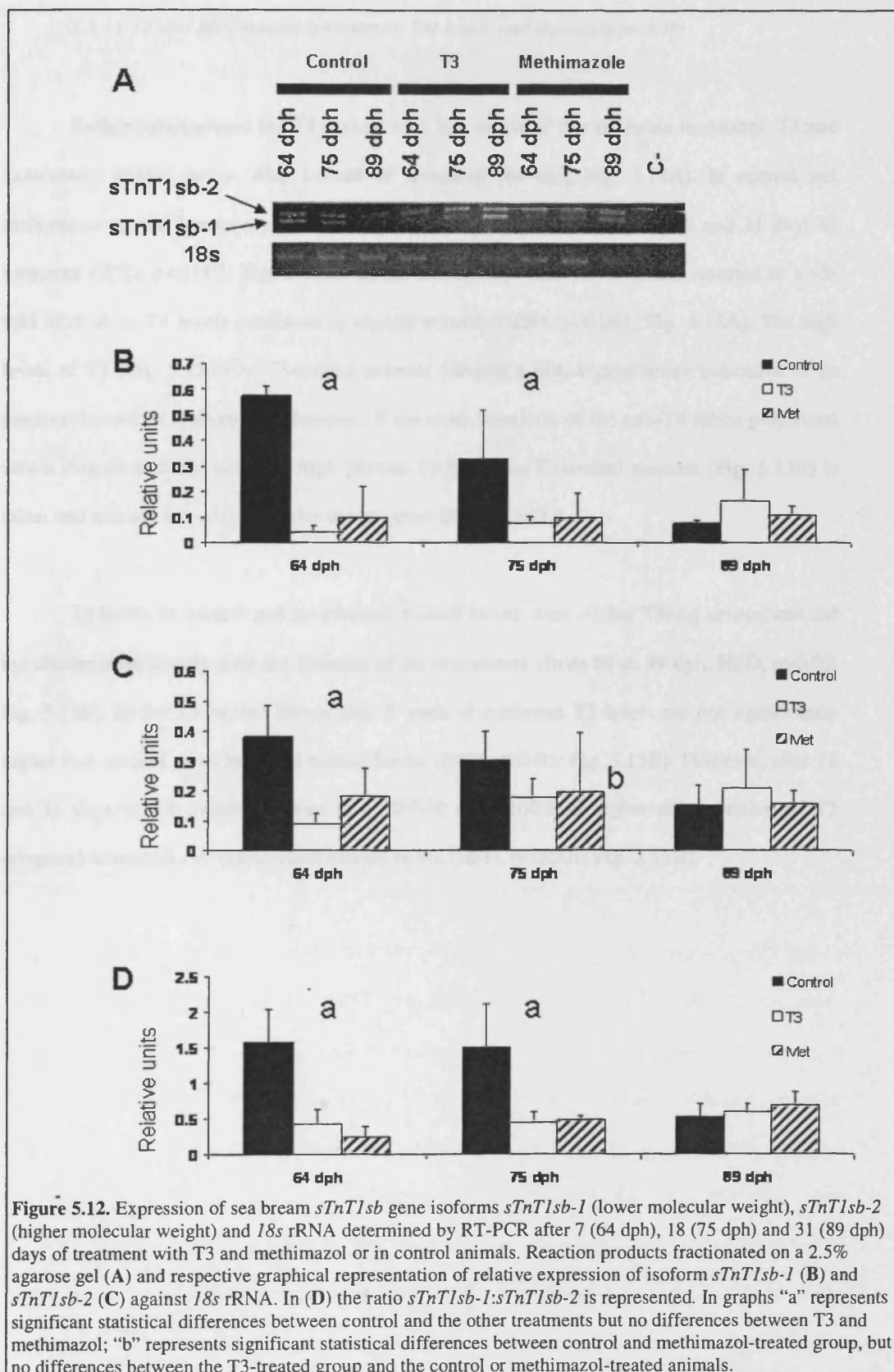


Figure 5.10. Expression of sea bream fTnT gene isoforms *afTnTsb* (higher molecular weight), *LfTnTsb* (lower molecular weight) and *18s* rRNA assessed by RT-PCR after 7 (64 dph), 18 (75dph) and 31 days (89 dph) treatment with T3, methimazol and control animals. Reaction products fractionated on a 2.5% agarose gel (A) and respective graphical representation of relative expression of isoform *afTnTsb* (B) and *LfTnTsb* (C) against *18s*. In (D) the ratio *afTnTsb*:*LfTnTsb* is presented. The *efTnTsb* isoform is not represented graphically since no expression is detected in any treatment at any sampling point. In the graphs “a” represents significant statistical differences between all treatments; “b” represents significant statistical differences between control and T3-treated group, but no differences when the methimazol-treated group is compared either with the control or T3-treated animals; “c” represents no significant statistical differences are found between control and T3-treated animals but methimazol is significantly different.

The expression of *sTnT2sb* and *iTnTsb* in sea bream larvae treated for 7 (64 dph), 18 (75 dph) or 31 (89 dph) days with T3 or methimazol are not significantly different from control larvae (one-way ANOVA, $p > 0.05$; Fig. 5.11). Indicating T3 neither induces nor represses expression of *sTnT2* or *iTnT* (Fig. 5.11B) in sea bream.



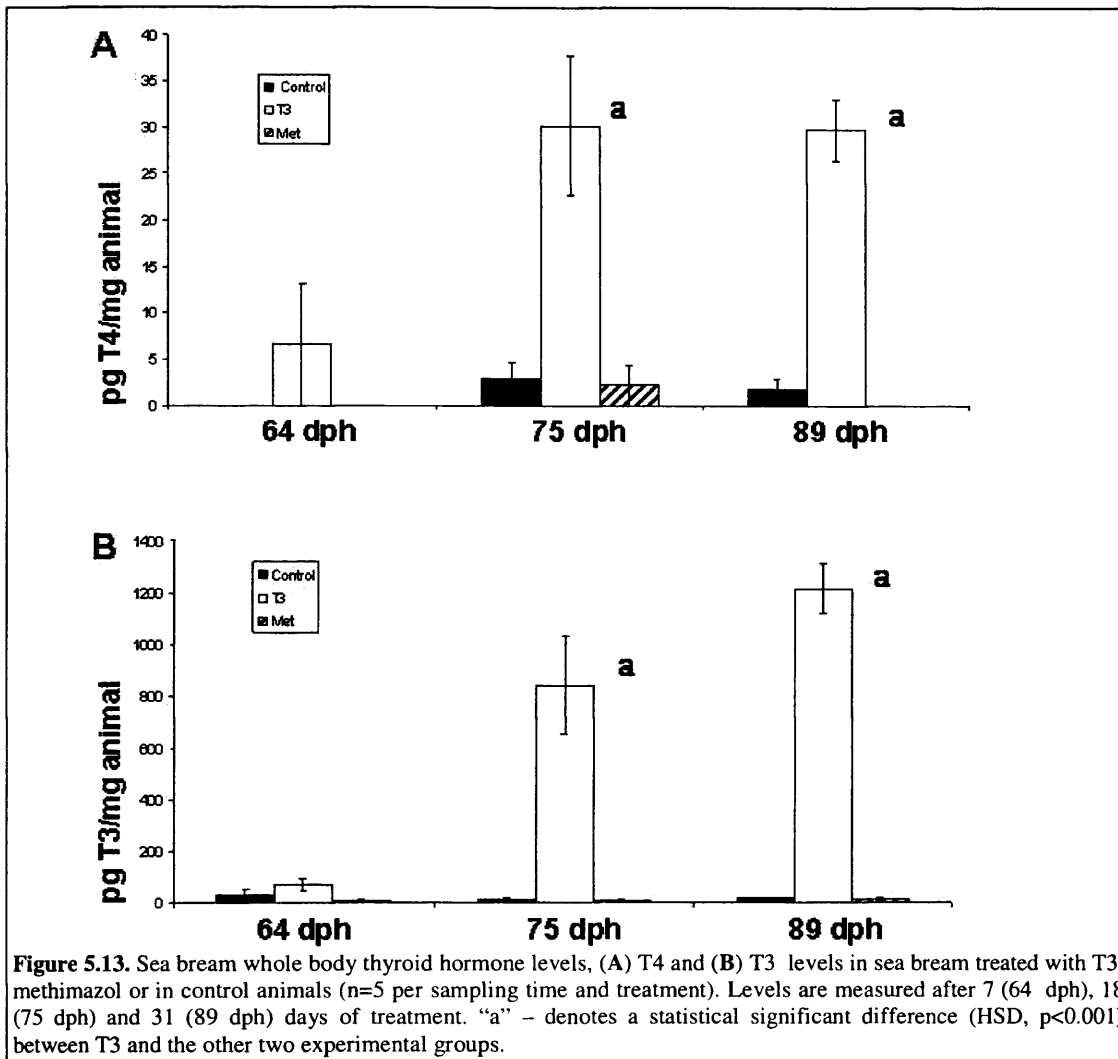
In contrast, sTnT1sb is significantly downregulated at the end of the first week of treatment with T3 and methimazol compared to the control larvae (HSD, $p < 0.05$; Fig. 5.12). Moreover, T3 and methimazol diminish sTnT1sb isoform expression with the same effectiveness (HSD, $p < 0.05$; Fig. 5.12A and B). Treatment had a greater effect on expression of sTnT1sb-1 isoform than on sTnT1sb-2. Both treatments decreased sTnT1sb-1 isoform expression from the first week of treatment to a level only attained in 89dph control fish (31 days of treatment; Fig. 5.12A and B). In the case of sTnT1sb-2, after 18 days of treatment no significant differences in isoform expression were observed between control and T3-treated animals (HSD, $p > 0.05$), although in the methimazol treated animals it was significantly lower than in the control (HSD, $p < 0.05$; Fig. 5.12A and C). In control animals after the first 18 days of experiment the ratio between sTnT1sb-1 and sTnT1sb-2 is ~1 and decreases to ~0.5 in 89dph (Fig. 5.12D) and sTnT1sb-2 becomes the most abundant sea bream sTnT1 gene isoform a feature characteristic of adult sea bream red muscle (Fig. 5.9). The change to an adult expression profile of the ratio of sTnT1sb isoforms occurs after only 1 week of treatment with T3 or methimazol compared to the control larvae and the effect persists throughout the entire treatment time (HSD, $p < 0.05$; Fig. 5.12D).



5.3.11 T3 and Methimazol treatments: TH levels and thyrocyte activity

Radioimmunoassays for T4 reveals very low levels of this hormone in control, T3 and methimazol treated larvae after 1-week of treatment (64 dph, Fig. 5.13A). In control and methimazol treated larvae a significant increase in T4 levels occurs after 18 and 31 days of treatment (HSD, $p < 0.001$; Fig. 5.13A). From 18 days onwards T3-treatment resulted in a ~5-fold increase in T4 levels compared to control animals (HSD, $p < 0.001$; Fig. 5.13A). The high levels of T4 (Fig. 5.13A) in T3-treated animals (despite a histological index indicative of an inactive thyroid) is ambiguous. However, if the cross reactivity of the anti-T4 rabbit polyclonal serum (Sigma-Aldrich) with the high plasma T3 levels in T3-treated animals (Fig. 5.13B) is taken into account it readily explains the apparent increase in T4.

T3 levels in control and methimazol treated larvae were ~10pg T3/mg animal and did not change significantly over the duration of the experiment (from 64 to 89 dph; HSD, $p > 0.05$; Fig. 5.13B). In the T3 treated larvae after 1 week of treatment T3 levels are not significantly higher than control or methimazol treated larvae (HSD, $p > 0.05$; Fig. 5.13B). However, after 18 and 31 days of T3 treatment there is a 50-fold and ~100-fold higher concentration of T3 compared to control and methimazol treated larvae (HSD, $p < 0.001$; Fig. 5.13B).



To further analyse thyroid status after T3 and methimazol treatments thyroid follicle number (Fig. 5.14A) and thyrocyte cell height (index of thyroid activity, (Kalisnik et al., 1977; Cooley et al., 2001) (Fig. 5.14B), was assessed during normal sea bream ontogeny and during treatment with T3 and methimazol (Fig. 5.14). In control larvae, follicle number is constant through the course of the experiment (HSD, p>0.05; Fig. 5.14B). However, control thyrocyte cell height is greater in 7 and 18 days of treatment (64 dph and 75 dph respectively) than at the end of the experiment (HSD, p<0.001; Fig. 5.14A and C). Moreover, in days 7 and 18 colloid is absent or has a vesicular aspect indicative of high follicle activity (Fig. 5.14). At the end of the experiments 50% of the follicles appear inactive and have a squamous appearance (Fig. 5.14A).

Methimazol treatment has no effect on follicle number (2-Way ANOVA, $p>0.05$; Fig. 5.14A) but significantly increase thyrocyte cell height over 18 days of treatment compared to control fish (2-Way ANOVA, $p<0.001$; Fig. 5.14A and C) and although thyrocyte height decreases at the end of treatment (HSD, $p<0.001$; Fig. 5.14A and C) it is still significantly higher than control larvae (HSD, $p<0.001$). Moreover, thyroid follicles in methimazol treated animals lack or contain colloid with vesicles located at the apical side of the thyrocytes which is indicative of intense activity (Fig. 5.14A). However, at the end of the experiment over half of the follicles examined appear inactive (Fig. 5.14C). Analysis of larval T4 and T3 concentrations and thyroid follicle activity revealed that in sea bream methimazol does not have an anti-thyroidogenic activity. In fact, in sea bream methimazol treatment seems to moderately stimulate thyrocyte activity (Fig. 5.14). The lack effect of methimazol on the TH production in sea bream may explain its contradictory effect on TnT expression.

T3 treatment significantly increases follicle number above control and methimazol treated fish by the end of treatment (HSD, $p<0.001$; Fig. 5.14). However there is a significant reduction in thyrocyte cell height in T3-treated fish compared to control and methimazol treated animals (HSD, $p<0.001$; Fig. 5.14A and C). The effect of T3 on thyrocyte cell height is evident by the end of the first week of the experiment and causes a 25% reduction in cell height compared to control and methimazol treated animals (HSD, $p<0.001$; Fig. 5.14A and C). This difference in thyrocyte cell height between the T3 treated group and the other two experimental groups is even more accentuated after 18 days of treatment (Fig. 5.14A and C). At this time thyrocyte cell height in T3 treated animals is almost half that of the control and 2/5 of the methimazol treated group (HSD, $p<0.001$; Fig. 5.14). At the end of the experiment thyrocyte cell height in the T3 treated group is significantly different from the methimazol treated animals (HSD, $p<0.001$; Fig. 5.14). The follicle lumen of T3 treated larvae contains abundant colloid and few vesicles for the duration of the experiment (Fig. 5.14A, indicative of low activity).

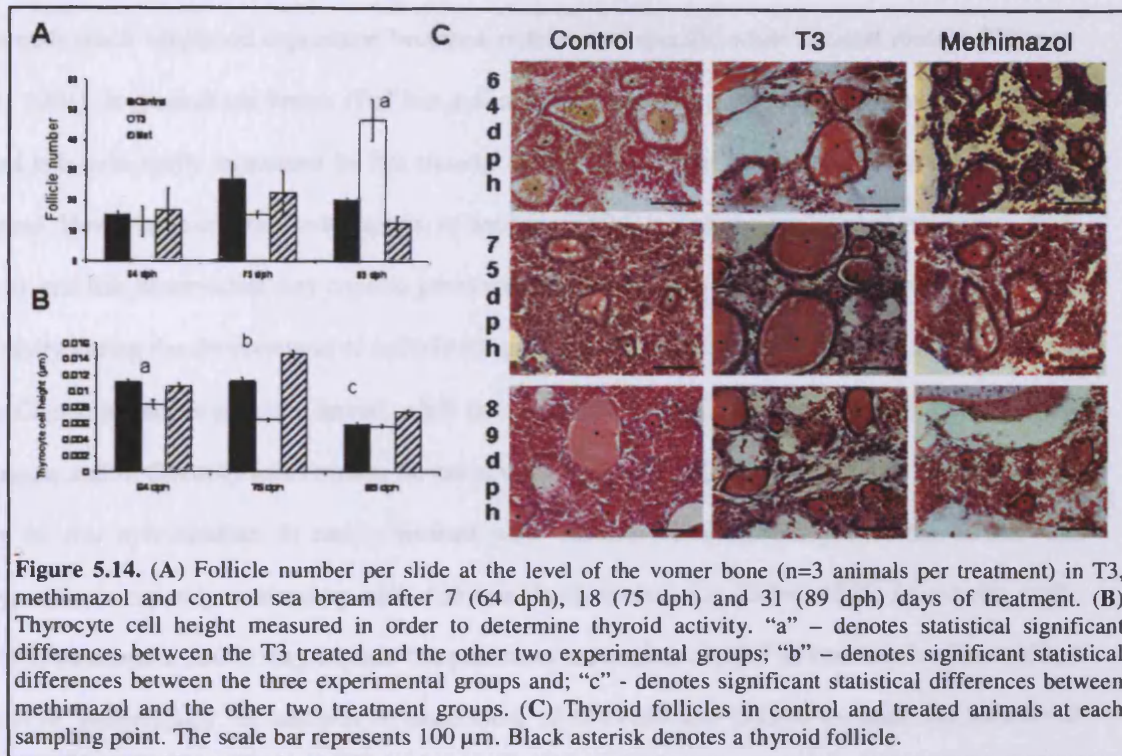


Figure 5.14. (A) Follicle number per slide at the level of the vomer bone ($n=3$ animals per treatment) in T3, methimazol and control sea bream after 7 (64 dph), 18 (75 dph) and 31 (89 dph) days of treatment. (B) Thyrocyte cell height measured in order to determine thyroid activity. "a" – denotes statistical significant differences between the T3 treated and the other two experimental groups; "b" – denotes significant statistical differences between the three experimental groups and; "c" – denotes significant statistical differences between methimazol and the other two treatment groups. (C) Thyroid follicles in control and treated animals at each sampling point. The scale bar represents 100 µm. Black asterisk denotes a thyroid follicle.

5.4 Discussion

5.4.1 Molecular characterization of sea bream *fTnT* gene - *fTnTsb*

The deduced protein sequence of the cDNA clones for *fTnT* splice variants in sea bream gives rise to three proteins that differ in the N-terminal region but are identical in the mid- and C-terminal region (Fig. 5.4). A similar situation is found for *fTnT* genes in terrestrial vertebrates (Briggs et al., 1984; Breitbart et al., 1985; Hastings et al., 1985; Briggs et al., 1987; Gahlmann et al., 1987; Briggs et al., 1988; Briggs and Schachat, 1989; Briggs and Schachat, 1993; Morgan et al., 1993; Wu et al., 1994; Jin, 1996; Jin et al., 1996; Wang and Jin, 1997; Jin et al., 1998a; Ogut and Jin, 1998; Perry, 1998; Wang and Jin, 1998; Bucher et al., 1999; Bastide et al., 2002; Jozaki et al., 2002). The embryonic *fTnT* isoform in sea bream is larger (33.8 kDa) than *afTnTsb* and *LfTnTsb*, with a predicted molecular weight of ~28 kDa which is similar to terrestrial vertebrate *fTnT* proteins (Perry, 1998; Jin et al., 2000b).

In tetrapods *fTnT* genes are initially expressed in different skeletal muscle types but as animals reach adulthood expression becomes restricted to specific white skeletal muscle (Wang et al., 2001). In general sea bream *fTnT* has a similar expression pattern to that observed in tetrapods and it is principally expressed in fast muscle and is absent from cardiac muscle and non-muscle tissue. However in contrast to tetrapods, in sea bream *fTnT* is also present in adult red muscle (Fig. 5.3), and this observation may explain previous biochemical data demonstrating fast tissue ATPase activity during the development of red (slow) muscle in sea bream (Mascarello et al., 1995). In fact, in *Clupea harengus* yolk-sac larvae, adult fast myosin light chain isoforms were detected in slow muscle and in *Oncorhynchus mykiss* larvae several fast-muscle specific genes have been identified by *in situ* hybridisation in newly formed slow muscle fibres (Chauvigne et al., 2006). The hyperplastic capacity retained by adult fish muscle (Koumans and Akster, 1995; Mascarello et al., 1995; Mommsen, 2001) may explain the persistent expression of *fTnT* in both adult white and red muscle. Interestingly, in addition to expression of sTnT2sb and iTnTsb in adult sea bream red muscle, efTnTsb and afTnTsb are also present (Fig. 5.8 and 5.9). The co-expression of sea bream TnT genes (sTnT2sb, iTnTsb, efTnTsb and afTnTsb) in adult red muscle is similar to what occurs during early embryonic muscle development (Fig. 5.8 and 5.9) and may suggest that, *de novo* formation of new red muscle fibres in adults recapitulates embryonic muscle development.

The various *fTnT* protein isoforms found in sea bream arise from alternative splicing of two exons (exon IV and V in Fig. 5.6) located in the 5' region of the gene. Alternative splicing is responsible for the differing sequence of the N-terminal region of the sea bream *fTnT* proteins (Fig. 5.4) and also for their divergent pI and size. The occurrence of *fTnT* splice variants in teleosts is not restricted to the sea bream or the halibut (Chapter 4) and database searches reveal the existence of homologous cDNA sequences in *Tetraodon*, medaka and zebrafish (Fig. 5.4). A similar situation also occurs in tetrapods, and in chicken wing muscle about 79 different TnT proteins are identified by 2D-SDS-PAGE analysis (Yao et al., 1992) and in mouse the mRNA of at least 10 different isoforms of the *fTnT* gene have been identified (Breitbart et al., 1985). Alternative 5'-exon splicing of the mouse *fTnT* gene can generate 64 different isoforms (Perry, 1998). This huge genomic

heterogeneity in tetrapod *fTnT* isoforms is further increased by the presence in avian and mammalian *fTnT* genes of two mutually exclusive alternatively spliced exons in the 3'-region (exon 16 and 17) which give rise to different C-terminal protein domains (Wang and Jin, 1997; Jin et al., 1998b; Perry, 1998; Bucher et al., 1999; Jozaki et al., 2002). In the present study no teleost C-terminal *fTnT* variants have been found (Fig. 5.4; Chapter 3) and the predicted C-terminal *fTnT* protein is most similar to the protein encoded by tetrapod exon 17. This seems to indicate that the alternatively spliced C-terminal exon 17 in tetrapods may be the exon present in *fTnT* of the common ancestors of fish and land vertebrates and that exon 16 may have arisen in the terrestrial vertebrate lineage. The greater heterogeneity of tetrapod *fTnT* transcripts compared to teleosts is probably a consequence of the greater number of specialized muscles in tetrapods which express alternatively spliced *fTnT* isoforms (Perry, 1998; Jin et al., 2000b).

In *Fugu* and *Tetraodon* the putative *fTnT* genes are composed of 14 putative exons, have a well conserved gene organisation (Fig. 5.6) and are respectively, ~7.5 Kb and ~5 Kb. This is in contrast to the ~16 Kb *fTnT* gene in rat and more than 33 Kb gene in quail (Bucher et al., 1999) which are composed of 19 and 25 exons respectively. Despite the greater number of exons in terrestrial vertebrate *fTnT* there is conservation of the overall gene organisation in teleosts. In sea bream, *Fugu* and *Tetraodon* only 2 alternatively spliced exons (exon IV and V; Fig. 5.6) have been identified. Zebrafish, differs from the other teleosts as it has two *fTnT* genes which are each composed of 12 exons and are 12 and 15 Kb respectively (Hsiao et al., 2003). Database searches reveal alternative splicing of zebrafish *fTnTb* gene also occurs and two different cDNAs coding for different isoforms (Fig. 5.4) of one gene have been identified in the present study. One of the predicted zebrafish proteins contains 4 additional amino acids (EYDE), homologous to the sea bream EYD peptide found in the *efTnTsb* and *afTnTsb* isoforms (Fig. 5.4). Mouse, rat and chicken, contain a significantly greater number of *fTnT* isoforms (13, 10 and 25 respectively) than fish (Breitbart et al., 1985; Wang and Jin, 1997; Perry, 1998), this has been related to their differential expression in specialised muscles of terrestrial vertebrates (Perry, 1998; Jin et al., 2000b).

Interestingly the biochemical characteristics of the embryonic-specific inserts of *fTnT* in sea bream (54 aa), *Tetraodon* (48 aa), human (8 aa) (Perry, 1998), rat (13 aa) and rabbit (12 aa) (Briggs and Schachat, 1993) are similar and the high glutamic acid content they encode confers an acidic pI to the protein. The occurrence of fetal *fTnT* splice variants in teleosts and terrestrial vertebrates (Briggs and Schachat, 1993; Morgan et al., 1993; Briggs et al., 1994; Wang and Jin, 1997), suggests that the fetal/embryonic specific exon arose before fish and terrestrial vertebrates diverged and that similar constraints exist in early muscle development in aquatic and terrestrial vertebrates. In fact, in the *fTnT* genes of *Fugu*, *Tetraodon* (this work, Fig. 5.6), rat and quail (Bucher et al., 1999) the alternatively spliced exons of the N-terminal region share exactly the same codon splitage combination. Moreover, a similar situation is also observed for the last two *fTnT* exons XIII and XIV in *Fugu* and *Tetraodon* (Fig. 5.6) which share the same codon splitage combination as the mutually exclusive exons 16 and 17 and the last C-terminal constitutively spliced exon (18) in rat and quail (Bucher et al., 1999).

5.4.2 Molecular characterisation of the *sTnT* and *iTnT* genes found in Sea bream

The deduced amino acid sequence of *sTnT1sb* and *sTnT2sb* reveals conserved primary structure when compared to other vertebrate groups. The central and C-terminal regions encoded by *sTnT1sb* and *sTnT2sb* are highly conserved and contain the tropomyosin and troponin C and I binding motifs (Perry, 1998, Hinkle and Tobacman, 2003, Jin et al., 2000). In common with what has been observed in other vertebrates the N-terminal segment is highly variable and has been proposed to be involved in tuning the overall conformation and function of the protein (Ogut and Jin, 1996, Hinkle and Tobacman, 2003). In common with zebrafish (Hsiao et al., 2003), sea bream possess an intronless *TnT* gene which seems to be a characteristic exclusive to teleosts (Fig. 5.5). The N-terminal region of sea bream *iTnT* protein is most divergent from other vertebrate TnTs but the last two thirds of the molecule is well conserved and contains the motifs for interaction with tropomyosin, troponin I and troponin C (Perry, 1998; Jin et al., 2000; Hinkle and Tobacman, 2003).

The predicted molecular weights of sTnT1sb and sTnT2sb are 32kDa and 28.4kDa respectively, and are similar to the predicted size of other vertebrate TnT proteins (Perry, 1998, Jin et al., 2000). The differences in size between the predicted sea bream sTnT proteins arise because of the different length of the N-terminal region. The longer N-terminal regions in the two sTnT1sb isoforms are rich in negatively charged residues and this is reflected by their lower pI of 5.72 and 5.42. The same is true of iTnTsb in which the majority of the additional 27 amino acids in the N-terminal region are glutamic acid (Fig. 5.2). It remains to be established if the differences between the predicted proteins arising from *sTnT1sb* and *sTnT2sb* lead to functional differences.

Northern blot (Fig. 5.3) and RT-PCR analysis of adult sea bream tissue (Fig. 5.9) indicates that the tissue distribution of *sTnT* in sea bream also appears to be conserved when compared with other vertebrate group. Transcripts from both *sTnT1sb* and *sbTnT2sb* are specific for striated skeletal red muscle and in the Atlantic salmon (*Salmo salar*), two immunoreactive sTnT proteins have been identified in red muscle, although their relationship to the forms identified in sea bream remain to be established (Waddleton et al., 1999). The relative abundance of the two sea bream transcripts is significantly different and the longer, acidic form of *sTnT1* in adult red muscle is of very low abundance compared to *sTnT2*. RT-PCR analysis of *iTnTsb* shows that it is expressed predominantly in adult white muscle (Fig. 5.9). The zebrafish intronless *TnT* gene has been classified as a slow *TnT* (Hsiao et al., 2003). The classification in the zebrafish of *iTnT* was based on *in situ* hybridisation analysis of zebrafish embryos and larvae and phylogenetic analysis which did not include teleost *sTnT*. Based upon the more extensive analysis of *sTnT* in the present study we propose that there is no compelling evidence supporting the classification of the intronless teleost *TnT* as an *sTnT* and that it should be classified as an independent group.

The present study reports for the first time in vertebrates the presence of two *sTnT* genes and an intronless *TnT* gene. Despite extensive studies in tetrapods, only splice variants, which give rise to different protein isoforms have previously been reported (Wang and Jin, 1997; Bucher et al., 1999; Briggs and Schachat, 1993; Jin et al., 1998; Nakada et al., 2002; Farza et

al., 1998; Yonemura et al., 2000; Yonemura et al., 2002; Gahlmann et al., 1987; Samson et al., 1994). Extensive database searches of the human genome in the present study failed to identify additional genes for *sTnT*. In contrast, similar searches of the *Fugu* genomic database and EST databases of medaka and zebrafish led to the identification of orthologues of both *sTnT1sb* and *sTnT2sb*.

The maximum-parsimony phylogenetic analysis (Swofford et al., 2001) performed in the present study clusters the *sTnT1sb* sequence groups with tetrapod *sTnT*. Several fish *sTnT* are also placed in this clade including a zebrafish low molecular weight *sTnT* isoform and an *sTnT* from *Ictalurus punctatus* (Fig. 5.5). A separate *sTnT* group occurs which is composed only of teleostei *sTnT2* proteins, suggesting that these cDNAs constitute a new family of *sTnT* genes different from *sTnT1sb* and the higher vertebrate *sTnT* genes previously described. The new *sTnT2* family appears to be specific to the fish lineage and may have arisen as a consequence of a teleost specific genome duplication proposed to have occurred 300 to 450 million years (My) ago (Taylor et al., 2001). Notably, the teleosts *iTnT* sequences used in the phylogenetic analysis group together and apart from any other vertebrate *TnT*, constituting a further new teleost specific *TnT* group (Fig. 5.5). Intronless *TnT* genes have not been described in any non-teleost species. Their presence in sea bream, *Fugu* and zebrafish suggests that integration into the genome of a reverse transcribed *TnT* mRNA (possibly encoding a larval isoform given the acidic nature of the *iTnT* proteins) may have occurred after the separation of the tetrapod and teleost lineages. To better characterise the different *TnT* forms in fish and establish when and how they arose in the euteleost lineage requires further information about teleost *TnTs*. Remarkably, when compared to the halibut, in the sea bream no cDNA that corresponded to a product of the sea bream Af*TnT* (Chapter 3) was found whereas in the halibut no cDNA that could represent an orthologue of the sea bream *sTnT1* gene was cloned. Furthermore, the phylogenetic trees obtained (Fig. 5.5; Chapter 3) clearly segregated those genes from each other. Moreover, at the protein level the Af*TnT* and *sTnT1sb* present striking differences with the former giving rise to fast-like *TnT* proteins and the latter yielding

typical vertebrate sTnT proteins. These evidences show that in the halibut the AfTnT gene and in the sea bream the sTnT1 gene might constitute species-specific red muscle genes and strongly suggest that in teleosts red muscle development and function might present species-specific adaptations aimed to respond to specific physiological and functional demands.

In silico comparison of the sea bream *sTnT1sb* and *sTnT2sb* genes with the *Fugu* genome revealed the putative genomic organisation is similar to higher vertebrates. In particular, the putative genomic organisation of sea bream and *Fugu sTnT2* derived by Spidey analysis (www.ncbi.nlm.nih.gov) indicates it is composed of 12 exons and 11 introns and spans ~2 Kb (Fig. 5.7). This gene organisation is similar to the mouse and human *sTnT* gene, which is composed of 14 exons (Barton et al., 1999, Huang et al., 1999).

Spidey analysis against the *Fugu* mayffold M000253 matched the entire sea bream intronless *TnT* to a putative single exon gene. However, it was only possible to compare the coding region of this intronless sea bream *TnT* with the *Fugu* genomic sequence. The likelihood that the intronless *TnT* gene probably arose in the teleost genome by reverse transcription of an ancient *troponin T* mRNA and the finding that it is still expressed in a muscle specific manner during development of zebrafish (Hsiao et al., 2003) and sea bream (present study) and in adult muscle of sea bream (Fig. 5.9A and D) is quite remarkable since these intronless genes commonly degenerate to processed pseudogenes (Harrison et al., 2002). It remains to be established if the teleost *iTnT* mRNA is also translated to a functional protein but given the sequence conservation it seems highly likely. The selective evolutionary pressures that might explain the survival of this gene in the teleost genomes are unknown. It will be of interest to establish if the additional forms of *sTnT* and the *iTnT* genes in fish are related to the additional complexity of fish muscle, which is composed of striated red muscle, pink muscle and white muscle.

5.4.3 Developmental expression from embryonic stages to adult of *fTnTsb*

In common with mouse (Wang et al., 2001) and zebrafish (Hsiao et al., 2003), the expression of *fTnT* in the sea bream occurs only after the most anterior somites are formed (36hpf, Fig. 5.8). This correlates well with the fact that in the zebrafish, and probably in all teleosts, the migration of the adaxial cells (progenitors of the red muscle layer) (Devoto et al., 1996) from their position immediately adjacent to the notochord to the surface of the developing somite constitutes the signal for white muscle differentiation (Henry and Amacher, 2004). The *efTnTsb* isoform is dominant in late embryonic stages but is downregulated immediately after hatching and is substituted by *LfTnTsb* that becomes the most abundant isoform in larvae and early juvenile stages, while in adult white muscle *afTnTsb* is the most abundant isoform (Fig. 5.8). Studies of muscle protein in juvenile flounder (Yamano et al., 1991a), sole (*Solea solea*) and turbot (*Scophthalmus maximus*) (Focant et al., 2003) and halibut (Chapter 3), reveal that in common with sea bream two TnT isoforms (molecular weight range 34-32.5 kDa) exist in white muscle. In juvenile post-metamorphic sole the lower molecular weight TnT isoform is predominant whereas in adult white muscle both isoforms are present in similar amounts (Focant et al., 2003) which is reminiscent of the pattern of transcript expression in sea bream (Fig. 5.8). The pattern of *fTnT* isoform expression in flounder (Yamano et al., 1991a) and halibut (Chapter 3) is somewhat different from sea bream and repression of the higher molecular weight embryonic form only occurs during the larval to juvenile metamorphosis. Differences in *fTnT* expression in fish probably reflect differences in their developmental ontogeny resulting from the different functional and physiological constraints that pelagic and flatfish face. Remarkably, the sea bream *fTnT* isoform expression profile bears more similarities to isoform ontogeny in chicken breast muscle (Yao et al., 1992) where there is a gradual transition from an embryonic to chick *fTnT* isoform, immediately after hatching, and a subsequent switch during maturation to an adult type *fTnT* isoform. The change in *fTnT* isoforms in chickens is predicted, as also occurs in sea bream, to result in a change in the pI of the expressed proteins from acidic to basic (Yao et al., 1992). The shift from acidic to basic *fTnT* proteins in fast skeletal vertebrate muscle has been related to changes in pH and Ca^{2+} sensitivity necessary for correct

contraction and is directly related to the hypervariable N-terminal region of *fTnT* isoforms (Wang and Jin, 1997; Jin et al., 2000b; MacFarland et al., 2002; Nosek et al., 2004). The presence of an acidic exon in chicken pectoralis *fTnT*'s is responsible for its higher tolerance to pH changes and for the decrease in both the interaction and assembly of *fTnT* with Troponin I (TnI) and Tropomyosin (Tm) (Jin et al., 2000b).

The change in *fTnT* isoforms during ontogeny in vertebrates appears to be important for functional adaptability (Nosek et al., 2004) and the impact of different *fTnT* isoforms on muscle function in fish remains to be established but is probably associated with changes in the hydrodynamic environment as well as different locomotive strategies, respiration and intracellular environments (Osse, 1990; Johnston, 1994; Koumans and Akster, 1995; Johnston et al., 1997; Patruno et al., 1998; Osse and van den Boogaart, 1999; Watabe, 1999; Verhagen, 2004). In fact, until the gills are fully functional, which only occurs at the end of the larval stage, most gas exchanges occurs through the skin and muscle that constitute the major respiratory surface of teleosts fish larvae. In fact muscle tissue in teleost embryos and larvae has different metabolic regimes than adult muscle and consequently a different cellular environment. During the larval stage white muscle is mainly aerobic and rich in mitochondria which contrasts to the anaerobic adult white muscle (Johnston, 1994; Johnston et al., 1997; Watabe, 1999). The *fTnT* isoform switching in sea bream appears to accompany the transition from larvae to juvenile and probably allows white-muscle to adapt to the changing functional and physiological demands during development.

5.4.4 Developmental expression of the sea bream *sTnT*

Studies during sea bream ontogeny by RT-PCR reveal that *sTnT2sb* and *iTnTsb* encode early appearing transcripts whereas *sTnT1sb* is only expressed after hatching and thereafter at higher levels (Fig. 5.9). However, after 75 dph *sTnT1* expression decreases substantially and in

adult red muscle only low levels of the higher molecular weight isoform is expressed, and *sTnT2sb* becomes the predominant *sTnT* gene being expressed in this tissue.

In common with the expression pattern of the intronless zebrafish *sTnT* gene (Hsiao et al., 2003), the sea bream, *sTnT2sb* and *iTnTsb* genes are expressed at 90% epiboly (18 hpf, Fig. 5.9). The precocious expression of *sTnT* genes in relation to the onset of somitogenesis may be linked to assembly of the first muscle fibres. Indeed, in zebrafish correct *cTnT* expression is essential to normal sarcomere assembly and contractility (Sehnert et al., 2002) of the heart and two different mutations in the zebrafish *cTnT* gene are responsible for *silent heart* mutant embryos (Sehnert et al., 2002). Similarly, in *Drosophila* over-expression of *TnT* in indirect flight muscles of transgenic flies leads to severe disruption of thin-filament assembly, accompanied by a decrease in expression of all other thin-filament proteins and impairment of flight in transgenic flies (Marco-Ferreres et al., 2005). The correct stoichiometric relationship between all the thin-filament proteins seems to be important for correct assembly of the muscle sarcomere (Sehnert et al., 2002; Marco-Ferreres et al., 2005).

At hatch the muscle of teleost fish is composed of two principal fibre types, a muscle layer derived from mesenchymal tissue adjacent to the notochord and a superficial monolayer derived from the mesenchymal tissue adaxial cell population which migrates from a position lateral to the notochord to the surface of the lateral body of the fish embryo (Devoto et al., 1996; Blagden et al., 1997; Cortés et al., 2003; Mascarello et al., 1995). Considerable differences in the ontogeny of muscle development exist between teleost fish. For example, in zebrafish the first muscle cells derived from the adaxial layer start to commit at late gastrula (Devoto et al., 1996) and a characteristic marker of differentiating red muscle tissue, slow myosin heavy chain (sMHC) mRNA and protein, is present in the superficial muscle monolayer (Blagden et al., 1997; Hsiao et al., 2003). In contrast, in sea bream and *Poecilia reticulata* sMHC is only detectable after hatching, well after the onset of somitogenesis (Devoto et al., 1996; Hsiao et al., 2003; Mascarello et al., 1995; Veggetti et al., 1993).

Sea bream *sTnT1sb* expression is only evident at 4dph and its subsequent increase in expression accompanies the increase in muscle mass and maturation of slow muscle fibres in sea bream larvae (Mascarello et al., 1995). The expression of *sTnT1sb* during larval development increases linearly up until 75 dph and decreases sharply thereafter (Fig. 5.9) at the initiation of the juvenile stage when presumably slow muscle tissue has formed and is entering a phase of hyperplastic growth (Mascarello et al., 1995). The pattern of expression of *sTnT1sb* during larval development, and sequence, genomic and phylogenetic analysis all support its classification as the orthologue of tetrapod *sTnT*. The apparently discordant observation that *sTnT1sb* is almost absent from adult red muscle and that *sTnT2sb* is the predominant form serves to underline the differences that exist between fish and tetrapod muscle development.

The switch from a predominantly larger acidic *sTnT1sb* form in larvae to a small basic form in adult red muscle (*sTnT2sb*) is intriguing. This change is reminiscent of the *cTnT* and *fTnT* isoform switch in cardiac muscle in tetrapods, and has been associated with functional changes in the protein and differences in contractibility and intracellular pH between fetal and adult heart muscle (Tobacman and Lee, 1987; MacFarland et al., 2002; Nosek et al., 2004). However, while in tetrapods the large acidic-to-small basic isoform switch in *cTnT* and *fTnT* is achieved through alternative splicing, in sea bream *sTnT* it is achieved by differential expression of two different genes. The functional significance of the acid-to-basic *sTnT* switch in sea bream remains to be established. In any event there is a clear difference in expression of *sTnT* genes, and probably red muscle development, between fish and tetrapods, since no clear developmentally regulated isoform switching is observed in tetrapod red muscle development (Wang and Jin, 1997; Bucher et al., 1999; Briggs and Schachat, 1993; Jin et al., 1998; Nakada et al., 2002; Farza et al., 1998; Yonemura et al., 2000; Yonemura et al., 2002; Gahlmann et al., 1987; Samson et al., 1994). Furthermore, there appears to be a coordinate expression pattern of *sTnT1sb* and *sTnT2sb* during developmental ontogeny of sea bream and the peak of *sTnT2sb* expression occurs before the peak in *sTnT1sb* expression (Fig. 5.9). It would appear in sea bream that the differential expression of the two *sTnT* genes and the isoforms of *sTnT1* may generate the diversity and account for the changing

structural and mechanical needs during development of red muscle thin filaments. In contrast, sTnT diversity in tetrapod red muscle occurs by differential expression of sTnT isoforms from a single gene (Perry, 1998). The reason for this difference is unknown but it could be a reflection of the additional complexity of fish muscles which has a layer of pink muscle which is absent from tetrapod muscle (Koumans and Akster, 1995). Moreover, the secondary myogenesis in fish, that starts at hatching, unlike tetrapods does not occur by hypertrophy of prenatal muscle fibres and hyperplasia continuous to be the most prominent muscle growth process taking place in fish muscle (Koumans and Akster, 1995, Mascarello et al., 1995). Only in late adult stages well after sexual maturation, does hypertrophy become the dominant muscle growth process (Koumans and Akster, 1995, Mascarello et al., 1995). The relative role of *iTnT*, *sTnT1* and *sTnT2* genes and their protein products in fish muscle growth still remains to be established. The results in sea bream may be indicative of subfunctionalization of the duplicate *sTnT* genes (Van de Peer et al., 2001, Lynch and Force, 2000, Force et al., 1999) and the *TnTs* in fish may be a good model system in which to investigate this process.

5.4.5 Sea bream *TnT* genes TH responsiveness

THs have been shown to play a role in vertebrate muscle development and muscle gene expression. In hyperthyroid newborn rats the transition of fast myosin heavy chains (MHC) from embryonic and perinatal to adult isoforms is accelerated and the opposite occurs in hypothyroid newborn rat. In general, in adult rats hypothyroidism increases slow MHC expression in skeletal and cardiac muscle and hyperthyroidism induces an opposite effect (Adams et al., 1999; Soukup and Jirmanova, 2000). In mammals, the responsiveness of muscle to TH is variable and slow muscle is more sensitive than fast muscle. Moreover, in rats THs are an important factor in MHC isoform expression in slow muscle (Soukup and Jirmanova, 2000) and normal TH levels are necessary for skeletal muscle phenotype (Vadaszova et al., 2004).

Fish muscle has also been shown to be responsive to THs and treatment changes the histological properties of developing zebrafish larvae muscle (Liu and Chan, 2002) and locomotion in *E. coioides* larvae (de Jesus et al., 1998). More specifically, in sea bream juveniles T4, but not T3, treatment increases myosin light chain 2 (MLC2) expression (Moutou et al., 2001). Moreover, in flounder, a pleuronectiform, THs drive the pelagic to benthic metamorphosis (Miwa and Inui, 1987a; Miwa et al., 1988) and associated muscle protein changes, which include a switch in MLC and *TnT* isoform expression (Yamano et al., 1991a; Yamano et al., 1994b). In particular, T3 treatment represses the flounder 41.5 kDa embryonic/larval *fTnT* isoform and induces precocious expression of a 34 kDa adult *fTnT* isoform whereas thiourea-induced hypothyroidism prevents these changes (Yamano et al., 1991a). Neither T3- or methimazol-treatment had any effect on *efTnT* expression in sea bream which contrasts to flounder, where T3-treatment accelerates *fTnT* pre- to post-metamorphic isoform changes and in which thiourea-induced hypothyroidism in pre-metamorphic larvae prevents metamorphosis and maintains embryonic/larval *fTnT* expression even though in control animals this expression had already terminated (Yamano et al., 1991a). Importantly, in sea bream T3 treatment did not induce the adult pattern of *fTnT* isoform expression where *afTnTsb* is predominant. Moreover, the change in the ratio between *afTnTsb:LfTnTsb* to an adult pattern only occurred after 31 days of T3-treatment and at the same time as in control animals suggesting that in the sea bream, *fTnT* splice variant expression during development is mediated by factors other than TH and seems to indicate that THs might not be involved at all in the developmental regulation of *fTnT* isoforms in sea bream. This is in striking contrast to the flounder (Yamano et al., 1991a) and halibut (Chapter 3). Although THs probably play a role in sea bream larvae/juvenile developmental switch, the sea bream belongs to an order that persists as a bilaterally symmetric fish throughout its life cycle and does not undergo a dramatic metamorphosis like flatfish. This fact taken together with the observation that in sea bream *efTnT* is downregulated immediately after hatching and that the differences found in the responsiveness of *fTnT* to T3 treatment between the sea bream and the flounder (Yamano et al., 1991a) and also *fTnT* isoform expression profile at halibut metamorphosis (Chapter 3), clearly

reinforces the notion that larval muscle development in teleosts may be species specific and associated with functional demands.

As has been discussed above and in contrast to what occurs in tetrapods, sea bream *sTnT* genes have a coordinated expression pattern during sea bream development (Gahlmann et al., 1987; Briggs and Schachat, 1993; Samson et al., 1994; Wang and Jin, 1997; Farza et al., 1998; Jin et al., 1998a; Perry, 1998; Barton et al., 1999; Bucher et al., 1999; Huang et al., 1999d; Jin et al., 2000b; Yonemura et al., 2000; Nakada et al., 2002; Wang et al., 2002; Yonemura et al., 2002). Gene expression of *sTnT1sb* (Fig. 5.12) and its splice variants in sea bream, but not *sTnT2sb* and *iTnT* (Fig. 5.11), are affected by both T3- and methimazol-treatment. That both T3 and the antagonist methimazol promote a *sTnT1sb* expression profile characteristic of adult red muscle may be explained by the lack of anti-thyroidogenic action of methimazol in the present study. The results obtained for *sTnT1sb* expression and the effect on the *sTnT1sb* isoform profile argue that T3 might be an important factor for sea bream, and probably other teleost, slow muscle final differentiation. The results from the present study indicate that *sTnT1sb* in sea bream is most sensitive to T3 and may suggest that in common with rats (Everts, 1996; Soukup and Jirmanova, 2000), teleost slow muscle is more TH sensitive than white muscle.

In summary, the expression of *fTnT* during the larval/juvenile transition in sea bream does not seem to be regulated by THs, which contrasts to the TH responsiveness found in flounder (Yamano et al., 1991a). In contrast, other teleost *TnT* genes, *sTnT1sb* seems to be under the control of THs during the larval/juvenile transition, although *sTnT2* and *iTnT* (Hsiao et al., 2003) less sensitive and unresponsive. It seems likely that despite the lower isoform heterogeneity of sarcomeric proteins and a lower number of specialised muscles in teleosts, in common with tetrapods, they have diverse and complex muscle development programs regulated by as yet unidentified genetic and molecular mechanisms.

CHAPTER 6

COORDINATION OF DEIODINASE AND

THYROID HORMONE RECEPTOR

EXPRESSION DURING THE LARVAL TO

JUVENILE TRANSITION IN SEA BREAM

6.1 Introduction

Thyroid hormones (TH) are amongst the most prominent factors controlling vertebrate development and homeostasis in the adult animal. In all vertebrates, TH are produced in thyroid follicles that in tetrapods are organised in a highly vascularised thyroid gland whereas in most teleosts assumes a more simple organisation as the follicles are scattered in the lower jaw around the aorta. Thyroid follicles produce mainly 5',3',5,3-tetraiodothyronine (T4) but the most active form of thyroid hormone is 3',5,3-triiodothyronine (T3) that is most able to interact with thyroid receptors (TR) present in the nucleus and transactivate or repress gene transcription (Zhang and Lazar, 2000; Jho et al., 2001; Power et al., 2001; Harvey and Williams, 2002; Bassett et al., 2003; Eckey et al., 2003; Buchholz et al., 2004; Jho et al., 2005; Kim et al., 2005; Tata, 2006; Yen et al., 2006). Two main types of nuclear TR are found in vertebrates designated TR α and TR β . These are encoded by separated genes, each of which also produces several alternatively spliced isoforms in all vertebrates (Yaoita et al., 1990; Wood et al., 1994; Llewellyn et al., 1998; Williams, 2000; Zhang and Lazar, 2000; Gauthier et al., 2001; Marchand et al., 2001; Nowell et al., 2001; Yen, 2001; Yen et al., 2006) that according to the nuclear specific context of co-factors and promoter organisation of the TH-target genes leads to either gene transactivation or repression .

In vertebrates, while all T4 is produced exclusively by the thyroid follicles most of serum T3 is produced in peripheral organs by deiodinases. Whereas in vertebrates TRs are the major mediators of TH action at a gene level, cell specific responsiveness to THs is also determined by selenoproteins known as iodothyronine deiodinases that act as cellular gatekeepers that give the hormone access to its nuclear targets (Darras et al., 1998; Darras et al., 2000; Kohrle, 2000; Bianco et al., 2002; Bianco and Larsen, 2005; Brown, 2005; Galton, 2005; Orozco and Valverde-R, 2005). Deiodinases can determine which cells respond or not to THs by activating the pro-hormone T4 to the hormone T3 through outer ring deiodination (ORD), or by inactivating, T4 and T3 to biological inactive metabolites (rT3 and T2 respectively) through

inner ring deiodination (IRD) (Bianco et al., 2002; Bianco and Larsen, 2005; Kuiper et al., 2005). Vertebrate deiodinases need a reducing co-factor for appropriate enzymatic activity and contain in their active site a selenocysteine (Sec) residue that is fundamental for removal of iodine from TH (Buettner et al., 2000; Kohrle, 2000; Bianco et al., 2002; Kuiper et al., 2002; Kuiper et al., 2003; Kuiper et al., 2005). The Sec residue is coded by the codon UGA that in normal circumstances would end translation, but that in the presence of a SElenoCysteine Insertion Sequence (SECIS) secondary structure, localised in the 3'UTR of the deiodinase mRNA, leads to insertion of a Sec residue in the growing deiodinase peptide (Kollmus et al., 1996; Buettner et al., 1998; Fagegaltier et al., 2000; Lambert et al., 2002). As described in chapter 4, in all vertebrates species studied 3 different deiodinase genes have been found (St Germain et al., 1994; Croteau et al., 1995; Croteau et al., 1996; Valverde et al., 1997; Davey et al., 1999; Hernandez et al., 1999; Sanders et al., 1999; Leonard et al., 2000; Orozco et al., 2002; Orozco et al., 2003; Sutija et al., 2003; Klaren et al., 2005; Bres et al., 2006): type 1 deiodinase (D1) an ORD that removes the 5'-iodine of rT3 (Visser, 1994; Mol, 1998; Darras et al., 1999; Bianco et al., 2002; Kuiper et al., 2005), type 2 deiodinase (D2) an exclusive ORD deiodinase which converts T4 to T3 (Mol, 1998; Van der Geyten et al., 2001a; Bianco et al., 2002; Bianco and Larsen, 2005; Kuiper et al., 2005) and type 3 deiodinase (D3) which is responsible for the inactivation of TH by IRD (Mol, 1998; Van der Geyten et al., 2001a; Bianco et al., 2002; Bianco and Larsen, 2005; Kuiper et al., 2005).

In vertebrates, with the exception of chicken where it is involved in TH-driven developmental changes in most tissues (Van der Geyten et al., 1997; Van der Geyten et al., 2001a; Van der Geyten et al., 2002), D1 is less important whilst D3 and D2 play a key role during development (Bianco et al., 2002; Brown, 2005; Galton, 2005; Orozco and Valverde-R, 2005). D3 expression and activity is fundamental for cellular responsiveness during development, and in rat eye development although TRs are necessary for retinal proliferation it is D3 that determines which cells respond (Forrest et al., 2002). During development of the rat cochlea correct timing in expression and activity of D2 assumes a crucial role where it is the

most important factor that mediates T3-action in postnatal development of hearing (Campos-Barros et al., 2000; Forrest et al., 2002; Ng et al., 2004). Similarly during brain development in rat there is a strong decrease in brain D3 expression and activity as birth approaches and a sharp increase in activity of both D1 and D2 during the same developmental period (Bates et al., 1999; Galton, 2005). In common with mammals but in contrast to chicken, D1 has little function in anuran metamorphosis while D2 and D3 are the deiodinases that coordinate TH action during this developmental period (Becker et al., 1997; Huang et al., 1999b; Shintani et al., 2002; Brown, 2005). Transgenic *X. laevis* that overexpress D3 develop normally up until early tadpoles but do not undergo a normal metamorphosis and fail to achieve the adult stage (Huang et al., 1999b). In general, during vertebrate development D3 protects the tissues against T3 until the precise moment it is required when D2 levels rise locally and produce intracellular T3 that triggers the appropriate morphological transformation.

Flatfish have been shown to undergo a dramatic, TH-promoted and TR-mediated, metamorphosis in that the symmetric larval becomes an asymmetric juvenile (Miwa and Inui, 1987a; Miwa et al., 1988; Yamano et al., 1991a; Yamano et al., 1994a; Yamano and Inui, 1995; Yamano and Miwa, 1998; Llewellyn et al., 1999; Power et al., 2001; Marchand et al., 2004; Safi et al., 2004). However the majority of teleosts are symmetric animals that after hatching also go through a larval phase which precedes the juvenile adult-like stage, thus implying a metamorphic-like developmental process (Balon, 1981; Balon, 1984). Although some information exists about T3 effects and TR expression during development of symmetrical teleosts (Llewellyn et al., 1998; Liu et al., 2000; Marchand et al., 2001; Nowell et al., 2001; Jones et al., 2002; Liu and Chan, 2002) little is known about their relationship with deiodinase expression during the round fish larval to juvenile metamorphosis. In the present study deiodinase genes were cloned from the sea bream (*Sparus aurata*) and their expression during sea bream embryonic, larval and juvenile development analysed in conjunction with RT-PCR of TR α (Sweeney, unpublished results) and TR β (Nowell et al., 2001).

6.2 Material and Methods

6.2.1 Isolation of sea bream D1 and D3 cDNAs

A sea bream larval cDNA library made from sea bream larvae from 1 day post-hatch (dph) up until 123 dph juveniles (Nowell et al., 2000) was plated at a density of 50,000 plaque forming units (pfu) per plate to give a total of 1,000,000 clones. Nitrocellulose lifts were performed and the complete cDNA clone of *Sparus aurata* D3 (Sweeney, unpublished results) labelled with ³²P-dCTP was used for screening. Nitrocellulose membranes were hybridised overnight with labelled probe at low stringency (60°C, 6xSSC, 5x Denhardt's solution, 100µg/ml tRNA, 0.1%SDS). The membranes were subsequently washed twice for 30 minutes at room temperature (1xSSC and 0.1%SDS) followed by two washes of 30 minutes at low stringency (55°C in 1xSSC and 0.1%SDS). The membranes were exposed overnight at -80°C to Biomax MS film (Kodak) and positive plaques selected for a second round of screening performed as described above. Isolated positive clones were selected and automatically excised into pBluescript SK+/- (Stratagene). DNA was purified using the Promega DNA Miniprep Wizard kit (accordingly to the manufacturer's instructions) and cDNA clones sequenced to give 3-fold coverage using BigDye Version 3 (Perkin-Elmer, UK) chemistry and an ABI 3700 sequencer. Identification of the selected clones was performed *in silico* using tBLASTx (Altschul et al., 1990) against the GenBank database in order to establish the most probable identity of the sea bream cDNA sequences. Further characterisation of the putative sea bream deiodinase cDNA clones was performed using SECISearch 2.19 software (Kryukov et al., 2003) in order to identify the presence of SECIS elements in the 3'UTR.

6.2.2 RT-PCR cloning of sea bream D2

Despite extensive screening it was not possible to isolate a sea bream D2 cDNA and so an RT-PCR strategy with degenerate primers was used instead. Multiple nucleotide sequence alignment (Clustal X, (Thompson et al., 1997) of cDNA sequences retrieved from GenBank was

used to design degenerate primers to conserved regions of vertebrate D2 sequences. The following primers were used: F1, CGNTCCATMTGGAAAYAGYTT; F2, TTYGGYTCGGCMACCTGACC; F3, CAYCCYTCTGAYGGNTGGGT; R1, GGTCAGGTKGCCGANCCRAA; R2, ACCCAWCCRTCAGANGGRTG; R3, GCATTGTTRTCCATRCARTC; R4, CCGTARSTSWKYTCCAGCCA with the following primer combinations: F1/R1, F1/R2, F1/R3, F1/R4, F2/R2, F2/R3, F2/R4, F3/R3 and F3/R4. All PCR reactions were performed using Sigma 2xReadyMix, 1.5 mM of MgCl₂ and 1 mM of each primer in a Techne TC-512 thermocycler using the following program: 5 minutes at 95°C followed by 35 cycles of 45 seconds at 95°C, 1 minute and 15 seconds at 55°C and 45 seconds at 72°C and a final extension time of 5 minutes at 72°C. All PCR reactions were performed using as template ~20ng of cDNA from adult liver and kidney samples (see below).

6.2.3 Phylogenetic analysis

Maximum-parsimony phylogenetic analysis with 1000 bootstraps (Fitch, 1971) was performed using PAUP 4.0b software (Swofford et al., 2001) in order to fully characterise the putative sea bream deiodinases DNA sequences isolated. The following vertebrate deiodinase sequences were retrieved from the GenBank or SwissProt databases: *Homo sapiens* D1, BC107170, hsD1; *H. sapiens* D2, AAD45494, hsD2; *H. sapiens* D3, BC017717, hsD3; *Mus musculus* D1, NM_007860; *M. musculus* D2, AAD11422, mmD2; *M. musculus* D3, NM_172129, mmD3; *Rattus norvegicus* D2, P70551, rnD2; *R. norvegicus* D3, P49897, rnD3; *Gallus gallus* D1, Y11110, ggD1; *G. gallus* D2, AAD33251, ggD2; *G. gallus* D3, Y11273, ggD3; *Xenopus laevis* D1, DQ098656, xlD1; *X. laevis* D2, AAK40121, xlD2; *X. laevis* D3, BC106400, xlD3; *Rana catesbeiana* D2, AAC42231, rcD2; *Danio rerio* (zebrafish) D1, AAO65268, zfD1; *D. rerio* D2, AAO065269, zfD2; *Fundulus heteroclitus* D1, AAO31952, fhD1; *F. heteroclitus* D2, AA262449, fhD2; *Scophthalmus maximus* D2, AAQ05027, smD2; *Oncorhynchus mykiss* D2, AAL25715, omD2; *Oreochromis niloticus* D1, CAA71995, onD1; *O. niloticus* D3, CAA71997, onD3; *Sparus aurata* D1, AJ619717, saD1 and previously isolated halibut cDNA sequences for D1 (hhD1- DQ856302), D2 (hhD2,

DQ856304) and D3 (hhD3, DQ856303). The deduced sea bream D1 (saD1, DQ888894), D2 (saD2, DQ888895) and D3 (saD3, DQ888896) protein sequences, together with the previous vertebrate deiodinases, were submitted to phylogenetic analysis using the ascidian *Halocynthia roretzi* iodothyronine deiodinase (hrDio, AAR25890) protein sequence as an outgroup. Before computational calculation of the maximum-parsimony tree all the vertebrate cDNA sequences were aligned using the Clustal X software (Thompson et al., 1997).

6.2.4 Animal Sampling

Sea bream eggs were collected at blastula (6 hours post-fertilization, hpf), 30% epiboly (12 hpf), 90% epiboly (18hpf), 2 somite stage (24 hpf), most posterior somite formation (36 hpf) and near hatching (43 hpf). Larvae were collected at hatching (1day post hatch – dph) and at 4, 15, 24, 46, 64 and 75 dph and 89 dph juveniles were also collected. The small size of the sea bream embryos and larvae meant that three different pools of several individuals (50-100mg) per developmental time were collected until 46 dph and thereafter individual fish were collected and analysed. Larvae and juveniles were anaesthetized in MS-222 (125mg/l, Sigma-Aldrich, Madrid, Spain) before being snap frozen in liquid Nitrogen and stored at -80°C until use. Classification of sea bream stages was based upon previous studies (Polo et al., 1991; Mascarello et al., 1995; Rowlerson et al., 1995; Patruno et al., 1998; Loy et al., 1999; Parra and Yufera, 2001). All animals were sacrificed in accordance with European legislation for Animal welfare.

6.2.5 Animal treatments

The sea bream were treated with T3 and methimazol as described in Chapter 5. The samples used for analysis of sea bream deiodinases and saTR α and saTR β expression were treated as described in Chapter 5.

6.2.6 Total RNA extraction

Pooled embryonic and larval sea bream samples as well as individual animals of late larval and juvenile stages were used to extract total RNA using Tri reagent (Sigma-Aldrich, Madrid, Spain). Three independent samples were analysed for each developmental stage. The T3 and methimazol treated animal samples were also extracted, in triplicate, using Tri reagent (Sigma-Aldrich) according to the manufacturer's instructions.

6.2.7 First strand cDNA synthesis

Before cDNA synthesis, total RNA of all samples was treated to prevent genomic DNA contamination using a DNA free kit (Ambion, Austin, TX, USA) accordingly to the manufacturer instructions. First strand cDNA synthesis (20 µl total reaction volume) was carried out with 0.5µg total RNA of the different sea bream embryonic, larval and juvenile stages. Synthesis reactions were carried out in 0.05M Tris-HCl, pH8.3, 0.075M KCl, 3mM MgCl₂, 0.01M DTT, 1mM dNTP, 5pmol/µl random hexamer primers, 4U of RNase inhibitor (Promega, Madison, WI, USA) and 10U of Superscript II reverse transcriptase (Invitrogen, Carlsbad, CA, USA). Each first stand cDNA reaction mix was incubated in a Techne TC-512 thermocycler (Staffordshire, UK) for 10 minutes at 25°C followed by 50 minutes at 42°C and synthesis was terminated by heating for 2 minutes at 70°C. cDNA was prepared individually for each sea bream developmental sample and adult tissue.

6.2.8 Developmental expression of sea bream D1, D2 and D3 – semi-quantitative RT-PCR analysis

The developmental expression of sea bream D1, D2 and D3 was analysed by semi quantitative RT-PCR during embryonic, larval and early juveniles stages. Experiments were conducted with sea bream D1, D2, D3 and 18s rRNA to determine optimal cDNA concentration

and RT-PCR cycle number to ensure that amplification occurred in the logarithmic phase of the reaction and could be measured by densitometry. The internal standard selected to normalise the amount of cDNA used in the reaction was the expression of 18s ribosomal RNA (rRNA).

Amplification reactions for sea bream D1, D2 and D3 were carried out in a 25 μ l reaction volume containing ~20 ng of cDNA for each of the samples described and 1.5 mM MgCl₂, 0.1 mM dNTP's, 1 pmol/ μ l of sea bream deiodinase specific forward and reverse primer (Table 6.1) and 0.6U *Taq* polymerase (Sigma-Aldrich, Madrid, Spain). The primers were designed for non-homologous regions of sea bream D1, D2 and D3 deiodinases after Clustal X (Thompson et al., 1997) multiple nucleotide sequence alignment.

Table 6.1. Sea bream deiodinase primers sequences used for developmental analysis of expression

Gene	Forward Primer	Reverse Primer
saD1	CGCCTGTGGTCACCATGAAGG	CCAAGATCTGTGCTGCACAC
saD2	CTTCATCAGCCACCTGCGAGC	CATACAGTCAGCCACCAGCTG
saD3	TGGTCCAGGAGCGGAGACAG	AGCATCAGCTGAGCGGCTC

The PCR reactions for saD1 were performed in an Techne TC-512 thermocycler (Staffordshire, UK), using the following cycle; 1 minute at 95°C followed by 37 cycles of 30 seconds at 95°C, 1 minute at 56°C and 30 seconds at 72°C, followed by a final step of 1 minute at 72°C. In the case of saD2 and saD3 the same thermocycle program was used but with, respectively, 35 or 36 cycles. Negative reactions without sample cDNA were also performed.

The normalising gene was 18s rRNA which was amplified for each sample in a 25 μ l reaction with ~20ng of cDNA, 1 pmol/ μ l of forward and reverse primer (5'-TCAAGAACGAAAGTCGGAGG-3' and 5'-GGACATCTAAGGGCATCACA-3' respectively), 1.5 mM MgCl₂, 0.1 mM dNTP's and 0.6U of *Taq* polymerase (Sigma-Aldrich, Madrid, Spain). The thermocycle program utilised was; 1 minute at 95°C followed by 16 cycles of 30 seconds at 95°C, 1 minute at 56°C and 30 seconds at 72°C, followed by a final step of 1

minute at 72°C. All RT-PCR reactions were fractionated on a 2.5% agarose gel and analysed by densitometry using LabWorks version 4.5 software (Ultra-Violet Products, Cambridge, UK) and results were expressed as the mean of three different samples per developmental stages with error bars representing standard error. In sea bream adult tissues only one sample was analysed.

RT-PCR analysis of sea bream deiodinase expression in control and T3 and methimazol treated animals was performed using the primers and RT-PCR conditions described above. The expression of 18s rRNA was used to normalise the expression of each sea bream deiodinase in each sample as described above. In order to determine if significant statistical differences occur between sea bream deiodinase genes in control and treatments groups 2-way analysis of variance was used (2-way ANOVA). If statistically significant differences were found a Holm-Sidak post-hoc multiple comparison analysis was performed. Statistical significance was considered if $p < 0.05$. All statistical analysis was performed using SigmaStat 3 software (SPSS, Inc).

6.2.9 Developmental expression of sea bream TR α and TR β - Taqman Quantitative RT-PCR analysis

Taqman quantitative RT-PCR (qPCR) was used to determine the expression of TR α and TR β during sea bream embryonic, larval and early juvenile stages. Sea bream embryonic samples at blastula (6hpf), 30% epiboly (12 hpf), 90% epiboly (18 hpf), most posterior somite formation (36 hpf), near hatching (43 hpf), 1 day post hatch (dph). 4, 24, 46, 64 and 75 dph and also 89 dph juveniles were analysed. Sea bream TR α (Sweeney, unpublished results) and TR β (Nowell et al., 2001) cDNA sequences were introduced in PrimerExpress V2 software (Perkin-Elmer) and Taqman qPCR probes and primers were designed (Table 6.2). Primers and probes were selected after ClustalX (Thompson et al., 1997) nucleotide multiple comparison in order to ensure the amplicon is located in a non-conserved region between TR α and TR β and by also considering a PrimerExpress penalty gap score below 100. The Taqman probes were labelled at

the 5'-end with FAM and at the 3'-end with TAMRA-6-FAM (OPERON). 18s rRNA was used as an internal standard using the primers and probes previously described (see Chapter 4). qPCR reactions for sea bream TRs were performed using the Eurogentec qPCR mastermix and ~20ng of sample cDNA with the primers and probe conditions (Table 6.2) or 1 μ L of 1/10000 dilution of sample cDNA for 18s rRNA. All reactions were carried out in 25 μ l volumes and a preliminary assay was performed to determine optimal primer and probe concentration.

Table 6.2. Quantitative RT-PCR primers and Taqman probes sequences and respective concentration used to analyse sea bream TR α and TR β expression and respective PCR efficiencies.

Gene	Sequence Forward Primer qPCR, Concentration (nM)	Sequence Taqman probe qPCR, Concentration (nM)	Sequence Reverse Primer qPCR, Concentration (nM)	PCR efficiency
TR α	ACCAAGATCATGACTCTGCAA 90	ACACGTGTCGTCGACTTCGCCAAG 300	AGCTCAGAGAACATGGGCAATT 90	72%
TR β	CGAGCTGCTGTTTCGCTATGA 90	CCCGAGAGCGAGACACTCACGCTAAA 200	CCCGTGTGACTGCCATCTC 90	70%

Taqman quantitative RT-PCR was performed and analysed using, respectively, an ABI 7700 qPCR thermocycler and software (Perkin-Elmer). The qPCR thermocycle program utilised was 10 minutes at 95°C followed by 40 cycles of 15 seconds at 95°C and 1 minute at 60°C.

For each sea bream gene to be analysed, a standard curve composed of 1/10 serial dilutions (1ng/ μ L to 1fg/ μ L) of cDNA plasmid of target genes were included in each PCR experiment. To normalise the qPCR results for TR α and TR β the expression of 18s rRNA was used. Results are presented as the mean of three individual samples per developmental time and the bars represent standard error. In order to compare expression between sea bream TR α and TR β analysis of variance between the standard curves for each sea bream TR gene was determined using GrapPad Prism software. Comparison between sea bream TR α and TR β expression was made if standard curves of the sea bream TRs had less than 5% variation. Differences between expression of sea bream TR α and TR β in each stage and between stages were determined by 2-Way analysis of variance (2-Way ANOVA) followed by Holm-Sidak post-hoc test (HSM) if significant differences were found. Differences were considered to be

statistically significant at $p < 0.05$. All statistical analysis was performed using SigmaStat3 software (SPSS Inc.).

6.3 Results

6.3.1 Isolation of sea bream deiodinases cDNA

Sea bream D1 (saD1) and D3 (saD3) deiodinase cDNA were isolated by cDNA library screening. However, it was not possible to isolate sea bream D2 (saD2) by library screening and a PCR cloning strategy with degenerate primers was used.

From the cDNA library screening a 1637 bp cDNA was isolated, composed of the full coding region but lacking part of the 3'UTR including the poly-adenylation signal and poly(A) tail. Analysis of the cloned cDNA by tBLASTx analysis (Altschul et al., 1990) gave a good match with a previously submitted sea bream deiodinase 1 sequence (Klaren et al., 2005), although the saD1 cDNA sequence cloned in the present work had a longer 3'UTR (Fig. 6.1A). The saD1 cDNA comprised the complete D1 protein of 248 amino acids (aa) (Fig. 6.1A) from nucleotide (nt) 34 to nt 777 where it terminates in a TAG codon (asterisk in Fig. 6.1A). A TGA codon (double underlined in Fig. 6.1A) at nt 409, encodes the Sec residue at aa 126 and is followed by a SECIS element in the 3'UTR (bold in Fig. 6.1A and A'). The saD1 SECIS element spanned nt 1028 to nt 1116 (bold in Fig. 6.1A) and was identified using SECISearch 2.19 software (Fig. 6.1A')(Kryukov et al., 2003). The predicted saD1 SECIS element is most like a form 1 SECIS elements with a canonical SECIS core element (bold and boxed in Fig. 6.1A') and adenine bulge (bold Fig. 6.1A').

A second cDNA (saD3) was also isolated from the sea bream larval cDNA library which was 1639 bp and in tBLASTx analysis (Altschul et al., 1990) shared greatest similarity with other vertebrates D3 sequences and was considered a product of the sea bream D3 locus

(Fig. 6.1B). Sequence analysis revealed that saD3 cDNA codes for a predicted protein of 268 aa from nt 68 to nt 871 where it terminates in a TAG codon (asterisk in Fig. 6.1B). The predicted saD3 cDNA has an in frame TGA codon at nt 461 (double underlined in Fig. 6.1B) that codes for a putative Sec residue at saD3 residue 132 (Fig. 6.1B). Further analysis in SECISearch 2.19 software (Kryukov et al., 2003) revealed that saD3 contains a SECIS element in the 3'UTR from nt 1361 to nt 1456 which resembles a form 2 SECIS element (Fig. 6.1B'). The saD3 SECIS is composed of a canonical SECIS core (bold and boxed in Fig. 6.1B') and adenosine bulge and taken with the sequence similarity analysis further confirms its designation as a D3.

Despite extensive screening of the sea bream larval cDNA library it was not possible to isolate a cDNA representing the sea bream D2 gene and a PCR cloning strategy was used. Degenerate primers were designed after Clustal X (Thompson et al., 1997) multiple protein sequence alignment of previously cloned tetrapod D2. Only the primer pair F2/R3 amplified a 275 bp PCR product from an adult sea bream liver cDNA sample which in tBLASTx analysis (Altschul et al., 1990), shared greatest similarity to D2 and was designated saD2 (Fig. 6.1C). The saD2 DNA presented an in frame TGA codon (double underlined in Fig. 6.1C) and coded for a predicted peptide of 91 aa that corresponds to about one quarter of other vertebrate D2 proteins but that includes the Sec residue (U in Fig. 6.1C) preceded by the highly specific phenylalanine (F) and serine (S) residues and two prolines (P) and a further F residues (boxed in Fig. 6.1C) characteristic of all vertebrate deiodinases (Bianco et al., 2002; Bianco and Larsen, 2005; Kuiper et al., 2005). Comparison of saD2 predicted protein sequence with the equivalent region in homologous vertebrate D2 peptide sequences revealed that it shares 94.5%, 93.4%, 89%, 85.7% and 82.4% identity respectively with *H. hippoglossus*, *F. heteroclitus*, *S. maximus*, *O. mykiss* and *D. rerio* but only ~73% identity with tetrapod D2 peptides.

C

```

1  TTGGGTTCGGCCACCTGACCCCCCTTTCATCAGCCACCTGCCAGCTTCCGGCAGTTGGTTGAGGACTTCA 70
   F G S A T U P P F I S H L P A F R Q L V E D F

71  GTGATGTCGCTGATTTCTGTTAGTGTACATTGATGAGGCTCACCCATCTGATGGCTGGGTAGCCCCCTCC 140
   S D V A D F L L V Y I D E A H P S D G W V A P P

141  TATGGGCTCTTGCTCTTTCAATGTCCGGAACATCAGAACCTGGAAGAGAGGCTAGGAGCTGCACGCAA 210
      M G S C S F N V R K H Q N L E E R L G A A R K

211  CTCATTGAGCAGTTTCCCTGCCACCACAATGTCAGCTGGTGGCTGACTGTATGGACAACAATGCA 276
      L I E Q F S L P P Q C Q L V A D C M D N N A

```

Figure 6.1. Nucleotide sequence and deduced protein sequence of sea bream deiodinases cDNAs saD1 (A) and saD3 (B). The double underline elicits the Sec (U) insertion codon TGA while (*) denotes the termination codon. In (B) the underlined denotes the putative poly(A) signal. The SECIS element of saD1 (A) and saD3 (B) is in depicted in bold. The SECISearch predicted SECIS element hairpin is shown for saD1 (A') and saD3 (B'). In both (A) and (B) the SECIS core is boxed and the conserved adenosines as well as the conserved SECIS core nucleotides are in bold. In (C) is represented the RT-PCR isolated saD2 nucleotide sequence and the predicted peptide sequence. The TGA Sec (U) insertion codon is double undelined. The boxed aa's represent highly conserved residues.

6.3.2 Phylogenetic relationships of sea bream deiodinases

In order to establish the phylogenetic relationship of sea bream deiodinases and further confirm their identity sequences were retrieved from GenBank and SwissProt databases and when necessary the protein sequence was deduced using the BioEdit software. Multiple protein sequence alignment was carried out in Clustal X software (Thompson et al., 1997) and then maximum-parsimony phylogenetic analysis with 1000 bootstraps with PAUP 4.2 version software (Swofford et al., 2001). The resulting phylogenetic tree places each sea bream deiodinase in separate clusters alongside their predicted vertebrate homologues (Fig. 6.2). Moreover, the sea bream deiodinases cluster specifically with other teleost homologue deiodinases used in the analysis. Despite using only a fragment (91 aa) of saD2 (Fig. 6.1C) it clustered with other vertebrate D2 sequences and more specifically with other teleost D2 sequences (Fig. 6.2).

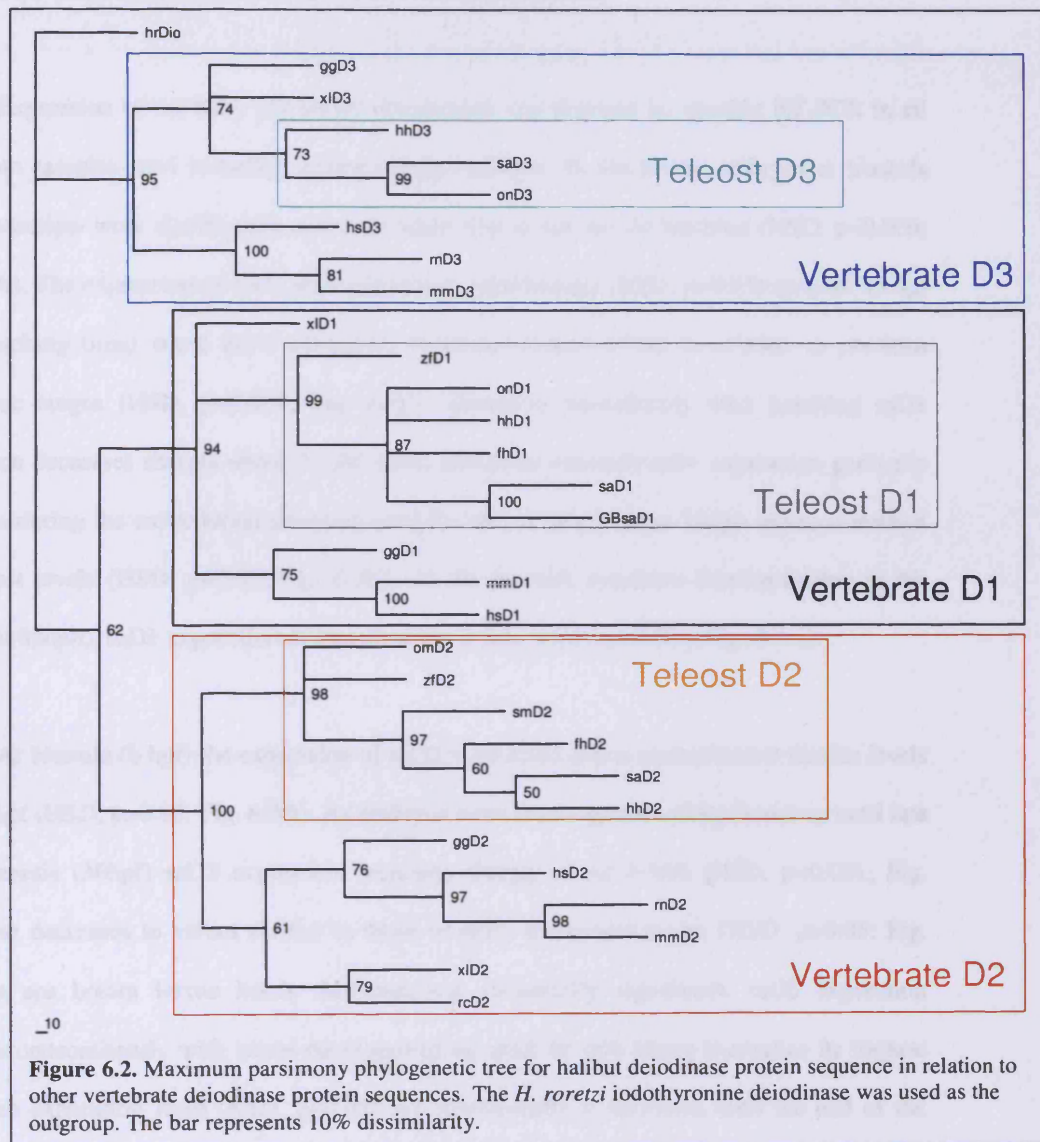


Figure 6.2. Maximum parsimony phylogenetic tree for halibut deiodinase protein sequence in relation to other vertebrate deiodinase protein sequences. The *H. roretzi* iodothyronine deiodinase was used as the outgroup. The bar represents 10% dissimilarity.

6.3.3 Developmental expression of sea bream deiodinases

Expression of the three sea bream deiodinases was detected by specific RT-PCR in all sea bream samples used including blastula stage embryos. In sea bream embryos at blastula saD1 transcripts were significantly more abundant than at the day of hatching (HSD, $p=0.006$; Fig. 6.3A). The expression of saD1 does not change significantly (HSD, $p>0.05$) up until 43 hpf (near hatching time) when saD1 expression increases almost 2-fold in relation to previous embryonic stages (HSD, $p<0.007$; Fig. 6.3C). However, immediately after hatching saD1 expression decreases sharply about 9-fold. From this point onwards saD1 expression gradually increases during the entire larval phase up until the end of larval life at 75dph where it reaches its highest levels (HSD, $p<0.05$; Fig. 6.3C). At the juvenile transition (corresponding to the sample at 89dph), saD1 expression decreases about 2-fold (HSD, $p<0.001$; Fig. 6.3A).

At blastula (6 hpf) the expression of saD2 is detected and is maintained at similar levels until 12hpf (HSD, $p>0.05$; Fig. 6.3B). As embryos enter somitogenesis (24hpf) and up until late somitogenesis (36hpf) saD2 expression increases sharply about 8-fold (HSD, $p<0.001$; Fig. 6.3B), but decreases to values similar to those of early embryonic stages (HSD, $p>0.05$; Fig. 6.3B) as sea bream larvae hatch. Although not statistically significant, saD2 expression increases concomitantly with larval development up until 46 dph where it reaches its highest post-hatch expression level (HSD, $p<0.05$) but subsequently it decreases until the end of the larval phase (75 dph; Fig. 6.3B). At the beginning of the juvenile stage (89 dph) expression of saD2 had increased to a similar level as 46 dph larvae (HSD, $p>0.05$; Fig. 6.3B).

saD3 mRNA is already detectable in blastula stage sea bream embryos and at early epiboly (12 hpf, 30% epiboly) expression increases more than 2-fold (HSD, $p<0.001$; Fig. 6.3C) and reaches its highest level of any of the sea bream developmental times analysed (HSD, $p<0.001$; Fig. 6.3C). After this peak in expression, saD3 mRNA levels return to levels very similar to those of blastula (HSD, $p>0.05$; Fig. 6.3C). The expression of saD3 shows no

significant change with hatching and throughout larval life up until early juvenile stage saD3 expression levels do not significantly change and are about 50% of 18s (HSD, $p > 0.05$; Fig. 6.3C).

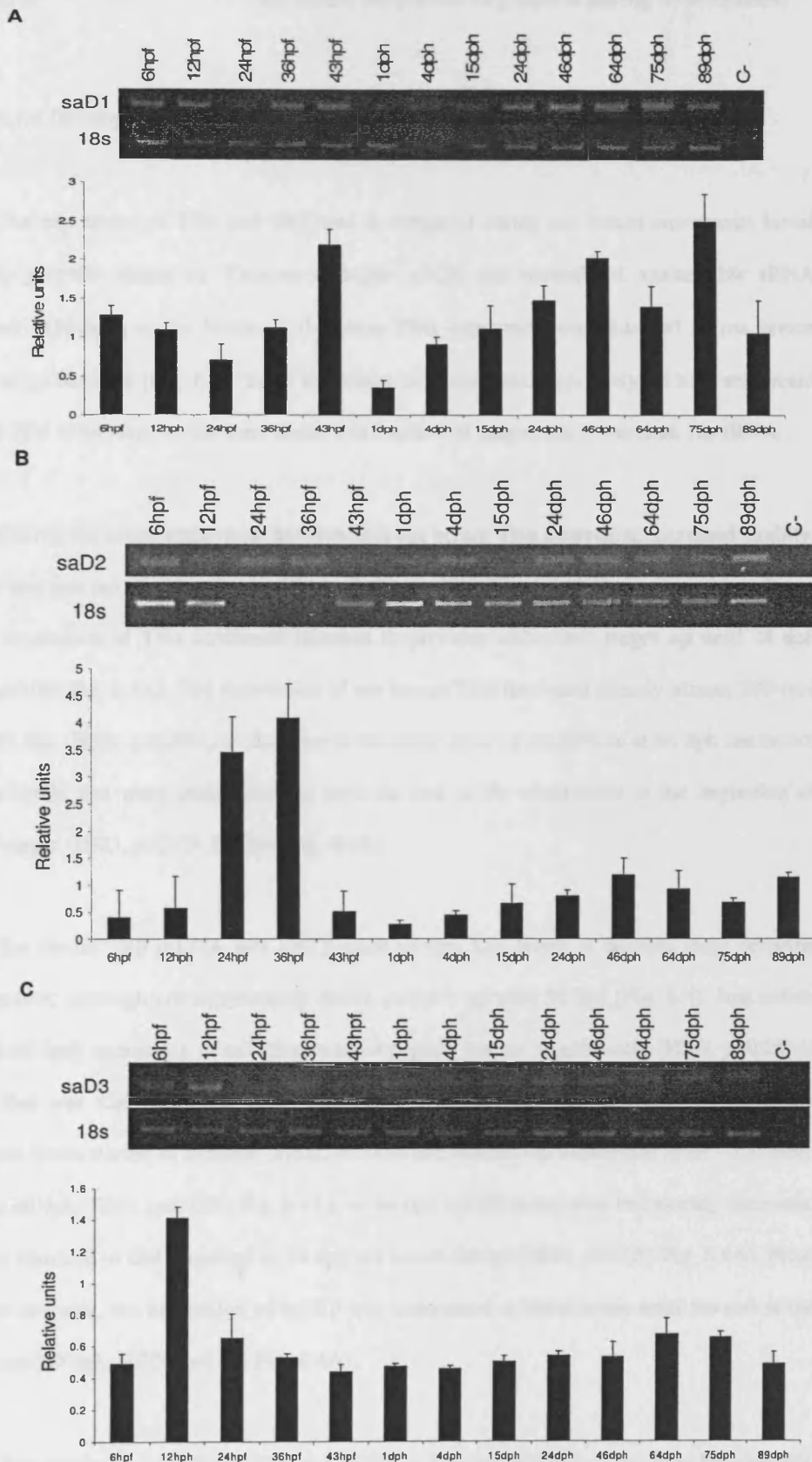


Figure 6.3. Semi quantitative RT-PCR expression of saD1 (A), saD2 (B) and saD3 (C) in sea bream embryonic, larval and juvenile stages. Ethidium bromide agarose gel and graphic representation of sea bream deiodinase genes normalised with 18s rRNA expression.

6.3.4 Developmental expression of sea bream TR α and TR β

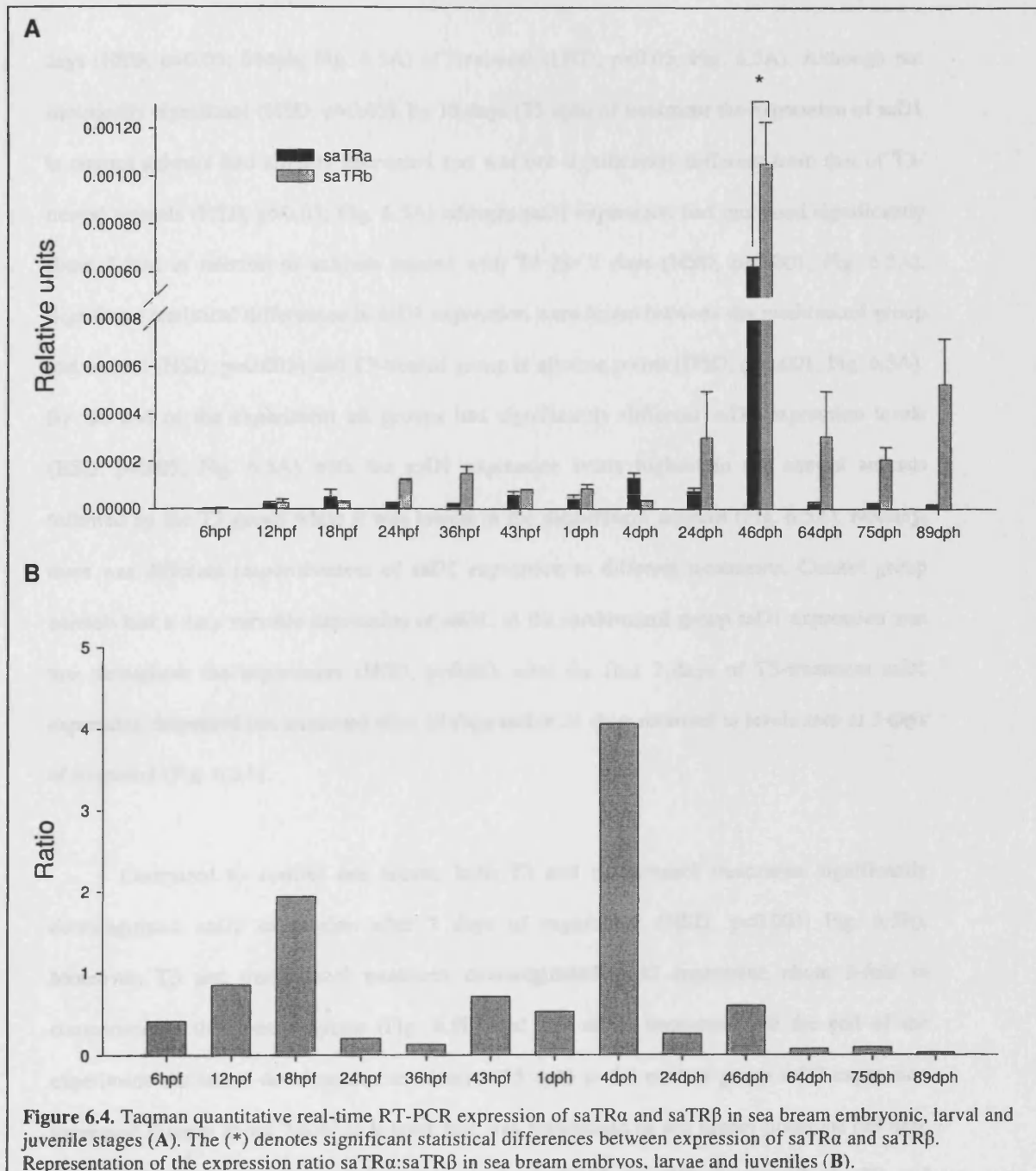
The expression of TR α and TR β was investigated during sea bream embryonic, larval and early juvenile stages by Taqman real-time qPCR and normalised against 18s rRNA expression. Although at the limits of detection TR α expression was detected in sea bream blastula stage embryos (Fig. 6.4). In all sea bream developmental ages analysed both sea bream TR α and TR β expression levels were about 7 to 6 orders of magnitude lower than 18s rRNA.

During the entire embryonic development sea bream TR α expression increased slightly, although this was not statistically significant (HSD, $p>0.05$; Fig. 6.4A). As soon as the embryos hatched expression of TR α continued identical to previous embryonic stages up until 24 dph (HSD, $p>0.05$; Fig. 6.4A). The expression of sea bream TR α increased sharply almost 200-fold only at 46 dph (HSD, $p<0.001$) to decrease in the same order of magnitude at 64 dph sea bream larval to levels that were maintained up until the end of the experiment at the beginning of juvenile stages (HSD, $p>0.05$; 89 dph; Fig. 6.4A).

Sea bream TR β mRNA was also present at very low levels in blastula stage embryos and increased, although not significantly (HSD, $p>0.05$) up until 36 hpf (Fig. 6.4). Just before hatching (43 hpf) expression of saTR β decreased slightly but not significantly (HSD, $p>0.05$) to a level that was maintained up until 4 dph (HSD, $p>0.05$; Fig. 6.4A). At 24 dph saTR β expression levels started to increase (HSD, $p>0.05$) and reached an expression level ~200 times higher at 46 dph (HSD, $p<0.001$; Fig. 6.4A). At 64 dph saTR β expression had already decreased to a level identical to that observed in 24 dph sea bream larvae (HSD, $p>0.05$; Fig. 6.4A). From this stage onwards, the expression of saTR β was maintained at these levels until the end of the experiment (89 dph; HSD, $p>0.05$; Fig. 6.4A).

The standard curves for saTR α and saTR β in Taqman qPCR had less than 5% variation between each other and the expression of both receptors was directly compared in each sea

bream developmental stage analysed. Differences in the expression of saTR α and saTR β were only found in 46 dph sea bream larvae (HSD, $p < 0.001$; Fig. 6.4A) although in the majority of other sea bream developmental stages the relationship between the absolute expression values of saTR α and saTR β differ (Fig. 6.4B). In sea bream blastula stage embryos the expression ratio of saTR α :saTR β was below 1 but it increased to almost two when embryos reached the end of epiboly (18 hpf; Fig. 6.4B). However, at 24 hpf at the beginning of somitogenesis this relation inverts dramatically (Fig. 6.4B). From this point onwards until immediately after hatching (1 dph) saTR β is more readily detected than saTR α (Fig. 6.4B). However, at 4 dph the ratio between the expression of the two receptors inverts again (Fig. 6.4B), although by 24 dph the ratio of saTR α :saTR β is below 1 and is maintained until the end of the experiment (Fig. 6.4B).



6.3.5 T3 and methimazol treatments - sea bream deiodinases expression

The expression of sea bream D1 was, in comparison with control animals, downregulated in the same manner in the T3 and methimazol experimental groups after only 7

days (HSD, $p > 0.05$; 64dph; Fig. 6.5A) of treatment (HSD, $p < 0.05$; Fig. 6.5A). Although not statistically significant (HSD, $p > 0.05$), by 18 days (75 dph) of treatment the expression of saD1 in control animals had slightly decreased and was not significantly different from that of T3-treated animals (HSD, $p > 0.05$; Fig. 6.5A) whereas saD1 expression had increased significantly about 3-fold in relation to animals treated with T3 for 7 days (HSD, $p < 0.001$; Fig. 6.5A). Significant statistical differences in saD1 expression were found between the methimazol group and control (HSD, $p = 0.008$) and T3-treated group in all time points (HSD, $p < 0.001$; Fig. 6.5A). By the end of the experiment all groups had significantly different saD1 expression levels (HSD, $p < 0.05$; Fig. 6.5A) with the saD1 expression being highest in the control animals followed by the T3 group while it was lowest in the methimazol animals (Fig. 6.5A). Notably, there was different responsiveness of saD1 expression to different treatments. Control group animals had a very variable expression of saD1, in the methimazol group saD1 expression was low throughout the experiment (HSD, $p > 0.05$), after the first 7 days of T3-treatment saD1 expression decreased but increased after 18 days and at 21 days returned to levels seen at 7 days of treatment (Fig. 6.5A).

Compared to control sea bream, both T3 and methimazol treatments significantly downregulated saD2 expression after 7 days of experiment (HSD, $p < 0.001$; Fig. 6.5B). Moreover, T3 and methimazol treatment downregulated saD2 expression about 3-fold in comparison to the control group (Fig. 6.5B) and this effect persisted until the end of the experiment. As larval development terminated (75 dph) in the control group saD2 expression decreased sharply about 7-fold to a level that was maintained in sea bream juveniles (89 dph; HSD, $p < 0.001$; Fig. 6.5B) and that did not show significant differences with the T3 and methimazol treated groups (HSD, $p > 0.05$; Fig. 6.5B). Notably, the T3 and methimazol treated group had a less variable saD2 expression compared to control animals at all experimental times (Fig. 6.5B).

The expression of saD3, up until 18 days of the experiment did not vary in control sea bream larvae (HSD, $p>0.05$), although by the end of the experiment saD3 expression had been downregulated (HSD, $p<0.05$; Fig. 6.5C). In methimazol treated larvae at day 7 and 18 of treatment saD3 expression was significantly different (HSD, $p<0.05$; Fig. 6.5C) from control larvae, but not from the T3-treated group (HSD, $p>0.05$). By the end of the experiment no differences were detected between the control and T3-treated animals (HSD, $p>0.05$), although expression of saD3 was significantly lower in methimazol treated sea bream (HSD, $p<0.05$; Fig. 6.5C).

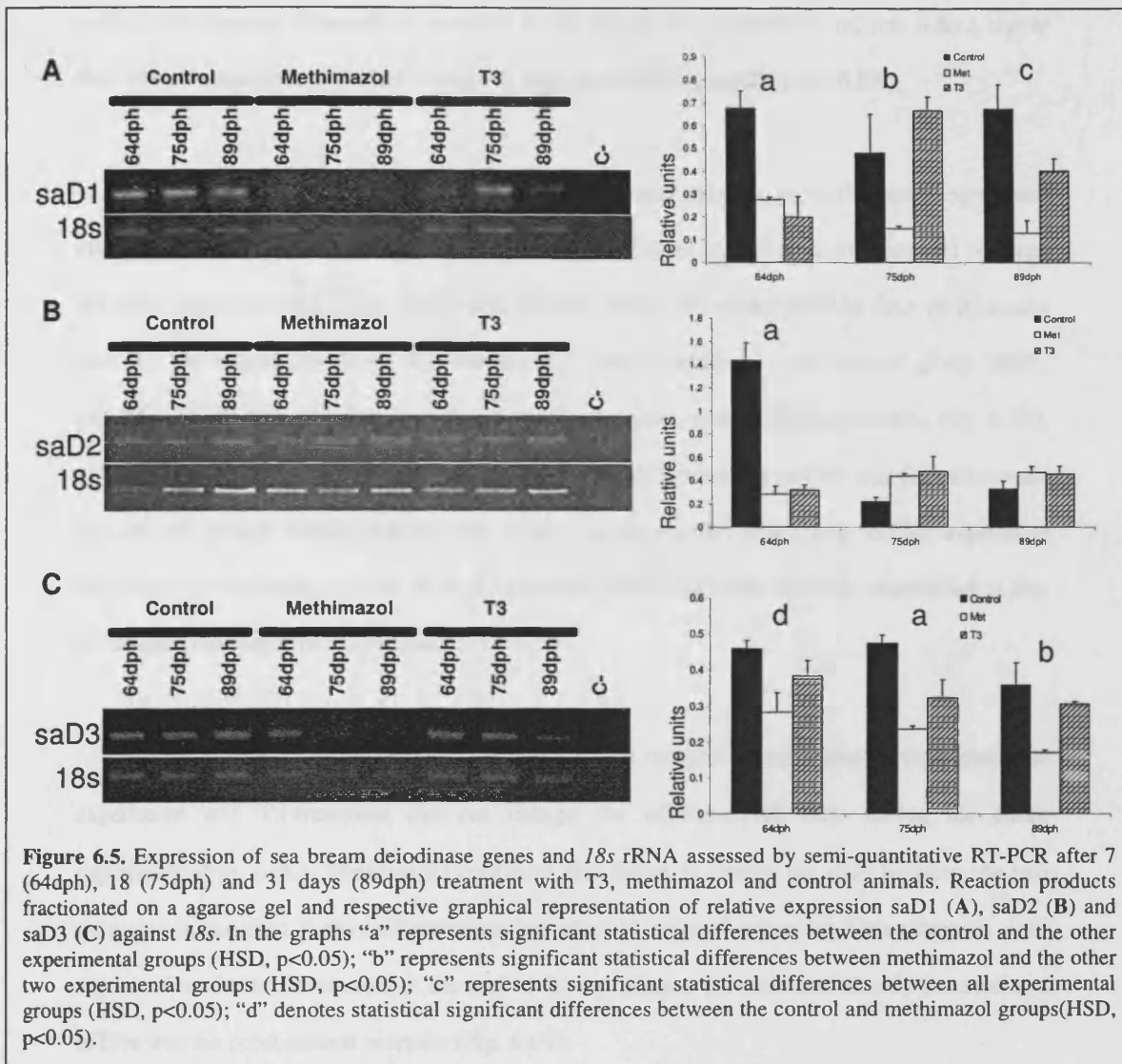


Figure 6.5. Expression of sea bream deiodinase genes and *18s* rRNA assessed by semi-quantitative RT-PCR after 7 (64dph), 18 (75dph) and 31 days (89dph) treatment with T3, methimazol and control animals. Reaction products fractionated on a agarose gel and respective graphical representation of relative expression saD1 (A), saD2 (B) and saD3 (C) against *18s*. In the graphs “a” represents significant statistical differences between the control and the other experimental groups (HSD, $p < 0.05$); “b” represents significant statistical differences between methimazol and the other two experimental groups (HSD, $p < 0.05$); “c” represents significant statistical differences between all experimental groups (HSD, $p < 0.05$); “d” denotes statistical significant differences between the control and methimazol groups (HSD, $p < 0.05$).

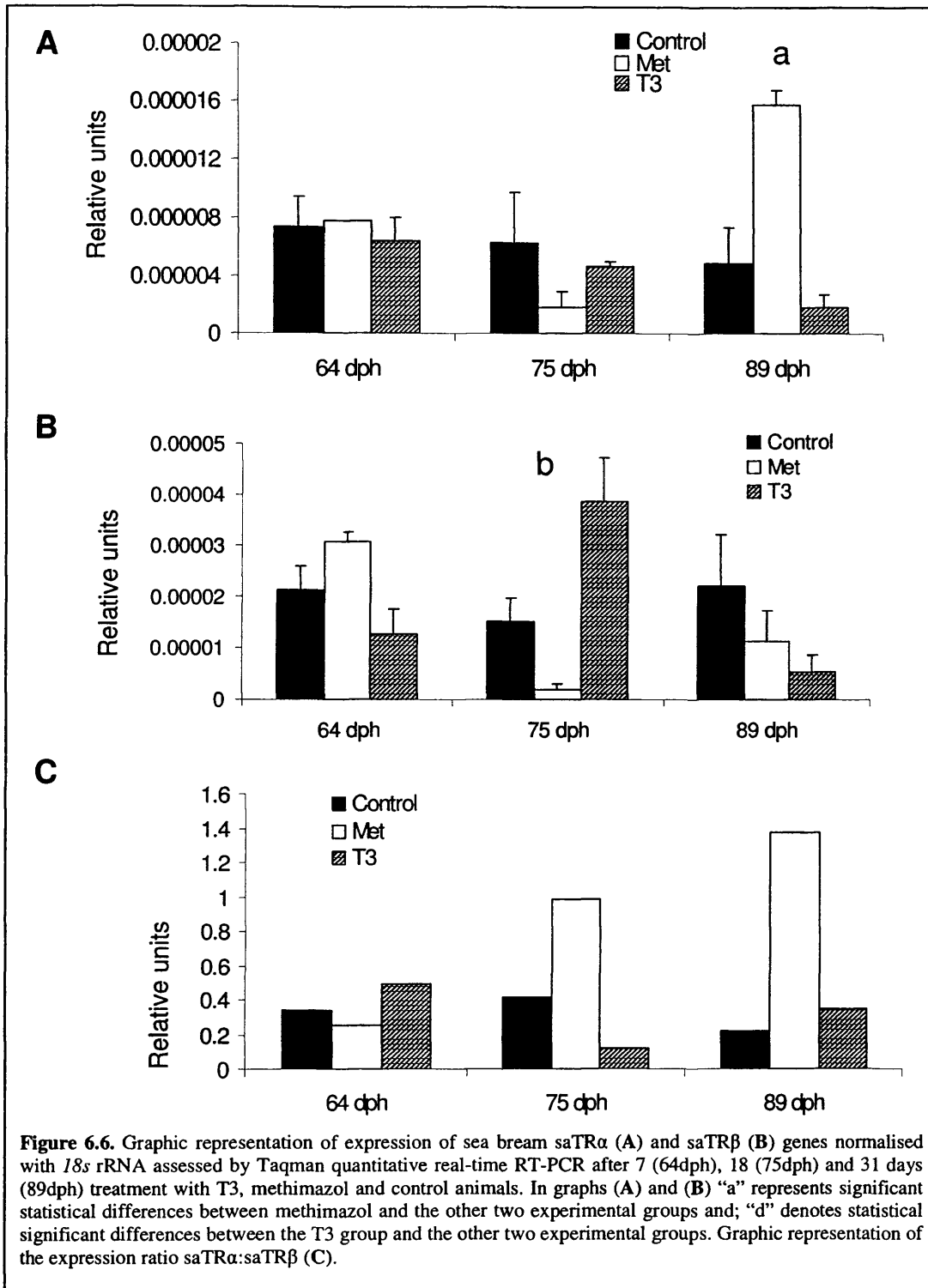
6.3.6 T3 and methimazol treatments - sea bream TR α and TR β expression

Treatment with T3 or methimazol did not significantly change saTR α expression after 18 days of treatment (HSD, $p > 0.05$; Fig. 6.6A). However, at the end of the experiment saTR α expression in the methimazol group was about 3 times higher than in the control group and about 5-fold higher than the T3-treated group (HSD, $p < 0.001$; Fig. 6.6A). Remarkably, the expression of saTR α declined in the methimazol group up until 18 days of treatment (HSD,

$p < 0.05$) but sharply increased in juveniles at the end of the experiment and was 6-fold higher than in sea bream collected after 18 days of treatment (HSD, $p < 0.001$; Fig. 6.6A).

In the control group expression of saTR β was constant throughout the entire experiment (HSD, $p > 0.05$; Fig. 6.6B) and no differences were observed after 7 days of treatment between the three experimental groups (HSD, $p > 0.05$; Fig. 6.6B). However, after 18 days of treatment with T3 the expression of saTR β was about 3 times higher than the control group (HSD, $p < 0.05$) and 10 times higher than the methimazol treated group (HSD, $p < 0.001$; Fig. 6.6B), although by the end of the experiment no significant differences in saTR β was found between any of the groups (HSD, $p > 0.05$; Fig. 6.6B). In the methimazol group saTR β expression decreased 10-fold from 7 to 18 days of treatment (HSD, $p = 0.006$) and was maintained at low levels until the end of the experiment (Fig. 6.6B).

In control sea bream TR β was the predominant receptor being expressed throughout the experiment and T3-treatment did not change the saTR α :saTR β ratio during the entire experiment (Fig. 6.6C). Methimazol treatment also failed to change the ratio between the two receptors in the first 7 days of treatment but after 18 days of treatment both receptors were expressed at similar levels and at the end of the experiment the ratio had already inverted and saTR α was the predominant receptor (Fig. 6.6C).



6.4 Discussion

6.4.1 Molecular characterisation of sea bream deiodinases

The cDNAs corresponding to sea bream deiodinase 1, 2 and 3 have been cloned. These were identified both by tBLASTx (Altschul et al., 1990) and maximum parsimony phylogenetic analysis (Swofford et al., 2001)(Fig. 6.2) that gave highly significant results with homologous vertebrates deiodinase proteins sequences. Further *in silico* analysis of the saD1 and saD3 cDNA sequences using the SECISearch version 2.19 software (Kryukov et al., 2003) identified in the 3'UTR of saD1 and saD3 a SECIS sequence responsible for the recruitment of the cellular factors that enable the usage of the TGA codon as a selenocysteine insertion codon (Kollmus et al., 1996; Copeland et al., 2000; Dumitrescu et al., 2005). As previously described (Klaren et al., 2005) the saD1 cDNA contained a SECIS element that resembles a form 1 element and in which the SECIS core (bold and boxed in Fig. 6.1A') is preceded by a guanine. The presence of a form 1 SECIS in saD1 is reminiscent of other vertebrate D1 transcripts (Sanders et al., 1997; Bianco et al., 2002; Orozco et al., 2003; Klaren et al., 2005). Interestingly, teleost D1 cDNAs described so far all have guanine just before the SECIS core (present study)(Sanders et al., 1997; Orozco et al., 2003; Klaren et al., 2005) with the exception of halibut in which the SECIS core region is preceded by an adenine (Chapter 4). In contrast to the previously described saD1 cDNA (Klaren et al., 2005) the cDNA found in the present study contains a longer 3'UTR although only a single SECIS element was found. This contrasts to *Oreochromis niloticus* D1 in which two SECIS elements have been found in the 3'UTR (Sanders et al., 1997).

In the case of saD3 the predicted SECIS element (Kryukov et al., 2003) most closely resembles a form 2 element (Fig. 6.1B') similar to that found for halibut D3 (Chapter 4). These results are in agreement with previous studies in other vertebrates that indicate that form 2 SECIS elements are more common in D3 transcripts (Fagegaltier et al., 2000; Bianco et al.,

2002) and contrast to *Oncorhynchus mykiss* in which D3 transcripts contain a form 1 SECIS elements (Bres et al., 2006). In common with halibut (Chapter 4) and *O. niloticus* (Sanders et al., 1999), in the sea bream only one isoform with one SECIS element was found, although in *O. mykiss* 2 different SECIS elements generated by alternative splicing occur (Bres et al., 2006).

The saD2 partial cDNA did not permit complete analysis and characterisation of this transcript in sea bream, although tBLASTx analysis (Altschul et al., 1990) and phylogenetic analysis (Fig. 6.2) support its designation as a sea bream D2. The cloned saD2 fragment presented an in frame TGA codon that coded for Sec and is flanked by specific residues (boxed in Fig. 6.1C) that are fundamental for correct D2 function and activity (Bianco et al., 2002; Bianco and Larsen, 2005).

6.4.2 Sea bream deiodinases, TR α and TR β present coordinated expression during development

In several teleosts maternally derived THs are present in the yolk sac of fertilised embryos (Tagawa and Hirano, 1987; Tagawa et al., 1990b; Tagawa and Hirano, 1991; Reddy et al., 1992; Power et al., 2001). In some species immersion of embryos in T4 and T3 solutions increased the resorption of the yolk sac and enhanced the rate of development whereas in other teleosts it delayed the expression of hatching enzymes (Leatherland, 1994) or even diminished survival (Mylonas et al., 1994). However, in TH deficient *Oryzias latipes* eggs or eggs from Great Lakes coho salmon with goitre there is no observed effect on development (Tagawa and Hirano, 1991; Leatherland, 1994). Nevertheless, these observations suggest that maternal TH might have a role in early developmental processes in some teleosts (Leatherland, 1994; Power et al., 2001). The expression of deiodinases and TR early in sea bream development (Fig. 6.3 and 7.4) strongly favour of this hypothesis. Furthermore, in *Danio rerio* (Essner et al., 1997; Essner et al., 1999; Liu et al., 2000; Liu and Chan, 2002), *Salmo salar* (Jones et al., 2002), sea bream (Llewellyn et al., 1998; Nowell et al., 2001) and halibut (Llewellyn et al., 1999) TR

expression has been shown to be present in early embryonic stages. In *D. rerio* in the absence of high TH levels TR α is probably involved in repression of gene transcription (Essner et al., 1997). Moreover, *D. rerio* embryos overexpressing TR α have significant hindbrain malformation that parallel those found in *D. rerio* with impaired retinoic acid function (Essner et al., 1999). On the other hand in *D. rerio* embryos D2 is expressed but not D1, suggesting that THs are already important for *D. rerio* embryonic development (Thisse et al., 2003). In fact, in *D. rerio* D2 is expressed at 24 and 36 hpf in the developing retina, adenohypophysis and intestine bulb and is downregulated in the retina and intestine bulb just before hatching (Thisse et al., 2003). Deiodinases and TR are simultaneously expressed in the sea bream together with THs (Szisch et al., 2005) indicating a role for THs during development. In common with *D. rerio*, sea bream D2 expression increases at 24 hpf up until 36 hpf and also decreases just before hatching (Fig. 6.3B) and the change in saD2 expression is correlated with an increase in saTR β expression at the same embryonic stages (Fig. 6.4). In contrast, in *Oreochromis mossambicus* although THs are present in embryonic stages no ORD activity is found suggesting differences may exist in the relative importance of THs in teleost development.

As sea bream enter the larval stage the expression of saD1, saD2, saTR α and saTR β start to increase and peaks at 46 dph from which point they decrease (Fig. 6.3A, B and 6.4). Moreover, a peak of THs is also observed in these larvae (Dr. Deborah Power, personal communication). The observed pattern of expression of these genes together with a peak in T3, during sea bream larval development is reminiscent of what occurs during halibut metamorphosis (Chapter 4)(Galay-Burgos et al., 2004) and in metamorphosing tissues of anurans or TH driven developmental events in mammals and birds (Yaoita and Brown, 1990; Becker et al., 1997; Van der Geyten et al., 1997; Campos-Barros et al., 2000; Zhang and Lazar, 2000; Huang et al., 2001; Van der Geyten et al., 2001a; Bianco et al., 2002; Forrest et al., 2002; Cai and Brown, 2004; Gereben et al., 2004; Ng et al., 2004; Brown, 2005; Galton, 2005). Again as observed during anuran (Yaoita and Brown, 1990; Becker et al., 1997; Huang et al., 2001; Cai and Brown, 2004; Brown, 2005) and more notably halibut metamorphosis (Chapter

4)(Galay-Burgos et al., 2004) there appears to be synergy between increased expression of D1 and D2 deiodinases, TRs, and T3 and this is probably responsible for the transition from larvae to juvenile in the sea bream.

6.4.3 Effect of T3 and methimazol treatment in sea bream deiodinase and TR expression

T3 is known to be a positive regulator of D1 expression in adult mammals (Berry et al., 1990; Berry et al., 1991a; Kohrle, 2000; Bianco et al., 2002). Moreover, positive and negative regulating TRE have been identified in the promoter region of the human D1 gene (Toyoda et al., 1995a; Jakobs et al., 1997b) (Zhang et al., 1998; Kim et al., 2004) and TR β knock-out mice reveal the receptor is the major transcription factor involved in D1 expression in the liver (Ammal et al., 2001). In liver of *O. mykiss* (Finsson and Eales, 1999) and *Fundulus heteroclitus* (Garcia-G et al., 2004) T4 and T3 treatment did not affect D1 activity and had a delayed effect on *F. heteroclitus* gene expression. Moreover, in *O. niloticus* T3 treatment did not affect liver and renal D1 activity (Mol, 1998) and hypothyroidism decreased its expression in kidney but upregulated it in liver, although in euthyroid fish D1 is only expressed in kidney (Van der Geyten et al., 2001b). The preceding results seem to suggest that THs might not have a direct action on teleost D1 expression although in the sea bream T3 treatment (89 dph; 31 days of treatment) influenced the expression of both saD1 and saTR β . The results from sea bream suggest D1 regulation in this species may be similar to that in mammals.

In adult rat and human pituitary tumour cells THs regulate D2 expression both at a pre- and post-transcriptional level (Burmeister et al., 1997; Tu et al., 1997; Kim et al., 1998; Bianco et al., 2002). In the sea bream T3 significantly down regulated saD2 expression and has a similar effect in *O. mykiss* and *F. heteroclitus* (Garcia-G et al., 2004; Bres et al., 2006). Surprisingly, promoter analysis of mammalian D2 genes reveals the presence of a cAMP responsive element but no TRE (Safran et al., 1996; Bartha et al., 2000; Canettieri et al., 2000; Song et al., 2000). The precise molecular mechanisms by which T3 regulates D2 transcription in

vertebrate still have to be elucidated (Bianco et al., 2002) and the characteristics of the teleost D2 promoters remain to be established.

In anurans D3 has a tissue specific responsiveness during metamorphosis and in *X. laevis* as T3 levels rise during climax D3 expression and activity in the tail increases but in the liver decreases (Wang and Brown, 1993; St Germain et al., 1994; Kawahara et al., 1999; Shintani et al., 2002; Brown, 2005). Moreover, both *in vivo* and *in vitro* T3 treatment and hyperthyroidism in mammals upregulate D3 expression in brain but decrease mRNA and activity levels in liver (Esfandiari et al., 1992; Croteau et al., 1995; Pallud et al., 1999; Tu et al., 1999). In teleosts, D3 expression and regulation by T3 appear to be tissue and species specific and in *O. mykiss* and *Salmo salar* T3 treated liver D3 mRNA and activity levels increased (Leatherland, 1994; Finnson and Eales, 1999; Bres et al., 2006) whereas in *O. niloticus* both D3 mRNA and activity are reduced (Mol et al., 1999). Conversely, in hyperthyroid *O. niloticus* brain D3 expression and activity increase but in *S. salar* increased T3 fails to influence brain D3 expression and activity (Morin et al., 1993). In the sea bream larvae and juveniles there was a significant reduction in whole body saD3 expression during T3 treatment. However, taking into consideration the tissue specific responses observed in adults of other vertebrates, it will be important in the future to carry out tissue specific analysis in the sea bream.

The effect of T3 on saTR α and saTR β appeared to depend on the duration of exposure to the hormone. Short term treatment (64 dph, 7 days of treatment; Fig. 6.6) had no apparent effect on saTR α and saTR β expression, although longer T3 exposure (75 dph; 18 days of treatment; Fig. 6.6) caused a significant upregulation in saTR β . The observed effect of T3 treatment on sea bream TRs contrast to the effect of T3 in *Scophthalmus maximus* where TR α expression was upregulated by T3 treatment but not TR β expression (Marchand et al., 2004). In fact, in *S. maximus* TR α expression was correlated with metamorphosis but not TR β suggesting that, in contrast to sea bream (present chapter), halibut (Chapter 5) and anurans (Yaoita and Brown, 1990; Buchholz et al., 2006), TR α is the major TR mediating T3 action in *S. maximus*

metamorphic development (Marchand et al., 2004). On the other hand in *D. rerio* T3 treatment upregulated both TR α 1 and TR β 1 (Liu et al., 2000; Liu and Chan, 2002). However, caution is required in the interpretation of such studies as tissue specific differences in responsiveness of TR occur. For example, in mice treated with T3 hepatic expression of TR β 1 and TR α 2 is downregulated whereas in the heart the opposite occurs (Sadow et al., 2003). Moreover, in tetrapods it has been extensively shown that T3 and TR action on gene expression are strongly dependent not only of the promoter context of the target genes but also from the context of co-activator and co-repressor proteins that exist in the nucleus of each cell at a particular time (Farsetti et al., 1997; Lin et al., 1997; Privalsky and Yoh, 2000; Sachs et al., 2000; Sachs et al., 2002; Buchholz et al., 2003; Paul and Shi, 2003; Jho et al., 2005; Paul et al., 2005a; Paul et al., 2005b). To better understand the role of TR in TH action in teleosts it will be important to characterise the TR promoters and also establish how putative TR co-regulators may act.

As discussed in Chapter 5 methimazol did not behave as an anti-thyroidogenic drug in sea bream, as it failed to decrease T4 and T3 levels and instead slightly stimulated thyrocyte activity (Chapter 5). These results are contradictory to the effect of methimazol in *O. niloticus* and *Sarotherodon melanotheron* (Mol et al., 1999; Van der Geyten et al., 2001b) and the reason for this difference remains to be established. However, in the sea bream larvae and juveniles methimazol treatment had a persistent repressive action on the expression of saD1 (Fig. 6.5A). In contrast, it initially down-regulated saD2 expression (75 dph; 18 days of treatment) but subsequently stimulated (89 dph; 31 days of treatment) its expression. This is in contrast with the stimulatory effect of methimazol on D1 and D2 expression and activity in *O. niloticus* and *S. melanotheron* and also in the rat (Croteau et al., 1996; Burmeister et al., 1997; Tu et al., 1997; Guadano-Ferraz et al., 1999; Mol et al., 1999; Van der Geyten et al., 2001b). In contrast, methimazol decreased D3 expression and activity in *O. niloticus* and in rats (Tu et al., 1999) (Van der Geyten et al., 2001b) and also on whole-body saD3 expression in sea bream larvae and juveniles (Fig. 6.5C). The coordinated downregulation of D3 expression and upregulation in D2 expression and activity levels in mammals is proposed to counteract diminished serum TH

levels in methimazol-induced hypothyroid animals (Kohrle, 2000; Bianco et al., 2002). That methimazol fails to reduce THs in sea bream may partially explain the differing effect of this drug on deiodinase expression. Taken together the biological significances of methimazol treatment on expression of sea bream deiodinases, TR and TnT (Chapter 5) genes together with the biochemical and histological data of thyroid activity (Chapter 5) is difficult to interpret but suggests that in the sea bream methimazol does not act as an anti-thyroidogenic drug.

In conclusion, in the symmetric teleost sea bream TH seems to be responsible for the transition from larvae to juvenile and the relationships between deiodinases, TRs and TH levels are strikingly similar to those observed in the halibut (Chapter 4) but also in anurans, thus implying that this developmental transition in sea bream, and possibly all other symmetric teleosts, is analogous to anuran and flatfish metamorphosis.

CHAPTER 7

GENERAL CONCLUSION

The importance of THs in development of anurans, birds and mammals has been recognised for a long time although, only in the late 1980's and early 1990's did evidence arise suggesting an important role for THs in teleost development. A notable example occurs in flatfish metamorphosis in which THs drive the change from a symmetric pelagic larvae to an asymmetric benthic juvenile. This is most dramatically characterised by the migration of one of the eyes to the opposite side of the head so that both eyes come to rest on the same side in juveniles and adult animals, although a myriad of other less obvious changes occur (Inui and Miwa, 1985; Miwa and Inui, 1987a; Miwa and Inui, 1987b; Miwa et al., 1988; Miwa and Inui, 1991; Yamano et al., 1991a; Miwa et al., 1992; Yamano et al., 1994b; Inui et al., 1995; Huang et al., 1998a). TH is presumed to mediate its effect by interacting with TRs which directly regulate TH-target genes through binding to specific thyroid response elements (TREs) (Yamano et al., 1994a; Yamano and Inui, 1995; Yamano and Miwa, 1998; Llewellyn et al., 1999; Power et al., 2001). TRs have also been cloned (Huang et al., 1998b; Llewellyn et al., 1998; Liu et al., 2000; Nowell et al., 2001; Liu and Chan, 2002) from round fish (which, have a less dramatic transition from larvae to juvenile) and again THs are shown to be important in development (Yamano et al., 1991c; Eales and Brown, 1993; Leatherland, 1994; Brown, 1997; de Jesus et al., 1998; Power et al., 2001), although little is known about the precise molecular mechanisms and pathways they influence. This is due in part to a lack of information about TH-target genes and about the expression of deiodinases during teleost development (Thisse et al., 2003). The results of the present thesis have gone some way towards remedying this situation and demonstrated that in the flatfish, Atlantic halibut, during the larval to juvenile metamorphosis, T3 levels rise, deiodinase D3 decreases its expression while D2 and TR (especially TR β) expression increase concomitantly and peak at climax when major organ and tissue transformations occurs (Galay-Burgos et al., 2004) (Chapter 4). Moreover, studies in developing sea bream (a symmetrical round fish) revealed that expression of D2, D1, TR α and TR β gradually increases while D3 expression is stable (Chapter 6). Furthermore, in sea bream between 40-50 dph the expression of D2, D1 and TRs (Chapter 6) and T3 level (Dr. Deborah Power, personal communication) peak prompting a change from larvae to juvenile adult-like

morphology. Once again in striking resemblance to halibut the expression of D1, D2 and TRs as well as T3 levels subsequently decrease as the animals become juveniles (Chapter 6; Dr. Deborah Power personal communication). The present data strongly supports the notion that halibut and sea bream metamorphosis are a similar developmental process in which THs play an important role. Moreover, taken with literature on THs in tetrapods the present study provides strong evidence that TH actions in development of all vertebrates have shared characteristics and are regulated by similar molecular mechanisms and homologous genes.

Nevertheless, despite the underlying similarity of metamorphosis in halibut and sea bream several key differences exist and probably reflect different life strategies of each teleost. The first regards the regulation of D3. In halibut, D3 expression decreases several-fold as the animals enter metamorphosis but increases immediately after metamorphosis (Chapter 4), whereas in the sea bream D3 expression maintains a constant profile from embryonic to early juvenile stage whilst expression of the T3 producing deiodinases (D1 and D2) increases (Chapter 6). Secondly, the way Troponin T genes are regulated in muscle at metamorphosis, presumably by T3 action, also shows striking differences between the two teleosts (Chapters 3 and 5). While in sea bream the fTnT developmental isoform expression profile does not seem to be affected by T3 (Chapter 5), in the halibut (Chapter 3) and other flatfishes (Yamano et al., 1991a; Focant et al., 2003), different splice variants are produced before and after metamorphosis. In the halibut, when the larval muscle changes into a juvenile adult-like phenotype the expression of the embryonic efTnThh isoform is totally downregulated at metamorphic climax (Chapter 3) in coordination with increasing T3 levels and high D2 and lower D3 expression (Chapter 4). Importantly, the small white muscle fibres that characterise the larval apical and lateral hyperplastic areas of larval muscle growth and the new satellite cells that occur just before climax co-express efTnThh, D2 and D3 suggesting T3 is needed for maintaining the proliferative larval muscle cells. Notably when halibut reaches metamorphic climax and TH levels peak, the expression of efTnThh terminates and the apical and lateral regions of hyperplastic larval growth become totally depleted (Chapter 3) while D2 and D3

expression is exclusively detected in the scattered putative juvenile/adult satellite cells responsible for the hyperplastic post-metamorphic growth of white muscle (Chapter 4)(Veggetti et al., 1993; Johnston, 1994; Koumans and Akster, 1995; Mascarello et al., 1995; Johnston et al., 1997; Mommsen, 2001). Overall, the results obtained strongly suggest that in the halibut T3 is not only essential for the switch between larval and juvenile muscle at metamorphosis but is also important for correct cellular homeostasis of larval muscle cells (Chapter 3 and 4). This data leads to the hypothesis that different cellular TH levels in halibut white muscle hyperplastic proliferative cells might occur and that the transition from a larval to a juvenile/adult phenotype occurs in a T3 dose dependent manner.

In contrast to the halibut, in sea bream the homologous efTnTsb isoform is downregulated immediately after hatching when TH levels are generally low (Eales and Brown, 1993; Leatherland, 1994; Szisch et al., 2005) and when D1, D2 and TR expression levels are also at their lowest (Chapter 6). Moreover, T3 treatment of late larval stages of sea bream (54 to 89dph) was not able to induce a change from a larval to an adult fTnT isoform expression profile (Chapter 5). This suggests that although conservation of developmental mechanisms occurs in halibut and sea bream metamorphosis, the effect of the hormone on muscle development at metamorphosis seems to be different in these two teleosts. Moreover, comparison of halibut with other flatfish showed there was different regulation of fTnT isoforms at metamorphosis. In *P. olivaceus* the fTnT isoform that corresponds to fTnThh-1 predominates in relation to the isoform corresponding to fTnThh-2; in both halibut and in *S. maximus* the two isoforms, fTnThh-1 and -2, are present in similar abundance (Chapter 3 and 5)(Yamano et al., 1991a; Focant et al., 2003). This further emphasises that teleost muscle in general, and more specifically fTnT isoform expression, responds to T3 in a species-specific manner. This hypothesis is further reinforced by the finding that sea bream and halibut red muscle TnT genes respond differently to THs (Chapter 3 and 5). In the halibut, two red muscle specific genes found and cloned (sTnT2hh and AfTnThh) did not show any change either in expression or in isoform profile during metamorphosis (Chapter 3). In turn, in the sea bream the

isolated sTnT2sb, as in the halibut, was not affected by T3 treatment, but sTnT1sb presented regulation of its isoforms that changed from a larval to an adult profile after T3 treatment (Chapter 5). Moreover, the fact that different, non-homologous TnT genes were found in sea bream and halibut and also in *D. rerio* (Hsiao et al., 2003) further highlights that in teleosts, muscle development might occur in a species-specific fashion in order to better comply with the ecological, mechanical and physiological demands on each species.

In the sea bream time did not allow for a search for keratin genes that are regulated during metamorphosis which prevented the study of changes in sea bream skin at this developmental time. However, in the halibut an epidermal keratin type I gene, hhKer1, was found that showed decreased expression throughout metamorphosis, which was almost completely repressed at climax and undetectable in adult skin (Chapter 2). This gene was shown to be a cellular marker of halibut larval basal and suprabasal cells and its expression was positively correlated with D3 expression in these cells but inversely correlated with increased D2 expression as well as increasing whole-body TH levels (Chapter 2 and 4). Again in halibut skin THs seem to have a role not only in the transition from a larval to an adult skin phenotype but also in the maintenance of cellular homeostasis of larval basal and suprabasal cells since expression of both D2 and D3 is observed in these cells in pre-metamorphic halibut larvae (Chapter 2 and 4). The fact that the adult molecular, cellular and histological characteristics of halibut deep epidermal cells only emerges at climax when only D2 is expressed in these cells (Chapter 2 and 4) leads us to hypothesise that in halibut skin, as in halibut muscle, T3 action to maintain or to induce the larval deep epidermal cells to an adult cell type might also be determined in a dose dependent manner. From an evolutionary perspective, THs seem to be an important factor in skin development of teleosts, anurans and mammals, but more specifically in keratin isoform regulation during skin development (Ellison et al., 1985; Jonas et al., 1985; Nishikawa et al., 1992; Tomic-Canic et al., 1992; Tomic-Canic et al., 1996a; Tomic-Canic et al., 1996b; Radoja et al., 1997; Jho et al., 2001; Watanabe et al., 2001; Watanabe et al., 2002; Radoja et al., 2004; Jho et al., 2005). In fact the evidence presented here strongly suggest that

early skin development in teleosts and terrestrial vertebrates is similar but, diverges in late skin development

Overall, the present study indicates that teleost metamorphosis occurs both in symmetric and asymmetric teleosts and that T3 might be the major hormone that drives this developmental event. Furthermore, the iodothyronine deiodinases and TRs expression (Chapters 4 and 6)(Galay-Burgos et al., 2004) in both fishes correlates in the same manner with TH levels and the morphological changes that occur at metamorphosis. Moreover, the relationships found between TH levels and these genes in sea bream and halibut are similar to the ones observed in anuran tissues at metamorphic climax and to TH-driven developmental events in mammals and birds thus strongly suggesting that the endocrinological, molecular and cellular pathways involved are conserved.

7.1 Future research in TH action in teleost development

The findings presented here indicate that halibut skin is an excellent model with which to study cellular TH effects in development. In fact, the way hhKer1 is regulated by THs in halibut should constitute a very interesting model to study negative gene regulation by TR and T3 in teleosts, especially in light of the finding of a putative non-canonical negative TRE in the *F. rubripes* Ker1 locus that closely resembles negative TREs found in mammalian keratin genes (Tomic-Canic et al., 1992; Tomic-Canic et al., 1996a; Radoja et al., 1997). Moreover, since after metamorphosis in teleosts the physiological function of skin changes from being the major larval gas exchange surface to an impermeable membrane (Mommensen, 2001), it would be very interesting to investigate the way in which THs influence this process.

In muscle the differences in post-hatch development between sea bream, a perciforme and halibut, a pleurinectiforme, are quite remarkable and deserve special attention in the future. A comparative study of the divergent molecular mechanisms of T3 action on muscle in the

closely related halibut and sea bream might constitute a valuable tool to understand not only the success of teleosts but also how apparently conserved developmental events at the molecular level change to adapt to different ecological, mechanistic and physiological demands.

Finally, tissues like the digestive tract, blood, cartilage and bone, not studied in the present work but that are known to change at metamorphosis in teleosts (Miwa and Inui, 1991; Miwa et al., 1992; Faustino and Power, 1998; Faustino and Power, 1999; Faustino and Power, 2001; Campinho et al., 2004) seem interesting tissues in which to further investigate the precise molecular mechanisms by which THs might act.

Appendix I

Blocking solution 2% or 1%

Preparation of 100ml of blocking solution:

2g or 1g blocking reagent (Boehringer Mannheim GmbH; for 2% and 1% solution, respectively). Dissolve in 100ml of maleic acid buffer (MAB, see below) at 65°C mixing occasionally. Cool to room temperature, aliquot and store at -20°C.

Bovine serum albumin solution (BSA, 10mg.ml-1)

Preparation of 10ml of solution:

100mg of bovine serum albumin (Randox, Ireland). Dissolve in 10ml of sterile water. Aliquot and store at -20°C.

CHAPS 2% (3-[3-cholamidpropyl]dimethylammonio]-1-propanesulfonate)

Preparation of 100ml of solution:

2g CHAPS (Sigma-Aldrich). Dissolve in 100ml of diethyl pyrocarbonate treated, sterile water (see below).

Citric Acid 2M

Preparation of 100ml of solution:

42g citric acid (Merck). Dissolve in 100ml of MilliQ water. Autoclave for 20 minutes at 121°C and store at room temperature.

50xDenhardt's solution

Preparation of 100ml of solution:

1g bovine serum albumin

1g ficoll (Sigma-Aldrich)

1g polyvinylpyrrolidone (PVP, Sigma-Aldrich)

Dissolve overnight at 4°C, filter, aliquot and store at -20°C.

DEPC treated Ethylenediaminetetraacetic acid (EDTA, 0.2M and 0.5M)

Preparation of 100ml solution:

7.6g (0.2M) EDTA (Sigma-Aldrich)

19g (0.5M) EDTA

Dissolve the appropriate quantity of EDTA for the molarity desired, in DEPC water (see below) by adjusting the pH to 8 with sodium hydroxide and mixing well. Adjust the final volume of the solution to 100ml with DEPC water. Store at room temperature.

Developing buffer (100mM TRIS-HCl, 100mM NaCl, 50mM MgCl₂, pH 9.5)

Preparation of 100ml of solution:

10ml of 1M tris-HCl solution, pH 9.5 (see below)

2ml of 5M sodium chloride solution (see below)

5ml of 1M magnesium chloride solution (see below)

Mix together appropriate volumes of the solution and make up to 100ml with double distilled water and use immediately.

Diethyl pyrocarbonate treated water (DEPC water)

Preparation of 100ml of solution:

Fill a 100ml Duran bottle with MilliQ water and add 10mL of DEPC (diethyl pyrocarbonate, Sigma-Aldrich). Mix vigorously and leave to stand at room temperature for at least 1 hour before autoclaving for 20 minutes at 121°C. Store at room temperature.

Eosin Y 1% aqueous solution

Preparation of 100ml solution:

1g eosin Y (C.I. 45380, Sigma-Aldrich)

Dissolve the eosin in 100ml of double distilled water and store until use.

Harris haematoxylin solution

Preparation of 100ml solution:

1g haematoxylin (C.I.75290, Merck)

10g aluminium potassium sulphate.12 H₂O (Merck)

0.25g mercuric oxide (Merck)

4ml glacial acetic acid

5ml absolute ethanol

Dissolve the haematoxylin in 5ml of absolute ethanol. Dissolve the aluminium potassium sulphate in 100ml of warmed distilled water. Combine the solutions and boil for 4 minutes, remove from heat and add the mercuric oxide, mix well and then boil for 1 minute or until the dye becomes a dark purple colour. Cool the solution rapidly, under running water and add 4ml of glacial acetic acid and filter. Immediately prior to use dilute 50:50 in absolute ethanol and filter the resulting solution. Store the stock solution in the dark at room temperature.

Hybridization buffer, for Northern blot

Preparation of 100ml solution:

25ml 20xSSC (see below)

10ml 50xDenhardt's solution (see above)

1ml sodium dodecyl sulphate solution 10% (SDS, see below)

1ml e. coli strain W tRNA (10mg/ml)

Mix all the reagents and make up the resulting solution to a final volume of 100ml with sterile DEPC water (see above). Store at -20°C.

***In situ* hybridization solution**

Preparation of 100ml solution:

50ml deionized formamide (Sigma-Aldrich)

20ml sterile 20xSSC Buffer (see below)

2ml 50xDenhardt's solution (see above)

2ml torula RNA yeast (50mg.ml⁻¹, see below)

2ml 2% CHAPS (see above)

1ml heparin (10 mg.ml⁻¹, see above)

Mix all the reagents together and adjust the pH to 6.0 with 2M citric acid solution (see above).

Make up the resulting solution to a final volume of 100ml with sterile DEPC water (see above).

Aliquot and store at -20°C.

Lithium chloride 4M (DEPC treated)

Preparation of 100ml solution:

16.96g lithium chloride (Sigma-Aldrich)

Dissolve in 100ml of DEPC water (see above) and store at room temperature.

Magnesium chloride solution 1M

Preparation of 100ml solution:

20.33g magnesium chloride, hexahydrate (Sigma-Aldrich)

Dissolve in 100ml of double distilled water and store at room temperature.

Maleic acid buffer (MAB; 100mM maleic acid, 150mM NaCl, 0.1% tween-20, pH 7.5)

Preparation of 100ml solution:

1.161g maleic acid (Sigma-Aldrich)

0.8775g sodium chloride (Sigma-Aldrich)

Dissolve in MilliQ water and adjust the pH to 7.5. Complete the volume to 100ml and autoclave for 20 minutes at 121°C. Allow to cool to room temperature and add 100ml of tween-20. Store at room temperature.

Paraformaldehyde 4% (PFA, pH 7.4), for tissue fixation

Preparation of 100ml solution:

4g paraformaldehyde (Sigma-Aldrich)

90ml of sterile MilliQ water

10mL sodium hydroxide (saturated solution)

Mix the paraformaldehyde in 90ml of water and heat to 65°C stirring continuously in a fume cupboard until the paraformaldehyde is completely dissolved. Allow the solution to cool to room temperature and then add 10ml of sterile 1M Phosphate Buffer pH 7.4 (PBS, see below) and with the sodium hydroxide correct the pH to 7.4 if necessary. The solution of fixative can be stored for 1 week at 4°C.

Phosphate buffer 1M pH 7.4 (PB), for the preparation of PFA solutions

Preparation of 100ml solution:

12.46g disodium hydrogen phosphate, dihydrate ($\text{Na}_2\text{HPO}_4 \cdot 2\text{H}_2\text{O}$, Merck)

4.68g sodium dihydrogen phosphate, dihydrate ($\text{NaH}_2\text{PO}_4 \cdot 2\text{H}_2\text{O}$, Merck)

Dissolve the reagents in 60ml of MilliQ water and adjust the pH to 7.4 and make the solution up to a final volume of 100ml. Autoclave the solution for 20 minutes at 121°C. Store at room temperature.

10x Phosphate buffered saline pH 7.0 (PBS)

To prepare 100ml:

7.597g sodium chloride

1.246g disodium hydrogen phosphate, dihydrate ($\text{Na}_2\text{HPO}_4 \cdot 2\text{H}_2\text{O}$)

0.48g sodium dihydrogen phosphate, dihydrate ($\text{NaH}_2\text{PO}_4 \cdot 2\text{H}_2\text{O}$)

Dissolve the reagents in 60ml of MilliQ water, adjust the pH to 7.0 and make the solution up to a final volume of 100ml. Autoclave the solution for 20 minutes at 121°C. Store the stock at room temperature. To prepare 100ml of 1xPBS Buffer dilute 10ml of 10xPBS buffer with 90ml of DEPC water (see above).

Phosphate-triton buffer (PBST)

Preparation of 100ml solution:

To 100ml of 1xPBS (see above) add 100mL of triton-X (Sigma-Aldrich) and mix well to completely dissolve the triton-X.

Phosphate-tween buffer (PTW)

Preparation of 100ml solution:

To 100ml of 1xPBS (see above) add 100mL of tween-20 and mix well to completely dissolve the tween-20.

Sodium acetate 3M, pH 5.2

Preparation of 100ml solution:

24.6g sodium acetate (Merck)

Dissolve the sodium acetate in 60ml of distilled water and adjust the pH to 5.2 with acetic acid. Make the final volume of the solution up to 100ml with distilled water. Store at room temperature.

Sodium chloride solution 5M

Preparation of 100ml solution:

29.25g sodium chloride

Dissolve the sodium chloride in 100ml of double distilled water. Store at room temperature.

20x sodium chloride-sodium citrate buffer (20x SSC)

Preparation of 100ml solution:

17.53g sodium chloride

8.82g sodium citrate

Dissolve all the reagents in 60ml of distilled water. Adjust the pH to 7.0 with acetic acid and complete the volume to 100ml. Autoclave the solution for 20 minutes at 121°C. Store the stock solution at room temperature. To prepare 100ml of 2xSSC dilute 10ml of 20xSSC with 90ml of sterile water. All other concentrations of SSC buffer should be prepared as described using the appropriate amount of concentrated solution.

Sodium dodecyl sulphate 10% (SDS)

Preparation of 100ml solution:

10g sodium dodecyl sulphate (SDS, Merck)

Dissolve in distilled water without agitation to avoid bubble formation. Store at room temperature.

10x Tris-borate-EDTA buffer (10x TBE)

Preparation of 100ml solution:

10.8g tris base (Sigma-Aldrich)

5.5g boric acid (Sigma-Aldrich)

10ml EDTA 0.5M pH 8.0 (see above)

Dissolve the salts in double distilled water and make the volume up to 100ml. Autoclave the solution for 20 minutes at 121°C. Store the stock solution at room temperature. To prepare 100ml of 1xTBE Buffer dilute 10ml of 10xTBE Buffer with 90ml of double distilled water (for gels to run DNA samples) or DEPC water (for gels to run RNA samples).

1M Tris-HCl solution, pH 7.5 (or pH 9.5)

Preparation of 100ml solution:

12.114g tris (Tris(hydroxymethyl)aminomethane)

Dissolve the tris in 60ml of double distilled water and adjust the pH to 7.5 or 9.5 with concentrated hydrochloric acid or sodium hydroxide respectively. Make the volume of the solution up to 100ml with distilled water. Store at room temperature.

Tris-NaCl solution (100 mM TRIS-HCl, 150 mM NaCl, pH 7.5)

Preparation of 100ml solution:

10ml of 1M tris-HCl solution, pH 7.5 (see above)

3ml of 5M sodium chloride solution (see above)

Mix both solutions and complete the volume to 100ml with double distilled water and use immediately.

0.1M TRIZMA buffer, pH7.5, 0.1% BSA (0.01% NaNO₃)

Preparation of 125 ml solution:

1.211g Tris base (Sigma) dilute with 100 ml of double distilled water

1.576g Tris HCl (Sigma) dilute with 100 ml of double distilled water

In order to obtain a 0.1M TRIZMA buffer pH 7.5 add 25 ml of Tris base solution to 100 ml of Tris HCl solution. In the day of the assay add 0.0125g of BSA (Sigma) and 0.00125g of NaNO₃.

0.07M Barbital buffer. pH 8.6, 0.1% BSA

Preparation of 500 ml:

7.22 g of Barbital (Sigma) diluted in 500 ml of double distilled water. In the day of the assay added 0.5g of BSA (Sigma).

8% (w/v) X-Gal

250 mg 5-bromo-4-chloro-3-indolyl-B-D-galactosidase dissolved in 3.13 ml of dimethylformamide.

IPTG

Preparation of 10 ml:

2 g of IPTG (Sigma) diluted in 8 ml of autoclaved double distilled water.

1M MgSO₄

Preparation of 1 litre:

246.4g of MgSO₄.7H₂O diluted in 1 litre of autoclaved double distilled water.

1M MgCl₂

Preparation of 1 litre:

203.3g MgCl₂.6H₂O diluted in 1 litre of autoclaved double distilled water.

SM buffer

Preparation of 1 litre:

5.8g of NaCl

2g of MgSO₄.6H₂O

2g gelatine

50ml of 1M Tris-HCl (pH 7.5).

Dilute in 1 litre of autoclaved double distilled water.

1xYT

Preparation of 1 litre:

16g of tryptone

5g of yeast extract

5g of NaCl

Dilute in 0.75 litres of double distilled water and adjust pH to 7.4 with NaOH. Make the volume to 1 litre with double distilled water and autoclave.

LB broth

Preparation of 1 litre:

10g of NaCl

10g of tryptone

5g of yeast extract

Dilute in 0.75 litres of double distilled water and adjust pH to 7 with NaOH. Make up volume to 1 litre with double distilled water and autoclave.

LB agar

Preparation of 1 litre:

10g of NaCl

10g of tryptone

5g of yeast extract

20g of agar

Dilute in 0.75 litres of double distilled water and adjust pH to 7 with NaOH. Make up volume to 1 litre with double distilled water and autoclave.

NZY agar

Preparation of 1 litre:

5g of NaCl

2g of MgSO₄.7H₂O

5g of yeast extract

10g of NZ amine (casein hydrolyzate)

15g of agar

Dilute in 0.75 litres of double distilled water and adjust pH to 7.5 with NaOH. Make up volume to 1litre with double distilled water and autoclave.

NZY Top agar

Preparation of 1 litre:

5g of NaCl

2g of MgSO₄.7H₂O

5g of yeast extract

10g of NZ amine (casein hydrolyzate)

0.7%(w/v) of agarose

Dilute in 1 litre of double distilled water and autoclave.

REFERENCES

- Abe, T., Suzuki, T., Unno, M., Tokui, T. and Ito, S.: Thyroid hormone transporters: recent advances. *Trends Endocrinol Metab* 13 (2002) 215-20.
- Adams, G.R., McCue, S.A., Zeng, M. and Baldwin, K.M.: Time course of myosin heavy chain transitions in neonatal rats: importance of innervation and thyroid state. *Am. J. Physiol* 276 (1999) R954-R961.
- Alibardi, L.: Immunocytochemical localisation of keratins, associated proteins and uptake of histidine in the epidermis of fish and amphibians. *Acta Histochemica* 104 (2002) 297-310.
- Altschul, S.F., Gish, W., Miller, W., Myers, E.W. and Lipman, D.: Basic local alignment search tool. *Journal of Molecular Biology* 215 (1990) 403-410.
- Altschul, S.F., Madden, T.L., Schaffer, A.A., Zhang, J., Zhang, Z., Miller, W. and Lipman, D.J.: Gapped BLAST and PSI-BLAST: a new generation of protein database search programs. *Nucleic Acids Research (Online)* 25 (1997) 3389-402.
- Amma, L.L., Campos-Barros, A., Wang, Z., Vennstrom, B. and Forrest, D.: Distinct tissue-specific roles for thyroid hormone receptors beta and alpha 1 in regulation of type 1 deiodinase expression. *Molecular Endocrinology (Baltimore, Md.)* 15 (2001) 467-75.
- Andersson, H., Kohn, L., Bernardini, I., Blom, H., Tietze, F. and Gahl, W.: Characterization of lysosomal monoiodotyrosine transport in rat thyroid cells. Evidence for transport by system H. *J Biol Chem* 265 (1990) 10950-10954.
- Aparicio, S., Chapman, J., Stupka, E., Putnam, N., Chia, J.M., Dehal, P., Christoffels, A., Rash, S., Hoon, S., Smit, A., Gelpke, M.D., Roach, J., Oh, T., Ho, I.Y., Wong, M., Detter, C., Verhoef, F., Predki, P., Tay, A., Lucas, S., Richardson, P., Smith, S.F., Clark, M.S., Edwards, Y.J., Doggett, N., Zharkikh, A., Tavtigian, S.V., Pruss, D., Barnstead, M., Evans, C., Baden, H., Powell, J., Glusman, G., Rowen, L., Hood, L., Tan, Y.H., Elgar, G., Hawkins, T., Venkatesh, B., Rokhsar, D. and Brenner, S.: Whole-genome shotgun assembly and analysis of the genome of *Fugu rubripes*. *Science* 297 (2002) 1301-10.
- Aranda, A. and Pascual, A.: Nuclear hormone receptors and gene expression. *Physiol Rev* 81 (2001) 1269-304.
- Attwood, T.K., Bradley, P., Flower, D.R., Gaulton, A., Maudling, N., Mitchell, A.L., Moulton, G., Nordle, A., Paine, K., Taylor, P., Uddin, A. and Zygouri, C.: PRINTS and its automatic supplement, prePRINTS. *Nucl. Acids Res.* 31 (2003) 400-402.
- Balon, E.K.: Saltatory processes and altricial to precocial forms in the ontogeny of fishes. *American Zoologist* 21 (1981) 573-596.
- Balon, E.K.: Reflections on Some Decisive Events in the Early Life of Fishes. *Transactions of the American Fisheries Society* 113 (1984) 178-185.
- Baqi, M., Botero, D., Gereben, B., Curcio, C., Harney, J.W., Salvatore, D., Sorimachi, K., Larsen, P.R. and Bianco, A.C.: Human type 3 iodothyronine selenodeiodinase is located in the plasma membrane and undergoes rapid internalization to endosomes. *The Journal of Biological Chemistry* 278 (2003) 1206-11.
- Baqi, M.M., Gereben, B., Harney, J.W., Larsen, P.R. and Bianco, A.C.: Distinct subcellular localization of transiently expressed types 1 and 2 iodothyronine deiodinases as determined by immunofluorescence confocal microscopy. *Endocrinology* 141 (2000) 4309-12.
- Bartalena, L. and Robbins, J.: Thyroid hormone transport proteins. *Clinics in Laboratory Medicine* 13 (1993) 583-598.

- Bartha, T., Kim, S.W., Salvatore, D., Gereben, B., Tu, H.M., Harney, J.W., Rudas, P. and Larsen, P.R.: Characterization of the 5'-flanking and 5'-untranslated regions of the cyclic adenosine 3',5'-monophosphate-responsive human type 2 iodothyronine deiodinase gene. *Endocrinology* 141 (2000) 229-37.
- Barton, P.J., Cullen, M.E., Townsend, P.J., Brand, N.J., Mullen, A.J., Norman, D.A., Bhavsar, P.K. and Yacoub, M.H.: Close physical linkage of human troponin genes: organization, sequence, and expression of the locus encoding cardiac troponin I and slow skeletal troponin T. *Genomics* 57 (1999) 102-9.
- Bassett, J.H.D., Harvey, C.B. and Williams, G.R.: Mechanisms of thyroid hormone receptor-specific nuclear and extra nuclear actions. *Molecular and Cellular Endocrinology* 213 (2003) 1-11.
- Bastide, B., Kischel, P., Puterflam, J., Stevens, L., Pette, D., Jin, J.P. and Mounier, Y.: Expression and functional implications of troponin T isoforms in soleus muscle fibers of rat after unloading. *Pflugers Archiv : European Journal of Physiology* 444 (2002) 345-52.
- Bates, J.M., St_Germain, D.L. and Galton, V.A.: Expression profiles of the three iodothyronine deiodinases, D1, D2, and D3, in the developing rat. *Endocrinology* 140 (1999) 844-51.
- Becker, K.B., Stephens, K.C., Davey, J.C., Schneider, M.J. and Galton, V.A.: The type 2 and type 3 iodothyronine deiodinases play important roles in coordinating development in *Rana catesbeiana* tadpoles. *Endocrinology* 138 (1997) 2989-97.
- Bejar, J., Borrego, J.J. and Alvarez, M.C.: A continuous cell line from the cultured marine fish gilt-head seabream (*Sparus aurata* L). *Aquaculture* 150 (1997) 143-153.
- Bergh, J.J., Lin, H.-Y., Lansing, L., Mohamed, S.N., Davis, F.B., Mousa, S. and Davis, P.J.: Integrin $\alpha_v\beta_3$ Contains a Cell Surface Receptor Site for Thyroid Hormone that Is Linked to Activation of Mitogen-Activated Protein Kinase and Induction of Angiogenesis. *Endocrinology* 146 (2005) 2864-2871.
- Bernier-Valentin, F., Kostrouch, Z., Rabilloud, R. and Rousset, B.: Analysis of the thyroglobulin internalization process using in vitro reconstituted thyroid follicles: evidence for a coated vesicle-dependent endocytic pathway. *Endocrinology* 129 (1991) 2194-2201.
- Berry, D.L., Rose, C.S., Remo, B.F. and Brown, D.D.: The expression pattern of thyroid hormone response genes in remodeling tadpole tissues defines distinct growth and resorption gene expression programs. *Developmental Biology* 203 (1998) 24-35.
- Berry, M.J., Banu, L. and Larsen, P.R.: Type I iodothyronine deiodinase is a selenocysteine-containing enzyme. *Nature* 349 (1991a) 438-40.
- Berry, M.J., Kates, A.L. and Larsen, P.R.: Thyroid hormone regulates type I deiodinase messenger RNA in rat liver. *Mol Endocrinol* 4 (1990) 743-748.
- Berry, M.J., Kieffer, J.D., Harney, J.W. and Larsen, P.R.: Selenocysteine confers the biochemical properties characteristic of the type I iodothyronine deiodinase. *The Journal of Biological Chemistry* 266 (1991b) 14155-8.
- Bianco, A.C. and Larsen, P.R.: Cellular and Structural Biology of the Deiodinases. *Thyroid* 15 (2005) 777-786.
- Bianco, A.C., Salvatore, D., Gereben, B., Berry, M.J. and Larsen, P.R.: Biochemistry, cellular and molecular biology, and physiological roles of the iodothyronine selenodeiodinases. *Endocrine Reviews* 23 (2002) 38-89.
- Bjorkman, U. and Ekholm, R.: Hydrogen peroxide generation and its regulation in FRTL-5 and porcine thyroid cells. *Endocrinology* 130 (1992) 393-399.

- Breitbart, R.E., Nguyen, H.T., Medford, R.M., Destree, A.T., Mahdavi, V. and Nadal-Ginard, B.: Intricate combinatorial patterns of exon splicing generate multiple regulated troponin T isoforms from a single gene. *Cell* 41 (1985) 67-82.
- Bres, O., Plohman, J.C. and Eales, J.G.: A cDNA for a putative type III deiodinase in the trout (*Oncorhynchus mykiss*): Influence of holding conditions and thyroid hormone treatment on its hepatic expression. *General and Comparative Endocrinology* 145 (2006) 92-100.
- Briggs, M.M., Jacoby, J., Davidowitz, J. and Schachat, F.H.: Expression of a novel combination of fast and slow troponin T isoforms in rabbit extraocular muscles. *Journal of Muscle Research and Cell Motility* 9 (1988) 241-7.
- Briggs, M.M., Klevit, R.E. and Schachat, F.H.: Heterogeneity of contractile proteins. Purification and characterization of two species of troponin T from rabbit fast skeletal muscle. *The Journal of Biological Chemistry* 259 (1984) 10369-75.
- Briggs, M.M., Lin, J.J. and Schachat, F.H.: The extent of amino-terminal heterogeneity in rabbit fast skeletal muscle troponin T. *Journal of Muscle Research and Cell Motility* 8 (1987) 1-12.
- Briggs, M.M., Maready, M., Schmidt, J.M. and Schachat, F.: Identification of a fetal exon in the human fast troponin T gene. *FEBS Letters* 350 (1994) 37-40.
- Briggs, M.M. and Schachat, F.: N-terminal amino acid sequences of three functionally different troponin T isoforms from rabbit fast skeletal muscle. *Journal of Molecular Biology* 206 (1989) 245-9.
- Briggs, M.M. and Schachat, F.: Origin of fetal troponin T: developmentally regulated splicing of a new exon in the fast troponin T gene. *Developmental Biology* 158 (1993) 503-509.
- Briggs, M.M. and Schachat, F.: Physiologically regulated alternative splicing patterns of fast troponin T RNA are conserved in mammals. *The American Journal of Physiology* 270 (1996) C298-305.
- Brown, D.D.: The role of thyroid hormone in zebrafish and axolotl development. *Proc Natl Acad Sci U S A* 94 (1997) 13011-6.
- Brown, D.D.: The Role of Deiodinases in Amphibian Metamorphosis. *Thyroid* 15 (2005) 815-821.
- Bru, C., Courcelle, E., Carrere, S., Beausse, Y., Dalmar, S. and Kahn, D.: The ProDom database of protein domain families: more emphasis on 3D. *Nucleic Acids Research* 33 (2005) D212-215.
- Bucher, E.A., Dhoot, G.K., Emerson, M.M., Ober, M. and Emerson, C.P.: Structure and evolution of the alternatively spliced fast troponin T isoform gene. *The Journal of Biological Chemistry* 274 (1999) 17661-70.
- Buchholz, D.R., Hsia, S.C., Fu, L. and Shi, Y.B.: A dominant-negative thyroid hormone receptor blocks amphibian metamorphosis by retaining corepressors at target genes. *Mol Cell Biol* 23 (2003) 6750-8.
- Buchholz, D.R., Paul, B.D., Fu, L. and Shi, Y.-B.: Molecular and developmental analyses of thyroid hormone receptor function in *Xenopus laevis*, the African clawed frog. *General and Comparative Endocrinology* 145 (2006) 1-19.
- Buchholz, D.R., Tomita, A., Fu, L., Paul, B.D. and Shi, Y.B.: Transgenic analysis reveals that thyroid hormone receptor is sufficient to mediate the thyroid hormone signal in frog metamorphosis. *Mol Cell Biol* 24 (2004) 9026-37.
- Buettner, C., Harney, J.W. and Larsen, P.R.: The 3'-untranslated region of human type 2 iodothyronine deiodinase mRNA contains a functional selenocysteine insertion sequence element. *The Journal of Biological Chemistry* 273 (1998) 33374-8.

- Buettner, C., Harney, J.W. and Larsen, P.R.: The Role of Selenocysteine 133 in Catalysis by the Human Type 2 Iodothyronine Deiodinase. *Endocrinology* 141 (2000) 4606-4612.
- Burmeister, L.A., Pachucki, J. and St_Germain, D.L.: Thyroid hormones inhibit type 2 iodothyronine deiodinase in the rat cerebral cortex by both pre- and posttranslational mechanisms. *Endocrinology* 138 (1997) 5231-7.
- Cahmann, H., Pommier, J. and Nunez, J.: Spatial requirement for coupling of iodotyrosine residues to form thyroid hormone. *Proc Natl Acad Sci USA* 74 (1977) 5333-5335.
- Cai, L. and Brown, D.D.: Expression of type II iodothyronine deiodinase marks the time that a tissue responds to thyroid hormone-induced metamorphosis in *Xenopus laevis*. *Developmental Biology* 266 (2004) 87-95.
- Callery, E.M. and Elinson, R.P.: Thyroid hormone-dependent metamorphosis in a direct developing frog. *Proceedings of the National Academy of Sciences of the United States of America* 97 (2000) 2615-20.
- Campinho, M.A., Moutou, K.A. and Power, D.M.: Temperature sensitivity of skeletal ontogeny in *Oreochromis mossambicus*. *Journal of Fish Biology* 65 (2004) 1003-1025.
- Campinho, M.A., Power, D.M. and Sweeney, G.E.: Identification and analysis of teleost slow muscle troponin T (sTnT) and intronless TnT genes. *Gene* 361 (2005) 67-79.
- Campos-Barros, A., Amma, L.L., Faris, J.S., Shailam, R., Kelley, M.W. and Forrest, D.: Type 2 iodothyronine deiodinase expression in the cochlea before the onset of hearing. *PNAS* 97 (2000) 1287-1292.
- Canettieri, G., Celi, F.S., Baccheschi, G., Salvatori, L., Andreoli, M. and Centanni, M.: Isolation of human type 2 deiodinase gene promoter and characterization of a functional cyclic adenosine monophosphate response element. *Endocrinology* 141 (2000) 1804-13.
- Carvalho, D., Dupuy, C., Gorin, Y., Legue, O., Pommier, J., Haye, B. and Virion, A.: The Ca²⁺- and reduced nicotinamide adenine dinucleotide phosphate-dependent hydrogen peroxide generating system is induced by thyrotropin in porcine thyroid cells. *Endocrinology* 137 (1996) 1007-1012.
- Celi, F.S., Canettieri, G., Mentuccia, D., Proietti_Pannunzi, L., Fumarola, A., Sibilla, R., Predazzi, V., Ferraro, M., Andreoli, M. and Centanni, M.: Structural organization and chromosomal localization of the human type II deiodinase gene. *European Journal of Endocrinology / European Federation of Endocrine Societies* 143 (2000) 267-71.
- Chambard, M., Depetris, D., Gruffat, D., Gonzalez, S., Mauchamp, J. and Chabaud, O.: Thyrotropin regulation of apical and basal exocytosis of thyroglobulin by porcine thyroid monolayers. *Journal of Molecular Endocrinology* 4 (1990) 193-199.
- Chanoine, C. and Hardy, S.: *Xenopus* muscle development: from primary to secondary myogenesis. *Dev Dyn* 226 (2003) 12-23.
- Chassande, O., Fraichard, A., Gauthier, K., Flamant, F., Legrand, C., Savatier, P., Laudet, V. and Samarut, J.: Identification of transcripts initiated from an internal promoter in the c-erbA alpha locus that encode inhibitors of retinoic acid receptor-alpha and triiodothyronine receptor activities. *Molecular Endocrinology* (Baltimore, Md.) 11 (1997) 1278-90.
- Chauvigne, F., Ralliere, C., Cauty, C. and Rescan, P.Y.: In situ hybridisation of a large repertoire of muscle-specific transcripts in fish larvae: the new superficial slow-

- twitch fibres exhibit characteristics of fast-twitch differentiation. *J Exp Biol* 209 (2006) 372-379.
- Chin, W.W. and Yen, P.M.: Molecular mechanisms of nuclear thyroid hormone action. In: Braverman, L.R. (Ed.), *Diseases of the Thyroid*. Humana Press, 1997, pp. 1-15.
- Chistiakov, D.A.: Thyroid-stimulating hormone receptor and its role in Graves' disease. *Molecular Genetics and Metabolism* 80 (2003) 377-388.
- Chua, K.L. and Lim, T.M.: Type I and II cytokeratin cDNAs from the zebrafish (*Danio rerio*) and expression patterns during early development. *Differentiation* 66 (2000) 31-41.
- Conrad, M., Lemb, K., Schubert, T. and Markl, J.: Biochemical identification and tissue-specific expression patterns of keratins in the zebrafish *Danio rerio*. *Cell Tissue Research* 293 (1998) 195-205.
- Cooley, H.M., Fisk, A.T., Wiens, S.C., Tomy, G.T., Evans, R.E. and Muir, D.C.: Examination of the behavior and liver and thyroid histology of juvenile rainbow trout (*Oncorhynchus mykiss*) exposed to high dietary concentrations of C(10)-, C(11)-, C(12)- and C(14)-polychlorinated n-alkanes. *Aquat Toxicol* 54 (2001) 81-99.
- Copeland, P.R., Fletcher, J.E., Carlson, B.A., Hatfield, D.L. and Driscoll, D.M.: A novel RNA binding protein, SBP2, is required for the translation of mammalian selenoprotein mRNAs. *Embo J* 19 (2000) 306-14.
- Corvilain, B., van Sande, J., Laurent, E. and Dumont, J.: The H₂O₂-generating system modulates protein iodination and the activity of the pentose phosphate pathway in dog thyroid. *Endocrinology* 128 (1991) 779-785.
- Coulombe, P.A., Hutton, E., Vassar, R. and Fuchs, E.: A function for keratins and a common thread among different types of epidermolysis bullosa simplex diseases. *The Journal of Cell Biology* 115 (1991) 1661-1674.
- Croteau, W., Davey, J.C., Galton, V.A. and St_Germain, D.L.: Cloning of the mammalian type II iodothyronine deiodinase. A selenoprotein differentially expressed and regulated in human and rat brain and other tissues. *The Journal of Clinical Investigation* 98 (1996) 405-17.
- Croteau, W., Whittlemore, S.L., Schneider, M.J. and St_Germain, D.L.: Cloning and expression of a cDNA for a mammalian type III iodothyronine deiodinase. *The Journal of Biological Chemistry* 270 (1995) 16569-75.
- Curcio-Morelli, C., Gereben, B., Zavacki, A.M., Kim, B.W., Huang, S., Harney, J.W., Larsen, P.R. and Bianco, A.C.: In vivo dimerization of types 1, 2, and 3 iodothyronine selenodeiodinases. *Endocrinology* 144 (2003) 937-46.
- D'Arezzo, S., Incerpi, S., Davis, F.B., Acconcia, F., Marino, M., Farias, R.N. and Davis, P.J.: Rapid Nongenomic Effects of 3,5,3'-Triiodo-L-Thyronine on the Intracellular pH of L-6 Myoblasts Are Mediated by Intracellular Calcium Mobilization and Kinase Pathways. *Endocrinology* 145 (2004) 5694-5703.
- Dai, G., Levy, O. and Carrasco, N.: Cloning and characterization of the thyroid iodide transporter. *Nature* (1996) 458-460.
- Dale, B.A., Holbrook, K.A., Kimball, J.R., Hoff, M. and Sun, T.T.: Expression of epidermal keratins and filaggrin during human fetal skin development. *J. Cell Biol.* 101 (1985) 1257-1269.
- Darras, V.M., Hume, R. and Visser, T.J.: Regulation of thyroid hormone metabolism during fetal development. *Mol Cell Endocrinol* 151 (1999) 37-47.

- Darras, V.M., Mol, K.A., van_der_Geyten and Kuhn, E.R.: Control of peripheral thyroid hormone levels by activating and inactivating deiodinases. *Annals of the New York Academy of Sciences* 839 (1998) 80-6.
- Darras, V.M., Van der Geyten, S. and Kuhn, E.R.: Thyroid hormone metabolism in poultry. *Biotechnology, Agronomy, Society and Environment* 4 (2000) 13-20.
- Davey, J.C., Schneider, M.J., Becker, K.B. and Galton, V.A.: Cloning of a 5.8 kb cDNA for a mouse type 2 deiodinase. *Endocrinology* 140 (1999) 1022-5.
- Davies, T., Marians, R. and Latif, R.: The TSH receptor reveals itself. *J. Clin. Invest.* 110 (2002) 161-164.
- Davis, P.J., Davis, F.B. and Cody, V.: Membrane receptors mediating thyroid hormone action. *Trends Endocrinol Metab* 16 (2005) 429-35.
- de Jesus, E.G., Toledo, J.D. and Simpas, M.S.: Thyroid hormones promote early metamorphosis in grouper (*Epinephelus coioides*) larvae. *General and Comparative Endocrinology* 112 (1998) 10-6.
- Deme, D., Pommier, J. and Nunez, J.: Specificity of thyroid hormone synthesis. The role of thyroid peroxidase. *Biochim Biophys Acta* 540 (1978) 73-82.
- Deshpande, V. and Venkatesh, S.G.: Thyroglobulin, the prothyroid hormone: chemistry, synthesis and degradation. *Biochimica et Biophysica Acta (BBA) - General Subjects* 1430 (1999) 157-178.
- Devoto, S., Melancon, E., Eisen, J. and Westerfield, M.: Identification of separate slow and fast muscle precursor cells in vivo, prior to somite formation. *Development* 122 (1996) 3371-3380.
- Dorit, R.L., Walker, W.F. and Barnes, R.D.: *Zoology*. Saunders College Publishing, Philadelphia, 1991.
- Dremier, S., Coulonval, K., Perpete, S., Vandeput, F., Fortemaison, N., Van Keymeulen, A., Deleu, S., Ledent, C., Clement, S., Schurmans, S., Dumont, J.E., Lamy, F., Roger, P.P. and Maenhaut, C.: The Role of Cyclic AMP and Its Effect on Protein Kinase A in the Mitogenic Action of Thyrotropin on the Thyroid Cell. *Ann NY Acad Sci* 968 (2002) 106-121.
- Dumitrescu, A.M., Liao, X.H., Abdullah, M.S., Lado-Abeal, J., Majed, F.A., Moeller, L.C., Boran, G., Schomburg, L., Weiss, R.E. and Refetoff, S.: Mutations in SECISBP2 result in abnormal thyroid hormone metabolism. *Nat Genet* 37 (2005) 1247-52.
- Dumont, J.E.: The action of thyrotropin on thyroid metabolism. *Vitam Horm* 29 (1971).
- Dunn, J. and Dunn, A.: Thyroglobulin: chemistry, biosynthesis, and proteolysis. In: Braverman LE (Ed.), *The Thyroid*, 8th edition. Utiger R. Lippincott Williams & Wilkins, Philadelphia, 2000, pp. 91-104.
- Eales, J.G. and Brown, S.B.: Measurement and regulation of thyroidal status in teleost fish. *Reviews in Fish Biology and Fisheries* 3 (1993) 299-347.
- Eckey, M., Moehren, U. and Baniahmad, A.: Gene silencing by the thyroid hormone receptor. *Molecular and Cellular Endocrinology* 213 (2003) 13-22.
- Einarsdóttir, I.E., Silva, N., Power, D.M., Smáradóttir, H. and Bjornsson, B.T.: Thyroid and pituitary gland development from hatching through metamorphosis of a teleost flatfish, the Atlantic halibut. *Anatomy and Embryology* 211 (2006) 47-60.
- Einarsdóttir, I.E., Silva, N., Power, D.M., Smáradóttir, H. and Bjornssona, B.T.: Thyroid and pituitary gland development from hatching through metamorphosis of a teleost flatfish, the Atlantic halibut. *Anatomy and Embryology* in press (2005).

- Eisen, A.Z. and Gross, J.: The role of epithelium and mesenchyme in the production of a. *Dev Biol* 12 (1965) 408-18.
- Ellison, T.R., Mathisen, P.M. and Miller, L.: Developmental changes in keratin patterns during epidermal maturation. *Developmental Biology* 112 (1985) 329-37.
- Ercson, L.: Exocytosis and endocytosis in the thyroid cell. *Mol Cell Endocrinol* 22 (1981) 1-24.
- Esfandiari, A., Courtin, F., Lennon, A.M., Gavaret, J.M. and Pierre, M.: Induction of type III deiodinase activity in astroglial cells by thyroid hormones. *Endocrinology* 131 (1992) 1682-1688.
- Essner, J.J., Breuer, J.J., Essner, R.D., Fahrenkrug, S.C. and Hackett, P.B.: The zebrafish thyroid hormone receptor alpha 1 is expressed during early embryogenesis and can function in transcriptional repression. *Differentiation; Research in Biological Diversity* 62 (1997) 107-117.
- Essner, J.J., Johnson, R.G. and Hackett, P.B.: Overexpression of thyroid hormone receptor alpha 1 during zebrafish embryogenesis disrupts hindbrain patterning and implicates retinoic acid receptors in the control of hox gene expression. *Differentiation; Research in Biological Diversity* 65 (1999) 1-11.
- Everts, M.E.: Effects of thyroid hormones on contractility and cation transport in skeletal muscle. *Acta Physiol Scand* 156 (1996) 325-33.
- Fagegaltier, D., Lescure, A., Walczak, R., Carbon, P. and Krol, A.: Structural analysis of new local features in SECIS RNA hairpins. *Nucl. Acids Res.* 28 (2000) 2679-2689.
- Fagman, H., Andersson, L. and Nilsson, M.: The developing mouse thyroid: embryonic vessel contacts and parenchymal growth pattern during specification, budding, migration, and lobulation. *Dev Dyn* 235 (2006) 444-55.
- Farsetti, A., Lazar, J., Phyllaier, M., Lippoldt, R., Pontecorvi, A. and Nikodem, V.M.: Active repression by thyroid hormone receptor splicing variant alpha2 requires specific regulatory elements in the context of native triiodothyronine-regulated gene promoters. *Endocrinology* 138 (1997) 4705-12.
- Farza, H., Townsend, P.J., Carrier, L., Barton, P.J., Mesnard, L., Bahrend, E., Forissier, J.F., Fiszman, M., Yacoub, M.H. and Schwartz, K.: Genomic organisation, alternative splicing and polymorphisms of the human cardiac troponin T gene. *Journal of Molecular and Cellular Cardiology* 30 (1998) 1247-53.
- Faustino, M. and Power, D.M.: Development of osteological structures in the sea bream: vertebral column and caudal fin complex. *Journal of Fish Biology* 52 (1998) 11-22.
- Faustino, M. and Power, D.M.: Development of the pectoral, pelvic, dorsal and anal fins in cultured sea bream. *Journal of Fish Biology* 54 (1999) 1094-1110.
- Faustino, M. and Power, D.M.: Osteologic development of the viscerocranial skeleton in sea bream: alternative ossification strategies in teleost fish. *Journal of Fish Biology* 58 (2001) 537-572.
- Fenton, B., Orozco, A. and Valverde, C.: Kinetic characterisation of skin inner-ring deiodinative pathway and its correlation with circulating levels of reverse triiodothyronine in developing rainbow trout. *J Endocrinol* 154 (1997) 547-54.
- Finsson, K.W. and Eales, J.G.: Effect of T3 treatment and food ration on hepatic deiodination and conjugation of thyroid hormones in rainbow trout, *Oncorhynchus mykiss*. *General and Comparative Endocrinology* 115 (1999) 379-86.
- Fitch, W.M.: Rate of change of concomitantly variable codons. *Journal of Molecular Evolution* 1 (1971) 84-96.

- Flamant, F. and Samarut, J.: Thyroid hormone receptors: lessons from knockout and knock-in mutant mice. *Trends in Endocrinology & Metabolism* 14 (2003) 85-90.
- Flanagan, J.A., Power, D.M., Bendell, L.A., Guerreiro, P.M., Fuentes, J., Clark, M.S., Canario, A.V.M., Danks, J.A., Brown, B.L. and Ingleton, P.M.: Cloning of the cDNA for sea bream (*Sparus aurata*) parathyroid hormone-related protein. *General and Comparative Endocrinology* 118 (2000) 373-382.
- Focant, B., Vanderwalle, P. and Hurliaux, F.: Expression of myofibrillar proteins and parvalbumin isoforms during the development of a flatfish, the common sole *Solea solea*: comparison with the turbot *Scophthalmus maximus*. *Comparative Biochemistry and Physiology B-Biochemistry & Molecular Biology* 135 (2003) 493-502.
- Forrest, D., Reh, T.A. and Rusch, A.: Neurodevelopmental control by thyroid hormone receptors. *Current Opinion in Neurobiology* 12 (2002) 49-56.
- Friesema, E.C., Jansen, J., Milici, C. and Visser, T.J.: Thyroid hormone transporters. *Vitam Horm* 70 (2005) 137-67.
- Fuchs, E. and Weber, K.: Intermediate filaments: structure, dynamics, function, and disease. *Annu Rev Biochem* 63 (1994) 345-82.
- Fujiwara, K., Adachi, H., Nishio, T., Unno, M., Tokui, T., Okabe, M., Onogawa, T., Suzuki, T., Asano, N., Tanemoto, M., Seki, M., Shiiba, K., Suzuki, M., Kondo, Y., Nunoki, K., Shimosegawa, T., Inuma, K., Ito, S., Matsuno, S. and Abe, T.: Identification of Thyroid Hormone Transporters in Humans: Different Molecules Are Involved in a Tissue-Specific Manner. *Endocrinology* 142 (2001) 2005-2012.
- Gahlmann, R., Troutt, A., Wade, R., Gunning, P. and Kedes, L.: Alternative splicing generates variants in important functional domains of human slow skeletal troponin T. *J. Biol. Chem.* 262 (1987) 16122-16126.
- Galay-Burgos, M., Pittman, K., Saele, O., Smaradottir, H. and Sweeney, G.E.: Thyroid hormone receptors in metamorphosing Atlantic halibut., *International Symposium on Fish Endocrinology, Castellón, Spain, September 5-9, 2004, Castellon, Spain, 2004.*
- Galton, V.A.: The Roles of the Iodothyronine Deiodinases in Mammalian Development. *Thyroid* 15 (2005) 823-834.
- Galton, V.A., Martinez, E., Hernandez, A., St_Germain, E.A., Bates, J.M. and St_Germain, D.L.: Pregnant rat uterus expresses high levels of the type 3 iodothyronine deiodinase. *The Journal of Clinical Investigation* 103 (1999) 979-87.
- Garcia-G, C., Jeziorski, M.C., Valverde-R, C. and Orozco, A.: Effects of iodothyronines on the hepatic outer-ring deiodinating pathway in killifish. *General and Comparative Endocrinology* 135 (2004) 201-209.
- Gardahaut, M.F., Fontaine-Perus, J., Rouaud, T., Bandman, E. and Ferrand, R.: Developmental modulation of myosin expression by thyroid hormone in avian skeletal muscle. *Development* 115 (1992) 1121-31.
- Gauthier, K., Chassande, O., Plateroti, M., Roux, J.P., Legrand, C., Pain, B., Rousset, B., Weiss, R., Trouillas, J. and Samarut, J.: Different functions for the thyroid hormone receptors TRalpha and TRbeta in the control of thyroid hormone production and post-natal development. *The Embo Journal* 18 (1999) 623-31.
- Gauthier, K., Plateroti, M., Harvey, C.B., Williams, G.R., Weiss, R.E., Refetoff, S., Willott, J.F., Sundin, V., Roux, J.P., Malaval, L., Hara, M., Samarut, J. and Chassande, O.: Genetic analysis reveals different functions for the products of

- the thyroid hormone receptor alpha locus. *Molecular and Cellular Biology* 21 (2001) 4748-60.
- Gavaret, J.-M., Cahnmann, H. and Nunez, J.: Thyroid hormone synthesis in thyroglobulin; the mechanism of the coupling reaction. *J Biol Chem* 256 (1981) 9167-9172.
- Gavaret, J.-M., Nunez, J. and Cahnmann, H.: Formation of dehydroalanine residues during thyroid hormone synthesis in thyroglobulin. *J Biol Chem* 255 (1980) 5281-5285.
- Gereben, B., Goncalves, C., Harney, J.W., Larsen, P.R. and Bianco, A.C.: Selective proteolysis of human type 2 deiodinase: a novel ubiquitin-proteasomal mediated mechanism for regulation of hormone activation. *Molecular Endocrinology* (Baltimore, Md.) 14 (2000) 1697-708.
- Gereben, B., Kollar, A., Harney, J.W. and Larsen, P.R.: The mRNA structure has potent regulatory effects on type 2 iodothyronine deiodinase expression. *Molecular Endocrinology* (Baltimore, Md.) 16 (2002) 1667-79.
- Gereben, B., Pachucki, J., Kollar, A., Liposits, Z. and Fekete, C.: Ontogenic Redistribution of Type 2 Deiodinase Messenger Ribonucleic Acid in the Brain of Chicken. *Endocrinology* 145 (2004) 3619-3625.
- Guadano-Ferraz, A., Escamez, M.J., Rausell, E. and Bernal, J.: Expression of type 2 iodothyronine deiodinase in hypothyroid rat brain indicates an important role of thyroid hormone in the development of specific primary sensory systems. *J Neurosci* 19 (1999) 3430-9.
- Guissouma, H., Becker, N., Seugnet, I. and Demeneix, B.A.: Transcriptional repression of TRH promoter function by T3: analysis by in vivo gene transfer. *Biochemistry and Cell Biology* 78 (2000) 155-163.
- Hadley, M.E.: *Endocrinology*, 3rd Edition. ed. Prentice-Hall International, London., 1992.
- Harvey, C.B. and Williams, G.R.: Mechanism of Thyroid Hormone Action. *Thyroid* 12 (2002) 441-446.
- Hastings, K.E., Bucher, E.A. and Emerson, C.P.: Generation of troponin T isoforms by alternative RNA splicing in avian skeletal muscle. Conserved and divergent features in birds and mammals. *The Journal of Biological Chemistry* 260 (1985) 13699-703.
- Henry, C.A. and Amacher, S.L.: Zebrafish slow muscle cell migration induces a wave of fast muscle morphogenesis. *Developmental Cell* 7 (2004) 917-923.
- Hernandez, A., Lyon, G.J., Schneider, M.J. and St_Germain, D.L.: Isolation and characterization of the mouse gene for the type 3 iodothyronine deiodinase. *Endocrinology* 140 (1999) 124-30.
- Hernandez, A., Martinez, M.E., Fiering, S., Galton, V.A. and St. Germain, D.: Type 3 deiodinase is critical for the maturation and function of the thyroid axis. *J. Clin. Invest.* 116 (2006) 476-484.
- Hernandez, A., Park, J.P., Lyon, G.J., Mohandas, T.K. and St_Germain, D.L.: Localization of the type 3 iodothyronine deiodinase (DIO3) gene to human chromosome 14q32 and mouse chromosome 12F1. *Genomics* 53 (1998) 119-21.
- Hesse, M., Magin, T.M. and Weber, K.: Genes for intermediate filament proteins and the draft sequence of the human genome: novel keratin genes and a surprisingly high number of pseudogenes related to keratin genes 8 and 18. *Journal of Cell Science* 114 (2001) 2569-2575.

- Hesse, M., Zimek, A., Weber, K. and Magin, T.M.: Comprehensive analysis of keratin gene clusters in humans and rodents. *European Journal of Cell Biology* 83 (2004) 19-26.
- Hodin, R.A., Lazar, M.A., Wintman, B.I., Darling, D.S., Koenig, R.J., Larsen, P.R., Moore, D.D. and Chin, W.W.: Identification of a thyroid hormone receptor that is pituitary-specific. *Science* 244 (1989) 76-9.
- Hollenberg, A., Monden, T., Flynn, T., Boers, M., Cohen, O. and Wondisford, F.: The human thyrotropin-releasing hormone gene is regulated by thyroid hormone through two distinct classes of negative thyroid hormone response elements. *Molecular Endocrinology* 9 (1995) 540-550.
- Hsiang, B., Zhu, Y., Wang, Z., Wu, Y., Sasseville, V., Yang, W.-P. and Kirchgessner, T.G.: A Novel Human Hepatic Organic Anion Transporting Polypeptide (OATP2). IDENTIFICATION OF A LIVER-SPECIFIC HUMAN ORGANIC ANION TRANSPORTING POLYPEPTIDE AND IDENTIFICATION OF RAT AND HUMAN HYDROXYMETHYLGLUTARYL-CoA REDUCTASE INHIBITOR TRANSPORTERS. *J. Biol. Chem.* 274 (1999) 37161-37168.
- Hsiao, C.D., Tsai, W.Y., Horng, L.S. and Tsai, H.J.: Molecular structure and developmental expression of the three muscle-type troponin T genes in zebrafish. *Developmental Dynamics* 227 (2003) 266-79.
<http://au.expasy.org>.
<http://fugu.hgmp.mrc.ac.uk>.
<http://medaka.lab.nig.ac.jp>.
- Huang, H., Cai, L., Remo, B.F. and Brown, D.D.: Timing of metamorphosis and the onset of the negative feedback loop between the thyroid gland and the pituitary is controlled by type II iodothyronine deiodinase in *Xenopus laevis*. *PNAS* 98 (2001) 7348-7353.
- Huang, H., Marsh-Armstrong, N. and Brown, D.D.: Metamorphosis is inhibited in transgenic *Xenopus laevis* tadpoles that overexpress type III deiodinase. *PNAS* 96 (1999a) 962-967.
- Huang, H., Marsh_Armstrong, N. and Brown, D.D.: Metamorphosis is inhibited in transgenic *Xenopus laevis* tadpoles that overexpress type III deiodinase. *Proceedings of the National Academy of Sciences of the United States of America* 96 (1999b) 962-7.
- Huang, L., Schreiber, A.M., Soffientino, B., Bengtson, D.A. and Specker, J.L.: Metamorphosis of summer flounder (*Paralichthys dentatus*): Thyroid status and the timing of gastric gland formation. *The Journal of Experimental Zoology* 280 (1998a) 413-420.
- Huang, L.Y., Miwa, S., Bengtson, D.A. and Specker, J.L.: Effect of triiodothyronine on stomach formation and pigmentation in larval striped bass (*Morone saxatilis*). *Journal of Experimental Zoology* 280 (1998b) 231-237.
- Huang, Q.Q., Brozovich, F.V. and Jin, J.P.: Fast skeletal muscle troponin T increases the cooperativity of transgenic mouse cardiac muscle contraction. *520 Pt 1* (1999c) 231-42.
- Huang, Q.Q., Chen, A. and Jin, J.P.: Genomic sequence and structural organization of mouse slow skeletal muscle troponin T gene. *Gene* 229 (1999d) 1-10.
- Huang, Q.Q. and Jin, J.P.: Preserved close linkage between the genes encoding troponin I and troponin T, reflecting an evolution of adapter proteins coupling the Ca(2+) signaling of contractility. *Journal of Molecular Evolution* 49 (1999) 780-8.
- Huang, S.A., Dorfman, D.M., Genest, D.R., Salvatore, D. and Larsen, P.R.: Type 3 iodothyronine deiodinase is highly expressed in the human uteroplacental unit

- and in fetal epithelium. *The Journal of Clinical Endocrinology and Metabolism* 88 (2003) 1384-8.
- Huang, T.S., Chopra, I.J., Boado, R., Soloman, D.H. and Chua Teco, G.N.: Thyroxine inner ring monodeiodinating activity in fetal tissues of the rat. *Pediatr Res* 23 (1988) 196-199.
- Hutton, E., Paladini, R.D., Yu, Q.C., Yen, M., Coulombe, P.A. and Fuchs, E.: Functional differences between keratins of stratified and simple epithelia. *The Journal of Cell Biology* 143 (1998) 487-499.
- Imboden, M., Goblet, C., Kom, H. and Vríz, S.: Cytokeratin 8 is a suitable epidermal marker during zebrafish development. *C R Acad Sci III* 320 (1997) 689-700.
- Inui, Y. and Miwa, S.: Thyroid-Hormone Induces Metamorphosis of Flounder Larvae. *General and Comparative Endocrinology* 60 (1985) 450-454.
- Inui, Y., Yamano, K. and Miwa, S.: The role of thyroid hormone in tissue development in metamorphosing flounder. *Aquaculture* 135 (1995) 87-98.
- Ishida, Y., Suzuki, K., Utoh, R., Obara, M. and Yoshizato, K.: Molecular identification of the skin transformation center of anuran larval skin using genes of *Rana* adult keratin (RAK) and SPARC as probes. *Development, Growth & Differentiation* 45 (2003) 515-526.
- Jaillon, O., Aury, J.-M., Brunet, F., Petit, J.-L., Stange-Thomann, N., Mauceli, E., Bouneau, L., Fischer, C., Ozouf-Costaz, C., Bernot, A., Nicaud, S., Jaffe, D., Fisher, S., Lutfalla, G., Dossat, C., Segurens, B., Dasilva, C., Salanoubat, M., Levy, M., Boudet, N., Castellano, S., Anthouard, V., Jubin, C., Castelli, V., Katinka, M., Vacherie, B., Biemont, C., Skalli, Z., Cattolico, L., Poulain, J., de Berardinis, V., Cruaud, C., Duprat, S., Brottier, P., Coutanceau, J.-P., Gouzy, J., Parra, G., Lardier, G., Chapple, C., McKernan, K.J., McEwan, P., Bosak, S., Kellis, M., Volff, J.-N., Guigo, R., Zody, M.C., Mesirov, J., Lindblad-Toh, K., Birren, B., Nusbaum, C., Kahn, D., Robinson-Rechavi, M., Laudet, V., Schachter, V., Quetier, F., Saurin, W., Scarpelli, C., Wincker, P., Lander, E.S., Weissenbach, J. and Roest Crollius, H.: Genome duplication in the teleost fish *Tetraodon nigroviridis* reveals the early vertebrate proto-karyotype. *Nature* 431 (2004) 946-957.
- Jakobs, T.C., Koehler, M.R., Schmutzler, C., Glaser, F., Schmid, M. and Kohrle, J.: Structure of the human type I iodothyronine 5'-deiodinase gene and localization to chromosome 1p32-p33. *Genomics* 42 (1997a) 361-3.
- Jakobs, T.C., Schmutzler, C., Meissner, J. and Kohrle, J.: The promoter of the human type I 5'-deiodinase gene--mapping of the transcription start site and identification of a DR+4 thyroid-hormone-responsive element. *European Journal of Biochemistry* 247 (1997b) 288-97.
- Jansen, J., Friesema, E.C., Milici, C. and Visser, T.J.: Thyroid hormone transporters in health and disease. *Thyroid* 15 (2005) 757-68.
- Jho, S.H., Radoja, N., Im, M.J. and Tomic-Canic, M.: Negative response elements in keratin genes mediate transcriptional repression and the cross-talk among nuclear receptors. *J Biol Chem* 276 (2001) 45914-20.
- Jho, S.H., Vouthounis, C., Lee, B., Stojadinovic, O., Im, M.J., Brem, H., Merchant, A., Chau, K. and Tomic-Canic, M.: The book of opposites: the role of the nuclear receptor co-regulators in the suppression of epidermal genes by retinoic acid and thyroid hormone receptors. *J Invest Dermatol* 124 (2005) 1034-43.
- Jin, J.P.: Alternative RNA splicing-generated cardiac troponin T isoform switching: a non-heart-restricted genetic programming synchronized in developing cardiac

- and skeletal muscles. *Biochemical and Biophysical Research Communications* 225 (1996) 883-9.
- Jin, J.P., Chen, A. and Huang, Q.Q.: Three alternatively spliced mouse slow skeletal muscle troponin T isoforms: conserved primary structure and regulated expression during postnatal development. *Gene* 214 (1998a) 121-9.
- Jin, J.P., Chen, A., Ogut, O. and Huang, Q.Q.: Conformational modulation of slow skeletal muscle troponin T by an NH₂-terminal metal-binding extension. *American Journal of Physiology. Cell Physiology* 279 (2000a) C1067-77.
- Jin, J.P., Huang, Q.Q., Ogut, O., Chen, A. and Wang, J.: Troponin T isoform regulation and structure-function relationships. *Basic and Applied Myology* 10 (2000b) 17-26.
- Jin, J.P. and Lin, J.J.: Rapid purification of mammalian cardiac troponin T and its isoform switching in rat hearts during development. *The Journal of Biological Chemistry* 263 (1988) 7309-15.
- Jin, J.P., Wang, J. and Ogut, O.: Developmentally regulated muscle type-specific alternative splicing of the COOH-terminal variable region of fast skeletal muscle troponin T and an aberrant splicing pathway to encode a mutant COOH-terminus. *Biochemical and Biophysical Research Communications* 242 (1998b) 540-4.
- Jin, J.P., Wang, J. and Zhang, J.: Expression of cDNAs encoding mouse cardiac troponin T isoforms: characterization of a large sample of independent clones. *Gene* 168 (1996) 217-21.
- Johnston, I.A.: Development and plasticity of fish muscle with growth. *Basic and Applied Myology* 4 (1994) 353-368.
- Johnston, I.A., Cole, N.J., Abercromby, M. and Vieira, V.L.A.: Embryonic temperature modulates muscle growth characteristics in larval and juvenile herring. *Journal of Experimental Biology* 201 (1998) 623-646.
- Johnston, I.A., Cole, N.J., Vieira, V.L.A. and Davidson, I.: Temperature and developmental plasticity of muscle phenotype in herring larvae. *Journal of Experimental Biology* 200 (1997) 849-868.
- Jonas, E., Sargent, T.D. and Dawid, I.B.: Epidermal keratin gene expressed in embryos of *Xenopus laevis*. *Proc Natl Acad Sci U S A* 82 (1985) 5413-5417.
- Jones, I., Rogers, S.A., Kille, P. and Sweeney, G.E.: Molecular cloning and expression of thyroid hormone receptor alpha during salmonid development. *General and Comparative Endocrinology* 125 (2002) 226-35.
- Jozaki, M., Hosoda, K. and Miyazaki, J.I.: Differential expression of mutually exclusive exons of the fast skeletal muscle troponin T gene in the chicken wing and leg muscles. *Journal of Muscle Research and Cell Motility* 23 (2002) 235-243.
- Kalisnik, M., Jakopin, P. and Sustarsic, J.: On the methodology of the thyroid epithelial cell thickness determination. *J Microsc* 110 (1977) 157-62.
- Kaneshige, M., Kaneshige, K., Zhu, X., Dace, A., Garrett, L., Carter, T.A., Kazlauskaitė, R., Pankratz, D.G., Wynshaw-Boris, A., Refetoff, S., Weintraub, B., Willingham, M.C., Barlow, C. and Cheng, S.: Mice with a targeted mutation in the thyroid hormone beta receptor gene exhibit impaired growth and resistance to thyroid hormone. *Proc Natl Acad Sci U S A* 97 (2000) 13209-14.
- Katz, D. and Lazar, M.A.: Dominant negative activity of an endogenous thyroid hormone receptor variant (alpha 2) is due to competition for binding sites on target genes. *The Journal of Biological Chemistry* 268 (1993) 20904-10.

- Kawahara, A., Gohda, Y. and Hikosaka, A.: Role of type III iodothyronine 5-deiodinase gene expression in temporal regulation of *Xenopus* metamorphosis. *Development, Growth and Differentiation* 41 (1999) 365-373.
- Kawai, A., Ikeya, J., Kinoshita, T. and Yoshizato, K.: A three-step mechanism of action of thyroid hormone and mesenchyme in metamorphic changes in anuran larval skin. *Dev Biol* 166 (1994) 477-88.
- Kester, M.H.A., Martinez de Mena, R., Jesus Obregon, M., Marinkovic, D., Howatson, A., Visser, T.J., Hume, R. and Morreale de Escobar, G.: Iodothyronine Levels in the Human Developing Brain: Major Regulatory Roles of Iodothyronine Deiodinases in Different Areas. *J Clin Endocrinol Metab* 89 (2004) 3117-3128.
- Kim, P. and Arvan, P.: Folding and assembly of newly synthesized thyroglobulin occurs in a pre-Golgi compartment. *J Biol Chem* 266 (1991) 12412-12418.
- Kim, P. and Arvan, P.: Calnexin and BiP act as sequential molecular chaperones during thyroglobulin folding in the endoplasmic reticulum. *J Cell Biol* 128 (1995) 29-38.
- Kim, P., Bole, D. and Arvan, P.: Transient aggregation of nascent thyroglobulin in the endoplasmic reticulum: relationship to the molecular chaperone, BiP. *J Cell Biol* 118 (1992) 541-549.
- Kim, S.-W., Harney, J.W. and Larsen, P.R.: Studies of the Hormonal Regulation of Type 2 5'-Iodothyronine Deiodinase Messenger Ribonucleic Acid in Pituitary Tumor Cells Using Semiquantitative Reverse Transcription-Polymerase Chain Reaction. *Endocrinology* 139 (1998) 4895-4905.
- Kim, S.-W., Ho, S.-C., Hong, S.-J., Kim, K.M., So, E.C., Christoffolette, M. and Harney, J.W.: A Novel Mechanism of Thyroid Hormone-dependent Negative Regulation by Thyroid Hormone Receptor, Nuclear Receptor Corepressor (NCoR), and GAGA-binding Factor on the Rat CD44 Promoter. *J. Biol. Chem.* 280 (2005) 14545-14555.
- Kim, S.-W., Hong, S.-J., Kim, K.M., Ho, S.-C., So, E.C., Harney, J.W. and Larsen, P.R.: A Novel Cell Type-Specific Mechanism for Thyroid Hormone-Dependent Negative Regulation of the Human Type 1 Deiodinase Gene. *Mol Endocrinol* 18 (2004) 2924-2936.
- Kimura, T., Okajima, F., Sho, K., Kobayashi, I. and Kondo, Y.: Thyrotropin-induced hydrogen peroxide production in FRTL-5 thyroid cells is mediated not by adenosine 3',5'-monophosphate, but by Ca²⁺ signaling followed by phospholipase-A2 activation and potentiated by an adenosine derivative. *Endocrinology* 136 (1995) 116-123.
- Kirfel, J., Magin, T.M. and Reichelt, J.: Keratins: a structural scaffold with emerging functions. *Cellular and Molecular Life Sciences (CMLS)* 60 (2003) 56-71.
- Klaren, P.H., Haasdijk, R., Metz, J.R., Nitsch, L.M., Darras, V.M., Van der Geyten, S. and Flik, G.: Characterization of an iodothyronine 5'-deiodinase in gilthead seabream (*Sparus auratus*) that is inhibited by dithiothreitol. *Endocrinology* 146 (2005) 5621-30.
- Kohrle, J.: The selenoenzyme family of deiodinase isozymes controls local thyroid hormone availability. 1 (2000) 49-58.
- Kollmus, H., Flohe, L. and McCarthy, J.E.: Analysis of eukaryotic mRNA structures directing cotranslational incorporation of selenocysteine. *Nucleic Acids Res* 24 (1996) 1195-201.
- Kouklis, P.D., Hutton, E. and Fuchs, E.: Making a connection: Direct binding between intermediate filaments and desmosomal proteins. *The Journal of Cell Biology* 127 (1994) 1049-1060.

- Koumans, J.T.M. and Akster, H.A.: Myogenic cells in development and growth of fish. *Comparative Biochemistry and Physiology a-Physiology* 110 (1995) 3-20.
- Krushna Padhi, B., Akimenko, M.-A. and Ekker, M.: Independent expansion of the keratin gene family in teleostean fish and mammals: An insight from phylogenetic analysis and radiation hybrid mapping of keratin genes in zebrafish. *Gene* 368 (2006) 37-45.
- Kryukov, G.V., Castellano, S., Novoselov, S.V., Lobanov, A.V., Zehtab, O., Guigo, R. and Gladyshev, V.N.: Characterization of Mammalian Selenoproteomes. *Science* 300 (2003) 1439-1443.
- Kuiper, G.G., Klootwijk, W. and Visser, T.J.: Substitution of cysteine for a conserved alanine residue in the catalytic center of type II iodothyronine deiodinase alters interaction with reducing cofactor. *Endocrinology* 143 (2002) 1190-8.
- Kuiper, G.G., Klootwijk, W. and Visser, T.J.: Substitution of cysteine for selenocysteine in the catalytic center of type III iodothyronine deiodinase reduces catalytic efficiency and alters substrate preference. *Endocrinology* 144 (2003) 2505-13.
- Kuiper, G.G.J.M., Kester, M.H.A., Peeters, R.P. and Visser, T.J.: Biochemical Mechanisms of Thyroid Hormone Deiodination. *Thyroid* 15 (2005) 787-798.
- Lamas, L., Taurog, A., Salvatore, G. and Edelhofer, H.: The importance of thyroglobulin structure in thyroid peroxidase-catalyzed conversion of diiodotyrosine to thyroxine. *J Biol Chem* 249 (1974) 2732-2737.
- Lambert, A., Lescure, A. and Gautheret, D.: A survey of metazoan selenocysteine insertion sequences. *Biochimie* 84 (2002) 953-9.
- Langeland, A. and A., K.: Fish development. In: Gilbert, J.R. (Ed.), *Embryology: Constructing the organism*. Sinauer, New York, 1997.
- Langlois, M.F., Zanger, K., Monden, T., Safer, J.D., Hollenberg, A.N. and Wondisford, F.E.: A unique role of the beta-2 thyroid hormone receptor isoform in negative regulation by thyroid hormone. Mapping of a novel amino-terminal domain important for ligand-independent activation. *The Journal of Biological Chemistry* 272 (1997) 24927-33.
- Langsteger, W.: Clinical aspects and diagnosis of thyroid hormone transport protein anomalies. *Current Topics in Pathology* 91 (1997) 129-161.
- Larsson, L., Li, X., Teresi, A. and Salviati, G.: Effects of thyroid hormone on fast- and slow-twitch skeletal muscles in young and old rats. *J Physiol* 481 (Pt 1) (1994) 149-61.
- Larsson, L., Muller, U., Li, X. and Schiaffino, S.: Thyroid hormone regulation of myosin heavy chain isoform composition in young and old rats, with special reference to IIX myosin. *Acta Physiol Scand* 153 (1995) 109-16.
- Lazar, V., Bidart, J.-M., Caillou, B., Mahe, C., Lacroix, L., Filetti, S. and Schlumberger, M.: Expression of the Na⁺/I⁻ Symporter Gene in Human Thyroid Tumors: A Comparison Study with Other Thyroid-Specific Genes. *J Clin Endocrinol Metab* 84 (1999) 3228-3234.
- Le Guellec, D., Morvan-Dubois, G. and Sire, J.Y.: Skin development in bony fish with particular emphasis on collagen deposition in the dermis of the zebrafish (*Danio rerio*). *Int J Dev Biol* 48 (2004) 217-31.
- Leatherland, J.F.: Reflections on the thyroidology of fishes: from molecules to humankind, Guelph, 1994.
- Leatherland, J.F. and Farbridge, K.J.: Chronic fasting reduces the response of the thyroid to growth hormone and TSH, and alters the growth hormone-related

- changes in hepatic 5'-monodeiodinase activity in rainbow trout, *Oncorhynchus mykiss*. *General and Comparative Endocrinology* 87 (1992) 342-53.
- Leeuw, T., Kapp, M. and Pette, D.: Role of innervation for development and maintenance of troponin subunit isoform patterns in fast- and slow-twitch muscle of the rabbit. *Differentiation* 55 (1994) 193-201.
- Leonard, D.M., Stachelek, S.J., Safran, M., Farwell, A.P., Kowalik, T.F. and Leonard, J.L.: Cloning, expression, and functional characterization of the substrate binding subunit of rat type II iodothyronine 5'-deiodinase. *The Journal of Biological Chemistry* 275 (2000) 25194-201.
- Leonard, J. and Köhrle, J.: Intracellular pathways of iodothyronine metabolism. In: Braverman, L. and Utiger, R. (Eds.), *The Thyroid*. Lippincott-Raven, Philadelphia, 2000, pp. 136-173.
- Lin, K., Chen, S., Zhu, X.G., Shieh, H., McPhie, P. and Cheng, S.: The gene regulating activity of thyroid hormone nuclear receptors is modulated by cell-type specific factors. *Biochem Biophys Res Commun* 238 (1997) 280-4.
- Liu, Y.W. and Chan, W.K.: Thyroid hormones are important for embryonic to larval transitory phase in zebrafish. *Differentiation; Research in Biological Diversity* 70 (2002) 36-45.
- Liu, Y.W., Lo, L.J. and Chan, W.K.: Temporal expression and T3 induction of thyroid hormone receptors alpha1 and beta1 during early embryonic and larval development in zebrafish, *Danio rerio*. *Molecular and Cellular Endocrinology* 159 (2000) 187-195.
- Llewellyn, L., Nowell, M.A., Ramsurn, V.P., Wigham, T., Sweeney, G.E., Kristjansson, B. and Halldorsson, O.: Molecular cloning and developmental expression of the halibut thyroid hormone receptor- α . *Journal of Fish Biology* 55 (1999) 148-155.
- Llewellyn, L., Ramsurn, V.P., Sweeney, G.E., Wigham, T. and Power, D.M.: Expression of thyroid hormone receptor during early development of the sea bream (*Sparus aurata*). *Annals New York Academy of Sciences* 839 (1998) 610-611.
- Lloyd, C., Yu, Q.C., Cheng, J., Turksen, K., Degenstein, L., Hutton, E. and Fuchs, E.: The basal keratin network of stratified squamous epithelia: Defining K15 function in the absence of K14. *The Journal of Cell Biology* 129 (1995) 1329-1344.
- Loy, B.A., Boglione, C. and Cataudella, S.: Geometric morphometrics and morpho-anatomy: a combined tool in the study of sea bream (*Sparus aurata*, sparidae) shape. *Journal of Applied Ichthyology* 15 (1999) 104-110.
- Macchia, P.E., Takeuchi, Y., Kawai, T., Cua, K., Gauthier, K., Chassande, O., Seo, H., Hayashi, Y., Samarut, J., Murata, Y., Weiss, R.E. and Refetoff, S.: Increased sensitivity to thyroid hormone in mice with complete deficiency of thyroid hormone receptor alpha. *Proceedings of the National Academy of Sciences of the United States of America* 98 (2001) 349-54.
- MacFarland, S.M., Jin, J.P. and Brozovich, F.V.: Troponin T isoforms modulate calcium dependence of the kinetics of the cross-bridge cycle: studies using a transgenic mouse line. *Archives of Biochemistry and Biophysics* 405 (2002) 241-6.
- MacLatchy, D.L. and Eales, J.G.: Properties of T4 5'-deiodinating systems in various tissues of the rainbow trout, *Oncorhynchus mykiss*. *General and Comparative Endocrinology* 86 (1992) 313-22.

- MacLatchy, D.L., Kawauchi, H. and Eales, J.G.: Stimulation of hepatic thyroxine 5'-deiodinase activity in rainbow trout (*Oncorhynchus mykiss*) by Pacific salmon growth hormone. 101 (1992) 689-91.
- Maia, A.L., Kieffer, J.D., Harney, J.W. and Larsen, P.R.: Effect of 3,5,3'-Triiodothyronine (T3) administration on *diol* gene expression and T3 metabolism in normal and type 1 deiodinase-deficient mice. *Endocrinology* 136 (1995) 4842-9.
- Maia, A.L., Kim, B.W., Huang, S.A., Harney, J.W. and Larsen, P.R.: Type 2 iodothyronine deiodinase is the major source of plasma T3 in euthyroid humans. *J. Clin. Invest.* 115 (2005) 2524-2533.
- Maranduba, C.M., Friesema, E.C., Kok, F., Kester, M.H., Jansen, J., Sertie, A.L., Passos-Bueno, M.R. and Visser, T.J.: Decreased cellular uptake and metabolism in Allan-Herndon-Dudley syndrome (AHDS) due to a novel mutation in the MCT8 thyroid hormone transporter. *J Med Genet* 43 (2006) 457-60.
- Marchand, O., Duffraisse, M., Triqueneaux, G., Safi, R. and Laudet, V.: Molecular cloning and developmental expression patterns of thyroid hormone receptors and T3 target genes in the turbot (*Scophthalmus maximus*) during post-embryonic development. *Gen Comp Endocrinol* 135 (2004) 345-57.
- Marchand, O., Safi, R., Escriva, H., Van Rompaey, E., Prunet, P. and Laudet, V.: Molecular cloning and characterization of thyroid hormone receptors in teleost fish. *Journal of Molecular Endocrinology* 26 (2001) 51-65.
- Marco-Ferreres, R., Arredondo, J.J., Fraile, B. and Cervera, M.: Overexpression of troponin T in *Drosophila* muscles causes a decrease in the levels of thin-filament proteins. *Biochemical Journal* 386 (2005) 145-152.
- Marino, M. and McCluskey, R.T.: Role of thyroglobulin endocytic pathways in the control of thyroid hormone release. *American Journal of Physiology-Cell Physiology* 279 (2000) C1295-C1306.
- Marsh-Armstrong, N., Cai, L. and Brown, D.D.: Thyroid hormone controls the development of connections between the spinal cord and limbs during *Xenopus laevis* metamorphosis. *Proc Natl Acad Sci U S A* 101 (2004) 165-70.
- Marsh-Armstrong, N., Huang, H., Remo, B.F., Liu, T.T. and Brown, D.D.: Asymmetric growth and development of the *Xenopus laevis* retina during metamorphosis is controlled by type III deiodinase. *Neuron* 24 (1999) 871-8.
- Martin-Belmonte, F., Alonso, M., Zhang, X. and Arvan, P.: Thyroglobulin is selected as luminal protein cargo for apical transport via detergent-resistant membranes in epithelial cells. *J Biol Chem* 275 (2000) 41074-41081.
- Martorana, M.L., Tawk, M., Lapointe, T., Barre, N., Imboden, M., Joulie, C., Geraudie, J. and Vriza, S.: Zebrafish keratin 8 is expressed at high levels in the epidermis of regenerating caudal fin. *Int J Dev Biol* 45 (2001) 449-52.
- Mascarello, F., Rowleron, A., Radaelli, G., Scapolo, P.A. and Veggetti, A.: Differentiation and growth of muscle in the fish *Sparus aurata* (L): I. Myosin expression and organization of fibre types in lateral muscle from hatching to adult. *Journal of Muscle Research and Cell Motility* 16 (1995) 213-22.
- Mascia, A., Nitsch, L., Di Lauro, R. and Zannini, M.: Hormonal control of the transcription factor Pax8 and its role in the regulation of thyroglobulin gene expression in thyroid cells. *The Journal of Endocrinology* 172 (2002) 163-76.
- Masson, P.: Some histological methods. Trichrome staining and their preliminary techniques. *Bulletin of the International Association of Medicine* 12 (1929) 75.

- Mathisen, P.M. and Miller, L.: Thyroid hormone induction of keratin genes: a two-step activation of gene expression during development. *Genes & Development* 1 (1987) 1107-17.
- Mathisen, P.M. and Miller, L.: Thyroid hormone induces constitutive keratin gene expression during *Xenopus laevis* development. *Molecular and Cellular Biology* 9 (1989) 1823-31.
- Mendive, F., Rivolta, C., Moya, C., Vassart, G. and Targovnik, H.: Genomic organization of the human thyroglobulin gene: the complete intron-exon structure. *European Journal of Endocrinology* (2001) 485-496.
- Mikkaichi, T., Suzuki, T., Tanemoto, M., Ito, S. and Abe, T.: The Organic Anion Transporter (OATP) Family. *Drug Metab Pharmacokinet* 19 (2004) 171-179.
- Miwa, S. and Inui, Y.: Effects of Various Doses of Thyroxine and Triiodothyronine on the Metamorphosis of Flounder (*Paralichthys-Olivaceus*). *General and Comparative Endocrinology* 67 (1987a) 356-363.
- Miwa, S. and Inui, Y.: Histological-Changes in the Pituitary-Thyroid Axis During Spontaneous and Artificially-Induced Metamorphosis of Larvae of the Flounder *Paralichthys-Olivaceus*. *Cell and Tissue Research* 249 (1987b) 117-123.
- Miwa, S. and Inui, Y.: Thyroid-Hormone Stimulates the Shift of Erythrocyte Populations During Metamorphosis of the Flounder. *Journal of Experimental Zoology* 259 (1991) 222-228.
- Miwa, S., Tagawa, M., Inui, Y. and Hirano, T.: Thyroxine Surge in Metamorphosing Flounder Larvae. *General and Comparative Endocrinology* 70 (1988) 158-163.
- Miwa, S., Yamano, K. and Inui, Y.: Thyroid-Hormone Stimulates Gastric Development in Flounder Larvae During Metamorphosis. *Journal of Experimental Zoology* 261 (1992) 424-430.
- Miya, M., Takeshima, H., Endo, H., Ishiguro, N.B., Inoue, J.G., Mukai, T., Satoh, T.P., Yamaguchi, M., Kawaguchi, A., Mabuchi, K., Shirai, S.M. and Nishida, M.: Major patterns of higher teleostean phylogenies: a new perspective based on 100 complete mitochondrial DNA sequences. *Molecular Phylogenetics and Evolution* 26 (2003) 121-138.
- Miyatani, S., Winkles, J.A., Sargent, T.D. and Dawid, I.B.: Stage-specific keratins in *Xenopus laevis* embryos and tadpoles: the XK81 gene family. *J. Cell Biol.* 103 (1986) 1957-1965.
- Mol, K.A., Van der Geyten, S., Kuhn, E.R. and Darras, V.M.: Effects of experimental hypo- and hyperthyroidism on iodothyronine deiodinases in Nile tilapia, *Oreochromis niloticus*. *Fish Physiology and Biochemistry* 20 (1999) 201-207.
- Mol, K.A., van der Geyten, S., Burel, C., Kuhn, E. R., Boujard, T., Darras, V. M.: Comparative study of iodothyronine outer ring and inner ring deiodination activities in five teleostean fishes. *Fish Physiology and Biochemistry* 18 (1998) 253-266.
- Moll, R., Franke, W.W., Schiller, D.L., Geiger, B. and Krepler, R.: The catalog of human cytokeratins: Patterns of expression in normal epithelia, tumors and cultured cell lines. *Cell* 31 (1982) 11-24.
- Mommsen, T.P.: Paradigms of growth in fishes. *Comparative Biochemistry and Physiology B-Biochemistry & Molecular Biology* 129 (2001) 201-219.
- Morgan, M.J., Earnshaw, J.C. and Dhoot, G.K.: Novel developmentally regulated exon identified in the rat fast skeletal muscle troponin T gene. *Journal of Cell Science* 106 (Pt 3) (1993) 903-8.
- Morin, P.P., Hara, T.J. and Eales, J.G.: Thyroid hormone deiodination in brain, liver, gill, heart and muscle of Atlantic salmon (*Salmo salar*) during photoperiodically-

- induced parr-smolt transformation. I. Outer- and inner-ring thyroxine deiodination. *General and Comparative Endocrinology* 90 (1993) 142-56.
- Moutou, K.A., Canario, A.V., Mamuris, Z. and Power, D.M.: Molecular cloning and sequence of *Sparus aurata* skeletal myosin light chains expressed in white muscle: developmental expression and thyroid regulation. *The Journal of Experimental Biology* 204 (2001) 3009-3018.
- Murakami, M., Araki, O., Hosoi, Y., Kamiya, Y., Morimura, T., Ogiwara, T., Mizuma, H. and Mori, M.: Expression and regulation of type II iodothyronine deiodinase in human thyroid gland. *Endocrinology* 142 (2001) 2961-7.
- Muresan, Z. and Arvan, P.: Thyroglobulin transport along the secretory pathway. *J Biol Chem* 272 (1997) 26095-26102.
- Muresan, Z. and Arvan, P.: Enhanced binding to the molecular chaperone BiP slows thyroglobulin export from the endoplasmic reticulum. *Mol Endocrinol* 12 (1998) 458-467.
- Murray, H.M., Hew, C.L. and Fletcher, G.L.: Spatial expression patterns of skin-type antifreeze protein in winter flounder (*Pseudopleuronectes americanus*) epidermis following metamorphosis. *J Morphol* 257 (2003) 78-86.
- Mylonas, C.C., Sullivan, C.V. and Hinshaw, J.M.: Thyroid hormones in brown trout (*Salmo trutta*) reproduction and early development. *Fish Physiology and Biochemistry* 13 (1994) 485-493.
- Nagaya, T. and Jameson, J.L.: Distinct dimerization domains provide antagonist pathways for thyroid hormone receptor action. *The Journal of Biological Chemistry* 268 (1993) 24278-82.
- Nakada, K., Miyazaki, J.I. and Hirabayashi, T.: Expression of multiple troponin T isoforms in chicken breast muscle regeneration induced by sub-serious implantation. *Differentiation* 70 (2002) 92-100.
- Nelson, J.S.: *Fishes of the World*, third edition ed. Wiley, New York, 1994.
- Ng, L., Goodyear, R.J., Woods, C.A., Schneider, M.J., Diamond, E., Richardson, G.P., Kelley, M.W., Germain, D.L.S., Galton, V.A. and Forrest, D.: Hearing loss and retarded cochlear development in mice lacking type 2 iodothyronine deiodinase. *PNAS* 101 (2004) 3474-3479.
- Nguyen, T.T., Chapa, F. and DiStefano, J.J., III: Direct Measurement of the Contributions of Type I and Type II 5'-Deiodinases to Whole Body Steady State 3,5,3'-Triiodothyronine Production from Thyroxine in the Rat. *Endocrinology* 139 (1998) 4626-4633.
- Nilsson, M., Björkman, U., Ekholm, R. and Ericson, L.E.: Polarized efflux of iodide in porcine thyrocytes occurs via a cAMP-regulated iodide channel in the apical plasma membrane. *Acta Endocrinologica* 126 (1992) 67-74.
- Nilsson, S., Makela, S., Treuter, E., Tujague, M., Thomsen, J., Andersson, G., Enmark, E., Pettersson, K., Warner, M. and Gustafsson, J.A.: Mechanisms of estrogen action. *Physiological Reviews* 81 (2001) 1535-65.
- Nishida, K., Honma, Y., Dota, A., Kawasaki, S., Adachi, W., Nakamura, T., Quantock, A.J., Hosotani, H., Yamamoto, S., Okada, M., Shimomura, Y. and Kinoshita, S.: Isolation and Chromosomal Localization of a Cornea-Specific Human Keratin 12 Gene and Detection of Four Mutations in Meesmann Corneal Epithelial Dystrophy. *American Journal of Human Genetics* 61 (1997) 1268-1275.
- Nishikawa, A., Shimizu-Nishikawa, K. and Miller, L.: Isolation, characterization, and in vitro culture of larval and adult epidermal cells of the frog *Xenopus laevis*. *In Vitro Cellular & Developmental Biology : Journal of the Tissue Culture Association* 26 (1990) 1128-34.

- Nishikawa, A., Shimizu-Nishikawa, K. and Miller, L.: Spatial, temporal, and hormonal regulation of epidermal keratin expression during development of the frog, *Xenopus laevis*. *Developmental Biology* 151 (1992) 145-53.
- Nosek, T.M., Brotto, M.A. and Jin, J.P.: Troponin T isoforms alter the tolerance of transgenic mouse cardiac muscle to acidosis. *Archives of Biochemistry and Biophysics* 430 (2004) 178-184.
- Nowell, M.A., Power, D.M., Canario, A.V., Llewellyn, L. and Sweeney, G.E.: Characterization of a sea bream (*Sparus aurata*) thyroid hormone receptor-beta clone expressed during embryonic and larval development. *General and Comparative Endocrinology* 123 (2001) 80-9.
- Nowell, M.A., Power, D.M., Guerreiro, P.M., Llewellyn, L., Ramsurn, V.V., Wigham, T. and Sweeney, G.E.: Cloning and Expression of an Elongation Factor-1alpha in Sea Bream (*Sparus aurata*) Larvae and Adult Tissue. *Marine Biotechnology* 2 (2000) 173-179.
- O'Mara, B.A., Dittrich, W., Lauterio, T.J. and St Germain, D.L.: Pretranslational regulation of type I 5'-deiodinase by thyroid hormones and in fasted and diabetic rats. *Endocrinology* 133 (1993) 1715-23.
- Ogut, O. and Jin, J.P.: Developmentally regulated, alternative RNA splicing-generated pectoral muscle-specific troponin T isoforms and role of the NH2-terminal hypervariable region in the tolerance to acidosis. *The Journal of Biological Chemistry* 273 (1998) 27858-66.
- Ohtaki, S., Nakagawa, H., Nakamura, M. and Yamazaki, I.: One- and two-electron oxidations of tyrosine, monoiodotyrosine, and diiodotyrosine catalyzed by hog thyroid peroxidase. *J Biol Chem* 257 (1982a) 13398.
- Ohtaki, S., Nakagawa, H., Nakamura, M. and Yamazaki, I.: Reactions of purified hog thyroid peroxidase with H₂O₂, tyrosine, and methylmercaptoimidazole (Goitrogen) in comparison with bovine lactoperoxidase. *J Biol Chem* 257 (1982b) 761.
- Orozco, A., Jeziorski, M.C., Linser, P.J., Greenberg, R.M. and Valverde_R, C.: Cloning of the gene and complete cDNA encoding a type 2 deiodinase from *Fundulus heteroclitus*. *General and Comparative Endocrinology* 128 (2002) 162-7.
- Orozco, A., Linser, P. and Valverde, C.: Kinetic characterization of outer-ring deiodinase activity (ORD) in the liver, gill and retina of the killifish *Fundulus heteroclitus*. *Comparative Biochemistry and Physiology. Part B, Biochemistry & Molecular Biology* 126 (2000) 283-90.
- Orozco, A. and Valverde-R, C.: Thyroid Hormone Deiodination in Fish. *Thyroid* 15 (2005) 799-813.
- Orozco, A., Villalobos, P., Jeziorski, M.C. and Valverde_R, C.: The liver of *Fundulus heteroclitus* expresses deiodinase type 1 mRNA. *General and Comparative Endocrinology* 130 (2003) 84-91.
- Osse, J.W.: Form changes in fish larvae in relation to changing demands of function. *Netherlands Journal of Zoology* 40 (1990) 362-385.
- Osse, J.W. and van den Boogaart, J.G.M.: Dynamic morphology of fish larvae, structural implications of friction forces in swimming, feeding and ventilation. *Journal of Fish Biology* 55 (1999) 156-174.
- Ottensen, O.H. and Olafsen, J.A.: Ontogenetic development and composition of the mucous cells and the occurrence of saccular cells in the epidermis of atlantic halibut. *Journal of Fish Biology* 50 (1997) 620-633.
- Pallud, S., Ramauge, M., Gavaret, J.M., Lennon, A.M., Munsch, N., St_Germain, D.L., Pierre, M. and Courtin, F.: Regulation of type 3 iodothyronine deiodinase

- expression in cultured rat astrocytes: role of the Erk cascade. *Endocrinology* 140 (1999) 2917-23.
- Parra, G. and Yufera, M.: Comparative energetics during early development of two marine fish species, *Solea senegalensis* (Kaup) and *Sparus aurata* (L.). *J Exp Biol* 204 (2001) 2175-2183.
- Patrino, M., Radaelli, G., Mascarello, F. and Candia-Carnevali, M.D.: Muscle growth in response to changing demands of functions in the teleost *Sparus aurata* (L.) during development from hatching to juvenile. *Anatomy and Embryology* 198 (1998) 487-504.
- Paul, B.D., Buchholz, D.R., Fu, L. and Shi, Y.B.: Tissue- and gene-specific recruitment of steroid receptor coactivator-3 by thyroid hormone receptor during development. *J Biol Chem* 280 (2005a) 27165-72.
- Paul, B.D., Fu, L., Buchholz, D.R. and Shi, Y.B.: Coactivator recruitment is essential for liganded thyroid hormone receptor to initiate amphibian metamorphosis. *Mol Cell Biol* 25 (2005b) 5712-24.
- Paul, B.D. and Shi, Y.B.: Distinct expression profiles of transcriptional coactivators for thyroid hormone receptors during *Xenopus laevis* metamorphosis. *Cell Res* 13 (2003) 459-64.
- Penel, C., Gruffat, D., Alquier, C., Benoliel, A. and O, C.: Thyrotropin chronically regulates the pool of thyroperoxidase and its intracellular distribution: a quantitative confocal microscopic study. *J Cell Physiol* 174 (1998) 160-169.
- Perry, S.V.: Troponin T: genetics, properties and function. *Journal of Muscle Research and Cell Motility* 19 (1998) 575-602.
- Pinky, Mittal, S., Yashpal, M., Ojha, J. and Mittal, A.K.: Occurrence of keratinization in the structures associated with lips of a hill stream fish *Garra lamta*(Hamilton)(Cyprinidae, Cypriniformes). *Journal of Fish Biology* 65 (2004) 1165-1172.
- Pizzagalli, F., Hagenbuch, B., Stieger, B., Klenk, U., Folkers, G. and Meier, P.J.: Identification of a Novel Human Organic Anion Transporting Polypeptide as a High Affinity Thyroxine Transporter. *Mol Endocrinol* 16 (2002) 2283-2296.
- Plateroti, M., Gauthier, K., Domon_Dell, C., Freund, J.N., Samarut, J. and Chassande, O.: Functional interference between thyroid hormone receptor alpha (TRalpha) and natural truncated TRDeltaalpha isoforms in the control of intestine development. *Molecular and Cellular Biology* 21 (2001) 4761-72.
- Polo, A., Yúfera, M. and Pascuala, E.: Effects of temperature on egg and larval development of *Sparus aurata* L. *Aquaculture* 92 (1991) 367-375.
- Porterfield, S.F. and Hendrich, C.E.: The role of thyroid hormones in prenatal and neonatal neurological. *Endocrine Reviews* 14 (1993) 94-106.
- Power, D.M., Llewellyn, L., Faustino, M., Nowell, M.A., Bjornsson, B.T., Einarsdottir, I.E., Canario, A.V.M. and Sweeney, G.E.: Thyroid hormones in growth and development of fish. *Comparative Biochemistry and Physiology C-Toxicology & Pharmacology* 130 (2001) 447-459.
- Privalsky, M.L. and Yoh, S.M.: Resistance to thyroid hormone (RTH) syndrome reveals novel determinants regulating interaction of T3 receptor with corepressor. *Molecular and Cellular Endocrinology* 159 (2000) 109-124.
- Radoja, N., Diaz, D.V., Minars, T.J., Freedberg, I.M., Blumenberg, M. and Tomic-Canic, M.: Specific organization of the negative response elements for retinoic acid and thyroid hormone receptors in keratin gene family. *J Invest Dermatol* 109 (1997) 566-72.

- Radoja, N., Stojadinovic, O., Waseem, A., Tomic-Canic, M., Milisavljevic, V., Teebor, S. and Blumenberg, M.: Thyroid hormones and gamma interferon specifically increase K15 keratin gene transcription. *Mol Cell Biol* 24 (2004) 3168-79.
- Raspe, E. and Dumont, J.: Tonic modulation of dog thyrocyte H₂O₂ generation and I-uptake by thyrotropin through the cyclic adenosine 3',5'-monophosphate cascade. *Endocrinology* 136 (1995) 965-973.
- Reddy, P., Brown, C., Leatherland, J. and Lam, T.: Role of thyroid hormones in tilapia larvae (*Oreochromis mossambicus*): II. Changes in the hormones and 5'-monodeiodinase activity during development. *Fish Physiology and Biochemistry* 9 (1992) 487-496.
- Reginato, M.J., Zhang, J. and Lazar, M.A.: DNA-independent and DNA-dependent mechanisms regulate the differential heterodimerization of the isoforms of the thyroid hormone receptor with retinoid X receptor. *The Journal of Biological Chemistry* 271 (1996) 28199-205.
- Richard, K., Hume, R., Kaptein, E., Sanders, J.P., van_Toor, H., De_Herder, W.W., den_Hollander, J.C., Krenning, E.P. and Visser, T.J.: Ontogeny of iodothyronine deiodinases in human liver. *The Journal of Clinical Endocrinology and Metabolism* 83 (1998) 2868-74.
- Roberts, R.J., Bell, M. and Young, H.: Studies on the skin of plaice (*pleuronectes platessa* L.) II. The development of larval plaice skin. *Journal of Fish Biology* 5 (1973) 103-108.
- Rosenberg, M., RayChaudhury, A., Shows, T.B., Le Beau, M.M. and Fuchs, E.: A Group of Type I Keratin Genes on Human Chromosome 17: Characterization and Expression. *Molecular and Cellular Biology* 8 (1988) 722-736.
- Rotllant, J., Worthington, G.P., Fuentes, J., Guerreiro, P.M., Teitsma, C.A., Ingleton, P.M., Balment, R.J., Canario, A.V.M. and Power, D.M.: Determination of tissue and plasma concentrations of PTHrP in fish: development and validation of a radioimmunoassay using a teleost 1-34 N-terminal peptide. *General and Comparative Endocrinology* 133 (2003) 146-153.
- Rousset, B., Selmi, S., Bornet, H., Bourgeat, P., Rabilloud, R. and Munari-silem, Y.: Thyroid hormone residues are released from thyroglobulin with limited alterations of the thyroglobulin structure. *J Biol Chem* 265 (1990) 10950-10954.
- Rowlerson, A., Mascarello, F., Radaelli, G. and Veggetti, A.: Differentiation and growth of muscle in the fish *Sparus aurata* (L): II. Hyperplastic and hypertrophic growth of lateral muscle from hatching to adult. *Journal of Muscle Research and Cell Motility* 16 (1995) 223-36.
- Rowlerson, A., Radaelli, G., Mascarello, F. and Veggetti, A.: Regeneration of skeletal muscle in two teleost fish: *Sparus aurata* and *Brachydanio rerio*. *Cell and Tissue Research* 289 (1997) 311-22.
- Sachs, L.M., Damjanovski, S., Jones, P.L., Li, Q., Amano, T., Ueda, S., Shi, Y.B. and Ishizuya_Oka, A.: Dual functions of thyroid hormone receptors during *Xenopus* development. *Comparative Biochemistry and Physiology. Part B, Biochemistry & Molecular Biology* 126 (2000) 199-211.
- Sachs, L.M., Jones, P.L., Havis, E., Rouse, N., Demeneix, B.A. and Shi, Y.B.: Nuclear receptor corepressor recruitment by unliganded thyroid hormone receptor in gene repression during *Xenopus laevis* development. *Mol Cell Biol* 22 (2002) 8527-38.
- Sadow, P.M., Chassande, O., Koo, E.K., Gauthier, K., Samarut, J., Xu, J., O_Malley, B.W. and Weiss, R.E.: Regulation of expression of thyroid hormone receptor

- isoforms and coactivators in liver and heart by thyroid hormone. *Molecular and Cellular Endocrinology* 203 (2003) 65-75.
- Saele, O., Solbakken, J., Watanabe, K., Hamre, K., Power, D.M. and Pittman, K.: Staging of Atlantic halibut (*hippoglossus hippoglossus* L.) from first feeding through metamorphosis, including cranial ossification independent of eye migration. *Aquaculture* 239 (2004) 445-465.
- Saele, O., Solbakken, J.S., Watanabe, K., Hamre, K. and Pittman, K.: The effect of diet on ossification and eye migration in Atlantic halibut larvae (*Hippoglossus hippoglossus* L.). *Aquaculture* 220 (2003) 683-696.
- Safi, R., Bertrand, S., Marchand, O., Duffraisse, M., de Luze, A., Vanacker, J.M., Maraninchi, M., Margotat, A., Demeneix, B. and Laudet, V.: The axolotl (*Ambystoma mexicanum*), a neotenic amphibian, expresses functional thyroid hormone receptors. *Endocrinology* 145 (2004) 760-72.
- Safran, M., Farwell, A.P. and Leonard, J.L.: Catalytic activity of type II iodothyronine 5'-deiodinase polypeptide is dependent upon a cyclic AMP activation factor. *The Journal of Biological Chemistry* 271 (1996) 16363-8.
- Saito, T., Endo, T., Kawaguchi, A., Ikeda, M., Nakazato, M., Kogai, T. and Onaya, T.: Increased Expression of the Na⁺/I⁻ Symporter in Cultured Human Thyroid Cells Exposed to Thyrotropin and in Graves' Thyroid Tissue. *J Clin Endocrinol Metab* 82 (1997) 3331-3336.
- Salvatore, D., Low, S.C., Berry, M., Maia, A.L., Harney, J.W., Croteau, W., St_Germain, D.L. and Larsen, P.R.: Type 3 iodothyronine deiodinase: cloning, in vitro expression, and functional analysis of the placental selenoenzyme. *The Journal of Clinical Investigation* 96 (1995) 2421-30.
- Salvatore, D., Tu, H., Harney, J.W. and Larsen, P.R.: Type 2 iodothyronine deiodinase is highly expressed in human thyroid. *The Journal of Clinical Investigation* 98 (1996) 962-8.
- Samson, F., Mesnard, L., Mihovilovic, M., Potter, T.G., Mercadier, J.J., Roses, A.D. and Gilbert, J.R.: A new human slow skeletal troponin T (TnTs) mRNA isoform derived from alternative splicing of a single gene. *Biochemical and Biophysical Research Communications* 199 (1994) 841-7.
- Sanders, J.P., Van_der_Geyten, S., Kaptein, E., Darras, V.M., Kuhn, E.R., Leonard, J.L. and Visser, T.J.: Characterization of a propylthiouracil-insensitive type I iodothyronine deiodinase. *Endocrinology* 138 (1997) 5153-60.
- Sanders, J.P., Van_der_Geyten, S., Kaptein, E., Darras, V.M., Kuhn, E.R., Leonard, J.L. and Visser, T.J.: Cloning and characterization of type III iodothyronine deiodinase from the fish *Oreochromis niloticus*. *Endocrinology* 140 (1999) 3666-73.
- Santos, C.R. and Power, D.M.: Identification of transthyretin in fish (*Sparus aurata*): cDNA cloning and characterisation. *Endocrinology* 140 (1999) 2430-3.
- Schaffeld, M., Bremer, M., Hunzinger, C. and Markl, J.: Evolution of tissue-specific keratins as deduced from novel cDNA sequences of the lungfish *Protopterus aethiopicus*. *Eur J Cell Biol* 84 (2005) 363-77.
- Schaffeld, M., Haberkamp, M., Braziulis, E., Lieb, B. and Markl, J.: Type II keratin cDNAs from the rainbow trout: implications for keratin evolution. *Differentiation* 70 (2002a) 292-299.
- Schaffeld, M., Hoffling, S., Haberkamp, M., Conrad, M. and Markl, J.: Type I keratin cDNAs from the rainbow trout: independent radiation of keratins in fish. *Differentiation* 70 (2002b) 282-291.

- Schaffeld, M., Hoffling, S. and Jurgen, M.: Sequence, evolution and tissue expression patterns of an epidermal type I keratin from the shark *Scyliorhinus stellaris*. *Eur J Cell Biol* 83 (2004) 359-68.
- Schaffeld, M., Knappe, M., Hunzinger, C. and Markl, J.: cDNA sequences of the authentic keratins 8 and 18 in zebrafish. *Differentiation* 71 (2003) 73-82.
- Schaffeld, M., Lobbecke, A., Lieb, B. and Markl, J.: Tracing keratin evolution: catalog, expression patterns and primary structure of shark (*Scyliorhinus stellaris*) keratins. *Eur J Cell Biol* 77 (1998) 69-80.
- Schneider, M.J., Fiering, S.N., Pallud, S.E., Parlow, A.F., St_Germain, D.L. and Galton, V.A.: Targeted disruption of the type 2 selenodeiodinase gene (DIO2) results in a phenotype of pituitary resistance to T4. *Molecular Endocrinology* (Baltimore, Md.) 15 (2001) 2137-48.
- Schneider, M.J., Fiering, S.N., Thai, B., Wu, S.-y., St. Germain, E., Parlow, A.F., St. Germain, D.L. and Galton, V.A.: Targeted Disruption of the Type 1 Selenodeiodinase Gene (Dio1) Results in Marked Changes in Thyroid Hormone Economy in Mice. *Endocrinology* 147 (2006) 580-589.
- Schreiber, A. and Brown, D.D.: Tadpole skin dies autonomously in response to thyroid hormone at metamorphosis. *Proc Natl Acad Sci U S A* 100 (2003) 1769-74.
- Schreiber, A.M., Cai, L. and Brown, D.D.: Remodeling of the intestine during metamorphosis of *Xenopus laevis*. *PNAS* 102 (2005) 3720-3725.
- Schreiber, G. and Richardson, S.J.: The evolution of gene expression, structure and function of transthyretin. *Comparative Biochemistry and Physiology. Part B, Biochemistry & Molecular Biology* 116 (1997) 137-60.
- Schussler, G.: The thyroxine-binding proteins. *Thyroid* 10 (2000) 141-149.
- Sehnert, A.J., Huq, A., Weinstein, B.M., Walker, C., Fishman, M. and Stainier, D.Y.R.: Cardiac Troponin T is essential in sarcomere assembly and cardiac contractility. *Nature Genetics* 31 (2002) 106-110.
- Shepherdley, C.A., Richardson, S.J., Evans, B.K., Kuhn, E.R. and Darras, V.M.: Thyroid Hormone Deiodinases during Embryonic Development of the Saltwater Crocodile (*Crocodylus porosus*). *General and Comparative Endocrinology* 126 (2002) 153-164.
- Shi, Y.B., Wong, J., Puzianowska-Kuznicka, M. and Stolow, M.A.: Tadpole competence and tissue specific temporal regulation of amphibian metamorphosis: roles of thyroid hormone and its receptors. *BioEssays* 18 (1986) 391-399.
- Shi, Y.B., Yaoita, Y. and Brown, D.D.: Genomic organization and alternative promoter usage of the two thyroid hormone receptor beta genes in *Xenopus laevis*. *The Journal of Biological Chemistry* 267 (1992) 733-8.
- Shimizu-Nishikawa, K. and Miller, L.: Calcium regulation of epidermal cell differentiation in the frog *Xenopus laevis*. *The Journal of Experimental Zoology* 260 (1991) 165-9.
- Shimizu-Nishikawa, K. and Miller, L.: Hormonal regulation of adult type keratin gene expression in larval epidermal cells of the frog *Xenopus laevis*. *Differentiation; Research in Biological Diversity* 49 (1992) 77-83.
- Shintani, N., Nohira, T., Hikosaka, A. and Kawahara, A.: Tissue-specific regulation of type III iodothyronine 5-deiodinase gene expression mediates the effects of prolactin and growth hormone in *Xenopus* metamorphosis. *Development, Growth & Differentiation* 44 (2002) 327-35.

- Sinha, S., Degenstein, L., Copenhaver, C. and Fuchs, E.: Defining the Regulatory Factors Required for Epidermal Gene Expression. *Mol. Cell. Biol.* 20 (2000) 2543-2555.
- Song, S., Adachi, K., Katsuyama, M., Sorimachi, K. and Oka, T.: Isolation and characterization of the 5'-upstream and untranslated regions of the mouse type II iodothyronine deiodinase gene. *Molecular and Cellular Endocrinology* 165 (2000) 189-198.
- Soukup, T. and Jirmanova, I.: Regulation of myosin expression in developing and regenerating extrafusal and intrafusal muscle fibers with special emphasis on the role of thyroid hormones. *Physiol Res* 49 (2000) 617-33.
- St Germain, D.L., Schwartzman, R.A., Croteau, W., Kanamori, A., Wang, Z., Brown, D.D. and Galton, V.A.: A thyroid hormone-regulated gene in *Xenopus laevis* encodes a type III iodothyronine 5-deiodinase. *Proceedings of the National Academy of Sciences of the United States of America* 91 (1994) 7767-71.
- Stevens, A.: The haematoxylin. In: Bancroft, J.D. and Stevens, A. (Eds.), *Theory and practice of histological techniques*. Churchill Livingstone, Edinburgh, 1990, pp. 107-118.
- Stoiber, W., Haslett, J.R. and Sanger, A.M.: Myogenic patterns in teleosts: what does the present evidence really suggest? *Journal of Fish Biology* 55 (1999) 84-99.
- Strait, K.A., Zou, L. and Oppenheimer, J.H.: Beta 1 isoform-specific regulation of a triiodothyronine-induced gene during cerebellar development. *Molecular Endocrinology* (Baltimore, Md.) 6 (1992) 1874-80.
- Sutija, M., Longhurst, T.J. and Joss, J.M.P.: Deiodinase type II and tissue specific mRNA alternative splicing in the Australian lungfish, *Neoceratodus forsteri*. *General and Comparative Endocrinology* 132 (2003) 409-417.
- Suzuki, K.-i., Utoh, R., Kotani, K., Obara, M. and Yoshizato, K.: Lineage of anuran epidermal basal cells and their differentiation potential in relation to metamorphic skin remodeling. *Dev Growth Differ* 44 (2002) 225-238.
- Suzuki, K., Sato, K., Katsu, K., Hayashita, H., Bach Kristensen, D. and Yoshizato, K.: Novel *Rana* keratin genes and their expression during larval to adult epidermal conversion in bullfrog tadpoles. *Differentiation* 68 (2001) 44-54.
- Swofford, D.L., Waddell, P.J., Huelsenbeck, J.P., Foster, P.G., Lewis, P.O. and Rogers, J.S.: Bias in phylogenetic estimation and its relevance to the choice between parsimony and likelihood methods. *Systematic Biology* 50 (2001) 525-539.
- Szisch, V., Papandroulakis, N., Fanouraki, E. and Pavlidis, M.: Ontogeny of the thyroid hormones and cortisol in the gilthead sea bream, *Sparus aurata*. *Gen Comp Endocrinol* 142 (2005) 186-192.
- Szkudlinski, M.W., Fremont, V., Ronin, C. and Weintraub, B.D.: Thyroid-Stimulating Hormone and Thyroid-Stimulating Hormone Receptor Structure-Function Relationships. *Physiol. Rev.* 82 (2002) 473-502.
- Tagawa, M. and Hirano, T.: Presence of thyroxine in eggs and changes in its content during early development of chum salmon, *Oncorhynchus keta*. *General and Comparative Endocrinology* 68 (1987) 129-135.
- Tagawa, M. and Hirano, T.: Effects of thyroid hormone deficiency in eggs on early development of the medaka, *Oryzias latipes*. *Journal of Experimental Zoology* 257 (1991) 360-366.
- Tagawa, M., Miwa, S., Inui, Y., Dejesus, E.G. and Hirano, T.: Changes in Thyroid-Hormone Concentrations During Early Development and Metamorphosis of the Flounder, *Paralichthys Olivaceus*. *Zoological Science* 7 (1990a) 93-96.

- Tagawa, M., Tanaka, M., Matsumoto, S. and Hirano, T.: Thyroid hormones in eggs of various freshwater, marine and diadromous teleosts and their changes during egg development. *Fish Physiology and Biochemistry* 8 (1990b) 515-520.
- Tannahill, L.A., Visser, T.J., McCabe, C.J., Kachilele, S., Boelaert, K., Sheppard, M.C., Franklyn, J.A. and Gittoes, N.J.: Dysregulation of iodothyronine deiodinase enzyme expression and function in human pituitary tumours. *56* (2002) 735-43.
- Tata, J.R.: Amphibian metamorphosis as a model for the developmental actions of thyroid hormone. *Molecular and Cellular Endocrinology* 246 (2006) 10-20.
- Thisse, C., Degrave, A., Kryukov, G.V., Gladyshev, V.N., Obrecht-Pflumio, S., Krol, A., Thisse, B. and Lescure, A.: Spatial and temporal expression patterns of selenoprotein genes during embryogenesis in zebrafish. *Gene Expression Patterns* 3 (2003) 525-532.
- Thompson, J.D., Gibson, T.J., Plewniak, F., Jeanmougin, F. and Higgins, D.G.: The CLUSTAL_X windows interface: flexible strategies for multiple sequence alignment aided by quality analysis tools. *Nucleic Acids Research (Online)* 25 (1997) 4876-82.
- Tietze, F., Kohn, L., Kohn, A., Bernardini, I., Andersson, H., Adamson, M., Harper, G. and Gahl, W.: Carrier-mediated transport of monoiodotyrosine out of thyroid cell lysosomes. *J Biol Chem* 264 (1989) 4762-4765.
- Tobacman, L. and Lee, R.: Isolation and functional comparison of bovine cardiac troponin T isoforms. *J. Biol. Chem.* 262 (1987) 4059-4064.
- Tomic-Canic, M., Day, D., Samuels, H.H., Freedberg, I.M. and Blumenberg, M.: Novel Regulation of Keratin Gene Expression by Thyroid Hormone and Retinoid Receptors. *J. Biol. Chem.* 271 (1996a) 1416-1423.
- Tomic-Canic, M., Freedberg, I.M. and Blumenberg, M.: Codominant Regulation of Keratin Gene Expression by Cell Surface Receptors and Nuclear Receptors. *Experimental Cell Research* 224 (1996b) 96-102.
- Tomic-Canic, M., Komine, M., Freedberg, I.M. and Blumenberg, M.: Epidermal signal transduction and transcription factor activation in activated keratinocytes. *J Dermatol Sci* 17 (1998) 167-81.
- Tomic-Canic, M., Sunjevaric, I. and Blumenberg, M.: A simple method for site-specific mutagenesis that leaves the rest of the template unaltered. *Methods Mol Biol* 57 (1996c) 259-67.
- Tomic-Canic, M., Sunjevaric, I., Freedberg, I.M. and Blumenberg, M.: Identification of the Retinoic Acid and Thyroid Hormone Receptor-Responsive Element in the Human K14 Keratin Gene. *Journal of Investigative Dermatology* 99 (1992) 842-847.
- Toyoda, N., Berry, M.J., Harney, J.W. and Larsen, P.R.: Topological Analysis of the Integral Membrane Protein, Type 1 Iodothyronine Deiodinase (D1). *J. Biol. Chem.* 270 (1995a) 12310-12318.
- Toyoda, N., Nishikawa, M., Mori, Y., Yoshimura, M., Masaki, H., Gondou, A., Yonemoto, T. and Inada, M.: Identification of a 27-kilodalton protein with the properties of type I iodothyronine 5'-deiodinase in human thyroid gland. *The Journal of Clinical Endocrinology and Metabolism* 74 (1992) 533-8.
- Toyoda, N., Zavacki, A.M., Maia, A.L., Harney, J.W. and Larsen, P.R.: A novel retinoid X receptor-independent thyroid hormone response element is present in the human type 1 deiodinase gene. *Molecular and Cellular Biology* 15 (1995b) 5100-12.

- Troyanovsky, S.M., Leube, R.E. and Franke, W.W.: Characterization of the human gene encoding cytokeratin 17 and its expression pattern. *European Journal of Cell Biology* 59 (1992) 127-137.
- Tu, H.M., Kim, S.W., Salvatore, D., Bartha, T., Legradi, G., Larsen, P.R. and Lechan, R.M.: Regional distribution of type 2 thyroxine deiodinase messenger ribonucleic acid in rat hypothalamus and pituitary and its regulation by thyroid hormone. *Endocrinology* 138 (1997) 3359-68.
- Tu, H.M., Legradi, G., Bartha, T., Salvatore, D., Lechan, R.M. and Larsen, P.R.: Regional expression of the type 3 iodothyronine deiodinase messenger ribonucleic acid in the rat central nervous system and its regulation by thyroid hormone. *Endocrinology* 140 (1999) 784-90.
- Turner, C.D. and Bagnara, J.T.: *General Endocrinology*. W.B. Saunders Company, Philadelphia, Pa. USA., 1976.
- Vadaszova, A., Zacharova, G., Machacova, K., Jirmanova, I. and Soukup, T.: Influence of thyroid status on the differentiation of slow and fast muscle phenotypes. *Physiology Research* 53 (2004) S57-61.
- Valverde, C., Croteau, W., Lafleur, G.J., Orozco, A. and Germain, D.L.: Cloning and expression of a 5'-iodothyronine deiodinase from the liver of *Fundulus heteroclitus*. *Endocrinology* 138 (1997) 642-8.
- van de Graaf, S., Ris-Stalpers, C., Pauws, E., Mendive, F., Targovnik, H. and de Vijlder, J.: Up to date with human thyroglobulin. *J Endocrinol* . 170 (2001) 307-321.
- Van der Geyten, S., Byamungu, N., Reyns, G.E., Kuhn, E.R. and Darras, V.M.: Iodothyronine deiodinases and the control of plasma and tissue thyroid hormone levels in hyperthyroid tilapia (*Oreochromis niloticus*). *J Endocrinol* 184 (2005) 467-479.
- Van der Geyten, S., Sanders, J.P., Kaptein, E., Darras, V.M., Kuhn, E.R., Leonard, J.L. and Visser, T.J.: Expression of chicken hepatic type I and type III iodothyronine deiodinases during embryonic development. *Endocrinology* 138 (1997) 5144-52.
- Van der Geyten, S., Segers, I., Gereben, B., Bartha, T., Rudas, P., Larsen, P.R., Kuhn, E.R. and Darras, V.M.: Transcriptional regulation of iodothyronine deiodinases during embryonic development. *Molecular and Cellular Endocrinology* 183 (2001a) 1-9.
- Van der Geyten, S., Toguyeni, A., Baroiller, J.-F., Fauconneau, B., Fostier, A., Sanders, J.P., Visser, T.J., Kuhn, E.R. and Darras, V.M.: Hypothyroidism Induces Type I Iodothyronine Deiodinase Expression in Tilapia Liver. *General and Comparative Endocrinology* 124 (2001b) 333-342.
- Van der Geyten, S., Van den Eynde, I., Segers, I.B., Kuhn, E.R. and Darras, V.M.: Differential expression of iodothyronine deiodinases in chicken tissues during the last week of embryonic development. *General and Comparative Endocrinology* 128 (2002) 65-73.
- Van der Geyten, S., Van Rompaey, E., Sanders, J.P., Visser, T.J., Kuhn, E.R. and Darras, V.M.: Regulation of thyroid hormone metabolism during fasting and refeeding in chicken. *Gen Comp Endocrinol* 116 (1999) 272-80.
- Vassart, G., Pardo, L. and Costagliola, S.: A molecular dissection of the glycoprotein hormone receptors. *Trends in Biochemical Sciences* 29 (2004) 119-126.
- Veggetti, A., Mascarello, F., Scapolo, P.A., Rowlerson, A. and Candia-Carnevali, M.D.: Muscle growth and myosin isoform transitions during development of a small teleost fish, *Poecilia reticulata* (Peters) (*Atheriniformes, Poeciliidae*): a

- histochemical, immunohistochemical, ultrastructural and morphometric study. *Anatomy and Embryology* 187 (1993) 353-361.
- Verhagen, J.H.G.: Hydrodynamics of burst swimming fish larvae; a conceptual model approach. *Journal of Theoretical Biology* 229 (2004) 235-248.
- Virion, A., Courtin, F., Deme, D., Michot, J., Kaniewski, J. and Pommier, J.: Spectral characteristics and catalytic properties of thyroid peroxidase-H₂O₂ compounds in the iodination and coupling reactions. *Arch Biochem Biophys* 242 (1985) 41-47.
- Virion, A., Pommier, J., Deme, D. and Nunez, J.: Kinetics of thyroglobulin iodination and thyroid hormone synthesis catalyzed by peroxidase: the role of H₂O₂. *Eur J Biochem* 117 (1981) 103-109.
- Visser, T.J.: Role of sulfation in thyroid hormone metabolism. *Chemico-Biological Interactions* 92 (1994) 293-303.
- von Mering, C., Jensen, L.J., Snel, B., Hooper, S.D., Krupp, M., Foglierini, M., Jouffre, N., Huynen, M.A. and Bork, P.: STRING: known and predicted protein-protein associations, integrated and transferred across organisms. *Nucl. Acids Res.* 33 (2005) D433-437.
- Wang, J. and Jin, J.P.: Primary structure and developmental acidic to basic transition of 13 alternatively spliced mouse fast skeletal muscle troponin T isoforms. *Gene* 193 (1997) 105-14.
- Wang, J. and Jin, J.P.: Conformational modulation of troponin T by configuration of the NH₂-terminal variable region and functional effects. *Biochemistry* 37 (1998) 14519-28.
- Wang, Q., Lin, J.L. and Lin, J.J.: A novel TCTG(G/C) direct repeat and an A/T-rich HMG2-binding site control the expression of the rat cardiac troponin T gene. *Journal of Molecular and Cellular Cardiology* 34 (2002) 1667-1679.
- Wang, Q., Reiter, R.S., Huang, Q.Q., Jin, J.P. and Lin, J.J.: Comparative studies on the expression patterns of three troponin T genes during mouse development. *The Anatomical Record* 263 (2001) 72-84.
- Wang, Z. and Brown, D.: Thyroid hormone-induced gene expression program for amphibian tail resorption. *J. Biol. Chem.* 268 (1993) 16270-16278.
- Warshawsky, D. and Miller, L.: Tissue-specific in vivo protein-DNA interactions at the promoter region of the *Xenopus* 63 kDa keratin gene during metamorphosis. *Nucleic Acids Res* 23 (1995) 4502-4509.
- Watabe, S.: Myogenic regulatory factors and muscle differentiation during ontogeny in fish. *Journal of Fish Biology* 55 (1999) 1-18.
- Watanabe, Y., Kobayashi, H., Suzuki, K., Kotani, K. and Yoshizato, K.: New epidermal keratin genes from *Xenopus laevis*: hormonal and regional regulation of their expression during anuran skin metamorphosis. *Biochimica Et Biophysica Acta* 1517 (2001) 339-50.
- Watanabe, Y., Tanaka, R., Kobayashi, H., Utoh, R., Suzuki, K., Obara, M. and Yoshizato, K.: Metamorphosis-dependent transcriptional regulation of *xak-c*, a novel *Xenopus* type I keratin gene. *Developmental Dynamics* 225 (2002) 561-70.
- Weinberger, C., Thompson, C.C., Ong, E.S., Lebo, R., Gruol, D.J. and Evans, R.M.: The *c-erb-A* gene encodes a thyroid hormone receptor. *Nature* 324 (1986) 641-6.
- Wheeler, S.J., Church, D.M. and Ostell, J.M.: Spidey: A Tool for mRNA-to-Genomic Alignments. *Genome Research* 11 (2001) 1952-1957.
- Wilkins, M.R., Gasteiger, E., Bairoch, A., Sanchez, J.-C., Williams, K.L., Appel, R.D. and Hochstrasser, D.F.: Protein Identification and Analysis Tools in the ExPASy

- Server. In: Link, A.J. (Ed.), 2-D Proteome Analysis Protocols. Humana Press, New Jersey, 1998.
- Williams, G.R.: Cloning and characterization of two novel thyroid hormone receptor beta isoforms. *Molecular and Cellular Biology* 20 (2000) 8329-42.
- Wood, W.M., Dowding, J.M., Haugen, B.R., Bright, T.M., Gordon, D.F. and Ridgway, E.C.: Structural and functional characterization of the genomic locus encoding the murine beta 2 thyroid hormone receptor. *Molecular Endocrinology* (Baltimore, Md.) 8 (1994) 1605-17.
- Wrutniak-Cabello, C., Casas, F. and Cabello, G.: Thyroid hormone action in mitochondria. *Journal of Molecular Endocrinology* 26 (2001) 67-77.
- Wu, Q.L., Jha, P.K., Raychowdhury, M.K., Du, Y., Leavis, P.C. and Sarkar, S.: Isolation and characterization of human fast skeletal beta troponin T cDNA: comparative sequence analysis of isoforms and insight into the evolution of members of a multigene family. *DNA and Cell Biology* 13 (1994) 217-233.
- www.fishbase.org, 2000.
- www.genoscope.cns.fr/externe/tetranew/.
- www.ncbi.nlm.nih.gov.
- www.thyroidmanager.org: The thyroid hormone and its diseases, 2003.
- Yamano, K., Araki, K., Sekikawa, K. and Inui, Y.: Cloning of thyroid hormone receptor genes expressed in metamorphosing flounder. *Developmental Genetics* 15 (1994a) 378-82.
- Yamano, K. and Inui, Y.: cDNA cloning of thyroid hormone receptor beta for the Japanese flounder. *General and Comparative Endocrinology* 99 (1995) 197-203.
- Yamano, K. and Miwa, S.: Differential gene expression of thyroid hormone receptor alpha and beta in fish development. *Gen Comp Endocrinol* 109 (1998) 75-85.
- Yamano, K., Miwa, S., Obinata, T. and Inui, Y.: Thyroid-Hormone Regulates Developmental-Changes in Muscle During Flounder Metamorphosis. *General and Comparative Endocrinology* 81 (1991a) 464-472.
- Yamano, K., Tagawa, M., Dejesus, E.G., Hirano, T., Miwa, S. and Inui, Y.: Changes in Whole-Body Concentrations of Thyroid-Hormones and Cortisol in Metamorphosing Conger Eel. *Journal of Comparative Physiology B-Biochemical Systemic and Environmental Physiology* 161 (1991b) 371-375.
- Yamano, K., Tagawa, M., Jesus, E.G., Hirano, T., Miwa, S. and Inui, Y.: Changes in whole body concentrations of thyroid hormones and cortisol in metamorphosing conger eel. *Journal of Comparative Physiology B: Biochemical, Systemic, and Environmental Physiology* 161 (1991c) 371-375.
- Yamano, K., Takano-Ohmuro, H., Obinata, T. and Inui, Y.: Effect of thyroid hormone on developmental transition of myosin light chains during flounder metamorphosis. *General and Comparative Endocrinology* 93 (1994b) 321-6.
- Yang, Y.Z., Burgos_Trinidad, M., Wu, Y. and Koenig, R.J.: Thyroid hormone receptor variant alpha2. Role of the ninth heptad in dna binding, heterodimerization with retinoid X receptors, and dominant negative activity. *The Journal of Biological Chemistry* 271 (1996) 28235-42.
- Yao, Y., Nakamura, M., Miyazaki, J.I., Kirinoki, M. and Hirabayashi, T.: Expression pattern of skeletal muscle troponin T isoforms is fixed in cell lineage. *Developmental Biology* 151 (1992) 531-540.
- Yaoita, Y. and Brown, D.D.: A correlation of thyroid hormone receptor gene expression with amphibian metamorphosis. *Genes & Development* 4 (1990) 1917-24.

- Yaoita, Y., Shi, Y.B. and Brown, D.D.: Xenopus laevis alpha and beta thyroid hormone receptors. *Proceedings of the National Academy of Sciences of the United States of America* 87 (1990) 7090-4.
- Yen, P.M.: Physiological and molecular basis of thyroid hormone action. *Physiol Rev* 81 (2001) 1097-142.
- Yen, P.M., Ando, S., Feng, X., Liu, Y., Maruvada, P. and Xia, X.: Thyroid hormone action at the cellular, genomic and target gene levels. *Molecular and Cellular Endocrinology* 246 (2006) 121-127.
- Yen, P.M. and Chin, W.W.: New advances in understanding the molecular mechanisms of thyroid hormone action. *Trends in Endocrinology and Metabolism* 5 (1994) 65-72.
- Yonemura, I., Hirabayashi, T. and Miyazaki, J.I.: Heterogeneity of chicken slow skeletal muscle troponin T mRNA. *Journal of Experimental Zoology* 286 (2000) 149-156.
- Yonemura, I., Mitani, Y., Nakada, K., Akutsu, S. and Miyazaki, J.I.: Developmental changes of cardiac and slow skeletal muscle troponin T expression in chicken cardiac and skeletal muscle. *Zoological Science* 19 (2002) 215-223.
- Zacharova, G., Mrackova, K., Jirmanova, I. and Soukup, T.: Stereological evaluation of the soleus muscle isografted into fast extensor digitorum longus (EDL) muscle in rats with different thyroid status. *Gen Physiol Biophys* 18 Suppl 1 (1999) 84-6.
- Zhang, C.-Y., Kim, S., Harney, J.W. and Larsen, P.R.: Further Characterization of Thyroid Hormone Response Elements in the Human Type 1 Iodothyronine Deiodinase Gene. *Endocrinology* 139 (1998) 1156-1163.
- Zhang, J. and Lazar, M.A.: The Mechanism of Action of Thyroid Hormones. *Annual Review of Physiology* 62 (2000) 439-466.
- Zimek, A., Stick, R. and Weber, K.: Genes coding for intermediate filament proteins: common features and unexpected differences in the genomes of humans and the teleost fish *Fugu rubripes*. *J Cell Sci* 116 (2003) 2295-2302.